



UNIVERSITEIT VAN PRETORIA  
UNIVERSITY OF PRETORIA  
YUNIBESITHI YA PRETORIA

Denkleiers • Leading Minds • Dikgopolo tša Dihlalefi

**Characterization of diesel emissions with respect to semi-volatile organic compounds in South African platinum mines and other confined environments**

By

Genna-Leigh Geldenhuys

Submitted in partial fulfilment of the requirements for the degree  
Master of Chemistry in the Faculty of Natural & Agricultural Sciences

University of Pretoria  
Pretoria  
2014



# Characterization of diesel emissions with respect to semi-volatile organic compounds in South African platinum mines and other confined environments



by  
Genna-Leigh Geldenhuys

Submitted in partial fulfilment of  
the requirements for the degree  
Master of Chemistry in the  
Faculty of Natural & Agricultural  
Sciences

University of Pretoria  
Pretoria  
2014

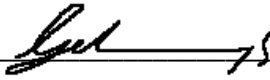


## Summary

Concentrations of diesel particulate matter (DPM) and polycyclic aromatic hydrocarbons (PAHs) in platinum mine environments are likely to be higher than in ambient air due to the use of diesel machinery in confined environments. PAHs may be present in gaseous or particulate phases each of which have different human health impacts due to their ultimate fate in the body. The sampling of both phases was made possible by means of small, portable denuder sampling devices consisting of two polydimethylsiloxane multi-channel traps connected in series and separated by a quartz fibre filter. Thermal desorption coupled with two dimensional gas chromatography with mass spectrometric detection (TD-GCxGC-ToFMS) was employed to analyse samples from three different platinum mines. The underground environments revealed that PAHs were predominantly found in the gaseous phase with naphthalene and mono-methylated derivatives being detected in the highest concentrations ranging from 0.15 – 8.73  $\mu\text{g}\cdot\text{m}^{-3}$ . Similarly higher gas phase PAH loading was found in the Daspoort Tunnel. The particle bound PAHs underground were found in the highest concentrations at the Load Haul Dump (LHD) vehicle exhaust with dominance of fluoranthene and pyrene and concentrations ranged from 0.52-109.60  $\text{ng}\cdot\text{m}^{-3}$ . This work highlighted the need to characterise both gaseous and particulate phases of PAHs in order to assess occupational exposure and demonstrated the successful application of these portable denuders in the mining environment.

## Declaration

I, Genna-Leigh Geldenhuys, declare that the dissertation, which I hereby submit for the degree Master of Chemistry at the University of Pretoria, is my own work and has not previously been submitted by me for a degree at this or any other tertiary institution.



---

Signature: Genna-Leigh Geldenhuys

21.11.2014

---

Date

## Acknowledgements

- First of all I would like to thank my Maker & Savior Jesus Christ for He gave me the strength and wisdom that I needed to complete my Masters degree.
- As the author of this project I would like to thank Impala Platinum Mine for providing me with the opportunity to do my Masters and for generously providing funding for my studies. Thank you specifically to Ref Makaloi (Processing Laboratory Manager) and Silke Burdack (HR) for the roles you played.
- Resources provided by Leco Africa; Microsep and Restek (USA) are gratefully acknowledged. Thanks to the CSIR, Centre for Mining Innovation, particularly Cecilia Pretorius. The Plat Mines are gratefully acknowledged for funding and guided underground sampling visits. Funding provided by the NRF and SASOL is gratefully acknowledged.
- The Germany-South Africa Year of Science programme is acknowledged for funding the ship exhaust project. The University of Rostock and the Helmholtz Zentrum München as well as all participants in the HICE campaign are thanked for providing the opportunity for the ship experiments to be conducted.
- Johan Marx from EroElectronics SA (Pty) Ltd. is thanked for his role in installing the continuous monitoring instrument in the tunnel and also for helping us in the sample and data retrieval from the instrument. The work done by Sifiso Nsibande and as well as the previous team that conducted sampling and traffic counts in the tunnel is also highly appreciated.
- A big thank you to the University of Pretoria Microscopy unit, specifically Antoinette Buys for all of your assistance with the scanning electron microscope.
- I would like to thank Dr Patricia Forbes, my supervisor, from the bottom of my heart for all of her guidance, support and encouragement throughout my studies. You were not only my supervisor but also my friend. Thank you to Prof Egmont Rohwer, my Co-Supervisor, for your valuable insight and for being a kind and approachable Head of the Chemistry Department.
- A very special thanks goes out to Yvette Naudé for always helping me with the instrument (or anything else) even when she had a million other things to do. You are a wonderful, patient person and I will always consider you a friend.
- A sincere thank you to David Masemula for working so hard and taking such pride in your work at all times and all the while with a smile on your face.
- I would like to give a warm thanks to PhD students: Niel Malan & Elize Hanekom for their constant willingness to share their knowledge with me and help me in any way necessary. Thank you for being the lovely and kind people that you are. On the same note I would like to thank my

fellow masters student and friend Sifiso Nsibande for all of his help and for being the provider of comical relief.

- I would like to give a very special thank you to my mom and my dad for being such supportive and loving parents I could not have done this without you and I love you both beyond words. To my beautiful sister and housemate Candice, thank you for your care and love during this stressful time.
- Last but definitely not least I would like to thank my fiancé, Cyle, for being my best friend and the love of my life. You are the buoy who floats my boat and always keeps my head above water.

## List of Abbreviations

1-OHP	1-Hydroxypyrene
8-OHdG	8-Oxo-2'-deoxyguanosine
ACGIH	American Conference of Government Industrial Hygienists
AnQ	Anthraquinone
AOEH	Applied Occupational and Environmental Hygiene
ASE	Accelerated solvent extraction
AZU	Azulene
CIS	Cooled injection system
CSIR	Council for Scientific and Industrial Research
DEE	Diesel exhaust emissions
DPM	Diesel particulate matter
DEP	Diesel exhaust particles
DNA	Deoxyribonucleic acid
EC	Elemental carbon
EDS	Energy dispersive spectrometry
EPA	Environmental Protection Agency
GC-FID	Gas chromatography-Flame ionisation detection
GCxGC-ToFMS	Two dimensional gas chromatography with time-of-flight mass spectrometric detection
GC-MS	Gas chromatography-Mass spectrometry
GDP	Gross domestic product
GFF	Glass fibre filter
HRTEM	High resolution transmission electron microscopy
HSE	Health and safety executive
LHD	Load haul dump
MSHA	Mine Safety and Health Administration
NIOSH	National Institute for Occupational Safety and Health
NIST	National Institute of Standards and Technology
OC	Organic carbon
OEL	Occupational exposure limit
OS	Oxidative stress
PAH	Polycyclic aromatic hydrocarbon
PCA	Principal component analysis
Plat mine	Platinum mine
PM	Particulate matter
PM <sub>2.5</sub>	Particulate matter with diameter ≤ 2.5 micron
PM <sub>10</sub>	Particulate matter with diameter ≤ 10 micron
QFF	Quartz fibre filter
RCD	Respirable combustible dust
ROS	Reactive oxygen species
SA	South Africa
SEM	Scanning electron microscopy
SIMRAC	Safety in Mines Research Advisory Committee
SOF	Soluble organic fraction
SVOC	Semi-volatile organic compound

TD	Thermal desorption
TEM	Transmission electron microscopy
TLV	Threshold limit value
TC	Total carbon
TM3	Trackless mining vehicles
USEPA	United States Environmental Protection Agency
UV	Utility vehicle
VOF	Volatile organic fraction
WHO	World Health Organisation

***PAH names in order of volatility***

NAP	Naphthalene
NAP 2M	2-methyl Naphthalene
NAP 1M	1-methyl Naphthalene
ACY	Acenaphthylene
ACE	Acenaphthene
FLU	Fluorene
1HPHA	1H-Phenylene
PHE	Phenanthrene
ANT	Anthracene
FLA	Fluoranthene
PYR	Pyrene
11HBaF	11H-Benzo[a]fluorene
7HBbF	7H-Benzo[b]fluorene
BghiF	Benzo[ghi]fluoranthene
BaA	Benz[a]anthracene
CHY	Chrysene
BcPHE	Benzo[c]phenanthrene
PER	Perylene
BbF	Benzo[b]fluoranthene
BkF	Benzo[k]fluoranthene
BjF	Benzo[j]fluoranthene
BaP	Benzo[a]pyrene
BeP	Benzo[e]pyrene
I123P	Indeno[1,2,3-cd]pyrene
BghiP	Benzo[ghi]perylene
dBahA	Dibenz[a,h]anthracene

***Sample names***

30MIN A	30 minute ambient sample from Plat mine A mine
30MIN B	30 minute ambient sample from Plat mine B mine
30MIN C	30 minute ambient sample from Plat mine C mine
WS A	Workshop sample from Plat mine A mine
WS B	Workshop sample from Plat mine B mine
WS C	Workshop sample from Plat mine C mine
LHD A	LHD sample from Plat mine A mine
LHD B	LHD sample from Plat mine B mine
LHD C	LHD sample from Plat mine C mine



10MIN A	10 minute ambient sample from Plat mine A mine
10MIN B	10 minute ambient sample from Plat mine B mine
10MIN C	10 minute ambient sample from Plat mine C mine
ND A	Non-diesel sample from Plat mine A mine
ND B	Non-diesel sample from Plat mine B mine

## Table of contents

Summary .....	ii
Declaration.....	iii
Acknowledgements.....	iv
List of Abbreviations .....	vi

### Chapter 1 : Introduction

1.1 The role of the mining industry .....	1
1.2 Polycyclic aromatic hydrocarbons .....	1
1.3 Problem statement .....	3
1.4 Regulatory context.....	5
1.5 Study areas.....	7
1.5.1 Platinum mines .....	7
1.5.2 The Daspoort Tunnel.....	7
1.5.3 HICE Campaign .....	9
1.6 Aim and objectives of the study .....	9
1.7 Hindrance to DPM monitoring in South Africa .....	9
1.8 Justification for the study .....	10
1.9 Research design .....	10
1.10 References .....	11

### Chapter 2 : Literature Review

2.1 Introduction.....	14
2.2 Diesel combustion engine.....	15
2.2.1 Basics of a diesel engine.....	15
2.2.2 Pollutants from diesel exhausts.....	16
2.2.3 Health effects of diesel emissions.....	19

2.2.4	Role of diesel in the mining industry .....	22
2.2.5	The role of diesel in the Daspoort Tunnel.....	26
2.3	Polycyclic aromatic hydrocarbons (PAHs).....	28
2.3.1	PAHs and their sources .....	28
2.3.2	Formation of PAHs .....	28
2.3.3	Properties and environmental fate of PAHs .....	28
2.3.4	Health effects of PAHs .....	33
2.3.5	PAHs which will be investigated in this study.....	36
2.3.6	PAH concentrations in different environments .....	36
2.4	Methods for PAH analysis .....	37
2.4.1	Sampling.....	39
2.4.2	Extraction of PAHs from airborne particles .....	45
2.4.3	Instrumental analysis .....	48
2.4.4	Challenges of analyzing DPM and PAHs.....	53
2.4.5	Microscopy based characterization of particulate matter .....	54
2.5	References.....	58

## **Chapter 3 : Experimental Methods and Optimisation**

3.1	Quality assurance.....	72
3.1.1	Handling .....	72
3.2	Platinum Mine study.....	73
3.2.1	CSIR personal particulate sampling.....	73
3.2.2	Gas and particulate PAH sampling .....	73
3.2.3	Analytical techniques-mine study.....	75
3.3	Daspoort Tunnel study.....	78
3.3.1	Gas phase sampling.....	78
3.3.2	Particulate phase sampling .....	79
3.3.3	Analytical techniques-tunnel study .....	81

3.4	Helmholtz Virtual Institute of Complex Molecular Systems in Environmental Health (HICE) campaign Germany 2012.....	82
3.4.1	Sampling and analysis .....	82
3.5	Method development for platinum mine study.....	84
3.5.1	Analysis of a NIST DPM reference material .....	92
3.6	Method validation-Mine study.....	94
3.6.1	Trap desorption repeatability .....	96
3.6.2	Filter homogeneity.....	97
3.6.3	Effect of the matrix as well as the desorption temperature and source temperature parameters.....	99
3.6.4	Desorption efficiency .....	101
3.6.5	Future validation .....	102
3.6.6	Calibration and linearity study .....	102
3.7	References.....	107

## Chapter 4 : Results and Discussion of Platinum Mine Study

4.1	Introduction.....	108
4.1.1	Sample Identification .....	110
4.1.2	Factors influencing analytical results.....	111
4.1.3	Observations made during the sampling campaign .....	112
4.2	Semi-volatile organic compound profiles expressed in relative % peak areas.....	114
4.3	Compound class profiles per sample expressed in total normalised peak areas.....	119
4.4	PAH profiles expressed as relative % peak areas.....	129
4.5	PAH profiles expressed as total normalized peak areas.....	134
4.6	Sample PAH fingerprints expressed as total normalised peak area for inter-mine comparison.....	138
4.7	Inter-sample comparisons.....	146
4.8	Other source indicators.....	151
4.9	Effectiveness of the denuder sampling device.....	152
4.10	Effect of ambient temperature and humidity.....	154

4.11 Quantification.....	155
4.12 Scanning electron microscopy.....	159
4.13 Principal component analysis.....	162
4.14 Diagnostic ratios.....	164
4.15 Conclusion.....	167
4.16 References.....	171

## **Chapter 5 : Results and Discussion of the Study Involving Other Environments where Diesel Engines are Used**

5.1 Introduction.....	173
5.2 Sample identification.....	173
5.3 Semi-volatile organic compound profiles for Daspoort Tunnel samples expressed as relative % peak areas.....	175
5.4 PAH profiles for Daspoort Tunnel samples expressed in relative % peak areas.....	179
5.5 PAH profiles for Daspoort Tunnel samples expressed in total peak areas.....	182
5.5.1 Gas phase samples.....	182
5.5.2 Particulate phase samples .....	183
5.6 HICE 2012 Campaign: Emissions from ship’s engine using light fuel oil.....	186
5.7 Conclusion.....	188
5.8 References.....	190

## **Chapter 6 : Conclusion**

6.1. Recommendations.....	195
---------------------------	-----

## List of Tables

Table 1-1 Priority PAHs as determined by the Environmental Protection Agency .....	2
Table 1-2 Carcinogenic classification of some PAH compounds according to the IARC monographs on the evaluation of carcinogenic risks to humans .....	4
Table 1-3 Summary of international exposure limits and guidelines pertaining to air concentrations of diesel exhaust particulate matter .....	5
Table 1-4 PAH exposure limits referring to all the PAHs that were found in the samples analysed in this study .....	6
Table 2-1 Comparison of concentrations of PAHs in different environments in $\text{ng.m}^{-3}$ .....	37
Table 3-1 Number and description of samples that were taken underground .....	74
Table 3-2. Sample name abbreviations and corresponding numbers .....	74
Table 3-3 Temperature, humidity, air velocity and sampled volume of each sample .....	75
Table 3-4 Method parameters for the instrumental analysis of the mine samples .....	77
Table 3-5 Description of the gas phase sampling parameters in the Daspoort Tunnel .....	79
Table 3-6 Description of the particulate phase sampling parameters in the Daspoort Tunnel .....	81
Table 3-7 Sample information for filter samples from the ship exhaust during different engine loads using light fuel oil .....	82
Table 3-8 Retention times of PAHs that have the same molecular ions .....	91
Table 3-9 PAHs, nitro PAHs and PAH derivatives that were detected in the NIST 2975 DPM reference material .....	93
Table 3-10 Certified NIST concentrations normalised to pyrene compared to sample results areas normalised to pyrene .....	94
Table 3-11 PAHs thermally desorbed (using the conditions in Table 3-4) from traps and the peak areas of n replicates .....	96
Table 3-12 PAHs thermally desorbed (using the conditions in Table 3-4) from filters and the peak areas of n replicates .....	97
Table 3-13 Coefficients of determination and limits of detection and quantification of PAHs on traps. 104	
Table 3-14 Coefficients of determination and limits of detection and quantification of PAHs on filters .....	105
Table 4-1 Diagnostic ratios of PAHs .....	109
Table 4-2. Sample name abbreviations and corresponding numbers .....	110
Table 4-3 Temperature, humidity, air velocity and sampled volume of each sample .....	111
Table 4-4 PAHs ( $\mu\text{g.m}^{-3}$ ) detected in the primary trap samples .....	155
Table 4-5 PAHs ( $\text{ng.m}^{-3}$ ) detected in the filter samples .....	156
Table 4-6 PAHs ( $\mu\text{g.m}^{-3}$ ) detected in the secondary trap samples .....	157
Table 4-7 Diagnostic ratios of PAHs in the different sample types of the mine samples .....	165
Table 5-1 Sample details for the gas phase sampling of PAHs in the Daspoort Tunnel using PDMS multi-channel (MC22) traps .....	173
Table 5-2 Sample details for the particulate sampling of PAHs in the Daspoort Tunnel using quartz fibre filters .....	174

## List of figures

Figure 1-1 Schematic map of the Bushveld Complex .....	7
Figure 1-2 Entrance to the Daspoort Tunnel (top) and an aerial view of the tunnel on Transoranje road showing surrounding communities (bottom) .....	8
Figure 2-1 The physico-chemical composition and structure of diesel particulate matter (Adapted by Matti Maricq 2007). .....	18
Figure 2-2 Trackless mining vehicles with diesel combustion engines used underground: utility vehicles (A&B), drill rig (C) and a LHD (D) .....	25
Figure 2-3 Daspoort Tunnel entrance (left) and pedestrian path inside the tunnel (right) .....	26
Figure 2-4 Transformation of naphthalene by •OH radical .....	30
Figure 2-5 Transformation of naphthalene by •NO <sub>3</sub> Radical .....	31
Figure 2-6 Transformation of benzo(a)pyrene by ozone .....	32
Figure 2-7 Schematic diagram of a denuder consisting of multi-channel silicone rubber traps and a quartz fibre filter .....	44
Figure 2-8 Total ion chromatogram showing the expected area for PAH elution .....	50
Figure 2-9 Representative SEM image of a carbonaceous particle agglomerate .....	57
Figure 3-1 Sampling setup used for the collection of semi-volatile organic compounds .....	73
Figure 3-2 A: Instrumental setup, showing GC-MS fitted with a Gerstel thermal desorber, B: TD system, C: PDMS trap to be inserted into the TD, D: filter placed in glass tube to be inserted into the TD .....	76
Figure 3-3 Photographs of swab samples and positions in the tunnel (573 m in length) where swab samples were taken (where TS = tunnel swab as defined in table 3.6) .....	80
Figure 3-4 Sampling setup for particulate samples for the HICE campaign .....	83
Figure 3-5 Sampling setup for particulate and gas phase PAH samples for the HICE campaign .....	83
Figure 3-6 Reconstructed ion 1D chromatogram of a 10 ng PAH mix standard for PAH masses (128, 142, 152, 154, 166, 178, 202, 228, 252, 276 & 278 Da) .....	86
Figure 3-7 Reconstructed ion 2D chromatogram of a 5 ng PAH mix standard for PAH masses (128, 142, 152, 154, 166, 178, 202, 228, 252, 276 & 278 Da) .....	86
Figure 3-8 Reconstructed 2D ion chromatograms of pure PAH standards for masses 178, 202, 228, 252 Da .....	87
Figure 3-9 Reconstructed 2D ion chromatograms of pure PAH standards for masses 178, 202, 228, 252 Da .....	88
Figure 3-10 Reconstructed 2D chromatogram of heavier PAHs in a 5ng standard. 252 mass was extracted. ....	89
Figure 3-11 Reconstructed 2D chromatogram showing the optimised separation of indeno(1,2,3-cd)pyrene and benzo(ghi)perylene in 2D GCxGC-ToFMS from a 5 ng standard .....	90
Figure 3-12 Reconstructed 2D chromatogram showing the optimised separation dibenz(a,h)anthracene in 2D GCxGC-ToFMS from a 5 ng standard chromatogram of PAHs in a 5ng standard .....	90
Figure 3-13 A: Tools used to punch filter sample, B: CSIR loaded filter which has been punched four times .....	98
Figure 3-14 Particulate sampling setup using 32 mm SKC cassettes .....	99
Figure 3-15 Absolute peak area of D-pyrene from spiked filters including: clean blank filter, loaded filter (analysed by method described in Section 3.2.3), loaded filter that was thermally desorbed (TD) at 300 °C (ST at 200 °C) as well a loaded filter that was analysed with a source temperature (ST) of 280°C (TD at 300 °C) (n=2). ....	101

Figure 3-16 PAH ion extracted chromatograms of a loaded trap sample (taken from the workshop at Plat mine B) after first (top chromatogram) and second (bottom chromatogram) desorption of the same trap.....	101
Figure 3-17 Calibration curves for naphthalene (top) and pyrene (bottom) from the PDMS traps across the range 0.1-10 ng.m <sup>-3</sup> .....	104
Figure 3-18 Calibration curves for benzo(k)fluoranthene (top) and benzo(a)pyrene (bottom) from filters across the range 0.001-1.0 ng.m <sup>-3</sup> .....	106
Figure 4-1 LHD vehicle used underground showing the size of the diesel powered engine next to a mine worker .....	113
Figure 4-2 Relative % peak areas of SVOC classes found in primary trap samples .....	114
Figure 4-3 Relative % peak areas of SVOC classes found in filter samples .....	116
Figure 4-4 Relative % peak areas of SVOC classes found in secondary trap samples .....	118
Figure 4-5 Composition of SVOCs from primary traps for 30 minute ambient diesel shaft samples.....	119
Figure 4-6 Composition of SVOCs from filters for 30 minute ambient diesel shaft samples .....	120
Figure 4-7 Composition of SVOCs from secondary traps for 30 minute ambient diesel shaft samples...	120
Figure 4-8 Composition of SVOCs from primary traps for LHD diesel shaft samples .....	122
Figure 4-9 Composition of SVOCs from filters for LHD diesel shaft samples.....	122
Figure 4-10 Composition of SVOCs from secondary traps for LHD diesel shaft samples .....	123
Figure 4-11 Composition of SVOCs from primary traps for workshop diesel shaft samples.....	124
Figure 4-12 Composition of SVOCs from filters for workshop diesel shaft samples .....	125
Figure 4-13 Composition of SVOCs from secondary traps for workshop diesel shaft samples.....	125
Figure 4-14 Composition of SVOCs from primary traps for ambient 10 minute non-diesel shaft samples .....	127
Figure 4-15 Composition of SVOCs from filters for ambient 10 minute non-diesel shaft samples.....	127
Figure 4-16 Composition of SVOCs from secondary traps for ambient 10 minute non-diesel shaft samples .....	128
Figure 4-17 A: Relative % peak areas of PAHs from the primary trap samples excluding sample # 14	
Figure 4-17 B: (insert) Relative % peak areas of PAHs from the primary trap samples including sample # 14 .....	130
Figure 4-18 Relative % peak areas of PAHs from the filter samples.....	131
Figure 4-19 Relative % peak areas of PAHs from the secondary trap samples .....	132
Figure 4-20 Total peak areas of PAHs from the primary trap samples.....	135
Figure 4-21 Total peak areas of PAHs from the filter samples .....	135
Figure 4-22 Total peak areas of PAHs from the secondary trap samples.....	136
Figure 4-23 Peak areas of PAHs detected in 30 minute ambient samples from primary traps. ....	138
Figure 4-24 Peak areas of PAHs detected in LHD exhaust samples from primary traps. ....	138
Figure 4-25 Peak area of PAHs detected in workshop samples from primary traps. ....	139
Figure 4-26 Peak area of PAHs detected in non-diesel samples from primary traps. ....	139
Figure 4-27 Peak areas of PAHs detected in 30 minute ambient samples from filters. ....	141
Figure 4-28 Peak areas of PAHs detected in LHD exhaust samples from filters.....	141
Figure 4-29 Peak areas of PAHs detected in workshop samples from filters. ....	141
Figure 4-30 Peak areas of PAHs detected in 10 minute ambient samples from filters. ....	142
Figure 4-31 Peak areas of PAHs detected in 30 minute ambient samples from secondary traps.....	143
Figure 4-32 Peak areas of PAHs detected in LHD exhaust samples from secondary traps. ....	144
Figure 4-33 Peak areas of PAHs detected in workshop samples from secondary traps. ....	144
Figure 4-34 Peak areas of PAHs detected in non-diesel samples from secondary traps.....	145
Figure 4-35 Peak areas of PAHs detected in 10 minute ambient samples from secondary traps.....	145
Figure 4-36 Comparison of LHD and 30 minute ambient primary trap samples.....	146



Figure 4-37 Comparison of LHD and 30 minute ambient filter samples .....	147
Figure 4-38 Comparison of the 10 minute and 30 minute ambient primary trap samples.....	147
Figure 4-39 Comparison of the 10 minute and 30 minute ambient filter samples .....	148
Figure 4-40 Comparison of the workshop and 10 minute ambient primary trap samples .....	148
Figure 4-41 Comparison of the workshop and 10 minute ambient filter samples.....	149
Figure 4-42 Comparison of the workshop and non-diesel ambient primary trap samples.....	149
Figure 4-43 Comparison of the workshop and non-diesel ambient filter samples .....	150
Figure 4-44 Total PAH peak area detected from each denuder component.....	152
Figure 4-45 PAH peak areas for different sample types from the different sampling media .....	153
Figure 4-46 Total particulate phase PAH peak areas per litre of air sampled with corresponding ambient temperature readings at each sampling site (filter samples) .....	154
Figure 4-47 Total gas phase PAH peak areas per litre of air sampled with corresponding ambient temperature readings at each sampling site (primary trap samples) .....	154
Figure 4-48 Plat mine A filter sample from a LHD operator at 800, 1400 & 7500 magnifications. ....	159
Figure 4-49 Plat mine B filter sample from a LHD operator at 800, 1500 & 6000 magnifications. ....	159
Figure 4-50 Plat mine C filter sample from a LHD operator at 800, 1500 & 10 000 magnifications. ....	159
Figure 4-51 102(Plat mine C) filter sample from a winch operator at 800, 1500 & 7500 magnifications. ....	160
Figure 4-52 105 (Plat mine B) filter sample from a winch operator at 220 & 800 magnifications. ....	160
Figure 4-53 Blank filter samples at 2500, 7500 & 9000 magnifications. ....	160
Figure 4-54 Score plot (left) and loading plot (right) resulting from PCA on samples with different sampling times: 10 minute and 30 minute ambient samples (with F; P; S denoting filter, primary trap and secondary trap respectively).....	163
Figure 4-55 Score plot (left) and loading plot (right) resulting from PCA on samples with different sampling sites: 10 minute ambient and LHD samples (with F; P; S denoting filter, primary trap and secondary trap respectively).....	164
Figure 5-1 Vehicle count in the Daspoort Tunnel .....	174
Figure 5-2 Relative % peak area SVOC profile of trap samples (gas phase) from the Daspoort Tunnel ..	175
Figure 5-3 Relative % peak area SVOC profile of filter samples from the Daspoort Tunnel where the blue box groups the denuder filters and the red box groups the swab samples. ....	177
Figure 5-4 Relative % peak area PAH profile for trap samples (gas phase) from the Daspoort Tunnel ...	179
Figure 5-5 Relative % peak area PAH profile for filter samples (particulate phase) from the Daspoort Tunnel where the blue box groups the swab samples. ....	180
Figure 5-6 Sum of all PAH peak areas detected in the Daspoort Tunnel trap samples .....	182
Figure 5-7 Sum of all PAH peak areas detected in the Daspoort Tunnel for all particulate samples .....	183
Figure 5-8 PAH peak areas detected in the denuder filter samples .....	184
Figure 5-9 Sum of all PAH peak areas detected in the swab filter samples.....	185
Figure 5-10 Sum of all PAH peak areas detected in the weekly filter samples.....	185
Figure 5-11 Relative % peak area of PAHs from a ship engine exhaust at different operating loads with LFO. ....	187
Figure 5-12 Number and relative % peak areas of detected PAHs from a ship engine exhaust emissions at different operating loads .....	188

## 1. Introduction

### 1.1 The role of the mining industry

South Africa (SA) is a developing country in which the mining sector contributes immensely to the country's revenue. SA is one of the world's leaders in diamond, gold, coal and base metal production and it is the largest producer of platinum. SA holds the world's largest natural reserves of gold and platinum group metals (platinum, palladium, rhodium, ruthenium, iridium and osmium). The platinum group metals mining industry generated R84 billion in sales, and was responsible for 36 % of the country's mining exports in 2011 (Chamber of Mines 2012a).

South African mining companies play a key role in the global industry in that the mining sector uses considerable services and inputs from the domestic economy which is crucial for direct and indirect job creation. Not only does the mining sector use local services and products from other domestic industries or businesses but it also supplies many related industries with mining products or by-products. According to the Chamber of Mines of South Africa (Chamber of Mines 2012b), the mining industry contributed 8.8 % directly and 18 % indirectly to the country's gross domestic product (GDP) in 2011 and in the past decade has contributed R1.9 trillion to both the country's GDP and export earnings.


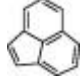
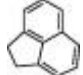
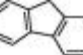
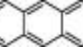
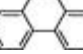
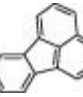

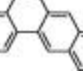


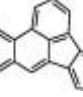
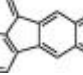

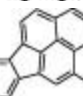
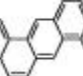
The mining process involves the use of diesel combustion engines for a number of underground operations. Combustion emissions contribute to ambient particulate and gaseous air pollutant levels, including those of semi-volatile organic compounds (SVOCs) and polycyclic aromatic hydrocarbons (PAHs). Exposure to these compounds are a cause for concern from a human health perspective (Lewtas 2007 & Ristovski *et al.* 2012).

### 1.2 Polycyclic aromatic hydrocarbons

PAHs are formed mainly as a result of incomplete combustion of organic material. The anthropogenic sources of PAHs include road traffic, wood fires and combustion of fossil fuels from industries. PAHs, by definition, contain only hydrogen and carbon atoms in the form of fused benzene rings which can be arranged linearly or in clustered and angular arrangements. However, derivatives of PAHs are also common where nitrogen, sulphur, oxygen, and other alkyl groups may be found attached to the benzene rings to form heterocyclic aromatic compounds (Lundstedt 2003). PAHs may be formed by pyrolysis of higher alkanes (found in fuel and plant materials) which can be envisioned as the "cracking"

of organic compounds resulting in smaller and significantly less stable molecules and radicals which condense and react to form PAHs. A list of common PAHs and their corresponding structures are included in Table 1-1 (US EPA 2013).

**Table 1-1 Priority PAHs as determined by the Environmental Protection Agency (US EPA 2013)**

Name	Abbr.	Formula	CAS no	Number of rings	MW (g.mol <sup>-1</sup> )	
Naphthalene	NAP	C <sub>10</sub> H <sub>8</sub>	91-20-3	2	128	
Acenaphthylene	ACY	C <sub>12</sub> H <sub>8</sub>	208-96-8	3	152	
Acenaphthene	ACE	C <sub>12</sub> H <sub>10</sub>	83-32-9	3	154	
Fluorene	FLU	C <sub>13</sub> H <sub>10</sub>	86-73-7	3	166	
Anthracene	ANT	C <sub>14</sub> H <sub>10</sub>	120-12-7	3	178	
Phenanthrene	PHE	C <sub>14</sub> H <sub>10</sub>	85-01-8	3	178	
Fluoranthene	FLA	C <sub>16</sub> H <sub>10</sub>	206-44-0	4	202	
Pyrene	PYR	C <sub>16</sub> H <sub>10</sub>	129-00-0	4	202	
Benzo(a)anthracene	BaA	C <sub>18</sub> H <sub>12</sub>	56-55-3	4	228	
Chrysene	CHY	C <sub>18</sub> H <sub>12</sub>	218-01-9	4	228	
Benzo(a)pyrene	BaP	C <sub>20</sub> H <sub>12</sub>	50-32-8	5	252	
Benzo(b)fluoranthene	BbF	C <sub>20</sub> H <sub>12</sub>	205-99-2	5	252	
Benzo(k)fluoranthene	BkF	C <sub>20</sub> H <sub>12</sub>	207-08-9	5	252	
Benzo(ghi)perylene	BghiP	C <sub>22</sub> H <sub>12</sub>	191-24-2	6	276	
Indeno[1,2,3-cd]pyrene	I123cdP	C <sub>22</sub> H <sub>12</sub>	193-39-5	6	276	
Dibenz(a,h)anthracene	dBahA	C <sub>22</sub> H <sub>14</sub>	53-70-3	6	278	

The atmospheric fate of PAHs is strongly dependent on the phase distribution of the PAH, i.e. whether it is associated with particles or if it is present in the gaseous form. Lighter PAHs tend to be present largely in the gas phase and less associated with particulate matter than the heavier PAHs under the same conditions (Vione *et al.* 2004).

Although particle-associated PAHs can undergo photolysis in the atmosphere, they are inclined to remain with the particle and be inhaled into the lungs while the gaseous PAHs tend to undergo photochemical reactions with radicals in the atmosphere (Vione *et al.* 2004).

Transformation of gas phase PAHs into polar derivatives, which are less volatile and potentially more toxic, occur via atmospheric photochemical reactions which are important as they define the atmospheric lifetime of the PAHs (Vione *et al.* 2004). Radiation from the sun can result in the formation of ozone ( $O_3$ ), hydroxyl ( $\bullet OH$ ) and nitrate ( $\bullet NO_3$ ) radicals which then can react with PAHs to form a wide range of derivatives (refer to Section 2.3.3 for reaction mechanisms). PAHs can also absorb light which can induce photoreactions such as photo-dimerisation and photo-oxidation. Photo-oxidation occurs upon irradiation of compounds in the presence of oxygen and it leads to the formation of oxy-PAHs (Vione *et al.* 2004). These reactions and transformations are expected to occur less in underground environments than in ambient environments due to the shafts being deep underground where there is no radiation present from the sun and lighting is minimal.

### 1.3 Problem statement

The wide use of mobile and stationary diesel machinery underground poses a risk to the health and safety of mine employees due to exposure to diesel exhaust emissions (DEE) which, as a whole was classified as being carcinogenic to humans (Group 1) by the International Agency for Research on Cancer (IARC) which forms part of the World Health Organization (IARC 2012, 2013). Evidence reveals that exposure is associated with an increased risk of lung cancer as well as other health complications such as respiratory and cardiovascular diseases (Lewtas 2007). The same problem also arises in the Daspoort Tunnel where a confined environment is polluted with diesel emissions from traffic which may have negative health impacts on pedestrians and cyclists commuting in the tunnel.

The organic carbon (OC) fraction of diesel particulate matter (DPM) from diesel emissions contains trace concentrations of polycyclic aromatic hydrocarbons (PAHs) which are semi-volatile organic compounds (Ono-Ogasawara & Smith 2004). It is of vital importance to study the organic species in particulate

matter, particularly PAHs, because they are ubiquitous and include several potent carcinogens (Bates *et al.* 2008). Environment induced cancer, cardiovascular disease as well as adverse reproductive effects have all been associated with electrophilic PAH compounds (see Table 1-2) (Lewtas 2007). Carcinogenicity of each PAH has been examined and benzo(a)pyrene is considered as one of the most carcinogenic PAHs hence its use as an environmental PAH exposure indicator (Ono-Ogasawara & Smith 2004).

This study will provide information regarding DPM characterization and PAH fingerprinting in large platinum mines as well as the Daspoort Tunnel in South Africa. The two types of confined environments (underground & tunnel) will be compared with more emphasis on the mining environments as it was the core focus of this study.

**Table 1-2 Carcinogenic classification of some PAH compounds according to the IARC monographs on the evaluation of carcinogenic risks to humans (IARC 2002, IARC 2010)**

Benzo[a]pyrene	1	carcinogenic to humans
Dibenzo[a,h]anthracene	2A	probably carcinogenic to humans
Benzo[a]anthracene	2B	possibly carcinogenic to humans
Benzo[k]fluoranthene	2B	possibly carcinogenic to humans
Chrysene	2B	possibly carcinogenic to humans
Indeno[1,2,3-cd]pyrene	2B	possibly carcinogenic to humans
Naphthalene	2B	possibly carcinogenic to humans
Acenaphthene	3	not classifiable as to its carcinogenicity to humans
Anthracene	3	not classifiable as to its carcinogenicity to humans
Benzo[b]fluoranthene	3	not classifiable as to its carcinogenicity to humans
Benzo[ghi]perylene	3	not classifiable as to its carcinogenicity to humans
Benzo[e]pyrene	3	not classifiable as to its carcinogenicity to humans
Fluoranthene	3	not classifiable as to its carcinogenicity to humans
Phenanthrene	3	not classifiable as to its carcinogenicity to humans
Pyrene	3	not classifiable as to its carcinogenicity to humans

## 1.4 Regulatory context

Limited data is currently available for DPM and PAH exposure in underground mines in South Africa. The lack of regulatory exposure limits for DPM and PAHs in South Africa makes it difficult for the mining industry to evaluate potential exposure effectively.

**Table 1-3 Summary of international exposure limits and guidelines pertaining to air concentrations of diesel exhaust particulate matter (Van Niekerk *et al.* 2002).**

Agency / Committee / Regulator	Date submitted	Exposure guideline/limit	Substance measured
Canadian ad hoc Diesel Committee	1990	1.50 mg.m <sup>-3</sup>	RCD
MSHA	2001	0.40 mg.m <sup>-3</sup>	TC
MSHA	2006	0.16 mg.m <sup>-3</sup>	TC
ACGIH	1996	0.15 mg.m <sup>-3</sup>	TC
ACGIH	1998	0.05 mg.m <sup>-3</sup>	TC
ACGIH	2001	0.02 mg.m <sup>-3</sup>	EC
Germany: General occupational environ.	1997	0.10 mg.m <sup>-3</sup>	EC
Germany: Underground non-coal mining	1997	0.30 mg.m <sup>-3</sup>	EC
Switzerland (road tunnels)	2001	0.20 mg.m <sup>-3</sup>	TC
NIOSH	2002	0.16 mg.m <sup>-3</sup>	EC

MSHA	- Mine Safety and Health Administration, United States of America
NIOSH	- National Institute for Occupational Safety and Health, United States of America
TC	- Total carbon
RCD	- Respirable combustible dust
ACGIH	- American Conference of Governmental Industrial Hygienists
EC	- Elemental carbon

The DPM in SA is currently monitored through the determination of the elemental carbon (EC) and organic carbon (OC) content by the National Institute for Occupational Safety and Health (NIOSH) 5040 method which is based on a gravimetric analysis whereby the mass of the EC and OC is extrapolated from data obtained by thermal optical analysis. The American Conference of Governmental Industrial Hygienists (ACGIH) limits are typically adopted by countries with no existing exposure limits (EL) where total carbon (TC) is regulated. The DPM limits proposed by ACGIH as well as other internationally proposed exposure limits can be seen in Table 1-3.

The Mining Occupational Health Advisory Committee (MOHAC) submission to the Mining Health and Safety Council (MHSC) recommends the introduction of an interim DPM exposure control value in South

Africa and gradually lowering this exposure control value by means of a “phased-in” approach as follows:

- ▶ January 2013 to December 2013 = 0.350 mg.m<sup>-3</sup> (TC)
- ▶ January 2014 to December 2014 = 0.250 mg.m<sup>-3</sup> (TC)
- ▶ January 2015 to December 2015 = 0.200 mg.m<sup>-3</sup> (TC)

The goal is to achieve less than 0.160 mg.m<sup>-3</sup> TC by January 2016 in trackless mines (Chamber of Mines 2012c).

Having seen in Table 1-2 that many PAHs have been classified as potential carcinogens, it sparks concern that these compounds are not readily regulated. Table 1-4 indicates the few PAHs that are being regulated and their corresponding exposure limits put forward by different agencies. NIOSH regulates two PAH compounds while the Occupational Safety and Health Administration (OSHA), an American agency, regulates five PAH compounds and the ACGIH regulates one PAH compound (NIOSH 1994). The ACGIH limits are typically adopted by countries such as South Africa who do not possess their own limits, which in this case would infer that only naphthalene has a regulated exposure limit of 10 ppm.

**Table 1-4 PAH exposure limits referring to all the PAHs that were found in the samples analysed in this study (OSHA Table Z-1 viewed 10 August 2013)**

PAH	Exposure limits		
	OSHA	NIOSH	ACGIH
acenaphthene	-	-	-
acenaphthylene	-	-	-
anthracene	0.2 mg.m <sup>-3</sup>	-	-
benz[a]anthracene	-	-	-
benzo[b]fluoranthene	-	-	-
benzo[k]fluoranthene	-	-	-
benzo[ghi]perylene	-	-	-
benzo[a]pyrene	0.2 mg.m <sup>-3</sup>	0.1 mg.m <sup>-3</sup>	-
benzo[e]pyrene	-	-	-
chrysene	0.2 mg.m <sup>-3</sup>	-	-
dibenz[a,h]anthracene	-	-	-
fluoranthene	-	-	-
fluorene	-	-	-
indeno[1,2,3-cd]pyrene	-	-	-
naphthalene	10 ppm	10 ppm	10 ppm
phenanthrene	0.2 mg.m <sup>-3</sup>	-	-
pyrene	-	-	-

## 1.5 Study areas

### 1.5.1 Platinum mines

Three platinum mines were focused on in this research. All three of the mines are situated on the western limb of the platinum belt (Bushveld Igneous Complex) in the North West province of South Africa (Fig. 1-1) and are all currently trading on the Johannesburg Stock Exchange. The mines will not be referred to by name in this report as the results are confidential.

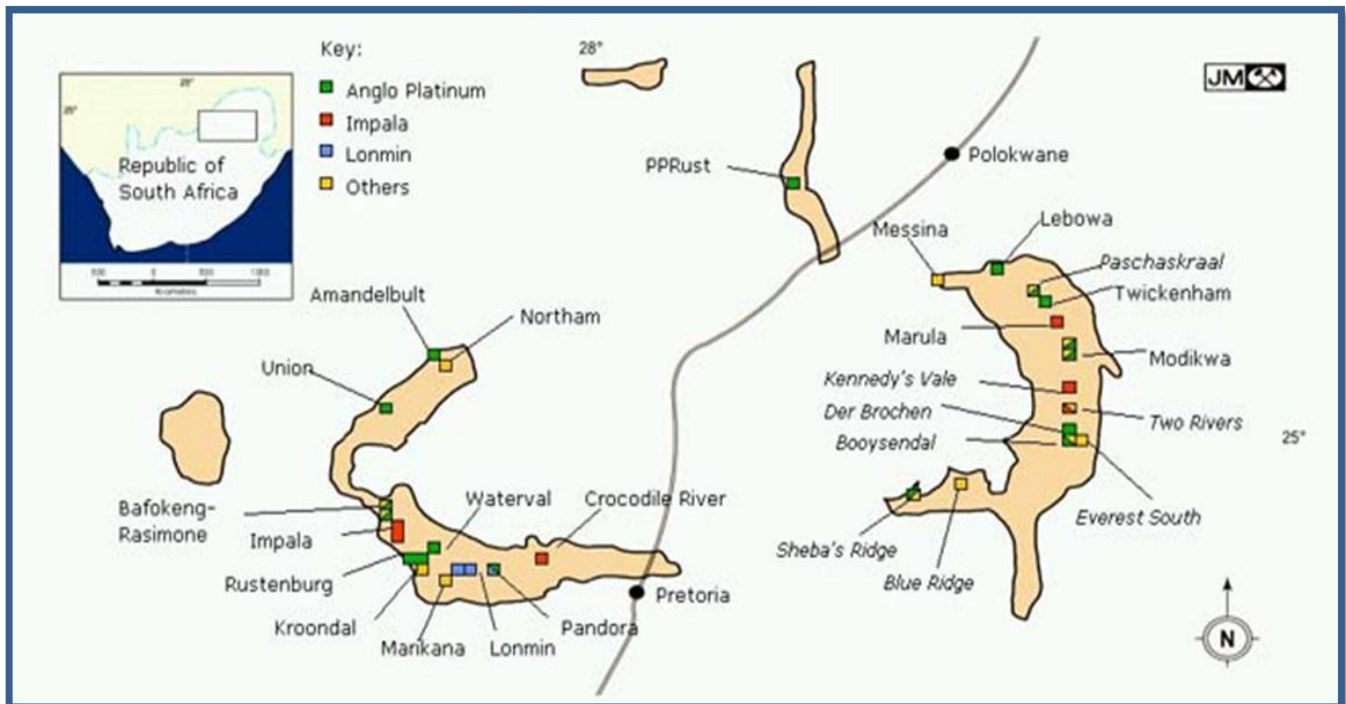


Figure 1-1 Schematic map of the Bushveld Complex (Bushveld Igneous Complex n.d)

### 1.5.2 The Daspoort Tunnel

An initial study of the concentrations of suspended particulate matter in the Daspoort Tunnel in Pretoria was undertaken in 2011 and it indicated that PM levels were of concern (Forbes *et al.* 2011). A particulate monitor was thus installed in the tunnel during February 2012 which captured data on PM concentrations every 10 minutes for a 6 week period.

It was important to characterise the nature of the PM from the tunnel in order to make informed decisions in as far as human health and environmental wellbeing is concerned.





Figure 1-2 Entrance to the Daspoort Tunnel (top) (Photographed by P. Forbes) and an aerial view of the tunnel on Transoranje road showing surrounding communities (bottom) (Transoranje Road, Pretoria, retrieved on May, 2012 from website <https://maps.google.com>).

The tunnel has a length of 573 m and it was constructed between the 1960's and 1970's. The tunnel consists of two traffic lanes and two footpaths. The tunnel provides a convenient link between the north of Pretoria and the central business district therefore commuters (adults, schoolchildren, cyclists) pass through the tunnel on a daily basis.

There is an exhaust ventilation system in place which was estimated to function efficiently for up to approximately 6000 cars. However since a 1974 study which concluded that the pollution concentrations did not present a hazard to pedestrians or motorists, the traffic has increased significantly and the maintenance of the ventilation system has not been up to standard (Wright *et al.* 2011). It is for these reasons that an initial study was conducted in 2011.

### 1.5.3 HICE Campaign

Sampling was carried out at the University of Rostock in Germany during the month of November in association with the 2012 Helmholtz Virtual Institute of Complex Molecular Systems in Environmental Health (HICE) sampling campaign where aerosol emissions from a ship diesel engine exhaust were sampled.

## 1.6 Aim and objectives of the study

The aim of the research conducted was to test the application of a novel portable denuder sampling device for underground environments and use the results to conduct a preliminary survey to evaluate exhaust emissions from different areas (from different mines) in shafts where diesel engines are used, as well as those where diesel engines are not used. Multi-channel silicone rubber traps were used in a denuder configuration to trap SVOCs, including PAHs, in gas and particle phases and the results were analysed using TD-GCxGC-ToFMS (Forbes *et al.* 2009 & 2012). The PAH emission profiles from different areas were compared as were the PAH fingerprints in both gaseous and particulate phases. Experimental detail is included in Chapter 3. The emission profiles from underground environments were compared to emission profiles from within the Daspoort Tunnel which are discussed in Chapter 5. This work highlights the need to establish occupational exposure limits (OELs) in South African regulations for PAHs existing in both gaseous and particulate phases.

## 1.7 Hindrance to DPM monitoring in South Africa

Several international agencies have imposed limits for DPM but these limits have been developed in countries where higher quality diesel fuel with low sulphur content is being used as well as the latest generation diesel engines (Tier 4+) with superior after treatment technologies. A constraint faced by the South African mining industry is the poor quality of fuel available in South Africa, which in turn limits the use of diesel engines with better fuel combustion and reduced emissions (Venter 2008).

The NIOSH 5040 method currently measures the OC content of DPM gravimetrically which is limited as it only accounts for particulate phase compounds with low volatility whereas PAHs are found in both gas and particulate phases with a wide range of volatility.

The analysis of semi-volatile organic compounds (including PAHs) found in DPM is difficult due to stringent sampling procedures that need to be followed preventing blow off of particle adsorbed

analytes as well as the possibility of adsorption of gas phase analytes onto the particles during sampling, which would lead to an erroneous estimation of impact and exposure. The instrumentation needed for this type of monitoring is also typically limited and is unsuitable for underground sampling environments.

## 1.8 Justification for the study

It is of vital importance to study the organic species in particulate matter, particularly PAHs, because they are ubiquitous and include several potent carcinogens (Bates *et al.* 2008). More so, it is imperative to be able to qualify the relative contributions of gas and particulate phase PAHs as they may have different environmental and health impacts i.e. deposition and uptake of inhaled toxic species in the human respiratory system depends on phase distribution (Temime-Roussel *et al.* 2004). PAH emissions are likely to be higher in confined environments such as road tunnels and in underground mining shafts both of which have diesel exhaust emissions as a potential source of PAHs.

## 1.9 Research design

Three participating underground platinum mines were involved in this study. Samples were taken from different mining environments in shafts that use trackless mining methods (use of diesel vehicles) and from a shaft that uses conventional track mining methods (no diesel vehicles). Multi-channel silicone rubber traps were used in a denuder configuration to trap PAHs in gas and particle phases. The type of samples was kept consistent for each different mine to allow for direct comparison and each denuder sample resulted in three separate samples representing the primary trap, the filter and the secondary trap. The three mines were visited over a period of 5 full days (not consecutively) during morning shifts to complete the sampling set. Samples were taken at a height to mimic a normal breathing environment. Denuders were disassembled and each individual component was analysed using TD-GCxGC-ToFMS.

## 1.10 References

- Bates, M., Bruno, P., Caputi, M., Caselli, M., de Gennaro, G. & Tutino, M. 2008, "Analysis of Polycyclic aromatic hydrocarbons (PAHs) in air borne particles by direct sample introduction thermal desorption GC/MS", *Atmospheric Environment*, vol. 42. pp. 6144-6151.
- Chamber of Mines of South Africa. 2012a, *Annual report 2012*.
- Chamber of Mines of South Africa. 2012b, *Facts and Figures 2012*.
- Chamber of Mines of South Africa. 2012c, "Diesel particulate matter position paper", OH&SPC circular, No. 58/12.
- Diesel emissions evaluation programme (DEEP). 2001, "Sampling for diesel particulate matter in mines", *CANMET: Mining and mineral science laboratories*, report (MMSL) 01-052
- Forbes, P.B.C. & Rohwer, E.R. 2009, "Investigations into a novel method for atmospheric polycyclic aromatic hydrocarbon monitoring", *Environmental Pollution*, vol. 157, no. 8-9, pp. 2529-2535.
- Forbes, P.B.C., Garland, R.M., Wright, C.Y., Louw, W., L. Phiri, L., Gawler, N., Mabe, M., Molisiwa, J. and Brown, J. 2011, "Air quality measurements in the Daspoort Tunnel, Pretoria", *National Air Quality Officers News*, July-September, pp. 11-13.
- Forbes, P.B.C., Karg, E.W., Zimmermann, R. & Rohwer, E.R. 2012, "The use of multi-channel silicone rubber traps as denuders for polycyclic aromatic hydrocarbons", *Analytica Chimica Acta*, vol. 730, pp. 71-79.
- IARC. 2002, "Overall Evaluations of Carcinogenicity to Humans", *International Association for Research on Cancer Monographs Series*, vol. 1-74.
- IARC. 2010, "Some Non-heterocyclic Polycyclic Aromatic Hydrocarbons and Some Related Exposures", *International Association for Research on Cancer Monographs Series*, vol. 92.
- IARC. 2012, Diesel engine exhaust carcinogenic 2012a, Press Release no. 213.

- IARC. 2013, Agents Classified by the IARC Monographs, vol 1-108, viewed 27 August 2013, <<http://monographs.iarc.fr/ENG/Classification/index.php>>.
- Lewtas, J. 2007, "Air pollution combustion emissions: Characterization of causative agents and mechanisms associated with cancer, reproductive, and cardiovascular effects", *Mutation Research - Reviews in Mutation Research*, vol. 636, no. 1-3, pp. 95-133.
- Lundstedt, S. 2003, *Analysis of PAHs and their transformation products in contaminated soil and remedial processes*, PhD, University of Umea, Sweden.
- OSHA Permissible Exposure Limits (PELS) from 29 CFR 1910.1000 Z-1 Annotated Table Z-1, U.S. Department of Labor, Occupational Safety & Health Administration, Washington, DC, U.S.A. viewed 10 August 2013 <<https://www.osha.gov/dsg/annotated-pels/tablez-1.html>>.
- Ono-Ogasawara, M. & Smith, T.J. 2004, "Diesel exhaust particles in the work environment and their analysis", *Industrial Health*, vol. 42, no. 4, pp. 389-399.
- Ristovski, Z.D., Miljevic, B., Surawski, N.C., Morawska, L., Fong, K.M., Goh, F. & Yang, I.A. 2012, "Respiratory health effects of diesel particulate matter", *Respirology*, vol. 17, no. 2, pp. 201-212.
- Schematic map of the Bushveld Complex, n.d.* Available from: <<http://www.globalhealthaction.net/index.php/gha/rt/printerFriendly/19520/html>> [5 April 2013]
- Temime-Roussel, B., Monod A., Massiani C. & Wortham H., 2004, "Evaluation of an annular denuder tubes for atmospheric PAH partitioning studies—1: evaluation of the trapping efficiency of gaseous PAHs", *Atmospheric Environment*, vol. 38, pp. 1913-1924.
- US EPA. 2013, List of priority pollutants, U.S. Environmental Protection Agency, viewed 13 February 2013, <<http://water.epa.gov/scitech/methods/cwa/pollutants.cfm>>
- Van Niekerk, W., Simpson, D., Fourie, M. & Mouton, G. 2002, "Diesel particulate emission in the South African mining industry", *Safety In Mine Research Advisory Committee*, no. SIM 020602, pp. 1-49.

Venter, I. 2008, "South Africa must introduce new emissions standards by 2012", *Toyota asserts*, 14 November 2008, viewed 27 June 2012, <<http://www.engineeringnews.co.za/article/south-africa-must-introduce-new-emissions-standards-by-2012-toyota-asserts-2008-11-14>>

Vione, D., Barra, S., de Gennaro, G., de Rienzo, M., Gilardoni, S., Perrone, M.G., & Pozzoli, L. 2004, "Polycyclic aromatic hydrocarbons in the atmosphere: monitoring, sources, sinks and fate" *Annali di Chimica*, vol 94, pp. 17-32

Wright, C., Garland, R. & Forbes, P. 2011, "Air Quality in the Daspoort Tunnel: a multidisciplinary, multi-institution collaboration" *Quest*, vol. 7(3), pp. 32-34.

## 2 Literature Review

### 2.1 Introduction

Atmospheric particles represent a critical component of the atmosphere which have an impact on both the environment as well as human health (Pöschl 2005). Diesel exhaust is a mixture of gaseous and particulate substances originating from unburnt fuel, lubricant oil and combustion products therefore contributing to air pollution caused by airborne particulates (Ono-Ogasawara & Smith 2004). Diesel engines are widely used in industries, for transportation, mining, construction and many others as they efficiently produce high power.

Occupational exposure to diesel engine exhaust (DEE) has been of great concern as the particles from these emissions contain toxic components. These contaminants may, at times, be present in high concentrations especially in confined work environments with inadequate ventilation. Literature suggests that there are a variety of health effects linked to Diesel Particulate Matter (DPM) exposures, such as lung cancer, heart disease and asthma in children (for example: Laumbach & Kipen 2012, Lewtas 2007, Metz 2004, Ristovski *et al.* 2012). The main constituents of DPM are elemental carbon (EC) and organic carbon (OC). The elemental carbon fraction has been widely researched, however the OC fraction, due to the difficulty of sampling and analysis, is far less researched. The OC fraction contains trace concentrations of polycyclic aromatic hydrocarbons (PAHs) and their methylated, nitrated and oxygenated derivatives (Ono-Ogasawara & Smith 2004). Emphasis was given to PAHs in this study, which is initiated with a literature review. The review will give a brief description as to the origin of PAH formation, specifically from diesel combustion engines, description of PAHs and PAHs of interest in this study. The chapter will review methods and analysis of PAHs as conducted by other researchers.

## 2.2 Diesel combustion engine

### 2.2.1 Basics of a diesel engine

A patent was lodged by Rudolf Diesel for the development of the diesel engine in 1892 (US EPA 2002). Diesel engines have high efficiencies and power outputs and are inexorably featured in our everyday lives, be it in the car that we drive or the industry where we are employed (Van Gerpen 2005).

In petrol engines: a fuel and air mixture is introduced into the engine cylinder, it is then compressed and ignited by a spark, hence the name spark-ignition engine. In contrast: a compression-ignition engine, such as a diesel engine, only permits air into the cylinder through the intake system. The air is then compressed to a high temperature and pressure which supports self-ignition when finely atomized fuel is sprayed into the air at high velocity. The engine is controlled by varying the volume of the fuel injected into the cylinder (Van Gerpen 2005).

At the top of the compression stroke, fuel is directly (injectors mounted at the top of the combustion chamber) or indirectly (pre-chamber or ante-chamber) injected into the engine cylinder of the engine by means of a fuel injector, which generates high injection pressure needed for fuel atomization, air-fuel mixing and combustion. The fuel injector contributes to the fuel distribution and consequently affects the performance, emissions and noise of the engine. The injector ensures that the fuel is atomised into small droplets which are injected at the end of the compression stroke, immediately exposing fuel droplets in the injection jet to the high gas temperature in the combustion chamber. The heat from the hot air in the combustion chamber, relative to the moderately cold fuel droplets, produces a strong exchange of heat. As the temperature exchange continues between the air and fuel, the evaporation at the droplet surface increases and the fuel vapour then mixes with the surrounding air and a series of spontaneous chemical reactions occur resulting in auto-ignition. The droplets get smaller as they continue to vaporise from their surfaces and burn until all the fuel in the droplets have burnt. The rapid expansion of combustion gases then forces the piston downward, supplying power to the crankshaft (Heywood 1988, Van Gerpen 2005).



Diesel fuel is heavier and oilier than petrol with a slower evaporation rate and a higher energy density. The boiling point of diesel is higher than that of water. It is the physical and chemical properties of the fuel that determines the quality of the fuel. It should be noted that best practices involving the storage and transportation of the fuel is crucial in order to prevent contamination, which could result in premature aging of engine or unwanted emissions. All aspects of the engine should be maintained to ensure optimum performance with minimum emissions at the same time prolonging the life-time of the engine (Heywood 1988, Van Gerpen 2005).

### 2.2.2 Pollutants from diesel exhausts

A pollutant is generally defined as a substance existing in greater than natural concentrations which has a net harmful effect on the environment and/or anything of value in the environment (Manahan 2000). Anthropogenic sources are of interest in this study particularly diesel emissions from the diesel engines used in the mining industry in South Africa as well as road vehicles in the Daspoort Tunnel. The effect of these pollutants on humans may be enhanced due to the confined nature of the tunnel and mine as well as the mining operations and type of equipment used underground.

Complete combustion of diesel fuel (derived from crude oil) should theoretically yield only  $\text{CO}_2$  and  $\text{H}_2\text{O}$  as combustion products in an internal combustion engine, however this depends on, amongst other things, the combustion efficiency of the engine (Ristovski *et al.* 2012). A trade off to the high combustion efficiency ( $\pm 98\%$  of fuel that is burnt), (Heywood 1988) is the small fraction of unburnt fuel and lubricating oil that yields significant incomplete combustion products that affect urban air quality and consequently, human respiratory health (Majewski & Khair 2006). Combustion emissions contain organic compounds that contribute to gaseous, semi-volatile and ambient particulate air pollutants that induce oxidative and genetic damage, toxicity, mutagenicity and inflammation (Lewtas 2007, Metz 2004, Ristovski *et al.* 2012). DEE is made up of 2 main constituents: gases and soot. The particulate (soot) portion of diesel exhaust is made up of particles such as carbon, particulate phase semi-volatile organic compounds (including PAHs and aliphatic hydrocarbons) and traces of metallic compounds (Ono-Ogasawara & Smith 2004).

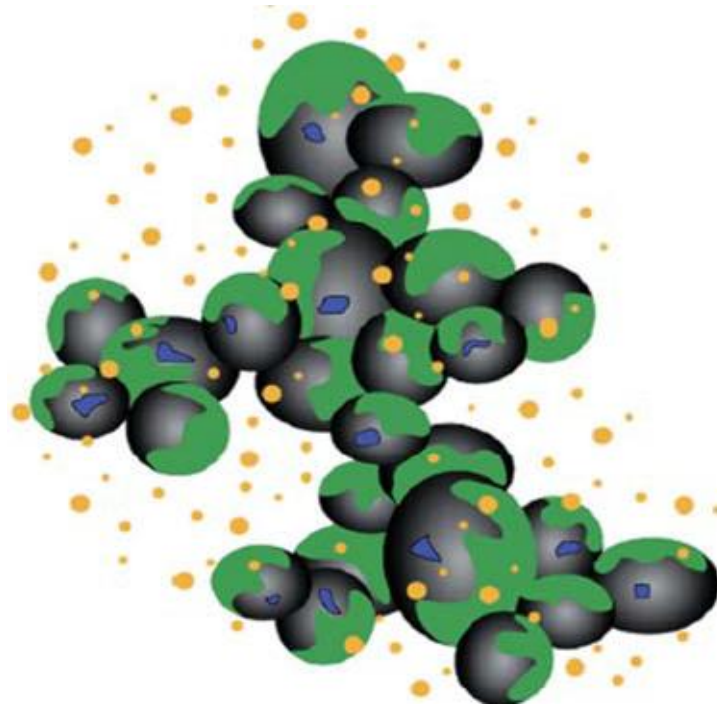
In a study of diesel fuel by Marr *et al.* the following PAHs were detected in the diesel fuel: naphthalene, acenaphthylene, acenaphthene, flourene, phenanthrene, fluoranthene, pyrene, chrysene and benzo(ghi)perylene. Benzo(a)anthracene and the heavier PAHs were below detection limits (Marr 1999). Naphthalene was the predominant PAH in diesel fuel with concentrations of up to  $1600 \text{ mg}\cdot\text{m}^{-3}$ . This is of concern as PAHs in vehicle exhaust can have several sources which include PAHs that are originally in the fuel that escape combustion. Other sources include pyrosynthesis from lower molecular weight aromatics as well as PAHs present in lubricating oil (Marr 1999). Diesel vehicles, gasoline vehicles, oil combustion as well as natural gas and wood combustion are all reported sources of PAHs.

Both the gases and the soot of diesel exhaust contain PAHs. Typical composition of DEP for a heavy-duty diesel engine (tested in a heavy-duty transient cycle) is described as follows: approximately 40 % of the total particulate matter (PM) mass is in the form of inorganic carbonaceous substances (elemental (EC) or black carbon (BC)), 30 % as organic carbonaceous substances (OC) that originate from unburned fuel and oil and the remaining 30 % consists of sulfate, water, ash and others (Kittelson 1998b, Watts 1995).

Typical number and mass size distribution of DEP is described by Kittelson who found that the number of ultrafine particles (defined as being less than 100 nm) is dominant in the number-size distribution as opposed to the larger particles which dominate the mass-size distribution (Kittelson 1998b). Ultrafine particles are either directly emitted from the engine or generated as a result of condensation of gaseous emissions (referred to as nucleation mode). The particles coagulate rapidly with larger particles or alternatively serve as nuclei of droplets in accumulation mode; therefore their life as an independent particle is short lived (Ono-Ogasawara & Smith 2004).

Most organic substances in the tailpipe of a diesel engine are present in the gaseous phase due to the high temperatures that are reached. However, they undergo cooling and dilution after being emitted into the air and during these processes, the low volatility material is adsorbed or condensed onto the PM surface (Ono-Ogasawara & Smith 2004). Initially, solid carbon and metal cores are produced in the engine cylinder but after emission, the high molecular weight pyrolysis products either condense or adsorb onto the surface of ultrafine PM. Unburned fuel or other inorganic compounds, including sulfate and water, also condense or adsorb onto the particles whereby agglomeration and coagulation of these small particles simultaneously occur (Ono-Ogasawara & Smith 2004). Therefore the structure of DPM can be described as an aggregation of primary and spherical carbon particles coated with adsorbed and condensed products which were formed during combustion (Ono-Ogasawara & Smith 2004). An

excellent visual representation of the composition and structure of diesel particulate matter is given in Fig. 2-1 where the black spheres represent the soot component of DPM, the green portion represents the condensed hydrocarbon or sulphate component and the blue spheres represent the metallic ash fraction. The yellow portion represents nucleation particles composed of condensed hydrocarbons and sulfates.



**Figure 2-1 The physico-chemical composition and structure of diesel particulate matter (Ristovski *et al.* 2012) (Adapted by Matti Maricq 2007).**

The composition of DPM depends on many factors including: the maintenance of the engine (Davies 2002), the type of fuel and lubricants that are used, the engine operating condition (e.g. load, speed, injection timing and strategy), the presence of after-treatment devices (Konstandopoulos, Zarvalis & Dolios 2007) and finally the level of dilution and its subsequent atmospheric processing once emitted from the tailpipe (Samy, Zielinska 2010, Zielinska, Samy & McDonald 2010).

Combustion ignition (CI) engines operate on the principle of internal mixture preparation (fuel has to mix with an oxidant (i.e. intake air) before combustion can occur (Heywood 1988)) therefore the process is characterised by a great degree of heterogeneity and is often referred to as diffusion flame combustion. During the diesel combustion process, the heterogeneous fuel-air mixture (in the cylinder) contributes to the formation of soot particles in high temperature regions of the combustion chamber

where the air/fuel ratio is fuel-rich and consists mostly of carbon with small amounts of hydrogen and other inorganic compounds (Heywood 1988). These soot particles contribute to the particulate level in the DEE as well as high molecular weight hydrocarbons that adsorb onto the particles during the expansion process in the exhaust pipe as the gas temperature decreases (Heywood 1988, Samy, Zielinska 2010, US EPA 2002).

All the diesel powered vehicles mentioned in Section 2.2.4 are sources of diesel emissions underground and the vehicles mentioned in Section 2.2.5 are sources in the Daspoort Tunnel. DPM present in underground atmospheres may pose a high risk towards the health and safety of employees working in the mines as a larger amount of particles are expected to exist in the work environment than in the ambient environment. This is due to the close proximity of the emission sources in a confined area (Ono-Ogasawara & Smith 2004). For the same reason, the confined space of road tunnels was of interest in this study.

### 2.2.3 Health effects of diesel emissions

The combined exposure to diesel particulate matter (DPM) and polycyclic aromatic hydrocarbons (PAHs) poses an increased risk to the health of employees as evidence confirms that diesel exhaust is a carcinogenic risk to humans (IARC 2012). Characterization of the DPM and PAHs in large platinum mines is therefore a priority and may indicate the need to establish Occupational Exposure Limits (OELs) in South African regulations.

The human carcinogenic potential of diesel exhaust has been evaluated by six organizations, including two international organizations, the International Agency for Research on Cancer (IARC), associated with the World Health Organization (WHO) (IARC 1989), and US agencies including the National Institute of Occupational Safety and Health (NIOSH), National Toxicology Program (NTP) and Environmental Protection Agency (EPA), as well as a state environmental agency, the California EPA (US EPA 2002).

As aforementioned, DEE contribute to gaseous, semi-volatile and ambient particulate air pollutants, all of which contain organic compounds that induce genetic and oxidative damage, toxicity, mutagenicity and inflammation (Lewtas 2007). DPM and its associated health risks have been evaluated and updated for more than two decades (IARC 1989, US EPA 2002). Cohort studies demonstrate that airborne PM, of

which DPM is a major contributor (Robinson *et al.* 2010), is accountable for causing respiratory mortality and morbidity (Pope & Dockery 2006).

The primary route by which DPM affects one's health is via inhalation into the respiratory system, however other routes such as skin absorption and translocation are also possible (Ristovski *et al.* 2012). Translocation is the migration of particles to secondary organs such as the brain, spleen or liver after inhalation, which causes negative health effects in the affected secondary organs (Ristovski *et al.* 2012). The inhalation route of exposure (being the main route) has been reported in numerous occupations such as: garage workers (Zaebst *et al.* 1991), truck drivers (Steenland, Deddens & Stayner 1998), miners (Birch, Dahmann & Fricke 1999, Birch & Cary 1996) and others (Stayner *et al.* 1998, Larkin *et al.* 2000).

As described in Section 2.2.2 the soot portion of diesel exhaust is made up of carbon as well as traces of metallic compounds and organic compounds (including PAHs and aliphatic hydrocarbons). The DPM surface area and the organic compounds that have been adsorbed onto the surface play an important role in chemical and cellular processes that can lead to the development of unfavorable respiratory health effects of which the mechanisms of damage involve: innate and acquired immunity, oxidative stress and inflammation (Kim *et al.* 2004, Xia *et al.* 2004, Healey *et al.* 2005, Ristovski *et al.* 2012).

Oxidative stress (OS) can be induced by ambient particulate matter with diameters less than or equal to  $2.5 \mu\text{m}$  ( $\text{PM}_{2.5}$ ) and is involved in carcinogenicity, genotoxicity and many other detrimental human health effects (Risom, Møller & Loft 2005), it develops when there is an imbalance between the production of reactive oxidation species (ROS- which can be directly generated on the DPM surface) and the availability of anti-oxidant defenses (Ristovski *et al.* 2012). ROS is a term which is used collectively and it refers to free radicals such as hydroxyl ( $\text{HO}\bullet$ ) and peroxy ( $\text{HOO}\bullet$ ,  $\text{ROO}\bullet$ ), ions such as superoxide ( $\text{O}_2^-$ ) and peroxynitrite ( $\text{ONOO}^-$ ), and molecules such as hydrogen peroxide ( $\text{H}_2\text{O}_2$ ) and hydro peroxides ( $\text{ROOH}$ ) (Ristovski *et al.* 2012). Subsequent studies indicate that PM interacts with biological systems through direct generation of ROS from soluble compounds, the surface of particles or from other disturbed processes in bodies (González-Flecha 2004, Risom, Møller & Loft 2005, Singh *et al.* 2007a, Singh *et al.* 2007b) which furthermore results in the OS process (Kim *et al.* 2004, Xia *et al.* 2004, Healey *et al.* 2005).

The hydroxyl radical (one of the ROS) can attack deoxyguanosine in DNA (the C-8 position) and produce a stable compound called 8-Hydroxy-20-deoxyguanosine (8-OHdG) that can be used as a biomarker of oxidative stress (Shigenaga & Ames 1991, Dalle-Donne *et al.* 2006) as it is excreted in the urine in a stable form and it is easily measured (Kasai *et al.* 1984).

*In situ* ROS is formed after particle deposition has occurred in the human respiratory tract whereas on the other hand *in situ* ROS production occurs via chemical species on the particle that have the potential to generate ROS such as quinines via a direct pathway (Grahame & Schlesinger 2007) or by phagocytic processes initiated by the presence of DPM in the lungs (the indirect pathway). These formations have gained substantial research attention, however numerous recent studies have shown that there exists an alternative to particle induced ROS which is particles that contain ROS referred to as exogenous ROS (Venkatachari *et al.* 2007).

Inflammatory response to DPM and other air pollutants is mediated by the immune system which shows responses to air pollutants that resemble that of the responses to pathogens found in infections (Ristovski *et al.* 2012). DPM is a transport vector for pathogens, which alter the subsequent inflammatory response. As with pathogens, DPM can access sites in the lung where it would otherwise not generally be found. A number of studies indicate that the mechanism by which DPM exerts its toxicity may be via OS (Ayres *et al.* 2008, Donaldson *et al.* 2005), which is a synergistic occurrence together with inflammation. Ayres *et al.* have noted that OS is a precursor to inflammation, with the occurrence of inflammation being able to generate more OS (Ayres *et al.* 2008).

The organic fraction of DPM is especially complex, containing numerous compounds including PAHs. It was interesting to note that DPM and its organic extracts were able to induce apoptosis as well as pro-inflammatory responses in lung tissue cells, while DPM that previously had its organic constituents extracted were no longer able to induce such responses in cells (Li *et al.* 2002). Organic components of DPM are implicated in the induction of oxidative stress (Ayres *et al.* 2008) and several other studies have demonstrated the toxicity of the organic fraction of DPM, therefore a summary of the health effects of PAHs follows in Section 2.3.

#### 2.2.4 Role of diesel in the mining industry

Trackless diesel machinery is used in many mining operations. These vehicles include: load haul dump vehicles (LHDs), utility vehicles (UVs), dump trucks and drill rigs. The UVs are primarily used for the logistics of material, equipment and personnel (Fig. 2-2 A & B). Drill rigs are used to drill holes into the rockface in which explosives are inserted and detonated for rock fragmentation (Fig. 2-2 C). The positioning of the cumbersome drill rigs into designated drilling areas is made possible by diesel powered engines. Diesel LHD vehicles (Fig. 2-2 D) are then used to load, haul and dump blasted ore and ore residue onto underground conveyor belts or dump trucks that will then transport and tip the ore into designated areas. These trackless vehicles are used in everyday mining operations and are unavoidable features in the foreseen future of mining. A cherry picker is also a widely used vehicle underground which is used to elevate material and personnel to abnormal heights for installation of piping and cabling and daily servicing of areas being mined. All the above mentioned diesel powered vehicles are sources of DPM underground. This is of concern due to the exposure of the miners, and other underground workers, to DEE which has been classified as being carcinogenic (IARC 2012). In this section several techniques that can be used to monitor DPM will be described.

Personal sampling is usually performed to measure the DPM exposure of individual workers or for assessing compliance with regulated exposure limits. There are presently two main analytical methods that can be used to measure workers' exposure to DPM, namely the Respirable Combustible Dust (RCD) method (used in most Canadian regulations) (Grenier & Butler 1996) and the NIOSH 5040 (NIOSH 2003) method, which will both be briefly discussed.

The sampling train of the RCD method consists of a cyclone (10 mm nylon cyclone to remove the non-respirable portion of the airborne dust), filter cassette, a length of tubing and a sampling pump operated at a constant flow of  $1.7 \text{ L}\cdot\text{min}^{-1}$  (Grenier & Butler 1996, DEEP 2001). The Mine Safety and Health Administration (MSHA) final ruling for metal and non-metal mines calls for a slightly different setup from the RCD method, which sees the addition of an impactor which is inserted between the cyclone and the filter cassette for the purpose of removing respirable dust particles  $> 0.9 \mu\text{m}$  in size (Grenier & Butler 1996, DEEP 2001).

The NIOSH 5040 method measures elemental carbon, organic carbon and total carbon. In this method, DPM is ashed from the sample filter when it is placed in a furnace at a temperature of 400 °C for a minimum period of 2 h. A silver membrane filter (25 mm diameter, 0.8 µm pore size) is required for the sampling process as silver acts as a catalyst, enabling the DPM to be burned at a lower temperature. The filter is weighed prior and post ashing to yield the mass of dust burned off in the process (RCD). This value is then used as an estimate of the DPM mass collected on the filter and the concentration is calculated using the mass, sampling flow rate and the total sampling time (DEEP 2001).

The Carbon Analysis NIOSH 5040 Method is more complex than the RCD method. In the NIOSH method the temperature and the analytical cell atmosphere are controlled to measure elemental carbon and organic carbon independently which are collected on a quartz fibre filter (37 mm in diameter). Light transmittance through the filter is then measured using a laser in order to determine the proportions of EC and OC. The mass of EC and OC are determined by the carbon dioxide which is produced during the controlled heating of the dust sample, with the sample flow rate and the sampling time used to calculate the airborne concentration of DPM (NIOSH 2003, DEEP 2001).

Three types of methods were used by van Niekerk *et al.* (2002) in order to determine diesel particulate matter which included the use of a Rupprecht and Patashnick (R&P) Series 5400 Ambient Carbon Particulate Monitor that had the capability of direct sampling and was used for quantification of EC associated with DPM in ambient air. Secondly, a laboratory-based Horiba Mexa 1370 PM Super Low Mass PM Analyser was used to analyse DPM that was captured on filters that were fitted to personal samplers. A size selective sampler was the third method used to differentiate between EC associated with DEE and carbon particles from other sources, e.g. coal dust present in coal mines. The investigation confirmed that determination of EC was the preferred method for quantification of exposure to diesel particulate emissions (van Niekerk *et al.* 2002).

In this same study by van Niekerk *et al.* PAH samples were collected with Gilair personal sampling pumps at a flow of 0.5 L.min<sup>-1</sup> and they were attached to relevant participants (mainly vehicle drivers). XAD-2 sampling tubes were used for sampling and a maximum of three samples were collected per day over a five-day collection period. Two of the PAH samples were collected underground and one at the security gate or at the ventilation office above ground. Extraction of the XAD-2 resin was done with accelerated solvent extraction (ASE<sup>®</sup>) based on NIOSH Method 3545. Analysis of the selected heterocyclic PAHs was performed by GC-MS analysis based on NIOSH Method 8270. The PAHs that were detected were anthracene (ANT), benz(a)anthracene (BaA), benz(b)fluoranthene (BbF), benz(k)fluoranthene (BkF),



benz(j)fluoranthene (BjF), benzo(a)pyrene (BaP), benzo(e)pyrene (BeP), benzo(ghi)perylene (BghiP), chrysene (CHY), cyclopentadienol(cd)pyrene (CcdPYR), dibenz(a,h)anthracene (dBahA), indeno(1,2,3-cd)pyrene (I123cdP) and pyrene (PYR). Where guidelines for individual PAHs have been set, concentrations did not exceed the individual guideline concentrations, however the total PAH concentrations on particular days were sometimes higher than the OSHA limit of  $0.2 \text{ mg.m}^{-3}$  for exposure to coal tar pitch volatiles (van Niekerk et.al. 2002).

Sampling and monitoring of DPM is done not only for compliance purposes but it can also aid in verifying the ventilation efficacy, confirm the maintenance state of an engine and measure the efficiency of exhaust treatment devices (DEEP 2001, van Niekerk et.al. 2002).



Figure 2-2 Trackless mining vehicles with diesel combustion engines used underground: utility vehicles (A&B), drill rig (C) and a LHD (D) (Photographed by G. Geldenhuys).

### 2.2.5 The role of diesel in the Daspoort Tunnel

Tunnels are man-made, unnatural constructions that aid in minimization of traffic congestion in areas where the topography poses building restrictions. In populated urban areas, the continuous influx of vehicles into the tunnel, especially during peak times, will lead to decreased average vehicle speed and ultimately saturation of tunnel lanes. Congestion periods will result in extended exposure periods to and increased concentrations of vehicle-induced emissions, hence an increased health hazard as DEE has recently been confirmed as a carcinogen (IARC 2012), as previously stated. Exposure time in a tunnel is typically short but due to the confined environment, pollutant concentrations are elevated to levels of potential health and safety risk. Safety becomes an issue as the presence of suspended particulate matter can decrease the visibility inside the tunnel and potentially cause car accidents (El-Fadel, Hashisho 2001). Occupational exposure is generally limited to workers responsible for cleaning and maintaining the tunnel.

The type of vehicles as well as the condition and age of their engines that pass through tunnels may also aggravate the pollutant situation. Vehicles are typically characterized into light duty vehicles (LDV) and heavy duty vehicles (HDV).



Figure 2-3 Daspoort Tunnel entrance (left) (Photographed by P. Forbes) and pedestrian path inside the tunnel (right) (Photographed by G. Geldenhuys).

PAHs were quantified by HPLC-UV during summer and winter months of 2003 in the Shing Mun tunnel in Hong Kong. The PAHs were collected on a combination of polyurethane foam and XAD-4 adsorbent resin (PUF/XAD-4/PUF) for gas phase PAHs and quartz fibre filter for particulate phase PAHs. Naphthalene (NAP), acenaphthylene (ACY), and acenaphthene (ACE) were the most abundantly found gas PAHs while

fluoranthene (FLA) and pyrene (PYR) were the most abundantly found in the particle phase. Phenanthrene (PHE), fluoranthene and pyrene were used as diesel markers (Ho *et al.* 2009).

Emissions of organic tracers (size resolved) from LDVs and HDVs were measured in a Californian roadway tunnel and although the sunlight, temperature, dilution and humidity conditions differ inside a tunnel compared to the conditions that are found outside a tunnel, it was noted that these conditions more closely approximate real-world conditions than dynamometer tests. In the study, air was sampled directly from inside the tunnel bore onto quartz fibre impaction strips and samples were analysed by GC-MSD. Very high PAH concentrations were detected and almost all measurements could be attributed to vehicles. The results demonstrated that lower molecular weight PAHs were emitted in relatively higher amounts by HDVs than that of the higher molecular weight PAHs and it was also seen that overall, the HDVs emitted significantly more PAHs as well as mass of PM. The distribution of different molecular weight PAHs was very different for HDV and LDV (Phuleria *et al.* 2006).

Determination and characterisation of profiles of PAHs were performed in a Gothenburg traffic tunnel in Sweden in 2001, in addition to two high traffic urban locations. In this particular study, 52–118 m<sup>3</sup> of air was sampled through the sampling train that consisted of a glass fibre filter (GFF) and two polyurethane foam plugs (PUFs) that were connected in series. After Soxhlet extraction, analysis was performed using high performance liquid chromatography (HPLC) with a fluorescence detector (FLD). Naphthalene and mono-methylated naphthalene derivatives (NAP 1M & NAP 2M) were detected with the highest concentrations on the PUFs whereas pyrene and fluoranthene had the highest concentration on the filter samples. It was found that although the PAH profiles of air samples from the tunnel and the urban sites were similar, the concentrations of PAHs from the tunnel air samples were one order of magnitude higher than in air samples from the two urban locations (Wingfors *et al.* 2001).

## 2.3 Polycyclic aromatic hydrocarbons (PAHs)

### 2.3.1 PAHs and their sources

Anthropogenic sources of PAHs include road traffic, wood fires and combustion of fossil fuels in industries, whilst natural sources include volcanic eruptions and forest fires (Lundstedt 2003, Forbes *et al.* 2012). The most dominant and ubiquitous source of PAHs in the environment is the incomplete combustion of fossil fuels such as petroleum and coal as well as the combustion of biomass such as wood. PAHs produced by combustion sources are pyrogenic PAHs which are the subject of this research.

### 2.3.2 Formation of PAHs

Polycyclic aromatic hydrocarbons are synthesized from saturated hydrocarbons under oxygen deficient conditions. Low molecular weight hydrocarbons act as precursors in the formation of PAHs by a process called pyrosynthesis which occurs at temperatures exceeding 500 °C. At this high temperature C-C and C-H bonds break to form free radicals which after dehydrogenation, combine to form aryl ring structures (Manahan 2000).

PAHs may also be formed from higher alkanes (in fuel and plant materials) by a process called pyrolysis which can be envisioned as the “cracking” of organic compounds to form smaller, less stable molecules and radicals which condense and react to form PAHs. The vehicles that are found in the tunnel and in underground environments use diesel fuel which undergo pyrolysis to form PAHs (Manahan 2000).

### 2.3.3 Properties and environmental fate of PAHs

The physicochemical properties of the PAHs predominantly control their fate in the environment however, concentration of oxidizing pollutants (e.g., NO<sub>x</sub>, O<sub>3</sub>, OH• radicals), biological degradation, light intensity, type of sorbent as well as temperature are natural processes that are also important factors that influence the fate of PAHs (Lima *et al.* 2005).

According to Atkinson and Arey, the fate of PAHs in the atmosphere is strongly dependent on whether the PAH is present in the gaseous form or is particle-associated (Atkinson & Arey 2003) and most of the PAHs that arise from incomplete combustion are associated with particles such as soot which will have an influence on the ultimate fate of these compounds in the atmosphere.

The gas and particulate phase distribution is typically determined by the vapour pressure of the PAH compound with the smaller, lower molecular weight PAHs (3-4 rings) being commonly present in the gas phase and larger, higher molecular weight PAHs (5 + rings) mostly seen in the particle phase in the atmosphere (Lima *et al.* 2005, Vione *et al.* 2004). Other factors that may influence partitioning of PAHs include: PAH concentration, ambient temperature, as well as the amount and type of fine particles that are present in the atmosphere (Lima *et al.* 2005, Vione *et al.* 2004).

PAHs tend to associate with particles rather than dissolve in water as they are hydrophobic compounds, which can be confirmed by the octanol-water partition coefficient,  $K_{ow}$ . PAHs range in solubility with the lowest molecular weight PAH namely naphthalene only being slightly soluble in water and the higher molecular weight PAHs, such as dibenz(a)anthracene, being extremely insoluble in water. PAHs also range in volatility from naphthalene being the most volatile to PAHs such as dibenz(a)anthracene being semi-volatile. Normally, the higher the mass of the compound and the more alkyl substitution, the lower its water solubility and vapour pressure (Lima *et al.* 2005).

Photolytic susceptibility of a compound is influenced in part by its absorption spectrum as well as the sorbent to which it is associated, i.e. the nature of the particle to which it is absorbed. PAHs absorb light over a wide range of wavelengths ( $\lambda$ ) and it is a common observation that the linear PAHs can absorb over a wider range of wavelengths (and up to higher wavelengths) than their angular isomers for example: phenanthrene absorbs in the region  $\sim$ 200-350 nm whereas the linear isomer, anthracene, absorbs in the range from  $\sim$ 200-390 nm. The difference in susceptibility between isomers, as shown, will ultimately have an influence on the relative proportion of these compounds during atmospheric transport (Lima *et al.* 2005) and light absorption can also induce photoreactions like photo-dimerisation and photo-oxidation, the latter occurring upon irradiation of compounds in the presence of oxygen leading to the formation of oxy-PAHs (Vione *et al.* 2004).

Photolysis and other atmospheric reactions (with  $O_3$ ,  $NO_2$ ,  $HNO_3$ , and  $N_2O_5$ ) of PAHs have been demonstrated to lead to loss of PAHs and their derivatives on numerous substrates (Finlayson-Pitts, Pitts Jr. 1999) which should be taken into account when considering the fate of a certain PAHs in the atmosphere. Particle-associated PAHs can undergo photolysis in the atmosphere but are inclined to remain associated with the particle and be inhaled into the lungs while the gaseous PAHs tend to undergo photochemical reactions, with some radicals in the atmosphere, to form polar derivatives which are potentially more toxic, have lower volatility and are more bioavailable (Atkinson & Arey 2003). These transformations are important as they define the atmospheric lifetime of the parent PAHs.

Radiation from the sun can result in the formation of ozone ( $O_3$ ), hydroxyl ( $\bullet OH$ ) and nitrate ( $\bullet NO_3$ ) radicals which then can react with PAHs to form a wide range of derivatives. This occurs in the troposphere. The reaction mechanisms for these transformations are discussed in the next section.

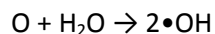
### Transformation of PAHs by $\bullet OH$ Radicals

The  $\bullet OH$  radical is an oxidising species and serves as a main sink for most organic compounds in the troposphere. The main source is represented by Equations 2-1 and 2-2 (Vione *et al.* 2004).

Equation 2-1



Equation 2-2



The  $\bullet OH$  radical can then react with PAHs to yield other radical intermediates (less volatile than parent PAHs) which can later react with oxygen or nitrogen oxides to yield different products. An example of the transformation of naphthalene by the  $\bullet OH$  radical is shown in Fig. 2-4.

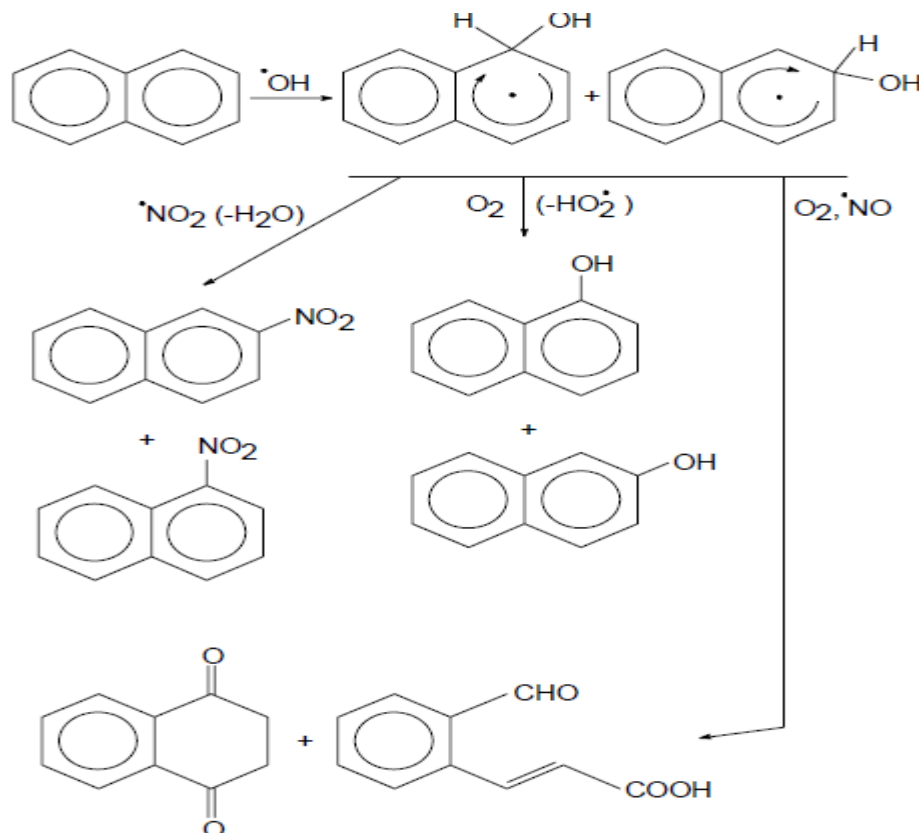


Figure 2-4 Transformation of naphthalene by  $\bullet OH$  radical (Vione *et al.* 2004).

### Transformation of PAHs by •NO<sub>3</sub> Radicals

Nitrate radicals are mainly formed in the atmosphere by reaction of nitrogen dioxide and ozone as represented by Equation 2-3. The radical can then transform PAHs as shown in Fig. 2-5 which illustrates the transformation of naphthalene (Vione *et al.* 2004).

#### Equation 2-3

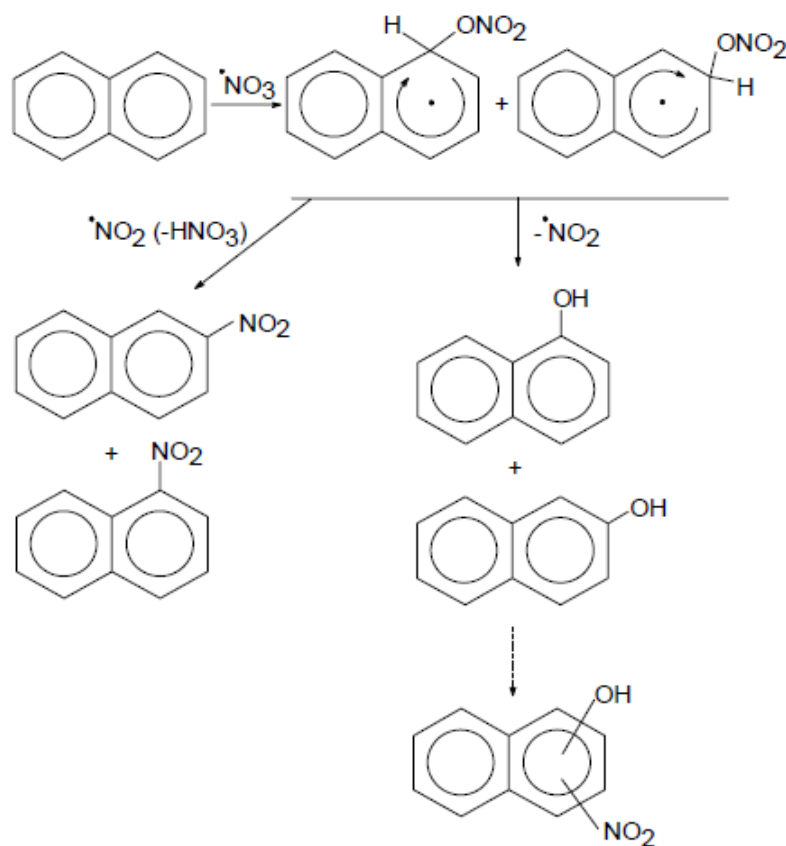
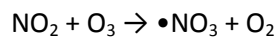


Figure 2-5 Transformation of naphthalene by •NO<sub>3</sub> Radical (Vione *et al.* 2004).



### Transformation of PAHs by O<sub>3</sub>

Ozone is a strong oxidant and can also react with PAHs to yield oxygenated intermediates (oxy-PAHs) which are less volatile and tend to associate with particulates in the atmosphere. An example of a transformation of a PAH (benzo(a)pyrene) by ozone is shown in Fig. 2-6 (Vione *et al.* 2004).

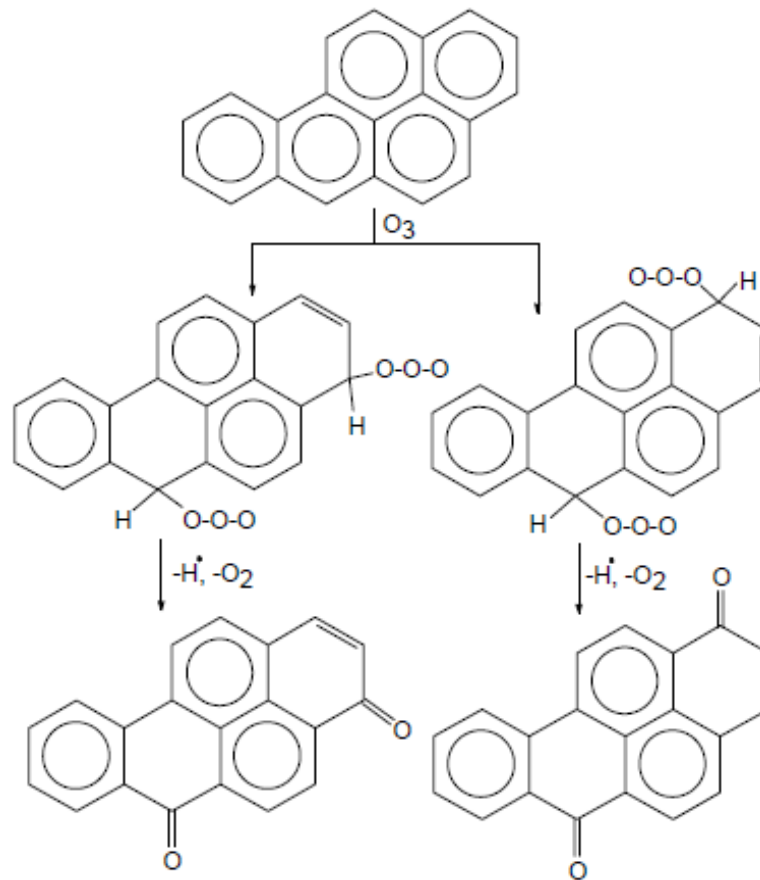


Figure 2-6 Transformation of benzo(a)pyrene by ozone (Vione *et al.* 2004)

### Removal of PAHs from the atmosphere

Wet or dry deposition are the two mechanisms by which PAHs are removed from the atmosphere with wet deposition offering simplicity in measurement as it is directly related to the amount of rain and snow precipitation. Normally, PAHs that are particulate bound are washed out from the atmosphere by precipitation whereas the PAHs present in the gas phase simply dissolve into raindrops or clouds. The direct fallout of particles containing adsorbed PAHs is what constitutes dry deposition and the

mechanism is more complex than wet deposition as it is dependent on the size and nature of particles to which the PAHs are adsorbed, which can vary vastly (Lima 2005). Both wet and dry deposition need to be considered to assess the total removal of PAHs from the atmosphere.

#### 2.3.4 Health effects of PAHs

Most of the organic compounds in DPM are sourced from unburnt fuel and lubricants and they consist of aliphatic and aromatic hydrocarbons which are of interest due to their toxicity to human and ecological life (Ono-Ogasawara & Smith 2004, Lewtas 2007). A significant number of PAHs are emitted from vehicle exhausts which range in size (molecular weight) from small naphthalene molecules which consist of only two fused benzene rings to heavier PAHs consisting of 5 or more rings, and as previously discussed, they also range in physiochemical and toxicity properties. In addition to the parent PAH compounds, alkyl substituted analogues as well as heterocyclic analogues containing ring nitrogen, sulphur and oxygen atoms are also possible emissions from combustion sources (Ono-Ogasawara & Smith 2004). The abovementioned compounds are electrophilic in nature and research has demonstrated their role in cardiovascular diseases, adverse reproductive effects and environment induced cancer (Lewtas 2007, IARC 2012). The carcinogenicity of each PAH has been examined and it was found that benzo(a)pyrene is one of the most carcinogenic PAHs hence its use as an environmental PAH exposure indicator (Ono-Ogasawara, Smith 2004).

PAHs are found in rural, urban and industrial environments and are therefore considered to be ubiquitous pollutants, which are often derived from anthropogenic sources (IARC 1985, National Research Council 1983). Humans can be exposed to PAHs by gaseous PAH inhalation, particulate PAH inhalation as well as skin absorption. DEE from transportation sources (including: buses, taxis, trucks, trains, ships etc.) was studied and occupational exposure to DEE was found to be associated with not only lung cancer but also bladder and lymphatic cancers (USEPA 2002, Lewtas 2007).

Since the 1960s, studies revealed evidence that supports the theory that chemical carcinogens such as PAHs produce electrophilic reactive compounds (such as epoxides) when metabolized, which occurs via various oxidative pathways. The resulting electrophilic compounds then covalently react with nucleophilic centers in DNA and other nucleophiles in the cell, such as proteins. DNA binding and mutations are a result of these reactions as is the initialization of multi-stage processes leading to genetic effects that can lead to cardiovascular damage, cancer and antagonistic reproductive effects (Lewtas 2007). As early as 1933 a study by Cook *et al.* recognised the carcinogenic constituent, BaP, in

coal soot (Cook, Hewett & Hieger 1933) which led to the use of genetic bioassays for mutagenic chemical detection as well as the detection of biomarkers of DNA adducts, protein adducts and oxidative damage in target tissues and cells (Harris *et al.* 1987, Phillips, Farmer 1995). Jongeneeren summarized the biomarkers of PAHs including protein and DNA adducts as well as various metabolites found in urine and blood (Jongeneelen 1997).

Both occupational and environmental research studies have seen the use of urinary PAH metabolites as biomarkers for PAH exposure (Jongeneelen, Bos & Anzion 1986, Goen *et al.* 1995, Szaniszló & Ungváry 2001). 1-hydroxypyrene (1-OHP) is one such biomarker and it consists of a hydroxylated PAH, namely pyrene, which is a semi-volatile PAH (classified as non-carcinogenic) that is distributed between the gas and particle phase in human exposure samples as well as in the ambient air (Williams *et al.* 1999). 1-OHP is a stable compound in urine and is easily quantified, thus it is the urinary metabolite that is most extensively used as a biomarker (Jongeneelen, Bos & Anzion 1986, Goen *et al.* 1995, Szaniszló & Ungváry 2001, Strickland & Kang 1999). Metabolic PAH activations involve three different pathways including the formation of o-quinones and syn-diol epoxides as well as the formation of radical cations which cause OS at deposition sites (by redox cycling) as a result of generated ROS (Bolton *et al.* 2000, Venkatachari *et al.* 2007, Cho *et al.* 2005).

According to studies, induced mutation, tumours and DNA adducts form due to emitted oxy- and nitro-PAH products derived from atmospheric transformations as well as combustion sources (Lewtas 2007). Labile DNA adducts may also form as a result of one electron oxidation which is an alternative carcinogenesis pathway which has been established to be the case for several PAHs (including dibenzo(a,l)pyrene) which are metabolized to phenols, oxidized to catechols then to quinines. The subsequent quinones then react with DNA resulting in apurinic sites and mutations (Cavalieri & Rogan 1995, Cavalieri & Rogan 2002).

Wei *et al.* (2010) confirmed reported associations between a mix of different PAHs and a urinary marker for oxidative stress in DNA namely 8-Oxo-2'-deoxyguanosine (8-OHdG). The purpose of the study was to investigate whether quinone-structured chemicals and particulate PAHs increase body burden of oxidative stress in humans exposed to heavy traffic volumes. In the study, two non-smoking security guards, who worked near a heavily trafficked road, were equipped with personal air sampler devices for 24 h per day in order to estimate exposures to anthraquinone (AnQ) as well as 24 PAHs in PM<sub>2.5</sub>. Urine samples were analyzed for 8-OHdG and source apportionment results suggest that vehicular emissions were the domineering source of exposure to PM<sub>2.5</sub>. Results indicated that exposures to 24 individual

PAHs and AnQ in ambient air originating from traffic emissions were significant with respect to increasing oxidative burdens in the human body (Wei *et al.* 2010). Among the 24 PAHs, the intermediate sized (4 ringed) PAHs accounted for approximately 70 % of the personal exposure to total PAHs whereas the 2, 3, 5 and 6 ringed PAHs only accounted for approximately 30 %. Pyrene, chrysene and benzo(b)fluoranthene were considered indicators of DEE and gasoline exhaust (Phuleria *et al.* 2006).

In a separate study, the same outcome was realised where levels of 8-OHdG adducts were increased by both PM and PAH exposure from the traffic related emissions which included DEE from diesel engines and vehicles and engines in *in vivo* or *in vitro* studies (Kim *et al.* 2003, Courter, Pereira & Baird 2007).

The study by Wei *et al.* in Beijing, China, revealed that personal exposure to 12 PAHs (corresponding to 16 US Environmental Protection Agency (EPA) PAHs) was 530.2 ng.m<sup>-3</sup>. This concentration was at least one order of magnitude higher than the same PAHs measured in other cities, for example, average ambient concentrations of 16 US EPA PAHs were 22.9 ng.m<sup>-3</sup> in Germany (Bari *et al.* 2009), 34.40–140 ng.m<sup>-3</sup> in California (Schauer & Cass 2000) and 67.12 ng.m<sup>-3</sup> in Rio de Janeiro, Brazil (De Almeida Azevedo, Moreira & Soares De Siqueira 1999). It was however noted that the studies conducted by Wei *et al.* were similar to previous studies conducted in China with ambient PAHs totalling 567.6 ng.m<sup>-3</sup> in Beijing (Wang *et al.* 2009) and 346 ng.m<sup>-3</sup> in particulate matter with diameters less than or equal to 10 micrometers (PM<sub>10</sub>) in northern parts of China (Liu *et al.* 2007b).

It is not only cancer or cardiovascular disease that is of concern when one is exposed to PAHs but the relationship between ambient air pollution (including PAHs) and reproductive outcomes has also been widely investigated which include studies in China (Wang *et al.* 1997), Korea (Ha *et al.* 2001), Brazil (Pereira *et al.* 1998) and Mexico (Loomis *et al.* 1999). These findings have all linked ambient air pollution exposure to problematic pregnancies.

A study in the Czech Republic by Binková *et al.* demonstrated that PAHs from PM<sub>2.5</sub> organic extracts from air samples in the Teplice district, were a major source of the embryo toxicity (measured by DNA adducts). These results were confirmed by a large population analysis (4800 pregnancies) conducted by Dejmek *et al.* who also noted that the first gestational month was the critical period for exposure in terms of fetal growth retardation (Binková *et al.* 1999, Dejmek *et al.* 2000). The occurrence of premature and/or low birth weight infants was shown to be influenced by the close proximity of households to heavy traffic roads in epidemiologic case–control studies in Los Angeles, California during 1994-1996 (Wilhelm, Ritz 2003, Ritz *et al.* 2002). Perera *et al.* conducted more specific reproductive

biomarker studies on the impact of PAHs (and other air pollutants derived from coal) on birth outcomes in a region of Poland (Perera *et al.* 1999).

### 2.3.5 PAHs which will be investigated in this study

Sixteen PAHs have been selected as priority pollutants by the US EPA and these PAHs were also the priority compounds in this study. These PAHs were listed and their corresponding structures were provided in Chapter 1. The World Health Organization (WHO) added 17 additional PAHs to make a total of 33 PAHs under its regulation (Poster *et al.* 2006). In Europe, ambient air legislation targets benzo(a)pyrene (value of  $1 \text{ ng.m}^{-3}$  for an averaging period of 1 year) as this compound carries the highest toxic load (toxicity multiplied by concentration) of any airborne PAH (Pandey, Kim & Brown 2011).

### 2.3.6 PAH concentrations in different environments

PAH ambient levels may vary depending on temporal and spatial changes as is evident in Table 2-1. The sampling location, in this case different environments (suburban, urban and tunnel) within different cities in different counties are compared to reveal variability in PAH concentrations.

From Table 2-1 it can be seen that ambient winter PAH concentrations were higher than ambient summer PAH concentrations in central Delhi, India. In that study, four samples (24 h) were collected during each month of the year with the winter season being classified as December-February and summer as March-May. PAH concentrations ranged from  $21.32\text{-}123.93 \text{ ng.m}^{-3}$  in summer and  $50.75\text{-}494.52 \text{ ng.m}^{-3}$  in winter, with the heavier PAHs showing the highest concentrations (Sharma 2008). The ambient air in Porto Alegre, Brazil showed much lower PAH concentrations ranging from  $0.055\text{-}2.295 \text{ ng.m}^{-3}$  where the 8° Distrito sampling station was located in an urban area with heavy traffic in Porto Alegre, Brazil, and was sampled for 24 h every 15 days between November 2001 and November 2002 (Dallarosa 2005).

A study was conducted in Sweden, in a traffic tunnel in Gothenburg, whereby  $52\text{-}118 \text{ m}^3$  of air was sampled in a period of 2-4 h for each sample. Both gas and particulate phase samples were collected and the results showed that the gas phase samples ranged from  $0.52\text{-}500 \text{ ng.m}^{-3}$  with the lighter 2 and 3 ringed PAHs having the highest concentrations. The particulate samples ranged from  $0.49\text{-}93.00 \text{ ng.m}^{-3}$  and included the heavier PAHs (Wingfors 2001).

Table 2-1 Comparison of concentrations of PAHs in different environments in ng.m<sup>-3</sup>

	<sup>a</sup> Winter filter (ambient)	<sup>a</sup> Summer filter (ambient)	<sup>b</sup> Filter PM <sub>10</sub> (ambient)	<sup>c</sup> Filter (tunnel)	<sup>c</sup> PUF (tunnel)	<sup>d</sup> Filter (tunnel)	<sup>d</sup> PUF/XAD -4/PUF (tunnel)	<sup>e</sup> Filter (suburban ambient)	<sup>e</sup> PUF (suburban ambient)
NAP	-	-	<DL <sup>#</sup>	0.69	500	13.6	572.7	-	-
NAP 2M	-	-	-	0.49	410	-	-	-	-
NAP 1M	-	-	-	<DL <sup>#</sup>	220	-	-	-	-
ACY	-	-	<DL <sup>#</sup>	0.63	43	<DL <sup>#</sup>	274.5	-	-
ACE	-	-	0.055	<DL <sup>#</sup>	17	<DL <sup>#</sup>	670.4	-	-
FLU	-	-	0.174	1.6	85	1.1	104.4	0.02	2.55
PHE	50.75	21.32	0.643	34.00	210.00	5.80	134.4	0.12	13.1
ANT	70.47	24.56	0.276	6.70	9.80	1.90	17.5	0.02	3.14
FLA	299.99	48.54	1.122	72.00	34.00	20.00	8.3	0.17	2.33
PYR	173.11	63.52	0.381	93.00	37.00	28.60	13.2	0.17	2.07
BaA +								0.69	0.49
CHY	224.51	51.46	2.080	11.90	0.52	13.60	0.8		
BbF	331.15	90.77	1.800*	2.70	<DL <sup>#</sup>	3.90	<DL <sup>#</sup>	0.71	0.01
BkF	121.20	46.03		0.55	<DL <sup>#</sup>	1.60	<DL <sup>#</sup>	-	-
BeF	-	-	-	2.40	<DL <sup>#</sup>	-	<DL <sup>#</sup>	-	-
BaF	-	-	-	2.40	<DL <sup>#</sup>	-	<DL <sup>#</sup>	-	-
BaP	86.50	31.25	1.090	-	-	2.10	<DL <sup>#</sup>	0.21	<DL <sup>#</sup>
BeP				-	-	<DL <sup>#</sup>	<DL <sup>#</sup>	0.35	0.03
PER	-	-	-	0.93	<DL <sup>#</sup>	-	<DL <sup>#</sup>	0.05	<DL <sup>#</sup>
IP	322.95	98.40	0.801	1.30	<DL <sup>#</sup>	0.15	<DL <sup>#</sup>	0.32	<DL <sup>#</sup>
DbahA	67.34	53.05	0.536	<DL <sup>#</sup>	<DL <sup>#</sup>	<DL <sup>#</sup>	<DL <sup>#</sup>	0.07	<DL <sup>#</sup>
BghiP	494.52	123.93	2.295	4.30	<DL <sup>#</sup>	6.00	<DL <sup>#</sup>	0.34	<DL <sup>#</sup>
I123cdP	-	-	-	-	-	3.00	<DL <sup>#</sup>	-	-
COR	-	-	-	2.10	<DL <sup>#</sup>		-	-	-

<sup>a</sup> India. Daryaganj, urban central Delhi with heavy vehicular traffic (Sharma 2008)

<sup>b</sup> Brazil, urban area with heavy traffic in Porto Alegre (Dallarosa 2005).

<sup>c</sup> Sweden. Traffic tunnel in Gothenburg, Sweden. Results for period 3 at tunnel exit (Wingfors 2001).

<sup>d</sup> Hong Kong. Shing Mun Tunnel, Hong Kong. Weekday noon samples considered (Ho 2009).

<sup>e</sup> Greece. Koropi suburban area (Vasilakos 2007)

<sup>#</sup> Detection Limit

\* Concentration for benzo(b)fluoranthene and benzo(k)fluoranthene

PAHs were determined at two suburban sites in Athens, Greece, (Koropi & Spata) during June and November 2003 where 14 PAHs were quantified by GC-MS in the collected samples. The air was drawn through a 102 mm glass-fibre filter (GFF) for initial particle collection followed by a polyurethane foam (PUF) plug to collect gas phase compounds. Each sampling period was approximately 24 h and the sample volume was approximately 300 m<sup>3</sup>. The total PAH concentration in the gas phase ranged between 0.01-13.10 ng.m<sup>-3</sup> while it was between 0.02-0.69 ng.m<sup>-3</sup> in the particulate phase. The colder periods revealed the maximum concentrations of the total PAHs (gas and particulate phase) with an

average of  $40.7 \text{ ng.m}^{-3}$ . The most abundant PAHs were phenanthrene, anthracene, fluorene, fluoranthene and pyrene. Molecular diagnostic ratios were used to identify potential sources of aerosol PAHs and the results revealed diesel and gasoline engines to be the dominant sources with other sources such as liquefied petroleum gas and coal combustion also contributing (Vasilakos 2007).

PAH samples (period of 1 or 2 h) were collected in the Shing Mun Tunnel, Hong Kong, during summer and winter (Ho 2009). Gas and particulate phase samples were taken and the results showed that the gas phase samples ranged from  $0.8\text{-}670.4 \text{ ng.m}^{-3}$  with the lighter 2 and 3 ringed PAHs having the highest concentrations. The particulate samples ranged from  $0.15\text{-}28.60 \text{ ng.m}^{-3}$  which included the heavier PAHs.

Although urban areas were common in these studies, it is evident that PAH concentrations vary from country to country and the different sampling and analysis techniques make it difficult to directly compare the findings, not to mention the fact that the number and types of PAH sources in each sampling vicinity is not known nor is the condition and age of the vehicular fleets that emit PAHs. All of these variables affect the PAH concentration.

The literature findings may give an idea as to what range of PAHs are to be expected which can be compared to the experimental findings of this study. However, underground mines have not been thoroughly investigated therefore there is no specifically comparable data in the literature. What can be concluded from Table 2-1 is that the ambient particulate samples taken in heavy traffic areas have higher concentrations of the heavier 5-6 ringed PAHs such as dibenz(a,h)anthracene and indeno(1,2,3-cd)pyrene than lighter 3-4 ringed particulate PAHs which is what is expected from vehicle exhaust emissions as per other studies.

Concentrations of PAHs sampled in the gas phase were found to be significantly higher than particle associated PAHs in tunnels (refer to Table 2-1), with a maximum concentration of  $670.4 \text{ ng.m}^{-3}$  for acenaphthene.

## 2.4 Methods for PAH analysis

### 2.4.1 Sampling

When reviewing sampling methods for PAHs, Li-bin *et al.* grouped the methods into active sampling and passive sampling. For active sampling a high-volume sampler and impingement collectors are used with filters. Passive sampling on the other hand is based on the migration of target compounds through a concentration gradient (Liu & Li-bin 2007a). For the scope of this study only active sampling was reviewed.

Concentration of airborne PAHs are in the order of  $\text{ng.m}^{-3}$  which necessitates large volumes of air to be sampled during which the PAHs are concentrated on a sorbent material, for gas phase collection, or a suitable filter material for particle phase collection, these sampling mediums will be briefly reviewed in the following sections.

#### Collection of particle-phase PAHs

GFFs are the most commonly used sampling media for particle-phase PAHs and most studies require the use of large sampling volumes to ensure sufficient collection of these compounds. Although large sampling volumes are employed in most studies, it should be noted that this is not the case for the specific flow rate and total sampling volume which vary between each study (Gustafson, Dickhut 1997, Omar *et al.* 2002, Yang *et al.* 2010, Castells, Santos & Galceran 2003, Zhang *et al.* 2009). Emfab is a modification of GFF in that it is coated with Teflon and it was successfully employed to collect particle phase PAHs from urban areas in Syria and the UK with total volume of sampled air being 900-1000  $\text{m}^3$  (flow rate of 650–750  $\text{L.min}^{-1}$ ) (Dimashki, Harrad & Harrison 2000).

Quartz-fibre filters (QFF) are another popular medium employed for the sampling of particle phase PAHs including methods that require low sampling volumes. In an urban area of Seoul, a study by Park *et al.* saw the collection of 16 priority PAHs on QFFs (102 mm diameter) (Park, Kim & Kang 2002) whilst Lottmann *et al.* collected 8 priority PAHs on QFFs (150 mm diameter) by sampling a total volume of 720  $\text{m}^3$ , at 1250  $\text{L.min}^{-1}$ , at a university campus in Strasbourg, France (Lottmann *et al.* 2007).

Depth filters such as quartz fibre and glass fibre filters offer high loading and retention capacities as well as fast flow rates which is why they are used for air pollution monitoring. Microfiber filters offer high



resistance to chemical attack and are biologically inert; they are also easily sterilized and easily stored (Msscscientific 2014). High-purity QFFs ( $\text{SiO}_2$ ) are used more often for air pollution monitoring as they have higher thermal stability and higher purity than GFFs. The quartz composition prevents the filters from reacting with acidic gases and due to the low level of alkaline earth metals, the artefact products of sulphates and nitrates are eliminated. This is unlike GFFs that can cause false readings as they may react with analytes. QFFs are heat treated for reduction of trace organic contaminants which is vital when sampling at trace levels as in this study (Msscscientific 2014).

Teflon filters are often reported for particulate phase PAH collection, however they are not as commonly used as the other fibrous filters as previously discussed. In a specific study, indoor Taiwanese coffee shops were divided into non-smoking and smoking zones and Teflon filters were mounted in personal environmental monitors for the collection of PAHs in  $\text{PM}_{2.5}$ . A sampling period of 8 h, at a flow rate of  $4 \text{ L}\cdot\text{min}^{-1}$ , was employed and it was consequently found (after analysis by GC-FID) that concentrations of PAHs were higher in smoking areas compared to non-smoking areas (Lung, Wu & Lin 2004).

Aluminium foil has high thermal conductivity and has also been tested for particulate phase PAH (along with other SVOCs) sampling (Falkovich, Rudich 2001b). Falkovich and Rudich collected urban  $\text{PM}_{10}$  samples on an aluminium foil substrate which was installed in an 8 stage cascade impactor at a flow rate of  $28.3 \text{ L}\cdot\text{min}^{-1}$  for a duration of 50 h. The aluminum foils were heated beforehand to  $500 \text{ }^\circ\text{C}$  for a duration of 24 h for quality assurance purposes. It was noted by the authors that the aluminum foil had very high efficacy for thermal desorption (TD) whereas QFF may be prone to unwanted pyrolysis of long-chain compounds during the TD process, which will lead to false readings (Falkovich, Rudich 2001b). A limitation to their studies was the fact that only particulate phase PAHs were determined and the gas phase PAHs, which are more abundant, were not considered. Also, the extended sampling time with the high sampling volume may result in overloading of the filter/foil beyond the loading capacity, which would give inaccurate estimations of particulate PAH exposure. The particulate on the filter may also be further underestimated due to blow off from the filter/foil (Forbes *et al.* 2012).

## Collection of gas-phase PAHs

Generally, gas phase collection follows the upstream collection of particulate matter which is why the focus of the following section will be on the sorbents used for collection of gas phase PAHs. There are generally three types of solid sorbents that are used for sampling organic compounds in air, namely: porous organic polymers, inorganic sorbents and carbon based porous material.

The first group is the polymer sorbents of which styrene–divinylbenzene copolymers (Porapak, Chromosorb), ethylvinylbenzene/divinylbenzene copolymers, polyvinylpyrrolidone, polyphenylene oxides (Tenax) and polyurethane foams are included. Inorganic sorbents include molecular sieves/zeolites, silica gels, magnesium silicates and aluminum oxides and the last group, the carbon based porous material, include sorbents such as carbon blacks, graphitized carbon blacks (Carbotrap, Carbo-pack, Carbograph), activated charcoals and graphitized molecular sieves.

The most frequently used sorbent that has been used for gas phase PAH sampling is PUF and it has shown its applicability for an extensive range of PAHs, including the 16 priority PAHs as well as their oxy- and nitro- derivatives.

Mandalakis *et al.* sampled 450–900 m<sup>3</sup> of air from an urban area, a coastal area and a background site in Athens, Greece during the month of July in 2000. The authors used a PUF plug with a diameter of 7.5 cm and a length of 8.0 cm to successfully collect 20 gas phase PAHs which ranged from 3.5 ng.m<sup>-3</sup> for the background site to 26.0 ng.m<sup>-3</sup> for the urban site (Mandalakis *et al.* 2002). In a later but similar Grecian study, Tsapakis and Stephanou passed 900 m<sup>3</sup> of urban air at a flow rate of 600 L.min<sup>-1</sup> through PUF in order to trap a total of 24 airborne PAHs, the study revealed that gas phase PAHs ranged from 31.4–84.7 ng.m<sup>-3</sup> (Tsapakis, Stephanou 2005). Dimashki *et al.* employed similar parameters with a flow rate of 650–750 L.min<sup>-1</sup> to obtain a sampling volume of 900–1000 m<sup>3</sup> from two urban locations in Syria and the UK (Dimashki, Harrad & Harrison 2000). More than one PUF plug can be used to increase efficacy of collection, this was demonstrated by Gustafson and Dickhut who trapped particulate phase PAHs on GFFs after which they trapped 14 priority gas-phase PAHs on two PUF plugs. This was at industrial and urban sites with a flow rate of 0.51–0.75 L.min<sup>-1</sup> and a total sampled volume of 172–665 m<sup>3</sup> of air (Gustafson, Dickhut 1996).

Not only can the number of sorbent devices be increased but mixed sorbents have also been used in various studies to enhance method sensitivities. As already mentioned, PUF samplers are the most frequently used sorbents which is why it is often used in combination with other sorbents i.e. Lee *et al.* used a glass cartridge containing a 5 cm PUF plug and a 2 cm PUF plug that were separated by 3 cm XAD-2 resin in order to collect PAHs in gas phase from a traffic impacted area (Lee *et al.* 1995), then, Wauters *et al.* used a mixed sorbent bed consisting of 1 cm polydimethylsiloxane (PDMS) foam, 120 mg of PDMS particles and 60 mg Tenax (TA) for the collection of 16 priority PAHs by sampling air at a rate of 100 mL.min<sup>-1</sup> for 24 h using personal air pump. The authors then compared the mixed sorbent bed method to the conventional method (high volume sampling onto a PUF sampler for a period of 24 h) and although they found contrasted sampling volumes, between 144 m<sup>3</sup> for mixed bed and a much higher 1296 m<sup>3</sup> for the conventional method, they found that the mixed bed approach yielded much better recoveries and was considered to be the superior of the two methods (Wauters *et al.* 2008b).

Depending on the amount and type of SVOC to be determined, there are a wide range of sorbents (and/or combinations thereof) to choose from that offer different suitability for analysis. There are associated disadvantages for every sorbent which need to be taken into consideration when developing an appropriate method.

During production, storage and shipping the sorbents will be affected by contamination therefore all sorbents have to be cleaned by extraction or thermal treatment prior to use. For carbon based and inorganic sorbents the contaminant removal is most effectively accomplished by heating in an inert gas stream of helium or nitrogen for a few hours, after which an added deactivation step may be required (depending on the intended use of the sorbent) for inorganic sorbents including: magnesium silicates, aluminum oxides and silica gels. Tenax can be thermally cleaned at 280-300 °C for 1 h in an inert stream of high purity helium or nitrogen, as traces of O<sub>2</sub> will lead to artefact formation on the sorbent. Most of the other polymer adsorbents such as PUF and XAD resins should be cleaned by solvent extraction and dry purging with pure nitrogen as they have limited thermal stability, however these steps are time consuming and necessitates the use of toxic organic solvents which is seen as a disadvantage of these sorbents. Their limited thermal stability (<200 °C) would not be suitable for the high temperatures that are incurred during a process such as thermal desorption.

After a certain time period has elapsed, solid sorbents may show background artefacts due photochemical or thermal degradation of the sorbent material, not to mention the fact that many

sorbents can react with reactive gases ( $O_2$ ,  $O_3$  or  $NO_x$ ) or certain adsorbed compounds resulting in unwanted reaction products in the analysis results. The process of artefact formation and/or degradation is inevitable when organic compounds, with limited stability, are exposed to reactive chemicals, high temperatures or active surfaces (Uhde 2009). The active surfaces of the adsorbents render them extremely sensitive to contamination therefore it is vital to practice quality control at all times. To avoid volatilization and loss of PAHs on the filter or sorbent, samples should be protected from light and kept at temperatures as low as  $-18\text{ }^\circ\text{C}$  until analysis is complete (Liu & Li-bin 2007a).

Traces of water can not only influence detector signals but it can also give rise to a high background noise level in GC-MS chromatograms and at elevated temperatures it has been demonstrated to damage fused silica columns due to hydrolysis. This should be taken into account when employing some inorganic sorbents as well as carbon based sorbents as they show reasonably high uptake of water. This characteristic renders inorganic and carbon based sorbents inappropriate for the sampling of PAHs underground where the relative humidity reaches 85 %. If such sorbents are used in high humidity environments (such as underground) then additional steps need to be employed in order to remove water during or after sampling, which will ultimately increase total analysis time and potentially cause loss of analyte recovery.

For solvent free sampling applying thermal desorption, polydimethylsiloxane (PDMS) has been used as a sorbent in the form PDMS traps (Baltussen *et al.* 1997) and more recently, quartz multi-channel PDMS traps (Forbes & Rohwer 2009). Thermal desorption has many advantages including decreased time and cost of analysis and reduced risk of analyte loss and possible introduction of contamination due to the fact that the entire sample is desorbed with no additional extraction or clean-up steps. The fact that no solvents are needed contributes to the cost saving factor but more so it eliminates the negative environmental impact of the solvents as well as the negative human health effects that are associated with the use of organic solvents. The disadvantages of TD are that the entire sample is used so no repeat analysis is possible, and compounds that are less volatile will not readily be desorbed so the method is less successful with high boiling point analytes.

## Denuder samplers

In 2012, Forbes *et al.* took into consideration the co-existence of particle and gas phase PAHs in the atmosphere. The differing phases have different health and environmental impacts and it is therefore necessary to quantify both as they occur naturally. Forbes *et al.* then went on to study the use of multi-channel (MC) silicone rubber traps as denuders for PAHs where two multi-channel silicone rubber traps were separated by a QFF for particle phase collection, as shown in Fig. 2.7 (Forbes *et al.* 2012).

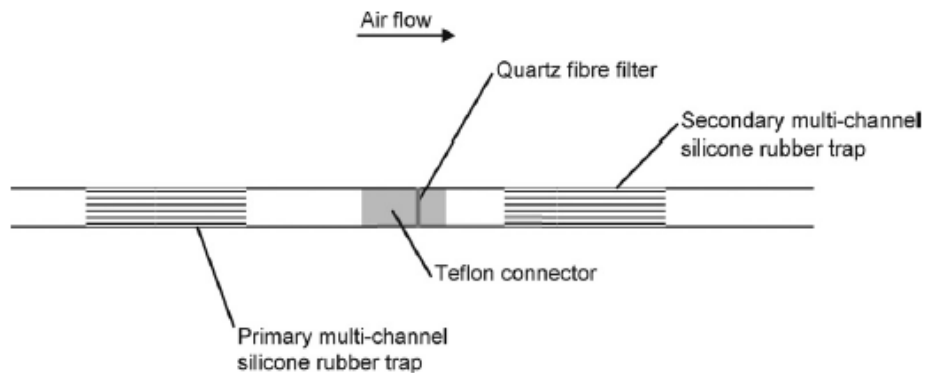


Figure 2-7 Schematic diagram of a denuder consisting of multi-channel silicone rubber traps and a quartz fibre filter (Forbes *et al.* 2011)

Each of the traps consisted of twenty-two parallel 55 mm long PDMS tubes with 0.3 mm inside diameter, 0.6 mm outside diameter, housed in a 178 mm long glass tube. To provide laminar air flow through these traps, flow rates of approximately  $0.5 \text{ L}\cdot\text{min}^{-1}$  were employed. Visual inspection of the traps prior and post sampling demonstrated successful particle collection on the filters, whilst the PDMS traps remained clean and particle free, which can be attributed to the different diffusion coefficients of the gas and particles. This denuder technology was later used to sample SVOC emissions from sugar cane burning and to sample diesel exhaust emissions (Forbes *et al.* 2012).

The standard sampling setup for gas and particulate phase sampling includes the use of a GFF filter with a PUF cartridge, with the air being drawn through the setup by a high volume sampler. There are limitations to this conventional method of PAH sampling including blow off and adsorption effects. Blow off from the filter occurs when the particulate phase has been sampled onto the filter but due to continuous airflow from the high volume sampler, the analyte on the filter could be lost due to blown off which would lead to an under estimation of particulate phase PAHs. Adsorption effects occur when particles on the filter adsorb gas phase particles which would ultimately result in an underestimation of

gas phase PAHs. In terms of physical limitations, the GFF/PUF sampling setup is not very easy to manoeuvre or transport and the setup is expensive.

The PDMS based denuders (as investigated by Forbes *et al.*) on the other hand are very small, lightweight and portable devices which are cost effective and easy to make. Blow off and adsorption effects are minimal due to the design of the denuder devices particularly due to the presence of the secondary trap.

Another denuder (and PUF alternative) was suggested by Possanzini *et al.* who tested a glass denuder that was coated with 20-40 mesh XAD-4 resin for trapping PAHs in the gas phase and contained a QFF for trapping PAHs in the particulate phase. A flow rate of 6 L.min<sup>-1</sup> over a period of 6 h allowed them to evaluate the efficacy as well as capacity of the denuder and they concluded that the collection efficiencies of the smaller, two and three ringed, PAHs were found to exceed 90 % [97 % for NAP, 90% for PYR] (Possanzini *et al.* 2004).

#### 2.4.2 Extraction of PAHs from airborne particles

The analysis of PAHs in DPM normally involves tedious extraction or clean-up steps, one commonly being Soxhlet extraction. Extraction methods are continuously being modified in order to reduce the amount of solvent required as well as to shorten the extraction time which has been demonstrated by various techniques including: sonication using a mixture of n-hexane : petroleum ether (1/1, v/v) as solvents (Aydin, Ozcan & Tor 2007, Christensen, Östman & Westerholm 2005), pressurized-fluid extraction (PFE) using a hexane:acetone mixture (Alexandrou *et al.* 2001) and supercritical fluid extraction (SCFE) using pure carbon dioxide (Hawthorne *et al.* 2000). Sonication is convenient and it reduces the solvent volume and extraction time, however, it is noteworthy that PAHs of higher molecular weight are less extractable.

PFE was used in a study by Bamford *et al.* who successfully quantified 28 nitro-PAHs (mono and dinitro compounds) as well as several isomers, in air samples and in DPM standard reference material (SRM). In the method approximately 100 mg of the particulate material from the air samples and 50 mg of the DPM SRMs (SRM 1650a and SRM 2975) were extracted using PFE with dichloromethane (DCM). PFE is operated at high temperatures and pressure which is why it offers an advantage over traditional extraction methods, such as Soxhlet extraction, in that the process is accelerated (Bamford *et al.* 2003).

In 2007 Aydin *et al.* used ultrasonic solvent extraction (USE) for the determination of PAHs in airborne particles that were trapped on GFFs. The aim of the study was to initially optimize the extraction procedure in order to increase the extraction efficacy with minimum solvent and time consumption. The extraction was optimized by the investigation of the following experimental parameters: type and volume of solvent, sonification time and number of extraction steps. The optimized mixture was selected as a mixture of n-hexane: petroleum ether (1/1, v/v) as it gave the highest recoveries ( $78 \pm 2$  to  $100 \pm 6$  %) with an optimum volume of 75 ml and an optimum sonication time of 45 min. When investigating the optimum number of steps, it was concluded that there was no significant difference ( $p > 0.05$ ) in the PAH recoveries when extracting with a solvent volume of 75 ml (for 45 min) once or dividing the 75 ml into three aliquots and extracting it three times for 15 minutes sequentially. When compared to the conventional Soxhlet extraction methods it was found that the optimized USE method was significantly faster and it reduced solvent consumption by 80 % (Aydin, Ozcan & Tor 2007).

Extraction of gaseous PAHs has been conducted most frequently from PUF using traditional solvent based methods however, methods where no solvent is required, such as thermal desorption (TD), are sufficiently advanced to allow comparison between various sorbent materials. TD has been introduced as an alternative method for extracting VOC and SVOCs in airborne PM as it is more sensitive and more readily automated than traditional extraction methods and it has the advantage of decreasing the time and cost of analysis as well as reducing the risk of analyte loss or contamination. However, a disadvantage of TD is the fact that dedicated instrumentation is required (Bates *et al.* 2008). The main advantage of TD is that no solvent extraction is required. Therefore there is no need for the use of toxic solvents which have adverse effects on the environment and human health which compensates for the limitations of TD.

Wei *et al.* were able to eliminate the use of toxic solvents in their one step microwave assisted desorption (MAD) method which was coupled to headspace solid-phase extraction (HS-SPME), however it could not be considered a fully solvent free method. In the study, 8 PAHs were adsorbed onto the XAD-2 sorbent after which they were desorbed into ethylene glycol. The PAHs were then evaporated into the headspace by microwave radiation and finally adsorbed onto a SPME fibre for MS detection which resulted in a recovery rate of  $>80$  % (Wei, Chang & Jen 2007). Even better recovery rates of  $>85$  % were achieved by Fan *et al.* using a solvent free TD method with a honeycomb-like sampler (320 sections of 1 cm long SPB-5 GC column) for the trapping of 8 gas phase PAHs (NAP, ACE, ACY, FLU, PHE, ANT, FLA and PYR). Although the recovery was good, it was suspected that temperature inhomogeneity in the TD

system resulted in large variability in the recoveries for FLA and PYR specifically with % RSDs of 36 % and 30 % respectively (Fan, Jung & Liou 2006). In another solvent free method, Wauters *et al.* employed a mixed sorbent-bed for collection of 16 priority PAHs which were then analysed by TD-GC-MS to reveal recoveries in the range of 80.5-118 % ((Wauters *et al.* 2008a).

A TD method and a standardized liquid extraction (LE) method were compared by Van Drooge *et al.* by the evaluation of recovery ratios of certain PAHs that were bound to particles which were trapped on QFFs. They found that the TD method showed higher recovery ratios than the LE method for PHE and ANT specifically however, the two methods were comparable for every other PAH (van Drooge 2009). Solvent free TD was further confirmed as a good alternative to solvent based methods by Bates *et al.* who achieved impressive recoveries in the range 99.1 % for BaA to 95.5 % for BghiP which were also trapped on QFFs (Bates 2008).

Falkovich and Rudich, 2001, published a paper on analysis of SVOCs in atmospheric aerosols by TD-GC-MS with direct sample introduction. They noted that conventional procedures including solvent extraction, pre-concentration, and in some cases, derivatization had the disadvantages of being time-consuming (up to 30 h), requiring large samples, and were not very sensitive as losses are inevitable due to the numerous steps. These reasons motivated them to explore thermal desorption as a sample introduction technique. They sought to use thermal desorption in conjunction with temperature and pressure-controlled sample introduction which was seen to be an improved technique than what had been published at that time. After sample introduction they heated the injector to 350 °C, at a rate of 200 °C min<sup>-1</sup>, and held it at 350 °C to attain thermal desorption after which the analyte proceeded into the GC column and MS for analysis. With this method they were successfully able to determine different classes of compounds. They noted that the technique was limited to compounds with a boiling point of up to 100 °C higher than that of the injector temperature and that compounds with boiling points closer to the injector temperature may escape during sample loading which would result in low sample recovery for those species (Falkovich & Rudich 2001a).



### 2.4.3 Instrumental analysis

The identification and characterization of PAHs and nitro PAHs in PM (specifically DPM for the purpose of this study) has been done using various analytical techniques and combinations thereof. GC-FID was used to quantify PAHs in Dehli, India (Sharma 2008), GC-MS, GC-flame ionization detection (FID) and high pressure liquid chromatography (HPLC) were used to analyse PAHs, hydrocarbons and PM in a tunnel in Gothenburg, Sweden (Wingfors 2001) and HPLC-with ultraviolet fluorescence detection (UV-FL) was used in Hong Kong to analyse and quantify 17 PAHs in the Shing Mun tunnel (Ho 2009). Methods using gas chromatography and mass spectrometry will be emphasized in the following sections as they were relevant to this study.

#### 2.4.3.1 Gas chromatography

In 2007, a review on development of analytical methods for PAHs by Liu *et al.* was published. They summarised the first EPA standard analytical method for atmospheric PAHs and went on to review other methods which emerged with development of technology. Among the modern methods they highlighted that chromatography was the principal technique in the analysis of air pollutants. They pointed out that among the chromatographic methods, HPLC, particularly reverse phase HPLC, was preferred over GC as one could use it without considering volatility and molecular weight. GC was however, preferred for analysis of oxy- and nitro-PAHs because of its high resolution, sensitivity and selectivity. Li-bin *et.al* also noted that due to the electronegative nature of the oxy- and nitro- groups combined with the aromatic rings of the PAHs, the most sensitive and selective detection of these compounds would be based on electron capture and thus reported negative-ion chemical ionization mass spectrometry (NCI-MS) as a widely used detection technique because it had the lowest limits of detection (Liu *et al.* 2007a).

In the previously mentioned paper that was published by Falkovich and Rudich on analysis of SVOCs in atmospheric aerosols, TD-GC-MS instrumentation was employed. The samples were collected on GFFs for a duration of 73 h using a pump flow rate of 28.3 L.min<sup>-1</sup>. The authors found that the fibre filters promoted pyrolysis of long-chain compounds and they therefore resorted to using aluminium foil instead. Upon analysis, they loaded their samples, a SRM, and piece of sampling filter into a disposable microvial inside the GC injector which initially vaporised VOCs with a low injector temperature with helium employed as the carrier gas. A temperature of 350 °C was used to attain thermal extraction of

the SVOCs, including PAHs, which then proceeded into the GC column and MS for analysis. With this method they successfully determined different classes of compounds (Falkovich, Rudich 2001a).

A TD-GC-MS technique for the quantification of PAHs in ambient particulate matter was developed by Waterman *et al.* in 2000, using the NIST Urban Dust SRM 1649a. The total chromatographic response for the SRM showed very good linearity with a correlation coefficient of 0.971 for a range of SRM weights of 1-5 mg (Waterman *et al.* 2000). In 2008 Bates *et al.* also evaluated the technique of TD-GC-MS in measuring airborne PAHs (4-6 rings) which were collected onto QFFs. Samples were collected using a low volume sampler with a volumetric flow of  $1 \text{ m}^3 \cdot \text{h}^{-1}$  for a period of 24 h. The method that was developed was applied to the analysis of PAH standards which were loaded on tubes packed with Carbograp2 and quartz wool, this allowed the repeatability, precision, sensitivity, recovery efficiency and desorption efficiency of the method to be determined. The resultant correlation coefficients were all above 0.997 (except for dBahA). The four quadrants of a filter were analysed to obtain a % RSD <9 % which implied that the filters were homogenous and SRM 1649a was also analysed to further verify the developed method (Bates *et al.* 2008).

#### 2.4.3.2 Two dimensional gas chromatography

Two dimensional gas chromatography (2D GCxGC) is an advanced technique where two different GC columns are connected in series therefore subjecting all compounds to two different modes of separation (such as polarity and volatility) which potentially results in superior separation than that of the conventional one dimensional GC methods. A thermal modulator is needed between the primary and secondary column in 2D GC to trap eluted compounds and then introduce them into the secondary column (Dimandja *et al.* 2003; Focant *et al.* 2003, Schoenmakers *et al.* 2003). This technique has been employed for numerous studies involving PAHs in different fields and it can be coupled with other instrumentation for detection. An example of an effective instrument coupling is GCxGC-ToFMS which allows for separation and detection of full scan spectra data at low  $\text{pg} \cdot \mu\text{L}^{-1}$  levels in injected liquid samples which is useful in the rapid determination of priority pollutants that have human and ecological health impacts (de Vos *et al.* 2011).

Aromatic compounds in heavy gas oil were characterized in Brazil by GCxGC-ToFMS whereby a HP-5 MS, 5 %- phenyl–95 %-methylsiloxane (30 m, 0.25 mm i.d., 0.25  $\mu\text{m}$  df) was employed as the primary column and a BPX-50, 50 %- phenyl–50 %-methylsiloxane (1.5 m, 0.1 mm i.d., 0.1  $\mu\text{m}$  df) as the secondary column. It was found that all of the aromatic fractions of the oil samples contained PAHs of which

naphthalene, alkylnaphthalenes, phenanthrene, alkylphenanthrenes, alkylpyrenes, benzo(a)anthracene, chrysene, alkylchrysenes, benzo(k)fluoranthene, benzo(a)pyrene, dibenzo(a,h)anthracene and benzo(g,h,i)perylene were detected (Ávila *et al.* 2012).

The high selectivity and sensitivity as well as the high separation power of GCxGC-MS have seen its increased use in environmental analysis and monitoring in the past few years (Panić 2006, Teruyo 2011). As an example: a method for rapid, non-targeted screening for environmental contaminants (including PAHs) in household dust was performed by Hilton *et al.* whereby a NIST reference material was extracted with hexane using ASE. The concentrated extract was analyzed by GCxGC-ToFMS where 106 PAHs (or analogues) were reported including all of the PAHs reported by NIST at a concentration of over 300 ng.g<sup>-1</sup> dust. It was noted that PAH classification was restricted by the definition of a region of the 2D chromatogram where PAHs are expected, as some other molecules may have similar mass spectral properties (refer to Fig. 2-8) (Hilton *et al.* 2009).

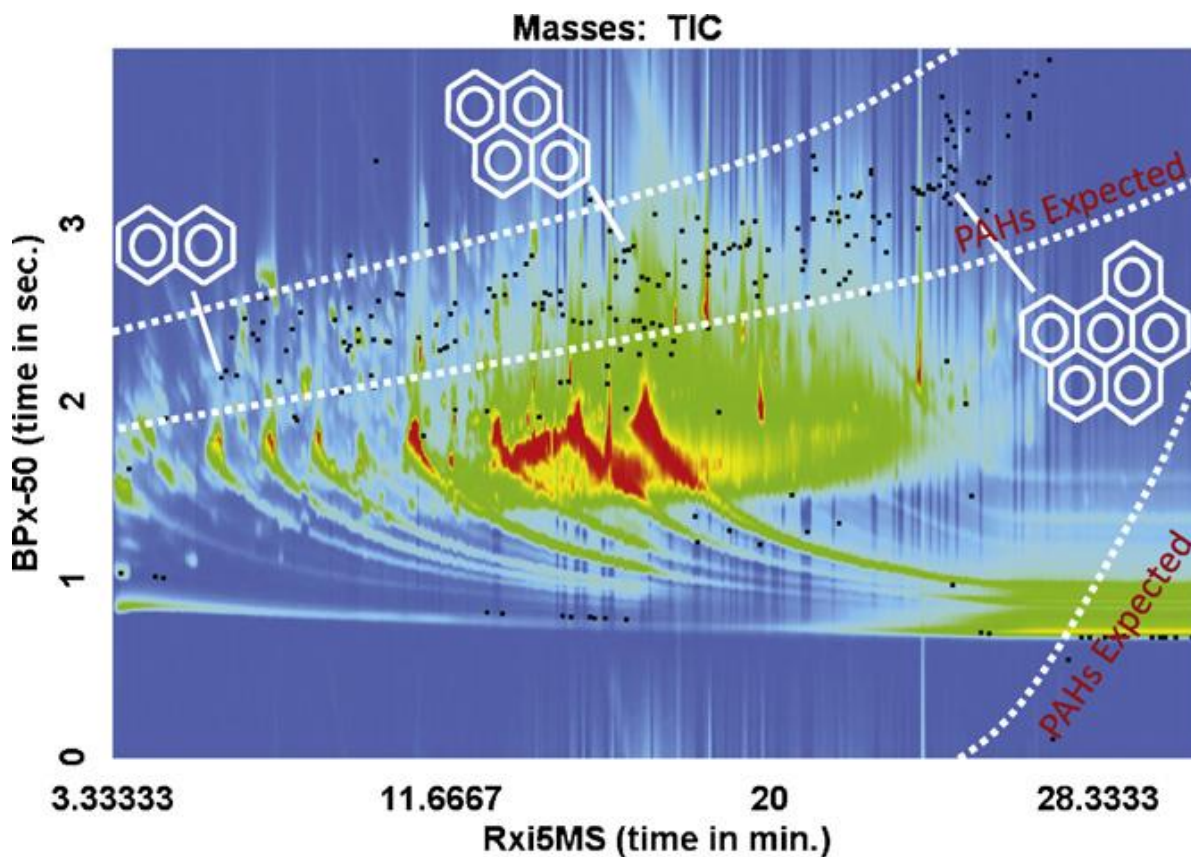


Figure 2-8 Total ion chromatogram showing the expected area for PAH elution (Hilton *et al.* 2009)

Other environmental samples, including soil extracts, were analysed for chlorinated and brominated PAHs by GCxGC that was coupled to high resolution time-of-flight mass spectrometry (HRTofMS). The results revealed the successful identification of 30 Cl<sup>-</sup>/Br<sup>-</sup> PAHs including 10 higher chlorinated PAHs (e.g. penta, hexa and hepta substitution of fluorene, phenanthrene, anthracene, fluoranthene, pyrene, chrysene, benz(a)anthracene, benzo(a)pyrene, benzo(b)fluoranthene and benzo(k)fluoranthene) in soil extracts without the use of standard material (Ieda *et al* 2011).

In 2010, Dasgupta showed that a GCxGC-ToFMS method could be optimized and applied to the analysis of grape and wine extracts for simultaneous analysis of 12 PAHs, 160 pesticides, 12 dioxin-like polychlorinated biphenyls (PCBs) and bisphenol. The method was effectively developed and optimized with recoveries of over 148 compounds ranging from 70 to 120 %. The limit of detection (LOD) and limit of quantification (LOQ) were calculated using the signal-to-noise (S/N) method (LOD set to 3 x S/N in a blank and LOQ at 10 x S/N in a blank) and the LOQs of the majority of the analytes were  $\leq 10 \mu\text{g.L}^{-1}$  with a few exceptions (Dasgupta 2010).

A highly sensitive method for the determination of particle associated PAHs and their derivatives (alkyl-, oxy- and nitro-PAHs) was developed by Fushimi *et al* who employed TD-GCxGC coupled with tandem mass spectrometry (MS/MS) with a selected reaction monitoring mode. Fan shaped gold foil (47 mm) was used to collect particles from an 8 L diesel engine, with no after treatment device, which included 18-32 nm exhaust particles as well as larger 100-180 nm accumulation-mode particles. The instrumental detection limits were 0.03–0.3 pg for PAHs and between 0.01–0.2 pg for the derivatives. The following PAHs were successfully quantified: phenanthrene, fluoranthene, pyrene, anthracene, benz(a)anthracene, chrysene, benzo(b) and (k) fluoranthene, benzo(a)pyrene, dibenzo(a,h)anthracene, indeno(1,2,3-cd)pyrene and benzo(g,h,i)perylene. The authors noted that the PAH profiles did not differ significantly between the different particle sizes, however they did differ among driving conditions (Fushimi *et al*. 2012).

### 2.4.3.3 Tandem MS/MS

The use of tandem mass spectrometry is gaining worldwide popularity and the number of applications involving this technique is growing significantly but it is a complex method and the instrumentation is expensive. In MS/MS the compounds are separated by mass, which is completely different to GC in which the compounds are separated by chemical properties (affinity for stationary phase). Tandem MS has high speed capabilities and allows for the analysis of complex mixtures as it offers the advantage of analytical selectivity and sensitivity, by reducing interferences from other sample components, even in the absence of prior chromatographic separation (Covey, Lee & Henion 1986). Tandem MS is less time consuming and requires less sample preparation and solvent use, which renders it an attractive analytical technique. This was also the general consensus by Hutzler *et al.* who are convinced that their method for the detection and analysis of 16 PAHs and nitro-PAHs, using LC-MS/MS, could be employed as a standard procedure for the quantification of carcinogenic PAHs in complex environmental mixtures (Hutzler, Luch & Filser 2011). In this particular study, diesel soot from old and new car engines as well as old and new truck engines (Euro 0 and Euro 4 engine technology for old and new vehicle respectively) were collected on filters and extracted by Soxhlet extraction with a SPE clean-up step, which prevented contamination of the MS with the polar matrix. Mass spectral data was collected in the multiple reaction monitoring (MRM) mode and the collision energy and potential parameters were optimized for each single analyte. The results for the NIST DPM 2975 SRM analysis confirmed that the developed LC-MS/MS method (using atmospheric pressure photoionization) was sensitive enough to detect the entire range of compounds stated by NIST and additional PAH species such as Db(a,l)P and Db(a,e)P which are also carcinogens. The quantification results showed higher amounts of analytes from car samples (1.89–2.41  $\mu\text{g}\cdot\text{g}^{-1}$ ) than the truck samples (0.01–0.11  $\mu\text{g}\cdot\text{g}^{-1}$ ) (Hutzler, Luch & Filser 2011).

A wide range of instrument coupling combinations and ionization methods exist for MS, depending on the type of analysis required, for example: Lintelmann *et al.* analysed oxygenated PAHs in ambient aerosols utilizing HPLC coupled to an atmospheric pressure chemical ionization (APCI) source and a tandem quadrupole (Q)-MS for MS/MS (Lintelmann, Fischer & Matuschek 2006) and in 2007, PAHs were analysed by LC-MS/MS using APCI or electron ionization (EI) with tropylium post-column derivatization (Lien, Chen & Wu 2007) and more recently, in 2010, Frenich *et al.* determined PAHs in airborne PM by GC-triple Q-MS/MS (Frenich, Ocana & Martínez Vidal 2010).

In other findings, Miller-Schulz *et al.* (2007) demonstrated a procedure for the analysis of 1-nitro pyrene (NP) in ambient PM samples that used stepwise 2D HPLC, on-line reduction, and MS/MS analysis. The

method involved ultrasonic extraction of ambient PM, in a 3:1 benzene:ethanol mixture, where the concentrate was analysed by HPLC after which 1-NP was isolated and converted to 1-aminopyrene (1-AP) via online reduction (in a catalytic Pt/Rh packed column) and then refocused on a trapping column, where eluent was passed through a second HPLC column prior to MS/MS detection. The analysis of NIST 1649a SRM revealed that the assay accuracy and precision was from  $53 \pm 9.2$  %. The LOD and LOQ were reported to be 152 and 221 fg on column respectively, which is orders of magnitude lower than what has been reported for other instrumentation with an approximate 10-fold improvement in sensitivity over HPLC methods employing chemiluminescence and/or fluorescence detection (Miller-Schulze *et al.* 2007).

#### 2.4.4 Challenges of analyzing DPM and PAHs

As discussed DPM is comprised of many different compounds either elemental or organic in nature, which renders DPM as a very complex matrix. Adding to the complexity of the matrix, the main obstacle in environmental analysis is that the analytes of interest are typically present in trace amounts. PAHs exist both in gas and particulate phases and are SVOCs, which makes the sampling of these compounds an extreme challenge where conventional sampling setups cannot be used especially in an underground environment.

The analysis of PAHs is normally a very time consuming task which often requires lengthy extraction and clean-up procedures, all of which introduce the risk of analyte loss and introduces the possibility additional contamination. The analysis of PAHs requires costly instrumentation with very low detection limits and instrument availability is an ever-present obstacle.

To overcome these challenges, a combination of different techniques covered in this literature study can be combined. Novel denuder devices can be used for sampling DPM underground where PAHs in both phases will be sampled in an effective, cost efficient and practical manner. The denuders can then be analysed by TD-GCxGC-ToFMS which requires no extraction or clean-up step as samples are directly analysed. The two dimensional GC offers high separation power, high sensitivity, high selectivity and the time of flight MS detection is sensitive and selective with high speed capability. The method has reduced analysis time and cost (although the instrument cost is significant) and there is no need for toxic organic solvents.

#### 2.4.5 Microscopy based characterization of particulate matter

Electron microscopy can provide details of individual particles as well as particle apportionment and it is often used in conjunction with bulk analytical methods as a complementary technique. It can also provide particle size information which is important from a human health perspective with respect to inhalation ie.  $PM_{2.5}$  is more likely to penetrate the deepest part of the lung, where oxygen enters the blood stream thus having adverse health implications (DEEE 2001). Transmission electron microscopy (TEM) and scanning electron microscopy (SEM) will be briefly discussed in this section specifically for their application in environmental studies for ambient  $PM_{2.5}$  characterisation as well as for individual particle analysis. Substrate interferences are often the cause for complications in fine PM characterization using electron microscopy. Energy Dispersive X-ray Spectroscopy (EDS/EDX) is frequently employed in conjunction with SEM for additional qualitative information whereby x-rays, that are characteristic to the parent element, are emitted due to the interaction of the electron beam with the sample. The resultant x-rays are detected and measured which can provide qualitative elemental composition information as well as elemental quantification if adequate standards are used.

In recent years a number of studies involving the application SEM and TEM techniques to environmental studies has been performed and will now be briefly overviewed. In 2012, Liati *et al.* used electron microscopy to investigate the PM ash deposits on a diesel particulate filter (DPF) from an operating light duty truck with the first ash sample being taken from the central part of the DPF and the second from the periphery which had lower ash deposits than the central sample. The following elements: O, S, Ca, P, Zn, Mg were found most frequently on irregularly shaped, usually round, agglomerates after detailed SEM imaging and EDX was performed and it was noted that Ca, S and O were often in the form of  $CaSO_4$  which is a common component in diesel ash. Other elements such as Al, Si and Fe were found in reduced amounts when compared with the other listed elements. The PM from the DPF exit, in the exhaust gas, was also imaged by SEM following EDX analysis and it showed the collection of ash particles and/or particle aggregates, which ranged in size from 200 to 600 nm, indicating that under normal engine operating conditions some large agglomerates may escape the DPF. The agglomerates were comprised of mainly Fe with small amounts of Ni and Cr which originated from the wear of the engine with Ca-, Zn- and Ti-oxides and small amounts of Sn and P also being present during the sampling of the exhaust (Liati *et al.* 2012).

TEM has the advantage of offering higher resolution information about the surface texture, morphology, size of individual ash particle as well as the internal structure thereof, which is why Liati *et al.* also opted for complementary TEM analysis of the periphery and center of the diesel particulate filters. The TEM images of ash from the DPF periphery showed ash agglomerates consisting of individual particles ranging in size between approximately 10-700 nm. Very fine, round, equi-dimensional crystalline particles (approximately 5 nm) were observed to form aggregates which were seen in both the centre and periphery samples. It was therefore concluded that the difference in temperature between DPF periphery and center did not have an effect on the ash aggregate densification (Liati *et al.* 2012).

In 2009 a study in El Paso, USA, was done involving indoor and outdoor PM which was comprised of both natural and anthropogenic matter. The PM samples were collected directly onto the TEM coated grid platforms using high volume air filters, electrostatic precipitation, and thermophoretic precipitation (TP) (Murr, Garza 2009). The principle of TP is based on the path of an aerosol particle in an aerosol stream, through a narrow slot between cold and hot plates, which experiences a thermal force (towards the lower temperature) with a magnitude dependent on the temperature gradient that exists between the two plates as well as the characteristic properties of the gas and particle (Dixkens *et al.* 1999). The collected PM was systematically characterized by TEM, EDS and SEM and from the work it could be concluded that 93 % of outdoor PM<sub>1</sub> was found to be crystalline and approximately 40 % of the PM<sub>1</sub>, in indoor and outdoor environments, was carbonaceous. Soot PM included multi-concentric fullerenes and multi-walled carbon nanotubes (MWCNTs) and was seen to consist of aggregated and branched fractal-like clusters of primary nanospherules, with diameters in the range of 25–75 nm. Over 80 % of all atmospheric nano-PM was aggregated with (MWCNT) aggregates and nano-PM soot aggregates containing up to  $3 \times 10^3$  primary nanoparticles (Murr, Garza 2009).

Chandler *et al.* characterized and compared DPM emissions using two techniques namely: measurements with a mobility particle sizer as well as analysis with a TEM instrument that had a resolution of 0.24 nm. Particulates were collected using a 3 mm TEM grid that was attached to the end of a metal probe that was placed at the engine exhaust in such a way that the TEM grid was parallel to the DEE flow during sampling. From the TEM analysis the DPM was found to be fractal aggregates of spherules and the comparison between the two methods revealed that the TEM diameters were consistently found to be approximately double the average mobility diameters for the specific diesel engine operating conditions. It could therefore be concluded that both experiments captured overall



trends in diesel aggregate sizes with respect to engine operating conditions (Chandler, Yingwu & Koylu 2007).

Kocbach *et al.* published work in 2006 regarding the analysis of combustion particles from vehicle exhaust and wood smoke that were collected on polycarbonate filters. The wood smoke samples were collected from a single stage combustion stove whereas the vehicle exhaust particles were collected from within a road tunnel during two seasons and a NIST DPM 2975 SRM was also analysed for verification and quality control. The samples were characterised using the following TEM techniques: high resolution transmission electron microscopy (HRTEM), electron energy-loss spectroscopy (EELS) and selected area electron diffraction (SAED). The samples were extracted by sonification and placed onto a micro grid (carbon filmed 200 mesh copper grid) for TEM analysis. The results revealed that wood samples contained carbon aggregates that consisted of tens to thousands of primary carbon particles whereas the tunnel samples contained mineral particles as well as carbon aggregates. The geometric diameters of primary carbon particles from the tunnel samples were in the range of 18-30 nm whilst 24-38 nm was observed for the wood smoke. The authors noted that although the wood and exhaust samples differed considerably, there was no significant difference between any of the vehicle exhaust samples (Kocbach *et al.* 2006).

Ancelet *et al.* studied PM from a road tunnel located in Wellington, New Zealand (Mount Victoria Tunnel) in order to gain a better understanding of the carbonaceous species that are emitted from vehicle exhausts. During their sampling programme (2008-2009) they collected samples using two co-located Gent samplers where the first sampler consisted of a stacked filter unit with coarse (PM<sub>10-2.5</sub>) Nucleopore polycarbonate membrane filters and fine (PM<sub>2.5</sub>) QFFs and the second sampler had the same stacked filter unit with coarse Nucleopore polycarbonate membrane filters but with Teflon filters for fine matter. The authors did this to accurately try to determine fine particle mass since they knew QFF had some positive and negative sampling artefacts. They placed their samplers on a ventilation outlet in the tunnel, where they sampled during peak traffic flows on weekdays, after which they performed carbon analysis, PAH analysis and SEM. An example of one of their SEM images is shown in Fig. 2-9. The SEM results confirmed the presence of carbonaceous aggregates as in all of the other reviewed studies (Ancelet *et al.* 2011).

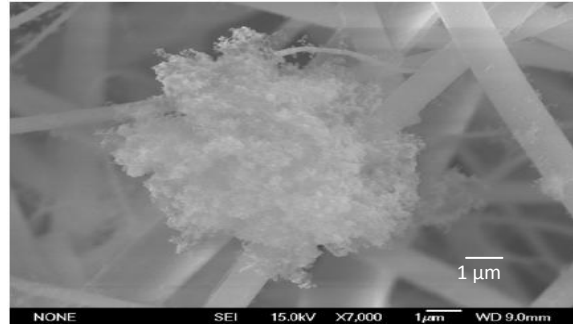


Figure 2-9 Representative SEM image of a carbonaceous particle agglomerate (Ancelet *et al.* 2011)

The majority of the samplers that are used in environmental studies are not suited for microscopic analysis and the lack of understanding of the limitations and advantages associated with these techniques limit their use in the industry, however it has proven to be enriching and useful as a complementary technique for DPM analysis.

## 2.5 References

- Alexandrou, N., Smith, M., Park, R., Lumb, K. & Brice, K. 2001, "The extraction of polycyclic aromatic hydrocarbons from atmospheric particulate matter samples by accelerated solvent extraction (ASE)", *International Journal of environmental Analytical Chemistry*, vol. 81, no. 4, pp. 257-280.
- Ancelet, T., Davy, P.K., Trompetter, W.J., Markwitz, A. & Weatherburn, D.C. 2011, "Carbonaceous aerosols in an urban tunnel", *Atmospheric Environment*, vol. 45, no. 26, pp. 4463-4469.
- Atkinson, R. & Arey, J. 2003, "Atmospheric degradation of volatile organic compounds", *Chemical Reviews*, vol. 103, no.12, pp. 4605-4638.
- Ávila, B.M.F., Pereira, R., Gomes, A.O. & Azevedo, D.A. 2011, "Chemical characterization of aromatic compounds in extra heavy gas oil by comprehensive two-dimensional gas chromatography coupled to time-of-flight mass spectrometry", *Journal of Chromatography A*, vol. 1218, no. 21, pp. 3208-3216.
- Aydin, M.E., Ozcan, S. & Tor, A. 2007, "Ultrasonic solvent extraction of persistent organic pollutants from airborne particles", *Clean - Soil, Air, Water*, vol. 35, no. 6, pp. 660-668.
- Ayres, J.G., Borm, P., Cassee, F.R., Castranova, V., Donaldson, K., Ghio, A., Harrison, R.M., Hider, R., Kelly, F., Kooter, I.M., Marano, F., Maynard, R.L., Mudway, I., Nel, A., Sioutas, C., Smith, S., Baeza-Squiban, A., Cho, A., Duggan, S. & Froines, J. 2008, "Evaluating the toxicity of airborne particulate matter and nanoparticles by measuring oxidative stress potential - A workshop report and consensus statement", *Inhalation Toxicology*, vol. 20, no. 1, pp. 75-99.
- Bamford, H.A., Bezabeh, D.Z., Schantz, M.M., Wise, S.A. & Baker, J.E. 2003, "Determination and comparison of nitrated-polycyclic aromatic hydrocarbons measured in air and diesel particulate reference materials", *Chemosphere*, vol. 50, no. 5, pp. 575-587.
- Bari, M.A., Baumbach, G., Kuch, B. & Scheffknecht, G. 2009, "Wood smoke as a source of particle-phase organic compounds in residential areas", *Atmospheric Environment*, vol. 43, no. 31, pp. 4722-4732.
- Bates, M., Bruno, P., Caputi, M., Caselli, M., de Gennaro, G. & Tutino, M. 2008, "Analysis of polycyclic aromatic hydrocarbons (PAHs) in airborne particles by direct sample introduction thermal desorption GC/MS", *Atmospheric Environment*, vol. 42, no. 24, pp. 6144-6151.
- Bertoni, G., Tappa, R. & Cecinato, A. 2001, "Environmental monitoring of semi-volatile polycyclic aromatic hydrocarbons by means of diffusive sampling devices and GC-MS analysis", *Chromatographia*, vol. 53, no. SPEC. ISS, pp. S312-S316.

- Binková, B., Veselý, D., Veselá, D., Jelínek, R. & Šrám, R.J. 1999, "Genotoxicity and embryotoxicity of urban air particulate matter collected during winter and summer period in two different districts of the Czech Republic", *Mutation Research - Genetic Toxicology and Environmental Mutagenesis*, vol. 440, no. 1, pp. 45-58.
- Birch, M.E., Dahmann, D. & Fricke, H. 1999, "Comparison of two carbon analysis methods for monitoring diesel particulate levels in mines", *Journal of Environmental Monitoring*, vol. 1, no. 6, pp. 541-544.
- Birch, M. & Cary, R. 1996, "Elemental carbon-based method for monitoring occupational exposures to particulate diesel exhaust", *Aerosol Science and Technology*, vol. 25, no. 3, pp. 221-241.
- Bolton, J.L., Trush, M.A., Penning, T.M., Dryhurst, G. & Monks, T.J. 2000, "Role of quinones in toxicology", *Chemical Research in Toxicology*, vol. 13, no. 3, pp. 135-160.
- Castells, P., Santos, F.J. & Galceran, M.T. 2003, "Development of a sequential supercritical fluid extraction method for the analysis of nitrated and oxygenated derivatives of polycyclic aromatic hydrocarbons in urban aerosols", *Journal of Chromatography A*, vol. 1010, no. 2, pp. 141-151.
- Cavalieri, E.L. & Rogan, E.G. 2002, "A Unified Mechanism in the Initiation of Cancer", *Annals of the New York Academy of Sciences*, vol. 959, no. 1, pp. 341-354.
- Cavalieri, E.L. & Rogan, E.G. 1995, "Central role of radical cations in metabolic activation of polycyclic aromatic hydrocarbons", *Xenobiotica*, vol. 25, no. 7, pp. 677-688.
- Chandler, M.F., Teng, Y. & Koylu, U.O. 2007, "Diesel engine particulate emissions: A comparison of mobility and microscopy size measurements", *Proceedings of the Combustion Institute*, no. 31, pp. 2971-2979.
- Cho, A.K., Sioutas, C., Miguel, A.H., Kumagai, Y., Schmitz, D.A., Singh, M., Eiguren-Fernandez, A. & Froines, J.R. 2005, "Redox activity of airborne particulate matter at different sites in the Los Angeles Basin", *Environmental Research*, vol. 99, no. 1, pp. 40-47.
- Christensen, A., Östman, C. & Westerholm, R. 2005, "Ultrasound-assisted extraction and on-line LC-GC-MS for determination of polycyclic aromatic hydrocarbons (PAH) in urban dust and diesel particulate matter", *Analytical and Bioanalytical Chemistry*, vol. 381, no. 6, pp. 1206-1216.
- Cook, J.W., Hewett, C.L. & Hieger, I. 1933, "The isolation of a cancer-producing hydrocarbon from coal tar. Parts I, II, and III", *Journal of the Chemical Society*. 1933, pp. 394-405.
- Courter, L.A., Pereira, C. & Baird, W.M. 2007, "Diesel exhaust influences carcinogenic PAH-induced genotoxicity and gene expression in human breast epithelial cells in culture", *Mutation Research - Fundamental and Molecular Mechanisms of Mutagenesis*, vol. 625, no. 1-2, pp. 72-82.

- Covey, T.R., Lee, E.D. & Henion, J.D. 1986, "High-speed liquid chromatography/tandem mass spectrometry for the determination of drugs in biological samples", *Analytical Chemistry*, vol. 58, no. 12, pp. 2453-2460.
- Dallarosa, J.B., Mõnego, J.G., Teixeira, E.C., Stefens, J.L. & Wiegand, F. 2005, "Polycyclic aromatic hydrocarbons in atmospheric particles in the metropolitan area of Porto Alegre, Brazil", *Atmospheric Environment*, vol. 39, no. 9, pp. 1609-1625.
- Dalle-Donne, I., Rossi, R., Colombo, R., Giustarini, D. & Milzani, A. 2006, "Biomarkers of oxidative damage in human disease", *Clinical Chemistry*, vol. 52, no. 4, pp. 601-623.
- Dasgupta, S., Banerjee, K., Patil, S.H., Ghaste, M., Dhumal, K.N. & Adsule, P.G. 2010, "Optimization of two-dimensional gas chromatography time-of-flight mass spectrometry for separation and estimation of the residues of 160 pesticides and 25 persistent organic pollutants in grape and wine", *Journal of Chromatography A*, vol. 1217, no. 24, pp. 3881-3889.
- Davies, B. 2002, "Diesel particulate control strategies at some Australian underground coal mines", *American Industrial Hygiene Association Journal*, vol. 63, no. 5, pp. 554-558.
- De Almeida Azevedo, D., Moreira, L.S. & Soares De Siqueira, D.S. 1999, "Composition of extractable organic matter in aerosols from urban areas of Rio de Janeiro city, Brazil", *Atmospheric Environment*, vol. 33, no. 30, pp. 4987-5001.
- DEEP (Diesel emissions evaluation programme). 2001, "Sampling for diesel particulate matter in mines", *CANMET: Mining and Mineral Science Laboratories*, report (MMSL) 01-052.
- Dejmek, J., Solanský, I., Beneš, I., Leníček, J. & Šrám, R.J. 2000, "The impact of polycyclic aromatic hydrocarbons and fine particles on pregnancy outcome", *Environmental Health Perspectives*, vol. 108, no. 12, pp. 1159-1164.
- Dimandja, J.D., Clouden, G.C., Colón, I., Focant, J., Cabey, W.V. & Parry, R.C. 2003, "Standardized test mixture for the characterization of comprehensive two-dimensional gas chromatography columns: The Phillips mix", *Journal of Chromatography A*, vol. 1019, no. 1-2, pp. 261-272.
- Dimashki, M., Harrad, S. & Harrison, R.M. 2000, "Measurements of nitro-PAH in the atmospheres of two cities", *Atmospheric Environment*, vol. 34, no. 15, pp. 2459-2469.
- Donaldson, K., Tran, L., Jimenez, L.A., Duffin, R., Newby, D.E., Mills, N., MacNee, W. & Stone, V. 2005, "Combustion-derived nanoparticles: A review of their toxicology following inhalation exposure", *Particle and Fibre Toxicology*, vol. 2.
- El-Fadel, M. & Hashisho, Z. 2001, "Vehicular emissions in roadway tunnels: A critical review", *Critical Reviews in Environmental Science and Technology*, vol. 31, no. 2, pp. 125-174.

- Falkovich, A.H. & Rudich, Y. 2001a, "Analysis of semivolatile organic compounds in atmospheric aerosols by direct sample introduction thermal desorption GC/MS", *Environmental Science and Technology*, vol. 35, no. 11, pp. 2326-2333.
- Falkovich, A.H. & Rudich, Y. 2001b, "Analysis of semivolatile organic compounds in atmospheric aerosols by direct sample introduction thermal desorption GC/MS", *Environmental Science and Technology*, vol. 35, no. 11, pp. 2326-2333.
- Fan, Z., Jung, K.H. & Lioy, P.J. 2006, "Development of a passive sampler to measure personal exposure to gaseous PAHs in community settings", *Environmental Science and Technology*, vol. 40, no. 19, pp. 6051-6057.
- Finlayson-Pitts, B.J. & Pitts Jr., J.N. 1999, "Polycyclic aromatic carbon (Chapter 10)", *Chemistry of the Upper and Lower Atmosphere*, pp. 436-546.
- Focant, J., Sjödin, A. & Patterson Jr., D.G. 2003, "Qualitative evaluation of thermal desorption-programmable temperature vaporization-comprehensive two-dimensional gas chromatography-time-of-flight mass spectrometry for the analysis of selected halogenated contaminants", *Journal of Chromatography A*, vol. 1019, no. 1-2, pp. 143-156.
- Forbes, P.B.C. & Rohwer, E.R. 2009, "Investigations into a novel method for atmospheric polycyclic aromatic hydrocarbon monitoring", *Environmental Pollution*, vol. 157, no. 8-9, pp. 2529-2535.
- Forbes, P.B.C., Karg, E.W., Zimmermann, R. & Rohwer, E.R. 2012, "The use of multi-channel silicone rubber traps as denuders for polycyclic aromatic hydrocarbons", *Analytica Chimica Acta*, vol. 730, pp. 71-79.
- Frenich, A.G., Ocana, R.M. & Martínez Vidal, J.L. 2010, "Determination of polycyclic aromatic hydrocarbons in airborne particulate matter by gas chromatography-triple quadrupole tandem mass spectrometry", *Journal of AOAC International*, vol. 93, no. 1, pp. 284-294.
- Fushimi, A., Hashimoto, S., Ieda, T., Ochiai, N., Takazawa, Y., Fujitani, Y. & Tanabe, K. 2012, "Thermal desorption - comprehensive two-dimensional gas chromatography coupled with tandem mass spectrometry for determination of trace polycyclic aromatic hydrocarbons and their derivatives", *Journal of Chromatography A*, vol. 1252, pp. 164-170.
- Goen, T., Gundel, J., Schaller, K. & Angerer, J. 1995, "The elimination of 1-hydroxypyrene in the urine of the general population and workers with different occupational exposures to PAH", *Science of the Total Environment*, vol. 163, pp. 195-201.
- González-Flecha, B. 2004, "Oxidant mechanisms in response to ambient air particles", *Molecular Aspects of Medicine*, vol. 25, no. 1-2, pp. 169-182.

- Grahame, T.J. & Schlesinger, R.B. 2007, "Health effects of airborne particulate matter: Do we know enough to consider regulating specific particle types or sources?", *Inhalation Toxicology*, vol. 19, no. 6-7, pp. 457-481.
- Grenier, M. & Butler, K. 1996, "Respirable Combustible Dust (RCD) Sampling and Analysis Protocol", Division Report MRL 96-029(TR). Natural Resources Canada, CANMET, Mining Research Laboratories.
- Gustafson, K.E. & Dickhut, R.M. 1996, "Particle/gas concentrations and distributions of PAHs in the atmosphere of southern Chesapeake Bay", *Environmental Science and Technology*, vol. 31, no. 1, pp. 140-147.
- Ha, E., Hong, Y., Lee, B., Woo, B., Schwartz, J. & Christiani, D.C. 2001, "Is air pollution a risk factor for low birth weight in Seoul?", *Epidemiology*, vol. 12, no. 6, pp. 643-648.
- Harris, C.C., Weston, A., Willey, J.C., Trivers, G.E. & Mann, D.L. 1987, "Biochemical and molecular epidemiology of human cancer: Indicators of carcinogen exposure, DNA damage, and genetic predisposition", *Environmental Health Perspectives*, vol. 75, pp. 109-119.
- Hawthorne, S.B., Grabanski, C.B., Martin, E. & Miller, D.J. 2000, "Comparisons of Soxhlet extraction, pressurized liquid extraction, supercritical fluid extraction and subcritical water extraction for environmental solids: Recovery, selectivity and effects on sample matrix", *Journal of Chromatography A*, vol. 892, no. 1-2, pp. 421-433.
- Healey, K., Lingard, J.J.N., Tomlin, A.S., Hughes, A., White, K.L.M., Wild, C.P. & Routledge, M.N. 2005, "Genotoxicity of size-fractionated samples of urban particulate matter", *Environmental and Molecular Mutagenesis*, vol. 45, no. 4, pp. 380-387.
- Heywood, J.B. 1988, "Engine types and their operations", in *Internal Combustion Engine Fundamentals*, 1<sup>st</sup> edn. eds. Duffy, A & Morriss, J.M, McGraw-Hill Higher Education, United States of America pp. 1-92.
- Hilton, D.C., Jones, R.S. & Sjödin, A. 2010, "A method for rapid, non-targeted screening for environmental contaminants in household dust", *Journal of Chromatography A*, vol. 1217, no. 44, pp. 6851-6856.
- Ho, K.F., Ho, S.S.H., Lee, S.C., Cheng, Y., Chow, J.C., Watson, J.G., Louie, P.K.K. & Tian, L. 2009, "Emissions of gas- and particle-phase polycyclic aromatic hydrocarbons (PAHs) in the Shing Mun Tunnel, Hong Kong", *Atmospheric Environment*, vol. 43, no. 40, pp. 6343-6351.

- Hutzler, C., Luch, A. & Filser, J.G. 2011, "Analysis of carcinogenic polycyclic aromatic hydrocarbons in complex environmental mixtures by LC-APPI-MS/MS", *Analytica Chimica Acta*, vol. 702, no. 2, pp. 218-224.
- IARC 1985, "Polynuclear aromatic compounds. Part 4. Bitumens, coal-tars and derived products, shale-oils and soot", *IARC Monographs on the Evaluation of Carcinogenic Risks to Humans*, vol. 35.
- IARC 1989, "Diesel and gasoline engine exhausts and some nitroarenes", *IARC Monographs on the evaluation of the carcinogenic risk of chemicals to humans*, vol. 46.
- IARC. 2012, Diesel Engine Exhaust Carcinogenic 2012a, Press Release no. 213.
- Ieda, T., Ochiai, N., Miyawaki, T., Ohura, T. & Horii, Y. 2011, "Environmental analysis of chlorinated and brominated polycyclic aromatic hydrocarbons by comprehensive two-dimensional gas chromatography coupled to high-resolution time-of-flight mass spectrometry", *Journal of Chromatography A*, vol. 1218, no. 21, pp. 3224-3232.
- Jongeneelen, F.J. 1997, "Methods for routine biological monitoring of carcinogenic PAH-mixtures", *Science of the Total Environment*, vol. 199, no. 1-2, pp. 141-149.
- Jongeneelen, F.J., Bos, R.P. & Anzion, R.B.M. 1986, "Biological monitoring of polycyclic aromatic hydrocarbons. Metabolites in urine", *Scandinavian Journal of Work, Environment and Health*, vol. 12, no. 2, pp. 137-143.
- Kasai, H., Hayami, H., Yamaizumi, Z., Saito, H. & Nishimura, S. 1984, "Detection and identification of mutagens and carcinogens as their adducts with guanosine derivatives", *Nucleic Acids Research*, vol. 12, no. 4, pp. 2127-2136.
- Kim, J.Y., Mukherjee, S., Ngo, L. & Christiani, D.C. 2004, "Urinary 8-hydroxy-2'-deoxyguanosine as a biomarker of oxidative DNA damage in workers exposed to fine particulates", *Environmental Health Perspectives*, vol. 112, no. 6, pp. 666-671.
- Kim, Y., Lee, C., Nan, H., Kang, J. & Kim, H. 2003, "Effects of genetic polymorphisms in metabolic enzymes on the relationships between 8-hydroxydeoxyguanosine levels in human leukocytes and urinary 1-hydroxypyrene and 2-naphthol concentrations", *Journal of Occupational Health*, vol. 45, no. 3, pp. 160-167.
- Kittelson, D.B. 1998a, "Engines and nanoparticles: A review", *Journal of Aerosol Science*, vol. 29, no. 5-6, pp. 575-588.
- Kittelson, D.B. 1998b, "Engines and nanoparticles: A review", *Journal of Aerosol Science*, vol. 29, no. 5-6, pp. 575-588.



- Kocbach, A., Li, Y., Yttri, K.E., Cassee, F.R., Schwarze, P.E. & Namork, E. 2006, "Physicochemical characterisation of combustion particles from vehicle exhaust and residential wood smoke", *Particle and Fibre Toxicology*, vol. 3, pp. 1-10.
- Konstandopoulos, A.G., Zarvalis, D. & Dolios, I. 2007, "Multi-instrumental assessment of diesel particulate filters", *SAE Paper*, no. 2007-01-0313, doi:10.4271/2007-01-0313.
- Larkin, E.K., Smith, T.J., Stayner, L., Rosner, B., Speizer, F.E. & Garshick, E. 2000, "Diesel exhaust exposure and lung cancer: Adjustment for the effect of smoking in a retrospective cohort study", *American Journal of Industrial Medicine*, vol. 38, no. 4, pp. 399-409.
- Laumbach, R.J. & Kipen, H.M. 2012, "Respiratory health effects of air pollution: Update on biomass smoke and traffic pollution", *Journal of Allergy and Clinical Immunology*, vol. 129, no. 1, pp. 3-11.
- Lee, W., Wang, Y., Lin, T., Chen, Y., Lin, W., Ku, C. & Cheng, J. 1995, "PAH characteristics in the ambient air of traffic-source", *Science of the Total Environment*, vol. 159, no. 2-3, pp. 185-200.
- Lewtas, J. 2007, "Air pollution combustion emissions: Characterization of causative agents and mechanisms associated with cancer, reproductive, and cardiovascular effects", *Mutation Research - Reviews in Mutation Research*, vol. 636, no. 1-3, pp. 95-133.
- Li, N., Kim, S., Wang, M., Froines, J., Sioutas, C. & Nel, A. 2002, "Use of a stratified oxidative stress model to study the biological effects of ambient concentrated and diesel exhaust particulate matter", *Inhalation Toxicology*, vol. 14, no. 5, pp. 459-486.
- Liat, A., Dimopoulos Eggenschwiler, P., Müller Gubler, E., Schreiber, D. & Aguirre, M. 2012, "Investigation of diesel ash particulate matter: A scanning electron microscope and transmission electron microscope study", *Atmospheric Environment*, vol. 49, pp. 391-402.
- Lien, G., Chen, C. & Wu, C. 2007, "Analysis of polycyclic aromatic hydrocarbons by liquid chromatography/ tandem mass spectrometry using atmospheric pressure chemical ionization or electrospray ionization with tropylium post-column derivatization", *Rapid Communications in Mass Spectrometry*, vol. 21, no. 22, pp. 3694-3700.
- Lima, A.L.C., Farrington, J.W. & Reddy, C.M. 2005, "Combustion-Derived Polycyclic Aromatic Hydrocarbons in the Environment—A Review", *Environmental Forensics*, vol. 6, no. 2, pp. 109-131.
- Lintelmann, J., Fischer, K. & Matuschek, G. 2006, "Determination of oxygenated polycyclic aromatic hydrocarbons in particulate matter using high-performance liquid chromatography-tandem mass spectrometry", *Journal of Chromatography A*, vol. 1133, no. 1-2, pp. 241-247.

- Liu, L., Liu, Y., Lin, J., Tang, N., Hayakawa, K. & Maeda, T. 2007a, "Development of analytical methods for polycyclic aromatic hydrocarbons (PAHs) in airborne particulates: A review", *Journal of Environmental Sciences*, vol. 19, no. 1, pp. 1-11.
- Liu, S., Tao, S., Liu, W., Liu, Y., Dou, H., Zhao, J., Wang, L., Wang, J., Tian, Z. & Gao, Y. 2007b, "Atmospheric polycyclic aromatic hydrocarbons in north China: A winter-time study", *Environmental Science and Technology*, vol. 41, no. 24, pp. 8256-8261.
- Loomis, D., Castillejos, M., Gold, D.R., McDonnell, W. & Borja-Aburto, V.H. 1999, "Air pollution and infant mortality in Mexico City", *Epidemiology*, vol. 10, no. 2, pp. 118-123.
- Lottmann, A., Cadé, E., Geagea, M.L., Delhomme, O., Grand, C., Veilleraud, C., Rizet, A.-., Mirabel, P. & Millet, M. 2007, "Separation of molecular tracers sorbed onto atmospheric particulate matter by flash chromatography", *Analytical and Bioanalytical Chemistry*, vol. 387, no. 5, pp. 1855-1861.
- Lung, S.C., Wu, M. & Lin, C. 2004, "Customers' exposure to PM 2.5 and polycyclic aromatic hydrocarbons in smoking/nonsmoking sections of 24-h coffee shops in Taiwan", *Journal of Exposure Analysis and Environmental Epidemiology*, vol. 14, no. 7, pp. 529-535.
- Lundstedt, S. 2003, *Analysis of PAHs and their transformation products in contaminated soil and remedial processes*, PhD, University of Umea, Sweden.
- Majewski, W.A. & Khair, M.K. 2006, *Diesel Emissions and Their Control*, Society of Automotive Engineers, vol. 303, SAE International, ISBN of 978-0-7680-0674-2.
- Manahan, S.E. 2000, *Environmental Chemistry*, 7<sup>th</sup> edn. Lewis Publishers, New York, pp. 20, 313.
- Mandalakis, M., Tsapakis, M., Tsoga, A. & Stephanou, E.G. 2002, "Gas-particle concentrations and distribution of aliphatic hydrocarbons, PAHs, PCBs and PCDD/Fs in the atmosphere of Athens (Greece)", *Atmospheric Environment*, vol. 36, no. 25, pp. 4023-4035.
- Marr, L.C., Kirchstetter, T.W., Harley, R.A., Miguel, A.H., Hering, S.V. & Hammond, S.K. 1999, "Characterization of polycyclic aromatic hydrocarbons in motor vehicle fuels and exhaust emissions", *Environmental Science and Technology*, vol. 33, no. 18, pp. 3091-3099.
- Matti Maricq, M. 2007, "Chemical characterization of particulate emissions from diesel engines: A review", *Journal of Aerosol Science*, vol. 38, no. 11, pp. 1079-1118.
- Metz, N. 2004, "Particulates and health effects from diesel engines", *AutoTechnology*, vol. 4, no. OCT., pp. 62-66.

- Miller-Schulze, J.P., Paulsen, M., Toriba, A., Hayakawa, K. & Simpson, C.D. 2007, "Analysis of 1-nitropyrene in air particulate matter standard reference materials by using two-dimensional high performance liquid chromatography with online reduction and tandem mass spectrometry detection", *Journal of Chromatography A*, vol. 1167, no. 2, pp. 154-160.
- Msscscientific. 2014, "Glass- and Quartz Fiber Filters", Chromatographie-Handel GmbH-Products for chromatography, spectroscopy, liquid management, sample preparation and thermostating, Berlin, Germany, viewed 28 April 2014, <[www.msscscientific.dehttp://www.msscscientific.de/glass\\_quartz\\_fiber\\_filters.pdf](http://www.msscscientific.de/glass_quartz_fiber_filters.pdf)>
- Murr, L.E. & Garza, K.M. 2009, "Natural and anthropogenic environmental nanoparticulates: Their microstructural characterization and respiratory health implications", *Atmospheric Environment*, vol. 43, no. 17, pp. 2683-2692.
- National Research Council. 1983, "Polycyclic Aromatic Hydrocarbons: Evaluation of Sources and Effects", Washington, DC: The National Academies Press.
- NIOSH. 2003, "Method 5040 - Elemental Carbon, Diesel Particulate: Method 5040", National Institute for Occupational Safety and Health, *NIOSH Manual of Analytical Methods (NMAM)*, Fourth Edition Issue 3 (Interim); March 2003.
- Omar, N.Y.M.J., Abas, M.R.B., Ketuly, K.A. & Tahir, N.M. 2002, "Concentrations of PAHs in atmospheric particles (PM-10) and roadside soil particles collected in Kuala Lumpur, Malaysia", *Atmospheric Environment*, vol. 36, no. 2, pp. 247-254.
- Ono-Ogasawara, M. & Smith, T.J. 2004, "Diesel exhaust particles in the work environment and their analysis", *Industrial Health*, vol. 42, no. 4, pp. 389-399.
- Pandey, S.K., Kim, K. & Brown, R.J.C. 2011, "A review of techniques for the determination of polycyclic aromatic hydrocarbons in air", *TrAC - Trends in Analytical Chemistry*, vol. 30, no. 11, pp. 1716-1739.
- Panić, O. & Górecki, T. 2006, "Comprehensive two-dimensional gas chromatography (GC×GC) in environmental analysis and monitoring", *Analytical and Bioanalytical Chemistry*, vol. 386, no. 4, pp. 1013-1023.
- Park, S.S., Kim, Y.J. & Kang, C.H. 2002, "Atmospheric polycyclic aromatic hydrocarbons in Seoul, Korea", *Atmospheric Environment*, vol. 36, no. 17, pp. 2917-2924.
- Pereira, L.A.A., Loomis, D., Conceição, G.M.S., Braga, A.L.F., Arcas, R.M., Kishi, H.S., Singer, J.M., Böhm, G.M. & Saldiva, P.H.N. 1998, "Association between air pollution and intrauterine mortality in Sao Paulo, Brazil", *Environmental Health Perspectives*, vol. 106, no. 6, pp. 325-329.

- Perera, F.P., Jedrychowski, W., Rauh, V. & Whyatt, R.M. 1999, "Molecular epidemiologic research on the effects of environmental pollutants on the fetus", *Environmental Health Perspectives*, vol. 107, no. 3, pp. 451-460.
- Phillips, D.H. & Farmer, P.B. 1995, "Protein and DNA adducts as biomarkers of exposure to environmental mutagens", *Environmental Mutagenesis*, eds. Phillips, D.H & Venitt, S., Bioscientific Publishers, Oxford, pp. 367-395.
- Phuleria, H.C., Geller, M.D., Fine, P.M. & Sioutas, C. 2006, "Size-resolved emissions of organic tracers from light and heavy-duty vehicles measured in a California roadway tunnel", *Environmental Science and Technology*, vol. 40, no. 13, pp. 4109-4118.
- Pope III, C.A. & Dockery, D.W. 2006, "Health effects of fine particulate air pollution: Lines that connect", *Journal of the Air and Waste Management Association*, vol. 56, no. 6, pp. 709-742.
- Pöschl, U. 2005, "Atmospheric aerosols: Composition, transformation, climate and health effects", *Angewandte Chemie - International Edition*, vol. 44, no. 46, pp. 7520-7540.
- Possanzini, M., Di Palo, V., Gigliucci, P., Tomasi Scianò, M.C. & Cecinato, A. 2004, "Determination of phase-distributed PAH in Rome ambient air by denuder/ GC-MS method", *Atmospheric Environment*, vol. 38, no. 12, pp. 1727-1734.
- Poster, D.L., Schantz, M.M., Sander, L.C. & Wise, S.A. 2006, "Analysis of polycyclic aromatic hydrocarbons (PAHs) in environmental samples: A critical review of gas chromatographic (GC) methods", *Analytical and Bioanalytical Chemistry*, vol. 386, no. 4, pp. 859-881.
- Risom, L., Møller, P. & Loft, S. 2005, "Oxidative stress-induced DNA damage by particulate air pollution", *Mutation Research - Fundamental and Molecular Mechanisms of Mutagenesis*, vol. 592, no. 1-2, pp. 119-137.
- Ristovski, Z.D., Miljevic, B., Surawski, N.C., Morawska, L., Fong, K.M., Goh, F. & Yang, I.A. 2012, "Respiratory health effects of diesel particulate matter", *Respirology*, vol. 17, no. 2, pp. 201-212.
- Ritz, B., Yu, F., Fruin, S., Chapa, G., Shaw, G.M. & Harris, J.A. 2002, "Ambient air pollution and risk of birth defects in southern California", *American Journal of Epidemiology*, vol. 155, no. 1, pp. 17-25.
- Robinson, A.L., Grieshop, A.P., Donahue, N.M. & Hunt, S.W. 2010, "Updating the conceptual model for fine particle mass emissions from combustion systems", *Journal of the Air and Waste Management Association*, vol. 60, no. 10, pp. 1204-1222.
- Samy, S. & Zielinska, B. 2010, "Secondary organic aerosol production from modern diesel engine emissions", *Atmospheric Chemistry and Physics*, vol. 10, no. 2, pp. 609-625.

- Schauer, J.J. & Cass, G.R. 2000, "Source apportionment of wintertime gas-phase and particle-phase air pollutants using organic compounds as tracers", *Environmental Science and Technology*, vol. 34, no. 9, pp. 1821-1832.
- Schoenmakers, P., Marriott, P. & Beens, J. 2003, "Nomenclature and conventions in comprehensive multidimensional chromatography", *LC-GC Europe*, vol. 16, no. 6, pp. 335-339.
- Sharma, H., Jain, V.K. & Khan, Z.H. 2008, "Atmospheric polycyclic aromatic hydrocarbons (PAHs) in the urban air of Delhi during 2003", *Environmental monitoring and assessment*, vol. 147, no. 1-3, pp. 43-55.
- Shigenaga, M.K. & Ames, B.N. 1991, "Assays for 8-hydroxy-2'-deoxyguanosine: A biomarker of in vivo oxidative DNA damage", *Free Radical Biology and Medicine*, vol. 10, no. 3-4, pp. 211-216.
- Singh, R., Kaur, B., Kalina, I., Popov, T.A., Georgieva, T., Garte, S., Binkova, B., Sram, R.J., Taioli, E. & Farmer, P.B. 2007a, "Effects of environmental air pollution on endogenous oxidative DNA damage in humans", *Mutation Research - Fundamental and Molecular Mechanisms of Mutagenesis*, vol. 620, no. 1-2, pp. 71-82.
- Singh, R., Sram, R.J., Binkova, B., Kalina, I., Popov, T.A., Georgieva, T., Garte, S., Taioli, E. & Farmer, P.B. 2007b, "The relationship between biomarkers of oxidative DNA damage, polycyclic aromatic hydrocarbon DNA adducts, antioxidant status and genetic susceptibility following exposure to environmental air pollution in humans", *Mutation Research - Fundamental and Molecular Mechanisms of Mutagenesis*, vol. 620, no. 1-2, pp. 83-92.
- Stayner, L., Dankovic, D., Smith, R. & Steenland, K. 1998, "Predicted lung cancer risk among miners exposed to diesel exhaust particles", *American Journal of Industrial Medicine*, vol. 34, no. 3, pp. 207-219.
- Steenland, K., Deddens, J. & Stayner, L. 1998, "Diesel exhaust and lung cancer in the trucking industry: Exposure- response analyses and risk assessment", *American Journal of Industrial Medicine*, vol. 34, no. 3, pp. 220-228.
- Strickland, P. & Kang, D. 1999, "Urinary 1-hydroxypyrene and other PAH metabolites as biomarkers of exposure to environmental PAH in air particulate matter", *Toxicology letters*, vol. 108, no. 2-3, pp. 191-199.
- Szaniszló, J. & Ungváry, G. 2001, "Polycyclic aromatic hydrocarbon exposure and burden of outdoor workers in Budapest", *Journal of Toxicology and Environmental Health - Part A*, vol. 62, no. 5, pp. 297-306.

- Tsapakis, M. & Stephanou, E.G. 2005, "Occurrence of gaseous and particulate polycyclic aromatic hydrocarbons in the urban atmosphere: Study of sources and ambient temperature effect on the gas/particle concentration and distribution", *Environmental Pollution*, vol. 133, no. 1, pp. 147-156.
- Uhde, E., Salthammer, Tunga. 2009, "Application of Solid Sorbents for the Sampling of Volatile Organic Compounds in Indoor Air", *Organic Indoor Air Pollutants. 2nd Edition*, Copyright © 2009 WILEY-VCH Verlag GmbH & Co. KGaA, Weinheim, ISBN: 978-3-527-31267-2.
- US EPA. 2002, Health Assessment Document for Diesel Engine Exhaust. U.S. Environmental Protection Agency, Office of Research and Development, National Center for Environmental Assessment, Washington Office, Washington, DC, EPA/600/8-90/057F.
- van Drooge, B.L., Nikolova, I. & Ballesta, P.P. 2009, "Thermal desorption gas chromatography–mass spectrometry as an enhanced method for the quantification of polycyclic aromatic hydrocarbons from ambient air particulate matter", *Journal of Chromatography A*, vol. 1216, no. 18, pp. 4030-4039.
- van Niekerk, W., Simpson, D., Fourie, M. & Mouton, G. 2002, "Diesel particulate emission in the South African mining industry", *Safety In Mine Research Advisory Committee*, no. SIM 020602, pp. 1-49.
- Vasilakos, C., Levi, N., Maggos, T., Hatzianestis, J., Michopoulos, J. & Helmis, C. 2007, "Gas-particle concentration and characterization of sources of PAHs in the atmosphere of a suburban area in Athens, Greece", *Journal of Hazardous Materials*, vol. 140, no. 1-2, pp. 45-51.
- Van Gerpen, J. 2005, "The Basics of diesel Engines and Diesel fuels", *The Biodiesel Handbook*, eds. Knothe, G., Van Gerpen, J & Krahl, J., AOCS Publishing, United States of America, pp. 1-92, DOI: 10.1201/9781439822357.ch3
- Venkatachari, P., Hopke, P.K., Brune, W.H., Ren, X., Leshner, R., Mao, J. & Mitchell, M. 2007, "Characterization of wintertime reactive oxygen species concentrations in Flushing, New York", *Aerosol Science and Technology*, vol. 41, no. 2, pp. 97-111.
- Vione, D., Barra, S., de Gennaro, G., de Rienzo, M., Gilardoni, S., Perrone, M.G., & Pozzoli, L. 2004, "Polycyclic aromatic hydrocarbons in the atmosphere: monitoring, sources, sinks and fate" *Annali di Chimica*, vol 94, pp. 17-32.
- Wang, Q., Shao, M., Zhang, Y., Wei, Y., Hu, M. & Guo, S. 2009, "Source apportionment of fine organic aerosols in Beijing", *Atmospheric Chemistry and Physics Discussions*, vol. 9, no. 2, pp. 9043-9080.
- Wang, X., Ding, H., Ryan, L. & Xu, X. 1997, "Association between air pollution and low birth weight: A community-based study", *Environmental Health Perspectives*, vol. 105, no. 5, pp. 514-520.

- Waterman, D., Horsfield, B., Leistner, F., Hall, K. & Smith, S. 2000, "Quantification of polycyclic aromatic hydrocarbons in the NIST Standard Reference Material (SRM1649A) urban dust using thermal desorption GC/MS", *Analytical Chemistry*, vol. 72, no. 15, pp. 3563-3567.
- Watts, W.F. 1995, "Assessment of occupational exposure to diesel emissions", *Diesel Exhaust: A Critical Analysis of Emissions, Exposure, and Health Effects*, Health Effects Institute (HEI), Cambridge, pp. 109-123.
- Wauters, E., Van Caeter, P., Desmet, G., David, F., Devos, C. & Sandra, P. 2008a, "Improved accuracy in the determination of polycyclic aromatic hydrocarbons in air using 24 h sampling on a mixed bed followed by thermal desorption capillary gas chromatography-mass spectrometry", *Journal of Chromatography A*, vol. 1190, no. 1-2, pp. 286-293.
- Wauters, E., Van Caeter, P., Desmet, G., David, F., Devos, C. & Sandra, P. 2008b, "Improved accuracy in the determination of polycyclic aromatic hydrocarbons in air using 24 h sampling on a mixed bed followed by thermal desorption capillary gas chromatography-mass spectrometry", *Journal of Chromatography A*, vol. 1190, no. 1-2, pp. 286-293.
- Wei, M., Chang, W. & Jen, J. 2007, "Monitoring of PAHs in air by collection on XAD-2 adsorbent then microwave-assisted thermal desorption coupled with headspace solid-phase microextraction and gas chromatography with mass spectrometric detection", *Analytical and Bioanalytical Chemistry*, vol. 387, no. 3, pp. 999-1005.
- Wei, Y., Han, I., Hu, M., Shao, M., Zhang, J.J. & Tang, X. 2010, "Personal exposure to particulate PAHs and anthraquinone and oxidative DNA damages in humans", *Chemosphere*, vol. 81, no. 10, pp. 1280-1285.
- Wilhelm, M. & Ritz, B. 2003, "Residential proximity to traffic and adverse birth outcomes in Los Angeles County, California, 1994-1996", *Environmental Health Perspectives*, vol. 111, no. 2, pp. 207-216.
- Williams, R.W., Watts, R.R., Stevens, R.K., Stone, C.L. & Lewtas, J. 1999, "Evaluation of a personal air sampler for twenty-four hour collection of fine particles and semivolatile organics", *Journal of Exposure Analysis and Environmental Epidemiology*, vol. 9, no. 2, pp. 158-166.
- Wingfors, H., Sjödin, A., Haglund, P. & Brorström-Lundén, E. 2001, "Characterisation and determination of profiles of polycyclic aromatic hydrocarbons in a traffic tunnel in Gothenburg, Sweden", *Atmospheric Environment*, vol. 35, no. 36, pp. 6361-6369.
- Xia, T., Korge, P., Weiss, J.N., Li, N., Venkatesen, M.I., Sioutas, C. & Nel, A. 2004, "Quinones and aromatic chemical compounds in particulate matter induce mitochondrial dysfunction: Implications for ultrafine particle toxicity", *Environmental Health Perspectives*, vol. 112, no. 14, pp. 1347-1358.

- Yang, F., Zhai, Y., Chen, L., Li, C., Zeng, G., He, Y., Fu, Z. & Peng, W. 2010, "The seasonal changes and spatial trends of particle-associated polycyclic aromatic hydrocarbons in the summer and autumn in Changsha city", *Atmospheric Research*, vol. 96, no. 1, pp. 122-130.
- Zaebst, D.D., Clapp, D.E., Blade, L.M., Marlow, D.A., Steenland, K., Hornung, R.W., Scheutzle, D. & Butler, J. 1991, "Quantitative determination of trucking industry workers' exposures to diesel exhaust particles", *American Industrial Hygiene Association Journal*, vol. 52, no. 12, pp. 529-541.
- Zhang, S., Zhang, W., Wang, K., Shen, Y., Hu, L. & Wang, X. 2009, "Concentration, distribution and source apportionment of atmospheric polycyclic aromatic hydrocarbons in the southeast suburb of Beijing, China", *Environmental Monitoring and Assessment*, vol. 151, no. 1-4, pp. 197-207.
- Zielinska, B., Samy, S. & McDonald, J.D. 2010, "Atmospheric Transformations of Diesel Emissions", *HEI Research report*, Health Effects Institute, Issue 147, pp. 5-60.



## 3 Experimental Methods and Optimisation

### 3.1 Quality assurance

#### 3.1.1 Handling

##### Empty traps

The inside of the glass tube was rinsed with hexane using a Pasteur pipette and the outside was wiped with a hexane saturated paper towel. The same was done using  $\text{CH}_2\text{Cl}_2$ . The procedure was repeated after which the clean traps were baked overnight in an oven at approximately  $100\text{ }^\circ\text{C}$  before use.

##### Multi-channel PDMS traps (MCT)

The MCTs were conditioned at  $250\text{ }^\circ\text{C}$  for 2 hours with  $\text{H}_2$  flow of *ca*  $10\text{ cm}^3\text{ min}^{-1}$ . This was done with a Gerstel TC2 Tube Conditioner coupled to an Aux-controller 163.

##### Filters

Quartz fibre filter punches (Whatman) were placed in a 100 ml beaker. Methanol was added to the beaker and swirled for approximately 1 minute and then decanted off. Dichloromethane was then added to the beaker, containing the punches, swirled for approximately 1 minute and then decanted off (punches were fragile at this stage so extra care was taken). The procedure was repeated and the clean filter punches were then placed in an oven at  $100\text{ }^\circ\text{C}$  for 30 minutes to dry. The clean, dry punches were then stored in an amber vial in a desiccator.

##### Teflon connectors and end caps

Teflon connectors and end caps were placed in a 100 ml beaker and rinsed with hexane followed by  $\text{CH}_2\text{Cl}_2$ . The procedure was repeated and the connectors and end caps were left to air dry before use.

##### Post sampling storage

PDMS traps were wrapped in aluminum foil after the sampling period to prevent light assisted reactions or transformations and were stored in a freezer at  $-18\text{ }^\circ\text{C}$  to prevent heat assisted reactions or transformations. The loaded large personal sampling filters were kept in the freezer and only punched before analysis. The loaded filters from the denuder samples were stored with their corresponding Teflon connectors still intact in amber quartz vials to prevent any sample loss. The vials were then also placed in the freezer. When analyzing the filter, the Teflon connector was placed on the end of a clean,

empty glass tube with the loaded face of the filter facing towards the tube. The filter was then carefully positioned into the heating zone of the glass tube for thermal desorption.

## 3.2 Platinum Mine study

### 3.2.1 CSIR personal particulate sampling

Personal air samples were provided by the CSIR, which had been collected from various areas where the study participants were performing their duties for that particular day. The NIOSH 5040 method was employed in their collection where the sampling train consisted of a Gilair personal sampling pump and a SKC-DPM cassette with quartz fiber filter. Flow rates were calibrated with a Gilair Gilibrator. Sampling pumps with the cassettes were attached to study participants in such a fashion that cyclones were in the breathing zones of the candidates. Cassettes were kept refrigerated at approximately 4 °C until analysis.

### 3.2.2 Gas and particulate PAH sampling

Samples were taken in three different platinum mines. The number of samples as well as the type of sampling location was kept constant to allow for comparison. The PAH samples were collected with Gilair 3 personal sampling pumps (Sensidyne) attached to denuders via Tygon silicone tubing. The denuder consisted of two multi-channel silicone rubber traps (each trap: 178 mm long glass tube, 0.6 mm o.d.) each containing 22 parallel PDMS tubes (55 mm long, 0.3 mm i.d., 0.6 o.d.) separated by a 6 mm diameter QFF, held in position by a Teflon connector, this configuration allows for both gas and particulate phase sampling (Forbes 2012a). The gas phase SVOCs were trapped by the first (primary) trap as the polydimethylsiloxane served as a solvent for these compounds, the particles were then trapped downstream on the quartz fiber filter. The post filter trap (secondary trap) served to sample any remaining gas phase SVOCs, including PAHs, that had blown off from the filter or had experienced breakthrough from the primary trap. Fig. 3-1 graphically illustrates the sampling setup.

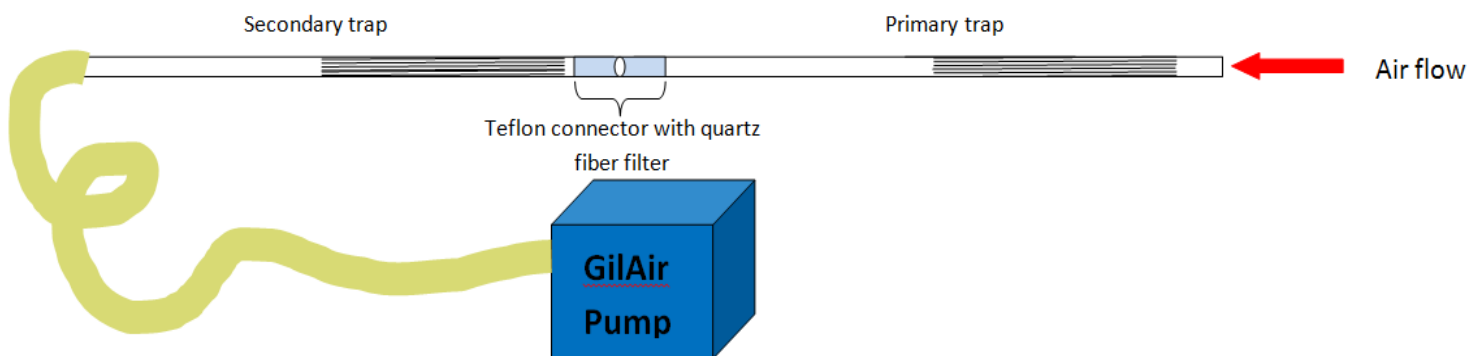


Figure 3-1 Sampling setup used for the collection of semi-volatile organic compounds

The GilAir pumps were calibrated prior to mine visits using a soap bubble flow meter set up. A flow rate of 500 mL.min<sup>-1</sup> was desired to prevent breakthrough of the more volatile SVOCs. The pumps were also calibrated post sampling to ensure the flow rate was maintained throughout the process. The ambient temperature and humidity at each sampling site was recorded using a Kestrel 4500 pocket weather tracker.

A minimum of 5 samples per mine were taken with each sample being a denuder that resulted in three individual samples. A total of 51 samples were thus obtained. The sample summary is given in Tables 3-1 to 3-3:

**Table 3-1 Number and description of samples that were taken underground**

Sample description	Shaft	Platinum mine A	Platinum mine B	Platinum mine C
Field blank		3	3	3
Workshop		3	3	3
10 min ambient	Diesel shaft	3		3
30 min ambient		3	3	3
LHD exhaust		3	3	3
Field blank	Non-diesel shaft	3		
10 min ambient		3	3	
Total		21	15	15

**Table 3-2 Sample name abbreviations and corresponding numbers**

Sample Description	Abbreviation	Number	Colour
30 minute ambient sample from Plat mine A	30MIN A	1	BLUE
30 minute ambient sample from Plat mine B	30MIN B	2	RED
30 minute ambient sample from Plat mine C	30MIN C	3	GREEN
Workshop sample from Plat mine A	WS A	4	
Workshop sample from Plat mine B	WS B	5	
Workshop sample from Plat mine C	WS C	6	
LHD sample from Plat mine A	LHD A	7	
LHD sample from Plat mine B	LHD B	8	
LHD sample from Plat mine C	LHD C	9	
10 minute ambient sample from Plat mine A	10MIN A	10	
10 minute ambient sample from Plat mine B	10MIN B	11 <sup>#</sup>	
10 minute ambient sample from Plat mine C	10MIN C	12	
Non-diesel sample from Plat mine A	ND A	13	
Non-diesel sample from Plat mine B	ND B	14	

# Not sampled due to sampling equipment constraints

**Table 3-3 Temperature, humidity, air velocity and sampled volume of each sample**

Sample no:	Temperature (°C)	Humidity (%)	Ambient air velocity (m.s <sup>-1</sup> )	Volume sampled (L)	Sampling flow rate (L.min <sup>-1</sup> )
1	31.4	63.0	0.4	14.5	0.483
2	23.2	55.0	0.8	33.4	1.115
3	25.2	70.0	0.7	30.0	1.000
4	27.3	36.0	0.0	5.0	0.503
5	20.4	49.8	-	4.9	1.115
6	22.8	47.2	0.0	7.0	1.000
7	27.3	36.0	0.0	5.0	0.503
8	23.2	55.0	0.8	11.1	1.115
9	20.7	76.0	-	5.0	1.000
10	31.4	63.0	0.4	5.0	0.503
11	-	-	-	-	-
12	22.3	81.6	0.9	10.0	1.000
13	30.9	48.3	0.5	5.0	0.503
14	23.2	62.4	8.45	22.3	1.115

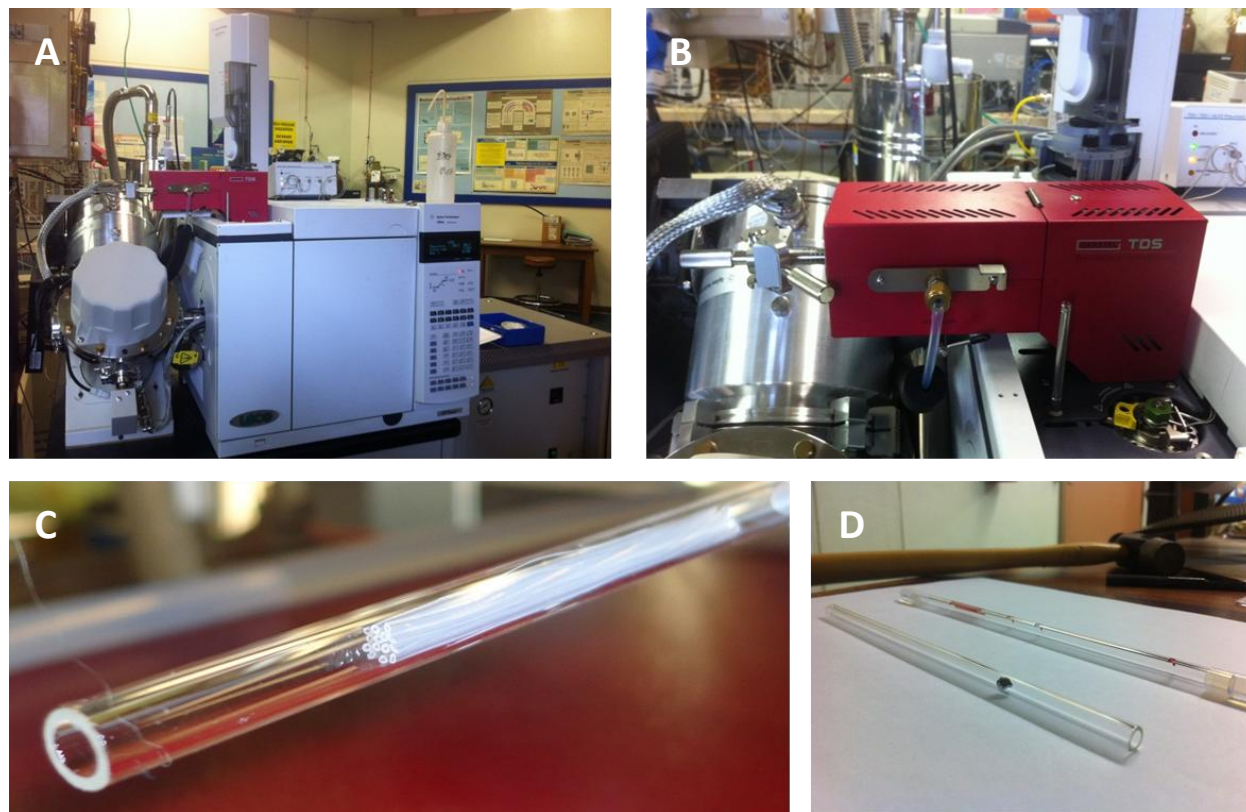
### 3.2.3 Analytical techniques-mine study

The method used in this study was based on a previously employed PAH analysis method which was used by Forbes in 2012 who investigated particle emissions from household fires in South Africa (Forbes 2012b). A LECO Pegasus 4D instrument (LECO, St. Joseph, MI, USA) was equipped with an Agilent Technologies 7890 GC (Palo Alto, CA, USA) and an Agilent 7683B autosampler, a quadjet dual-stage modulator and a secondary oven (Fig. 3-2 A). Data acquisition and processing was executed by ChromaTOF software version 4.0 (LECO Corp., St. Joseph, MI). A Gerstel 3 TDS was employed at the back inlet for sample introduction (Fig. 3-2 B). Synthetic air was used for the hot jets and liquid nitrogen (LN<sub>2</sub>) was used to cool nitrogen gas for the cold jets with an AMI Model 186 liquid level controller to maintain sufficient levels.

The GC column set consisted of a Restek Rxi-5Sil, 5 %-phenyl–95 %-methylsiloxane (30 m, 0.25 mm i.d., 0.25 µm df) as the first dimension (1D) and a Restek Rxi-200, 50 %-phenyl–50 %-methylsiloxane (1.5 m, 0.1 mm i.d., 0.1 µm df) as the second dimension (2D). The method parameters for the mine sample analysis are given in Table 3-4. PDMS traps were analysed as is and the filters were inserted into the heating zone of a glass tube for desorption (refer to Fig. 3-2 C and D).

Raw data results from the instrument were then sorted to remove all siloxanes (which were due to artefacts from the traps and filter or column bleed) and to remove all compounds with a NIST library match similarity of less than 80 %. After sorting, the remaining compounds were then classified into acid anhydrides, acids, aldehydes, esters, ketones, heterocyclic nitrogen-containing compounds, non-

heterocyclic nitrogen containing compounds, PAHs, PAH derivatives, saturated hydrocarbons, unsaturated hydrocarbons and the remaining compounds were classified as “other”.



**Figure 3-2 A:** Instrumental setup, showing GC-MS fitted with a Gerstel thermal desorber, **B:** TD system, **C:** PDMS trap to be inserted into the TD, **D:** filter placed in glass tube to be inserted into the TD (Photographed by G. Geldenhuys).

Once the data had been acquired, the data was processed by a predefined processing method whereby individual peaks were automatically detected on the basis of a 50:1 signal to noise ratio. Compound identification was performed by inspection and comparison of automatically acquired individual peak areas with literature mass spectra as well as the retention times and elution order obtained from the analysis of pure and mixed PAH standards.

A standard mixture solution of 2000  $\mu\text{g}\cdot\text{mL}^{-1}$  PAHs in  $\text{C}_6\text{H}_6:\text{CH}_2\text{Cl}_2$  (50:50) was acquired from Supelco (Bellefonte, USA). A stock solution of 1000  $\mu\text{g}\cdot\text{mL}^{-1}$  was prepared from which calibration standards of 5, 10, 20, and 30  $\mu\text{g}\cdot\text{mL}^{-1}$  were prepared and used to initially calibrate the instrument. Later, further dilutions of the calibration standards were prepared (refer to Section 3.6.6).

Table 3-4 Method parameters for the instrumental analysis of the mine samples

<b>Thermal desorption method</b>	
Flow mode	Splitless
Initial temperature	30 °C
Final temperature	280 °C
Desorption flow rate	100 mL.min <sup>-1</sup>
Ramp rate	60 °C min <sup>-1</sup>
Hold time	5 min
<b>Cooled injection system (CIS) method</b>	
Initial temperature	-50 °C
Final temperature	280 °C
Ramp rate	12 °C min <sup>-1</sup>
Hold time	5 min
<b>Gas chromatography method</b>	
Carrier gas	Helium
Column flow rate	1.0 mL.min <sup>-1</sup>
Constant flow mode	yes
Mode	Solvent vent
Primary column	Rxi-5Sil, (30 m, 0.25 mm i.d., 0.25 µm df)
Secondary column	Rxi-200, 50 % (1.79 m, 0.15 mm i.d., 0.15 µm df)
Primary oven initial temperature	40 °C
Primary oven final temperature	315 °C
Ramp	10 °C min <sup>-1</sup>
Hold time	5 min
Secondary oven initial temperature	45 °C
Secondary oven final temperature	320 °C
Ramp	10 °C min <sup>-1</sup>
Hold time	5 min
Transfer line temperature	280 °C
Modulation period	4 s
Modulator offset	30 °C
<b>Mass spectrometry method</b>	
Start mass	50
End mass	500
Electron energy	70 eV
Ion source temperature	200 °C
<b>Data processing method</b>	
Minimum S/N	50

Thousands of peaks were found in the two-dimensional chromatograms when the automated peak identification routine was used based on deconvolution methods. Single ion masses of PAHs were extracted and classified and the NIST library (NIST 08) was consulted to compare the similarities of spectra, where only library matches of greater than 80 % were then used for tentative identification purposes.

Peak areas were an indication of the concentration of a given substance. In order to do inter-mine or inter-sample comparisons, the peak areas were used simply as the sum of the volume normalised peak areas (i.e. peak area per litre sampled) obtained for a specific compound class or a specific PAH.

Relative % peak areas were calculated by using the peak area of a given compound, divided by the total peak area (sum of every peak in sample) multiplied by 100 which was useful to see the apportionment patterns or profiles of a sample using relative amounts of the compounds.

Principle component analysis (PCA) was performed using JMP 10 software and was based on covariance. Score plots, loading plots and eigenvalue bar graphs were generated (Wold *et al.* 1987).

### 3.3 Daspoort Tunnel study

#### 3.3.1 Gas phase sampling

In June 2011, air samples were actively taken at different positions and at different times from inside the Daspoort Tunnel, using a GilAir portable sampling pump operating at  $439 \text{ mL}\cdot\text{min}^{-1}$ . The pump drew air through a single multi-channel silicone rubber trap (MC22) (similar to Fig. 3-1) which was used according to the method described by Forbes *et al.* (2011). The sampling was performed for 10 min for each sample after which the samples were stored as per Section 3.1. Two denuder sets were used to sample gas and particulate phase PAHs (see Section 3.2.2 for details of the denuder setup).

The 1.0 m sampling height from the ground was used to represent the height of a person inside a vehicle and 1.5 m for that of a pedestrian in the tunnel.

**Table 3-5 Description of the gas phase sampling parameters in the Daspoort Tunnel**

Sample name	Sample type	Traffic time	Sample height (m)	Tunnel position
936	single trap	off peak	1.0	Entrance
934	single trap	peak	1.0	Entrance
928	single trap	off peak	1.5	Inside
927	single trap	off peak	1.0	Inside
926	single trap	peak	1.5	Inside
929	single trap	peak	1.0	Inside
550	denuder primary trap*	off peak	1.0	Entrance
324	denuder secondary trap#	peak	1.0	Inside
334	denuder primary trap#	peak	1.0	Inside

\*Indicating a component of denuder set 1

# indicating a component of denuder set 2

### 3.3.2 Particulate phase sampling

#### 3.3.2.1 Denuder filters

Two filters were obtained from the denuder sets mentioned in Table 3-5. Only one complete denuder (primary trap, secondary trap and filter) was obtained due to the loss of the secondary trap from the first set due to an instrumental malfunction.

#### 3.3.2.2 Swab sampling

Swab samples were taken from the pedestrian railings along the North-South (NS) lane of the tunnel (Fig. 3-3). Whatman quartz filter paper (cut into strips) was used to sample the visibly aged soot that was deposited on the rail. The aged soot samples were used to compare the “freshly” sampled particulate matter. Table 3.6 details the swab sampling parameters.



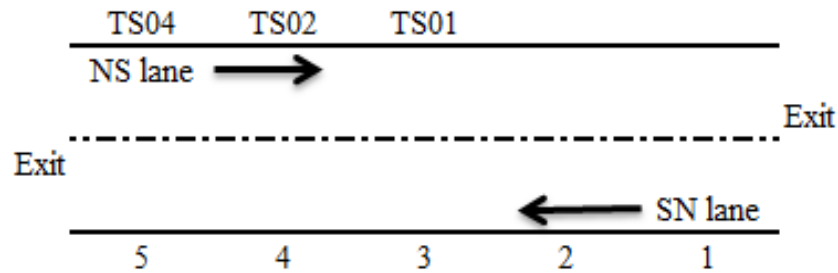


Figure 3-3 Photographs of swab samples and positions in the tunnel (573 m in length) where swab samples were taken (where TS = tunnel swab as defined in Table 3.6) (Photographed by P. Forbes)

### 3.3.2.3 Weekly filter samples

A Thermo Scientific Area Dust Monitor, Model ADR-1500 was used to sample particulate matter in the Daspoort Tunnel. The instrument used a “red cyclone” type of inlet that drew air at a flow rate of  $1.19 \text{ L}\cdot\text{min}^{-1}$  through a sensing chamber onto a Whatman 934-AH, 37 mm glass filter paper. The sensing chamber consisted of a light-scattering photometer which measured the intensity of light scattered by PM which was linearly proportional to the PM concentration (Thermo Scientific 2012). The mass concentrations were continuously monitored, averages were automatically recorded every 10 min and the PM loaded filter was removed after a week of sampling. The filter paper was then stored in a glass petri dish covered with aluminium foil to prevent photo degradation of the semi-volatile compounds (Forbes 2009). The weekly collected ADR loaded filters were manually punched using a 5 mm diameter punch to give a representative sample of the bulk matter. The punched disc was then placed into the heating zone of TD glass tube before being directly introduced into the GC column via a thermal desorber.

**Table 3-6 Description of the particulate phase sampling parameters in the Daspoort Tunnel**

Sample name	Sample type	Traffic time	Sample height (m)	Tunnel position
DTSF08	denuder filter*	off peak	1.0	entrance
DTSF09	denuder filter#	peak	1.0	inside
TS01	tunnel swab sample	-	from railing	¼ way inside
TS02	tunnel swab sample	-	from railing	middle
TS04	tunnel swab sample	-	from railing	entrance
WEEK 1	weekly filter	continuous	2.5	inside
WEEK 2	weekly filter	continuous	2.5	inside
WEEK 3	weekly filter	continuous	2.5	inside
WEEK 4	weekly filter	continuous	2.5	inside
WEEK 6	weekly filter	continuous	2.5	inside

\*Indicating a component of denuder set 1

# indicating a component of denuder set 2

### 3.3.3 Analytical techniques-tunnel study

The instrument parameters for the tunnel sample analysis were the same as for the mine sample analysis (refer to Section 3.2.3) except the system was equipped with an Agilent 6890 GC.

The temperature of the TDS (Gerstel TDS 3) was initially 30 °C for 30 min and ramped to 280 °C for 5 min at a 60 °C.min<sup>-1</sup> in the splitless mode. The desorbed semi-volatiles were then cryogenically focused onto a glass liner via a cooled injection system (CIS) using nitrogen at -40 °C, the temperature was then rapidly ramped at 12 °C.s<sup>-1</sup> to 280 °C.

The column set consisted of Rxi-5Sil, 5 % phenyl-95 % methylsiloxane (30 m, 0.25 mm i.d., 0.25 µm df) as the first dimension and Rxi-200 50 % phenyl-50 % methylsiloxane (1.5 m, 0.1 mm i.d., 0.1 µm df) as the second dimension. The primary oven temperature was programmed to an initial 40 °C for 3 min which was then ramped at 10 °C.min<sup>-1</sup> to 300 °C and held for 5 min. The secondary oven temperature was ramped from: 45 °C (3 min) at 10 °C. min<sup>-1</sup> to 305 °C (5 min). The total run time was 34 min.

The MS transfer-line temperature was set at 280 °C. The modulator temperature offset was 30 °C and the modulation period was 4 s with a hot pulse time of 1.0 s. The MS ion source temperature was set at 200 °C with the electron energy at 70 eV. The GC×GC-ToFMS data acquisition and processing was executed using ChromaTOF software, version 4.0, and the data acquisition rate was 100 spectra per second.

## 3.4 Helmholtz Virtual Institute of Complex Molecular Systems in Environmental Health (HICE) campaign Germany 2012

### 3.4.1 Sampling and analysis

Sampling was carried out at the University of Rostock in Germany during the month of November in association with the 2012 HICE campaign. The sampling setup consisted of two 81 mm long glass liners with a 5 mm quartz fibre filter that was placed between them. This configuration allowed for particulate phase sampling of PAHs. The one end of the liner was connected to the sample port via a Teflon adaptor which was fitted through a sized red adaptor and the other end was connected to a critical nozzle (8 Neu or D 18) via rubber tubing (see Fig. 3-4 and 3-5). A personal sampling pump could not be used as the back pressure from the experiment setup was too high for efficient pump operation. A critical nozzle was used which was calibrated to give the correct air flow. The flow rate obtained was thus 482.5 mL.min<sup>-1</sup> or 414 mL.min<sup>-1</sup> respectively and sampling was done for 10 min in both cases.

Four filter samples (Table 3-7) were taken during different engine loads using light fuel oil (LFO) which were analysed at the University of Pretoria with the same method used for the mine samples (refer to Section 3.2.3). The results can be seen in Chapter 5, following the tunnel results.

**Table 3-7 Sample information for filter samples from the ship exhaust during different engine loads using light fuel oil**

Sample Number	Engine load (%)	Sampling time	Flow rate (mL.min <sup>-1</sup> )	Experiment date
1	100	08h48-08h58	482.5	20 Nov 2012
2	75	09h10-09h20	414	20 Nov 2012
3	50	10h10-10h20	482.5	20 Nov 2012
4	25	10h25-10h35	482.5	20 Nov 2012

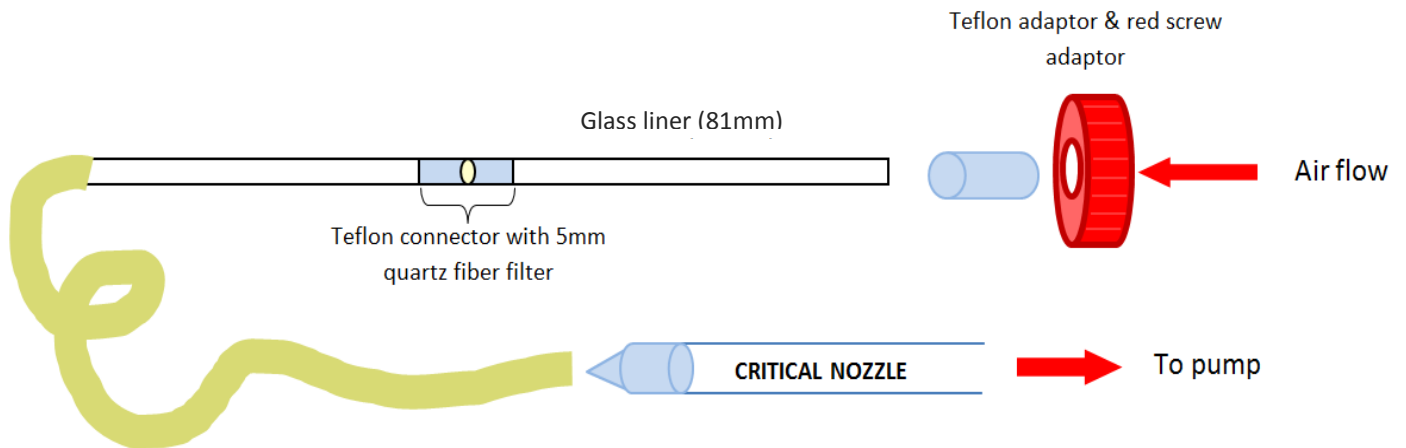


Figure 3-4 Sampling setup for particulate samples for the HICE campaign

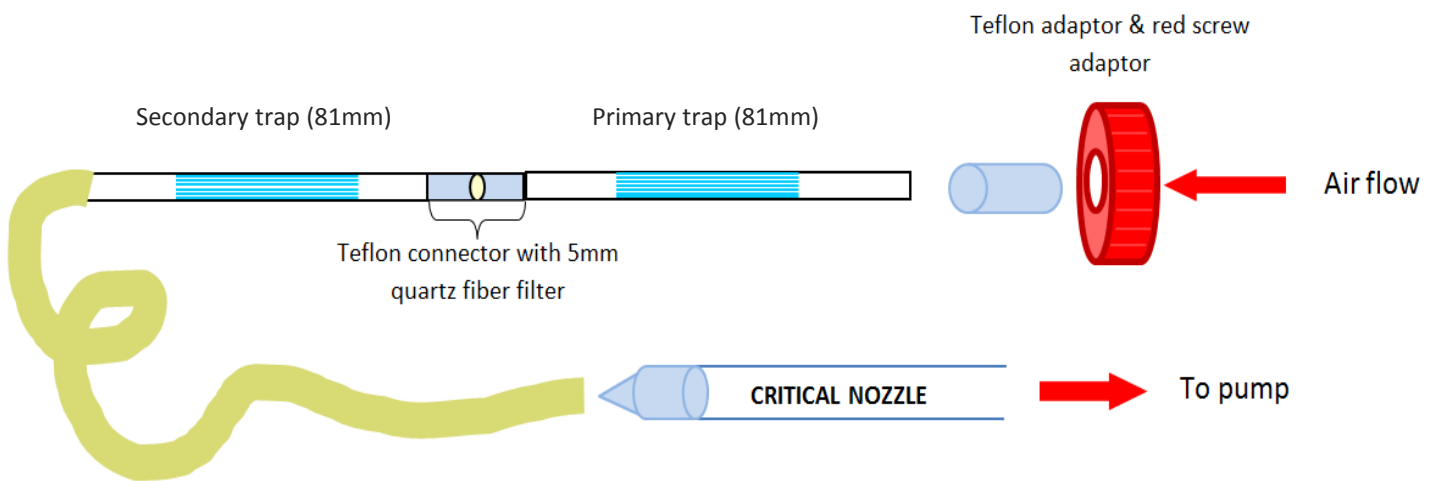


Figure 3-5 Sampling setup for particulate and gas phase PAH samples for the HICE campaign

A total of 12 denuders were also used for gas and particulate PAH sampling of the ship engine exhaust emissions during the use of light fuel oil (LFO) and heavy fuel oil (HFO) at different engine % loads. Sampling was carried out using denuder sampling devices which were made in the exact same manner as in Section 3.2.2, but the dimensions of the traps and filter were altered as seen in Fig. 3-4 and 3-5. These denuder samples are to be analysed at the Helmholtz Zentrum in Munich and were taken in parallel with many other samples applying diverse sampling techniques and those results are not reported here.

### 3.5 Method development for platinum mine study

A previously employed PAH analysis method was used as the starting point for the method development for this particular study (Forbes 2012b). The instrument was run in constant flow mode. Before commencing with the method development, the instrument was baked out (oven and TDS set to 300 °C for 30 min) and an empty glass tube was analysed to confirm that there was no contamination or carry over from previous analyses that remained in the system.

A 10 ng PAH mix standard was spiked onto a filter and then analysed in one dimension (no modulation) in order to initially identify the target analytes and evaluate the extent of separation in order to make adjustments to the method. The 1D method was first optimized before running in 2D to save time and prevent the unnecessary use of liquid nitrogen.

The 1D chromatogram showed good separation for the lighter PAHs and almost all of the PAHs could be clearly identified. The signal to noise ratio threshold was lowered from 500 to 50 which allowed the identification of the lower intensity peaks such as fluorene.

The heavier PAHs with masses higher than (and including) 252 g.mol<sup>-1</sup> were not initially seen in the 1D chromatogram. The desorption hold time was doubled from 5 minutes to 10 minutes and the solvent vent flow was increased from 50 mL.min<sup>-1</sup> to 100 mL.min<sup>-1</sup> to ensure that these heavier PAHs were eluted. The primary GC oven final temperature was increased to 315 °C with an offset of 20 °C to ensure elution of all of the PAHs and the oven ramp rate was decreased from 10 °C to 5 °C to prevent coelution of the heavier isomeric PAHs.

Another filter spiked with a 10 ng PAH mix standard was analysed in 1D with the new method parameters (see Fig. 3-6). The identification of all of the PAHs was successful (library match > 80 %) and analyte peaks were baseline resolved. Empty traps were run in between all standards and filter samples. Spiked filter samples were then run in 2D mode and the chromatogram and 3D plots (Fig. 3-7) revealed that good separation and identification of all of the PAHs was possible.

The method development went smoothly however obstacles were encountered.

## Obstacles encountered during chromatographic analysis

The column snapped at the secondary oven entrance, the secondary column lost 25 cm of length which would ultimately affect the results (retention times) however the length was still sufficient for good separation.

The press fit that was used to join the primary and secondary columns caused minor problems with the analysis. After the leak test passed in the morning, the results of the analysis revealed shifts in the retention times after which the leak profile view showed N<sub>2</sub> and O<sub>2</sub> peaks that were exceedingly large. The leak test was then repeated and confirmed that the relative abundances of N<sub>2</sub> and O<sub>2</sub> were above the allowed limits. The nuts were checked and monitored for leaks but it was found that it was the press fit that was loose and not sealing at the column interface. This leak obstacle would occur regularly and the press fit had to be secured numerous times a day and replaced at least weekly, as the leaks would get significantly worse. Not only did this cause time constraints and shifts in retention times but every time the press fit had to be changed, the column had to be cut. The solution to this problem was to install a mini union between the primary and secondary column as a replacement to the press fit and this proved to be successful.

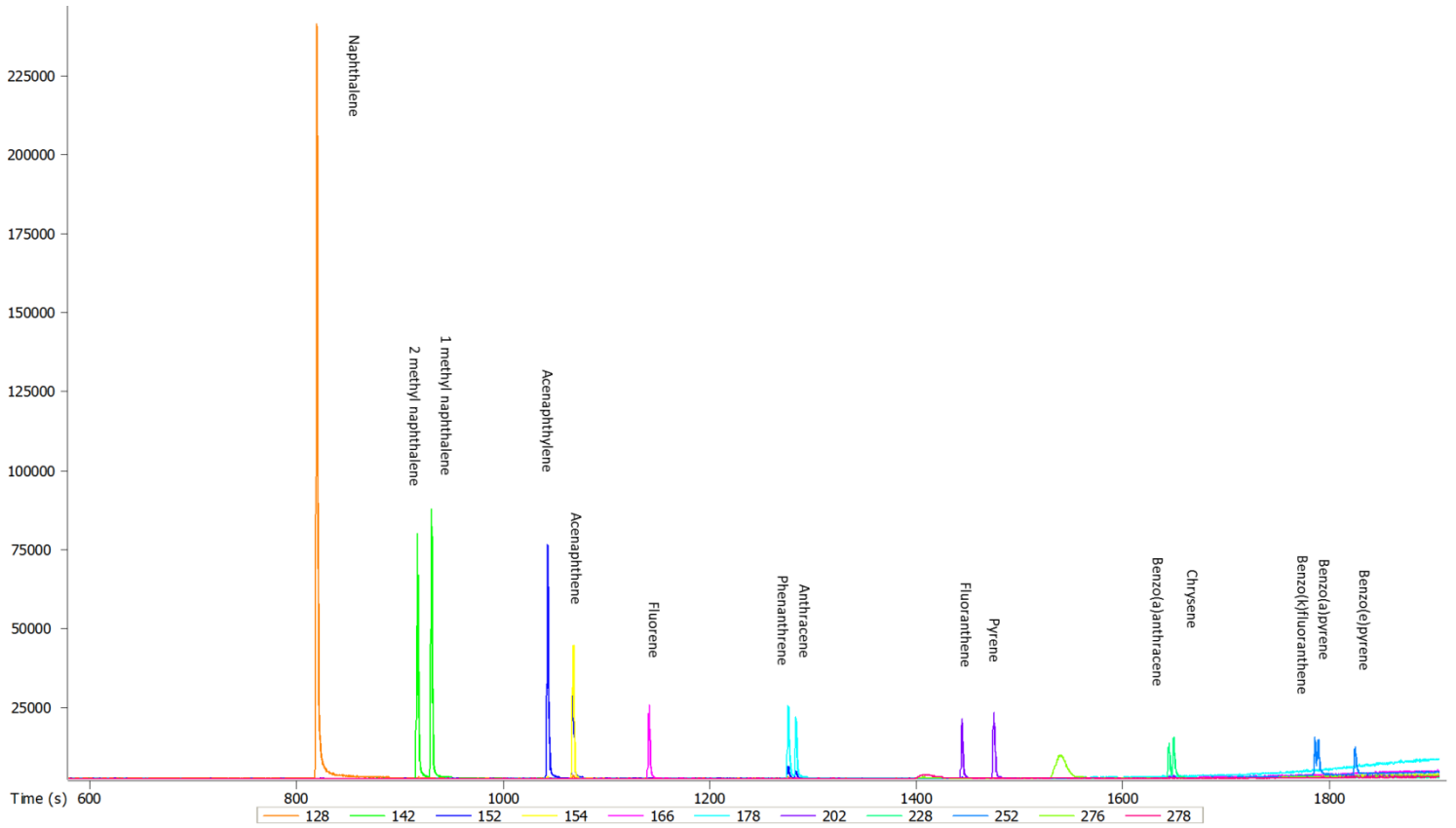


Figure 3-6 Reconstructed ion 1D chromatogram of a 10 ng PAH mix standard for PAH masses (128, 142, 152, 154, 166, 178, 202, 228, 252, 276 & 278 Da)

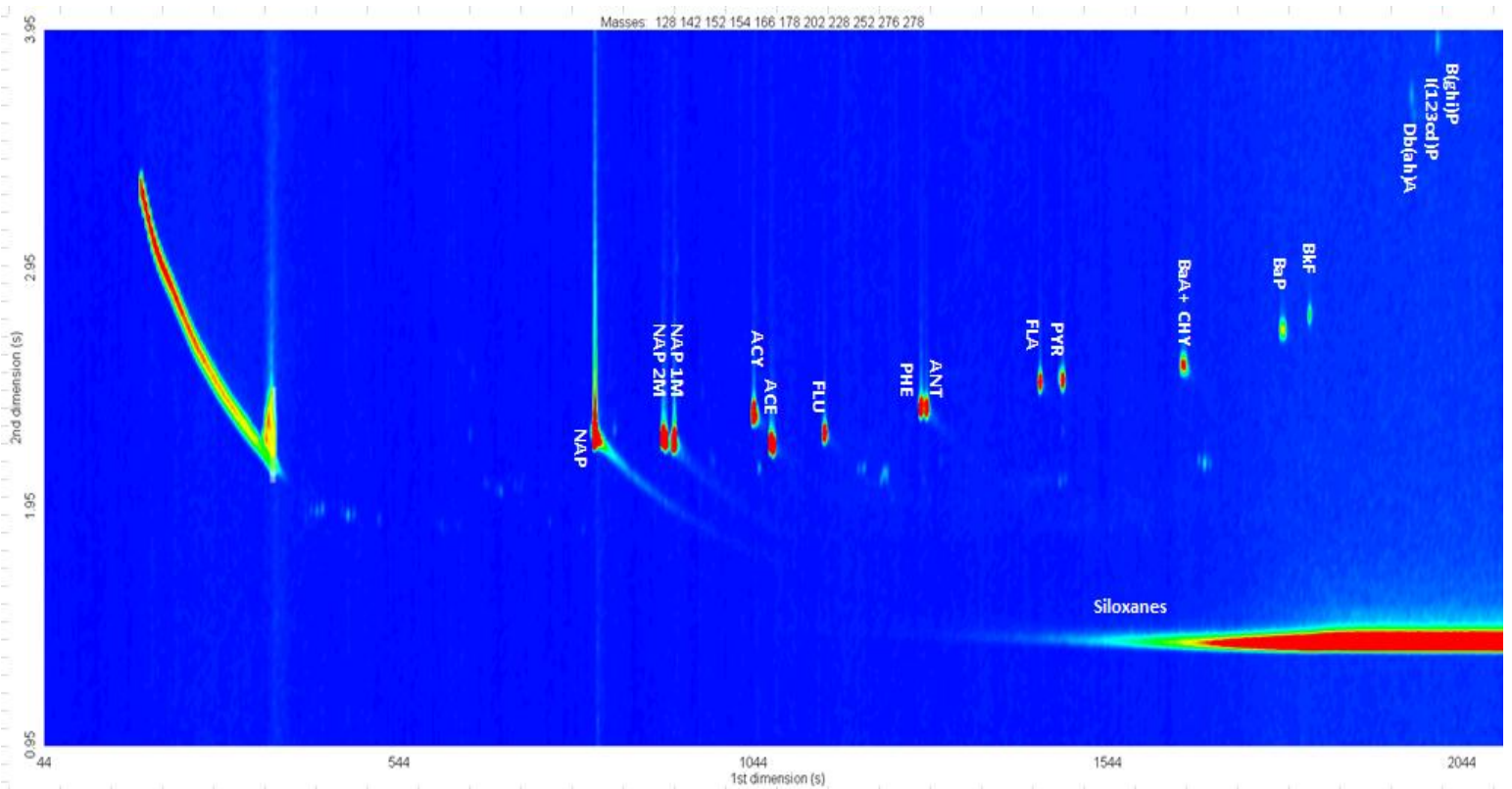


Figure 3-7 Reconstructed ion 2D chromatogram of a 5 ng PAH mix standard for PAH masses (128, 142, 152, 154, 166, 178, 202, 228, 252, 276 & 278 Da)

A difficulty arose in identifying the PAHs that possessed the same molecular weight (MW) and identical spectra such as the isomeric PAHs: phenanthrene and anthracene (MW 178), pyrene and fluoranthene (MW:202), benzo(a)anthracene and chrysene (MW: 228). Pure standards were prepared and analysed in order to identify each PAH and to distinguish the order of elution of these isomeric PAH pairs (Fig. 3-8 and 3-9).

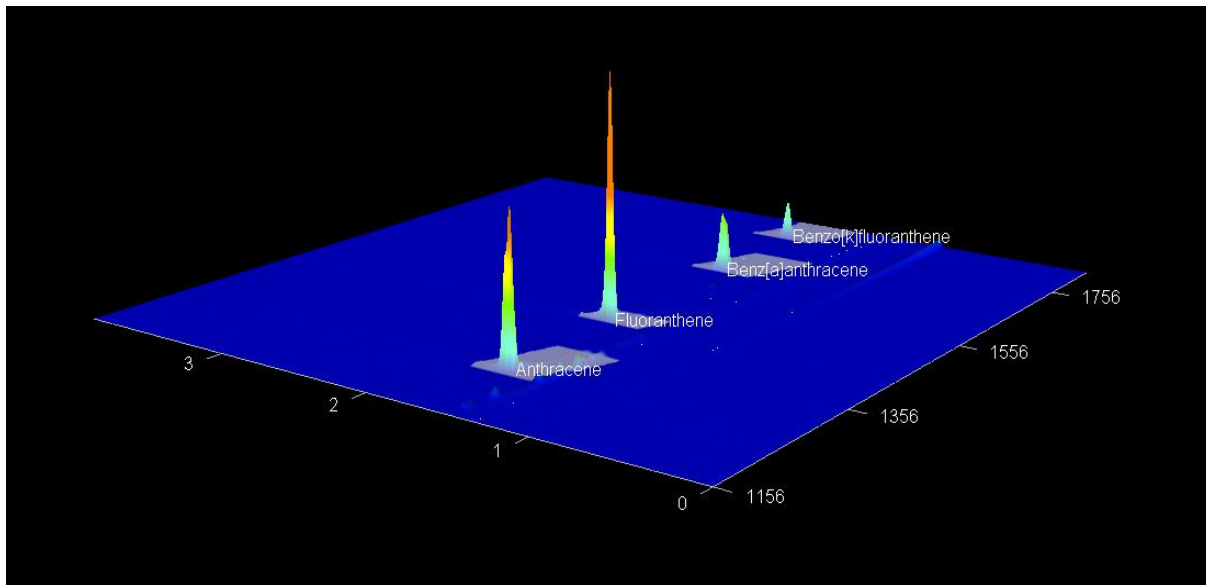
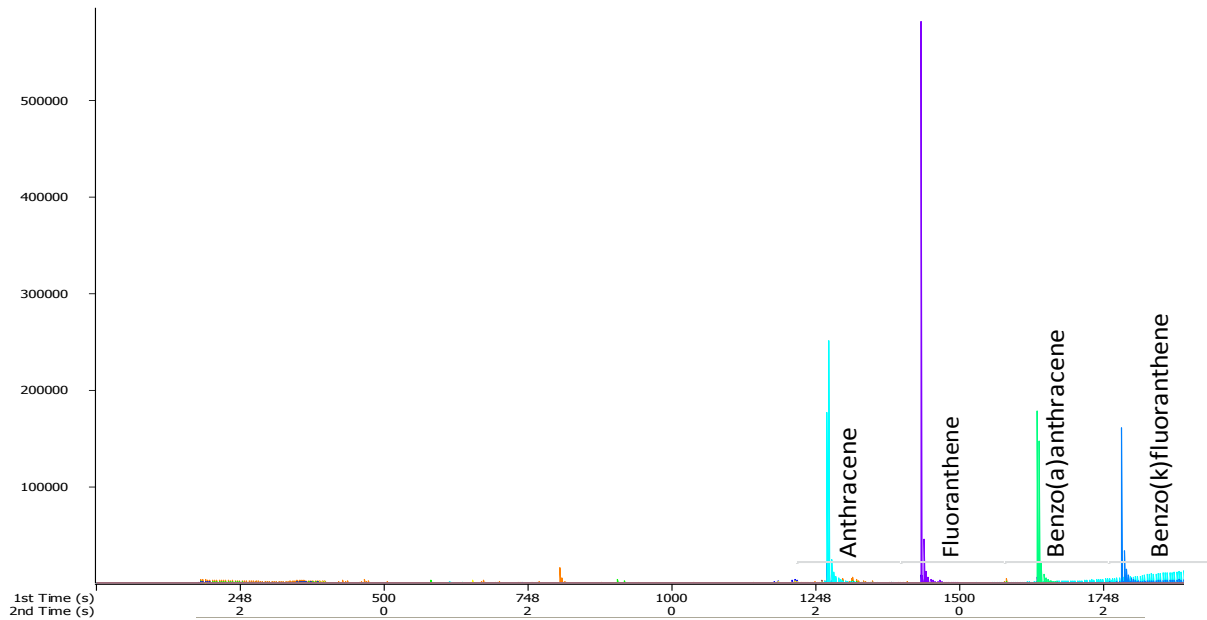


Figure 3-8 Reconstructed 2D ion chromatograms of pure PAH standards for masses 178, 202, 228, 252 Da



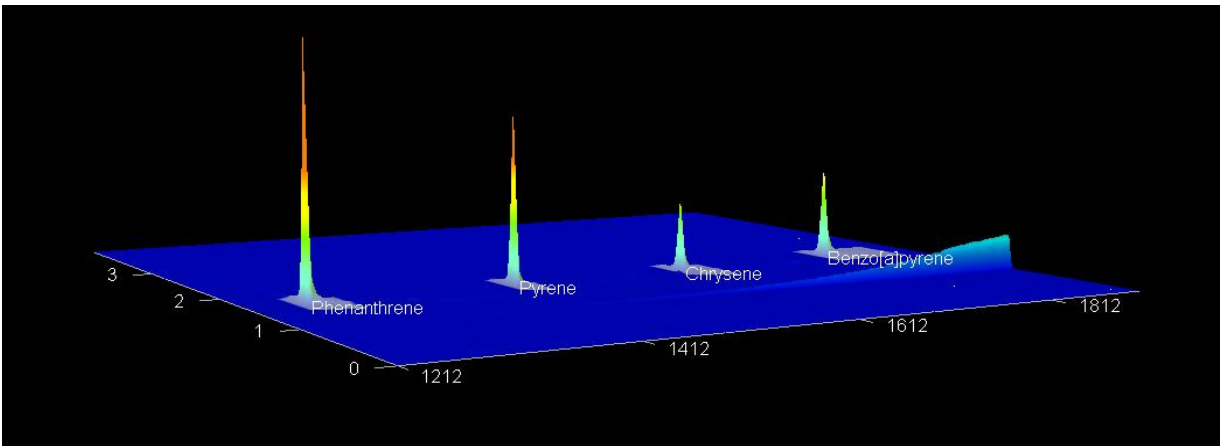
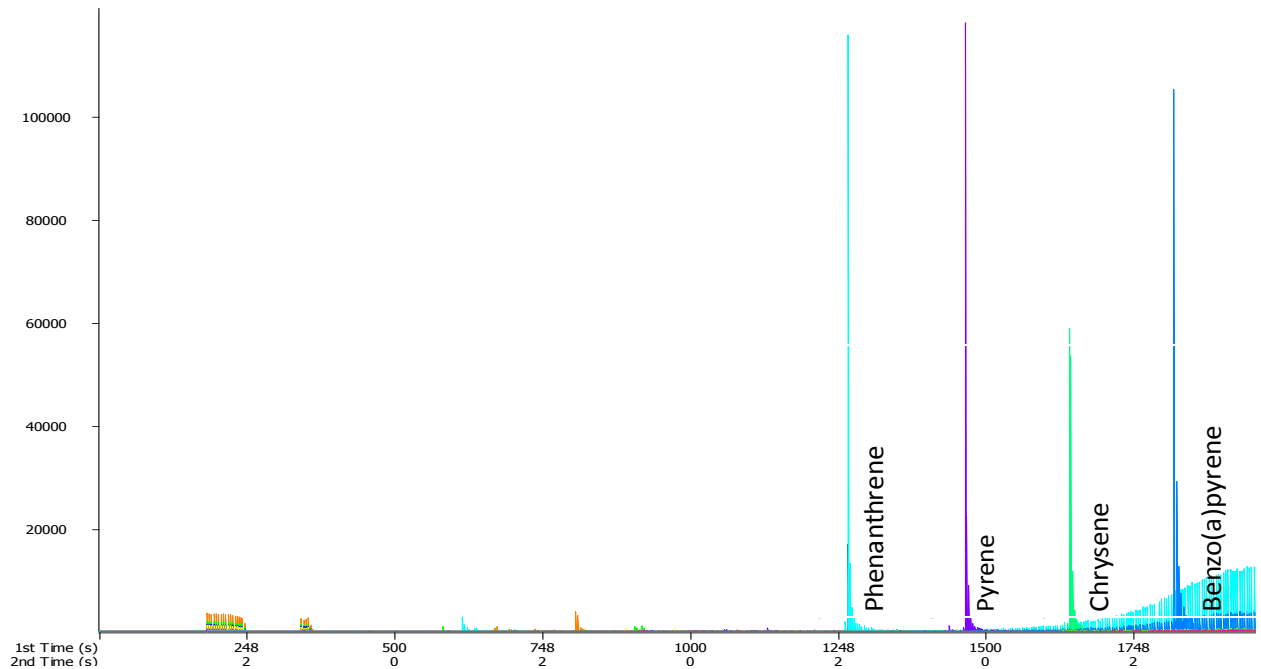
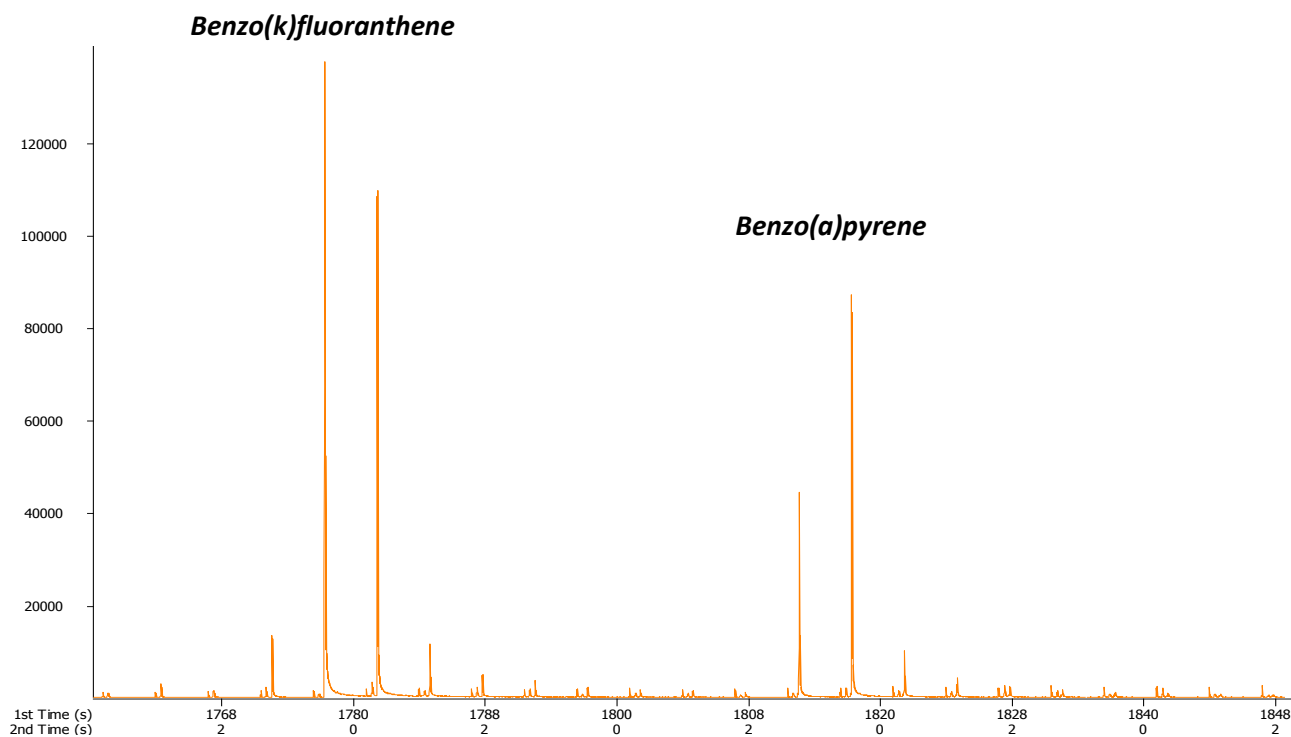


Figure 3-9 Reconstructed 2D ion chromatograms of pure PAH standards for masses 178, 202, 228, 252 Da

There were at least 5 known heavier PAHs that had the same mass at 252 amu and these all eluted close to each other, however pure standards of each of these heavier PAHs were analysed and the exact retention times were obtained. The benzopyrenes eluted close to each other just as the benzo fluoranthenes (b, j then k) eluted close to each other and in many cases would co-elute. This co-elution is a common problem often solved by reporting the value for benzo fluoranthenes as a whole as seen in

the literature (Schnelle-Kreis *et al.* 2011). Alternatively, the GC method can be adjusted to achieve optimum separation for compounds of mass of 252 amu.



**Figure 3-10 Reconstructed 2D chromatogram of heavier PAHs in a 5ng standard. 252 mass was extracted.**

The data showed benzo(k)fluoranthene and benzo(a)pyrene as single, separated peaks therefore co-elution was not a problem. This can be seen in the chromatograms of Fig. 3-10 representing the 5 ng standard.

The heaviest PAHs at 276 and 278 were also identified as they were included in the PAH mixed standard and the order of elution of indeno(1,2,3-cd)pyrene and benzo(ghi)perylene (both with mass 276 amu) was known (refer to Fig. 3-11).

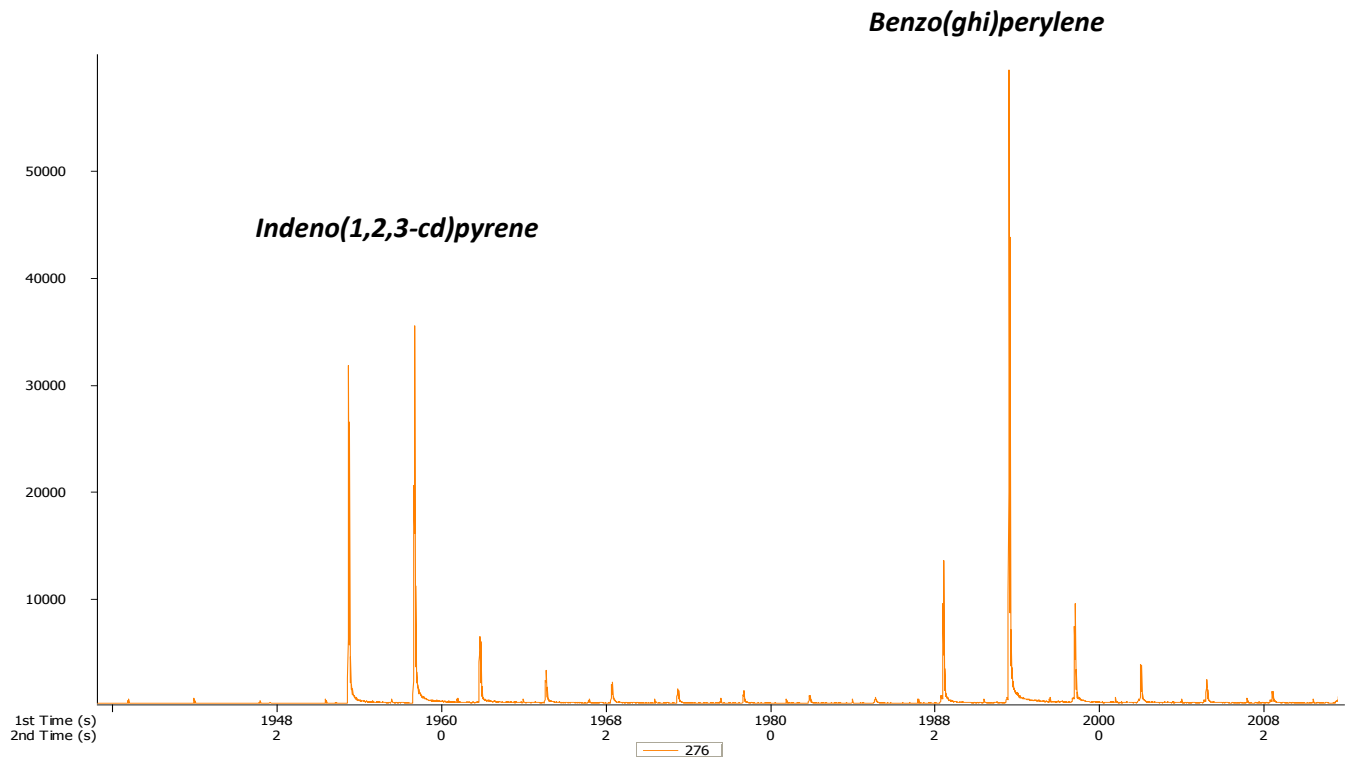


Figure 3-11 Reconstructed 2D chromatogram showing the optimised separation of indeno(1,2,3-cd)pyrene and benzo(ghi)perylene in 2D GCxGC-ToFMS from a 5 ng standard.

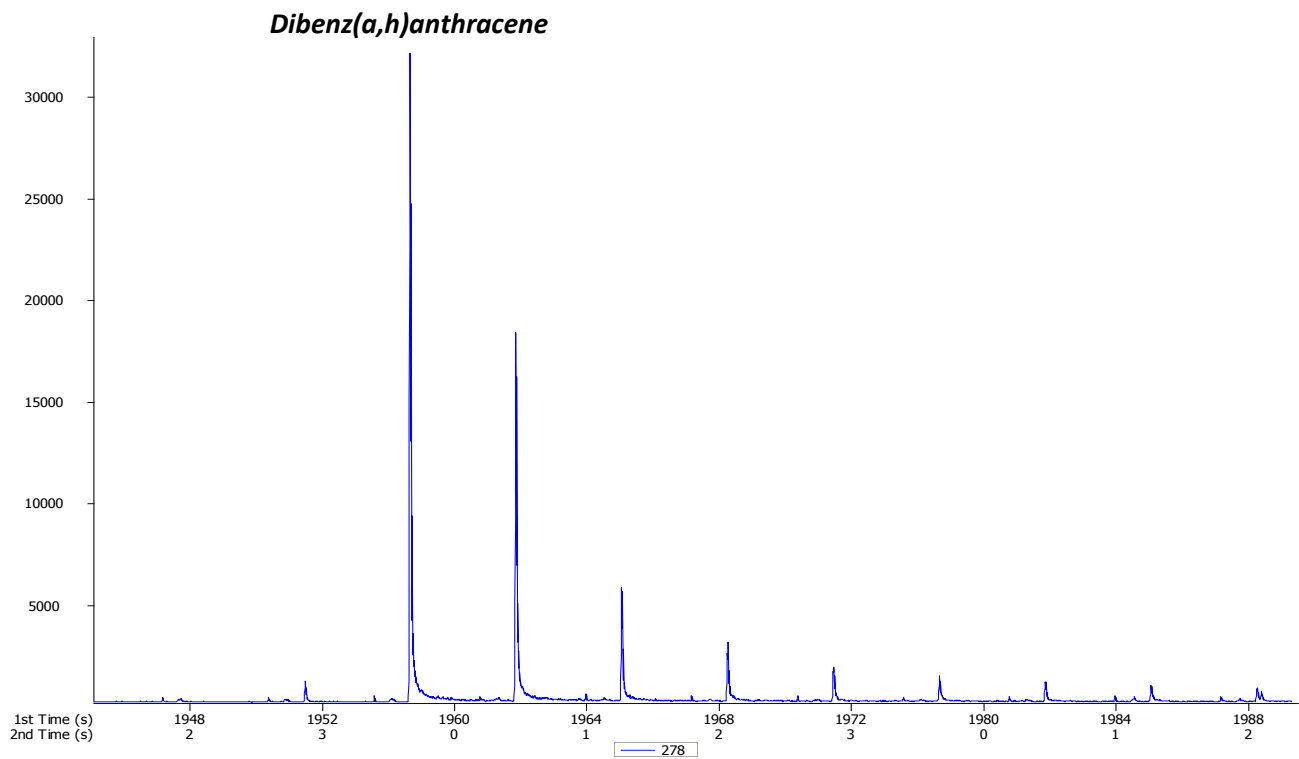


Figure 3-12 Reconstructed 2D chromatogram showing the optimised separation dibenz(a,h)anthracene in 2D GCxGC-ToFMS from a 5 ng standard chromatogram of PAHs in a 5ng standard.

The analysis of PAH standards, both pure and individual mixed standards, as well as NIST retention indexes that were consulted made it possible to assign retention times to all of the PAHs. The retention times are summarised in Table 3-8. Although the retention times changed slightly due to the shortening of the column, the order of elution as well as the difference in retention times can be used throughout the study to identify each of the 16 EPA PAHs.

**Table 3-8 Retention times of PAHs that have the same molecular ions**

PAHs	m/z	Retention time (s)	
		1st D	2nd D
Naphthalene	128	788	1.02
Naphthalene, 2-methyl-	142	888	1.01
Naphthalene, 1-methyl-	142	900	1.01
Acenaphthylene	152	1012	1.06
Acenaphthene	154	1040	1.00
Fluorene	166	1112	1.02
1H-Phenylene	166	1100	1.05
Phenanthrene	178	1252	1.07
Anthracene	178	1256	1.07
Fluoranthene	202	1420	1.12
Pyrene	202	1452	1.14
Benz[a]anthracene	228	1624	1.15
Chrysene	228	1632	1.18
Perylene	252	1816	1.24
Benzo[j]fluoranthene	252	1768	1.21
Benzo[k]fluoranthene	252	1772	1.22
Benzo[b]fluoranthene	252	1760	1.24
Benzo[a]pyrene	252	1808	1.31
Benzo[e]pyrene	252	1800	1.24
Indeno[1,2,3-cd]pyrene	276	1952	1.53
Benzo[ghi]perylene	276	1984	1.61
Dibenz[a,h]anthracene	278	1952	1.55

Loaded Occupational Hygiene particulate filters (archived mine samples which had been collected by the respective mine personnel) were obtained from the CSIR and used to ensure that the developed method would be sufficient for complex matrices such as diesel particulate matter. Matrix matched standards were employed for quantitation to account for the matrix effects (refer to Section 3.6.6.2). Heavily loaded, medium loaded and lightly loaded filters from each of the three mines were analysed. The numerous samples that were analysed revealed that the lighter PAHs namely naphthalene (MW: 128), acenaphthylene (MW: 152), acenaphthalene (MW: 154), fluorene (MW: 166), phenanthrene and anthracene (MW: 178) were detected in almost every sample.

The heavier PAHs (MW: 252, 276, 278) were not readily seen in the CSIR archived underground mine samples and it was uncertain if the heavier PAHs were not seen because they simply were not present or if they were not effectively desorbed. A NIST reference material was analysed in duplicate in Section 3.5.1 to determine the desorption efficiency in terms of the heavier PAHs.

### 3.5.1 Analysis of a NIST DPM reference material

A clean filter was weighed and the balance was tared after which a miniscule amount of the solid NIST 2975 DPM standard was placed on the filter and the mass was recorded. Toluene was spiked onto the edge of the filter using a micro syringe and by capillary action the entire filter was soaked in solvent in order to prevent blow off of the dry DPM standard. The filter was then carefully folded using tweezers and placed into an empty glass tube for thermal desorption.

The peak areas that were obtained from the NIST standard were significantly larger than the peak areas in the highest calibration standard. The absolute minimum amount of standard practically possible was weighed onto a filter (0.150-0.176 mg) which still proved to be too high. An additional problem was that the NIST standard reference material was found to be inhomogenous when samples of 100 mg were analysed (NIST 2009), therefore sampling such small aliquots would be expected to incur a significant variability. The exact weight of the DPM standard could not be reproduced and loss of the standard was of concern. However, the results could be used qualitatively in terms of determining the desorption efficiency (detection) of the heavier PAHs as seen in Table 3-9. A possible solution to this problem would be to decrease the amount of solid DPM NIST standard that is weighed at least 10 fold to obtain peak areas within the linear calibration range but this would be physically impossible. An aerosol generator could be useful to obtain the correct concentration range of the NIST standard in the correct form. If this could be done reproducibly, the DPM standard could possibly be used to semi-quantify compounds that are not present in the liquid PAH Mix standard, such as various PAH derivatives and nitro-PAHs

Table 3-9 PAHs, nitro PAHs and PAH derivatives that were detected in the NIST 2975 DPM reference material

Name	m/z	Formula	Certified concentration (mg.kg <sup>-1</sup> )
Phenanthrene	178	C <sub>14</sub> H <sub>10</sub>	17.0 ± 2.8
Anthracene	178	C <sub>14</sub> H <sub>10</sub>	0.038 ± 0.008
Fluoranthene	202	C <sub>16</sub> H <sub>10</sub>	26.6 ± 5.1
Pyrene	202	C <sub>16</sub> H <sub>10</sub>	0.90 ± 0.24
Benzo[ghi]fluoranthene	226	C <sub>18</sub> H <sub>10</sub>	10.2 ± 0.5
Chrysene	228	C <sub>18</sub> H <sub>12</sub>	4.56 ± 0.16
Benz[a]anthracene	228	C <sub>18</sub> H <sub>12</sub>	0.317 ± 0.066
Benzo[e]pyrene	252	C <sub>20</sub> H <sub>12</sub>	1.11 ± 0.10
Benzo[j]fluoranthene	252	C <sub>20</sub> H <sub>12</sub>	0.82 ± 0.11
Benzo[k]fluoranthene	252	C <sub>20</sub> H <sub>12</sub>	0.678 ± 0.076
Benzo[a]pyrene	252	C <sub>20</sub> H <sub>12</sub>	0.0522 ± 0.0053
Indeno[1,2,3-cd]pyrene	276	C <sub>22</sub> H <sub>12</sub>	1.4 ± 0.2
Dibenz[a,h]anthracene	278	C <sub>22</sub> H <sub>14</sub>	0.52 ± 0.08
Phenanthrene, 9-nitro	223	C <sub>14</sub> H <sub>9</sub> NO <sub>2</sub>	0.444 ± 0.047
Anthracene, 9-nitro-	223	C <sub>14</sub> H <sub>9</sub> NO <sub>2</sub>	2.97 ± 0.45
Pyrene, 1-nitro	247	C <sub>16</sub> H <sub>9</sub> NO <sub>2</sub>	34.8 ± 4.7
Fluoranthene, 3-nitro-	247	C <sub>16</sub> H <sub>9</sub> NO <sub>2</sub>	3.74 ± 0.59
Phenanthrene, 2-methyl-	192	C <sub>15</sub> H <sub>12</sub>	2.0 ± 0.2
Phenanthrene, 1-methyl-	192	C <sub>15</sub> H <sub>12</sub>	0.89 ± 0.11
Phenanthrene, 4-methyl-	192	C <sub>15</sub> H <sub>12</sub>	0.44 ± 0.09
Phenanthrene, 2,5-dimethyl-	206	C <sub>16</sub> H <sub>14</sub>	0.57 ± 0.08
Phenanthrene, 3,6-dimethyl-	206	C <sub>16</sub> H <sub>14</sub>	0.18 ± 0.02
Pyrene, 2-methyl	216	C <sub>17</sub> H <sub>12</sub>	0.040 ± 0.008
Pyrene, 4-methyl-	216	C <sub>17</sub> H <sub>12</sub>	0.022 ± 0.005

Table 3-10 represented the certified concentrations of the NIST 2975 DPM reference material which were normalised to pyrene to give ratios that can be compared to the ratios of the experimental peak areas of the same NIST 2975 DPM standards which have also been normalised to pyrene. This comparison was done in order to determine whether there was any discrimination towards higher mass PAHs which did not desorb as efficiently. According to Table 3-10 it can be seen that the certified and experimental ratios of the lighter PAHs (up to pyrene) were more comparable (in a similar range) with anthracene being overestimated in the experimental results. The ratios from the NIST certified ratios were however generally higher than what was found experimentally specifically for phenanthrene, fluoranthene and benzo(a)anthracene + chrysene.

The heavier PAHs show ratios of less than one for all PAHs except benzo(k)fluoranthene and indeno(1,2,3-cd)pyrene which had higher concentrations than pyrene in the certified NIST standard. The

experimental ratios concur with most of the certified ratios except for indeno(1,2,3-cd)pyrene which was underestimated. The heaviest PAHs (above 252 g.mol<sup>-1</sup>) had lower experimental ratios compared with the certified ratios, therefore there was a slight discrimination toward the higher mass PAHs above 252 g.mol<sup>-1</sup> which may be attributed to the desorption limitations, as well the use of peak areas instead of concentrations.

**Table 3-10 Certified NIST concentrations normalised to pyrene compared to sample results areas normalised to pyrene**

PAH	Mass (g.mol <sup>-1</sup> )	Certified NIST 2975 DPM	Experimental NIST 2975 DPM
Phenanthrene	178	18.89	16.27
Anthracene	178	0.04	1.08
Fluoranthene	202	29.56	18.94
Pyrene	202	1.00	1.00
Benzo(a)anthracene +Chrysene	228	12.43	4.48
Benzo[e]pyrene	252	0.75	0.14
Benzo[k]fluoranthene	252	1.23	2.06
Benzo(a)pyrene	252	0.06	0.30
Indeno(1,2,3-cd)pyrene	276	1.56	0.06
Dibenz(a,h)anthracene	278	0.58	0.004
Benzo(ghi)perylene	276	0.55	ND

### 3.6 Method validation-Mine study

Method validation is a crucial part of quality assurance in analytical chemistry and it aids in the demonstration that the method is fit for its intended purpose. The important performance characteristics of method validation include applicability, repeatability, linearity, precision and the limit of detection (LOD) and quantification (LOQ).

It was important to know that the results obtained were reproducible and that every time a new trap was used that the analytes could be reproducibly desorbed and detected in every different trap. It is for this reason that trap desorption repeatability was investigated in Section 3.6.1.

When analysing the large Occupational Hygiene filter samples, the punch taken should be a representative portion of the whole filter. A filter repeatability investigation was conducted where 4 different punches from the same filter sample were analysed (Section 3.6.2) This was not an issue for denuder filter samples as the entire filter was analysed at one time.

The method that was developed was fit for purpose for this study, however the method parameters may be further optimised for PAH analysis. Desorption temperature and the source temperature were individually investigated in Section 3.6.3 and although it was a very brief investigation, it leads to future recommendations for PAH analysis.

The relative standard deviation (% RSD) is a measure of variability obtained by dividing the standard deviation by the average after which it is multiplied by 100 to obtain a percentage expression. The % RSD values were used in the method validation study to test for repeatability.

The Dixon's Q-test was used to test for statistical outliers in an experimental data set, i.e. to see if a value could be validly rejected or not, where a Gaussian distribution of data was assumed whenever this test was applied (Ellison *et al.* 2009). This test was applied for the repeatability studies of the traps and filters and it was applied as follows:

1. The n values comprising the set of observations are arranged in ascending order

**Equation 3-1**

$$x_1 < x_2 < x_3 \dots \dots \dots < x_n$$

2. Q-value ( $Q_{exp}$ ) was calculated with a ratio defined as: the difference between the suspect value (outlier) and the closest value to that outlier value, divided by the range of the experimental values (Ellison *et al.* 2009). For testing  $x_n$  as a possible outlier, the corresponding equation would be as follows:

**Equation 3-2**

$$Q_{exp} = (x_n - x_{n-1}) / (x_n - x_1)$$

3. The  $Q_{exp}$  value was then compared to a critical Q-value ( $Q_{crit}$ ) found in literature tables with a confidence level (CL) of 95 % (Ellison *et al.* 2009).
4. If  $Q_{exp} > Q_{crit}$  then the suspect value was indeed an outlier and the value was rejected.
5. If  $Q_{exp} < Q_{crit}$  then the suspect value was retained and used in all subsequent calculations.

The null hypothesis for the Q-test is stated as follows:

- $H = 0$ : There is no significant difference between the suspect value and the rest of the experimental data and any differences must be exclusively attributed to random errors.
- $H \neq 0$ : There is a significant difference between the suspect value and the rest of the experimental data and the suspect value can be regarded as an outlier.



### 3.6.1 Trap desorption repeatability

Trap desorption repeatability was performed by spiking a conditioned PDMS trap with 5 ng of a PAH mix standard which was then analysed by TD-GCxGC-ToFMS. This was repeated five times (5 different traps) in order to obtain enough data for statistical analysis. The results are shown in Table 3-11.

Table 3-11 PAHs thermally desorbed (using the conditions in Table 3-4) from traps and the peak areas of n replicates

PAH	m/z	n	Average peak area	Std dev	% RSD
Naphthalene	128	4 <sup>#</sup>	17943215	1889692	10.5
Naphthalene, 2-methyl-	142	5	8668773	1622702	18.7
Naphthalene, 1-methyl-	142	5	7819045	1171543	15.0
Acenaphthylene	152	5	6435366	2485100	38.6
Acenaphthene	154	4 <sup>#</sup>	6192932	899104.2	14.5
Fluorene	166	5	5992514	1195062	19.9
Phenanthrene	178	5	8008831	972706.5	12.1
Anthracene	178	4 <sup>#</sup>	5154880	809129.3	15.7
Fluoranthene	202	5	4393696	847286.6	19.3
Pyrene	202	5	4585981	869575.4	19.0
Benz[a]anthracene	228	5	4059442	918666.8	22.6
Benzo[b]fluoranthene	252	5	3231265	710585.8	22.0
Benzo[a]pyrene	252	5	1246389	317516.8	25.5
Indeno[1,2,3-cd]pyrene	276	5	675319.8	206812.4	30.6
Benzo[ghi]perylene	276	5	743898.6	232192.5	31.2
Dibenz[a,h]anthracene	278	5	407811	146880	36.0

<sup>#</sup> Outliers were rejected

From Table 3-11 it can be seen that trap repeatability ranges from % RSD values of 10.5 % for naphthalene to a higher value of 38.6 % for acenaphthylene. Generally the % RSD is below 25 % for most of the PAHs which was acceptable for trace amounts. It was seen that PAHs heavier than pyrene show less repeatability, as the % RSD values are higher for these PAHs, which was expected as they may have been lost in the system due to its inability to volatilise the heavier PAHs. Or perhaps condensation of the heavier PAHs occurred which would result in the compounds being trapped in the system as it was not designed for the high boiling compounds. The low naphthalene % RSD is encouraging as it is the most volatile PAH and would be expected to have much higher % RSD values. % RSD values of approximately 15 % for PAHs were reported in another study (Schnelle-Kreis *et al.* 2011) which compare well with this study. Outliers were identified at 95 % CL and they were removed.

There were a number of factors that contributed to the % RSD values (TD repeatability) which include human error to a large extent. It should be noted that a different trap was used for each replicate in order to get an idea of the inter-trap repeatability. The traps were made by hand thus inter trap variability is expected due to: possible twisting of the PDMS tubes, as is the variability between different batches of tubing and the varying inner diameter of the glass tubes. The time taken to load the TD after spiking the trap, the accuracy of the syringe and analyst as well as the presence of tiny air bubbles all influence the repeatability of the results.

### 3.6.2 Filter homogeneity

Filter homogeneity was assessed by analysing an archived loaded quartz fibre filter punch obtained from the CSIR (from a platinum mine) by TD-GCxGC-ToFMS. The analysis was repeated to obtain enough data for statistical analysis. The results including the number of repeats are shown in Table 3-12.

**Table 3-12 PAHs thermally desorbed (using the conditions in Table 3-4) from filters and the peak areas of n replicates**

PAH	m/z	n	Average peak area	Std dev.	% RSD
Naphthalene, 2-methyl-	142	3 <sup>#</sup>	9094.90	2036.741	22.4
Naphthalene, 1-methyl-	142	2 <sup>#</sup>	7388.95	810.274	11.0
Phenanthrene	178	4	18252.50	4748.886	26.0
Pyrene	202	4	13640.25	1630.561	12.0
Chrysene	228	4	15300.75	7768.655	50.8
Benzo[k]fluoranthene	252	4	28362.50	8899.732	31.4
Benzo[a]pyrene	252	4	23030.83	10364.320	45.0

<sup>#</sup> Outliers were rejected

From Table 3-12 it can be seen that punches from the same filter were not very reproducible with % RSD values up to 45 % for benzo(a)pyrene and 50.8 % for chrysene. The loaded surface of filter is not completely consistent and homogeneous sample loading cannot be expected even though the punches that were taken (see Fig. 3-13) appeared identical and this should be taken into account for this statistical study. This again highlights the advantages of the denuder sampling device as the entire filter is desorbed therefore variability due to the inhomogeneous loading of the filter is not a problem.

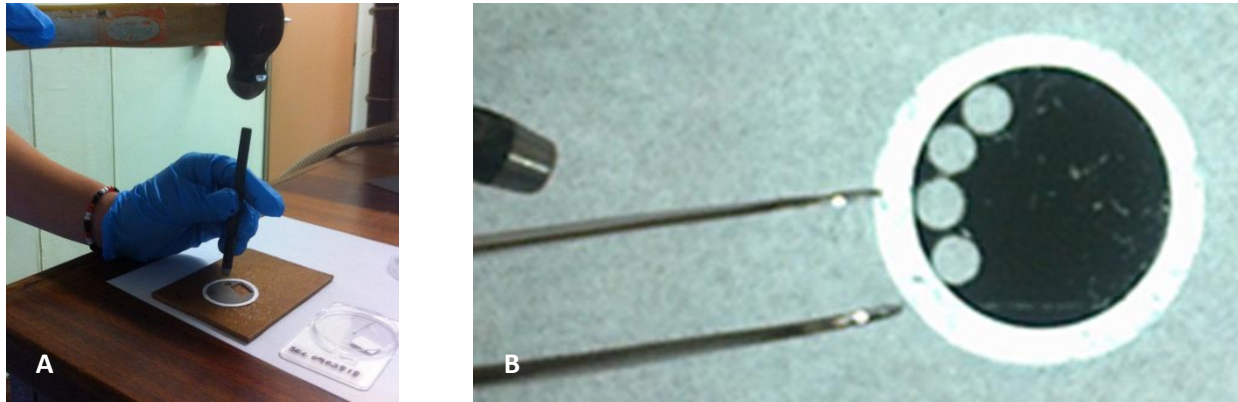


Figure 3-13 A: Tools used to punch filter sample, B: CSIR loaded filter which has been punched four times (Photographed by G. Geldenhuys).

The filter punches were analysed on different days therefore instrument stability may also have affected results. Whilst sampling, the filter was loaded more heavily in the centre of the filter paper which can be visibly noticed by the naked eye and can be confirmed with a closer look by SEM. One of the possible reasons that the edges of the filter differ from the centre is due to the sampling setup as seen in Fig. 3-14 where the outer edges of the filter are wedged between two layers of the cassette. The inlet is in the centre resulting in greater deposition of the heavier particles with larger inertia. This was however not an issue for the denuder filter samples as the entire filter was analysed. The filter punches were handled with tweezers to remove it from the punch and then to manoeuvre it into an empty glass tube for analysis. The filter punch was handled with great caution, however it should be noted that some degree of sample loss is inevitable.

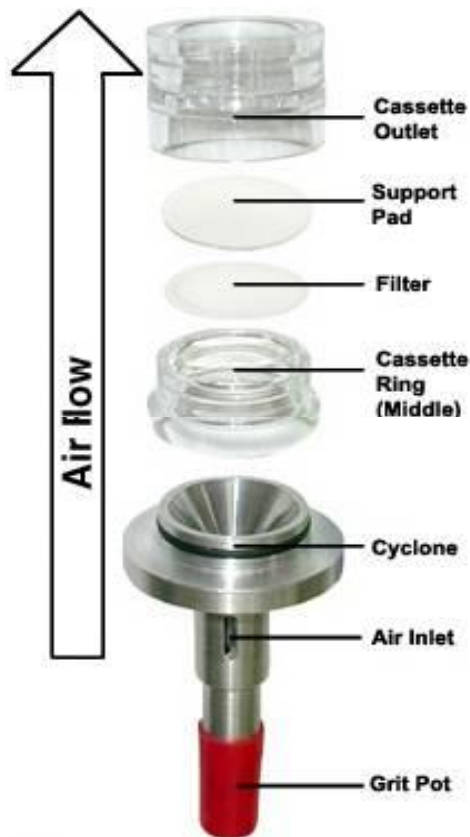


Figure 3-14 Particulate sampling setup using 32 mm SKC cassettes (Particulate sampling, n.d.).

### 3.6.3 Effect of the matrix as well as the desorption temperature and source temperature parameters

A clean, blank filter punch (6 mm) was spiked with a 10 ng deuterated pyrene standard in 1  $\mu$ L toluene which was then analysed by TD-GCxGC-ToFMS. The effect of the matrix was investigated by spiking the same amount of the D-pyrene onto a loaded filter punch which was then analysed in the same manner as the blank punch by TD-GCxGC-ToFMS. It should be noted that a random loaded filter was chosen to be used for this investigative analysis and although it does represent a DPM matrix, it does not by any means imply that all DPM matrixes will be the same. The peak area of the standard on a blank versus on a loaded punch with DPM matrix was compared.

An investigation into the effect of the desorption temperature (TD) and the source temperature (ST) parameters was performed by spiking loaded punches with 10 ng of a deuterated pyrene standard which was then analysed by TD-GCxGC-ToFMS. The developed method was used for analysis whereby

only the parameter under investigation would be changed. Analysis was done in duplicate for confirmation of the results.

The clean filter spiked with 10 ng D-pyrene revealed an average peak area of 3 023 851 which more than doubled to an average peak area of 8 531 214 when the same standard was spiked onto a loaded filter, which showed that the DPM matrix clearly enhanced the detected signal. The purest silica surface is the most active site for analyte interaction and would result in the poorest recovery as in the case of the clean and dry blank. The effect of the active silica is deactivated by the DPM matrix in the loaded filter therefore there is less analyte-silica interaction resulting in better recoveries (May *et al.* 2013). Moisture would also deactivate the active silica sites and this should be taken into consideration when interpreting the results.

Fig. 3-15 showed that increasing the thermal desorption temperature to 300 °C did not make a significant difference in the signal of the deuterated standard as the peak areas remain in the 8 000 000 range, it did however make a significant difference when the source temperature was changed to 280 °C which decreased the signal of the D-pyrene standard. The current method called for an ion source of 200 °C which was possible due to the open source structure of the LECO instrument which thus had less contamination from eluting species. If the source temperature was too low, the adsorptive effects within the ion source would result in tailing of the peaks so it was vital to ensure the analyte peaks were Gaussian in shape. The lowered signal seen when increasing the source temperature was possibly due to ion beam expansion which resulted in defocusing and thereby lowered sensitivity.

Increasing the TD temperature and the source temperature did not reveal improved signals therefore they were not employed. Sample duplicates confirmed the obtained peak areas and showed acceptable reproducibility (% RSD < 20, n=2). Pyrene is not considered a heavy PAH so the fact that the TD temperature had no effect on the observed signal may not be true for a heavier PAH, which is more affected by the desorption parameters therefore for future research a deuterated benzo(k)fluoranthene standard, for example, should be used for a similar investigation.

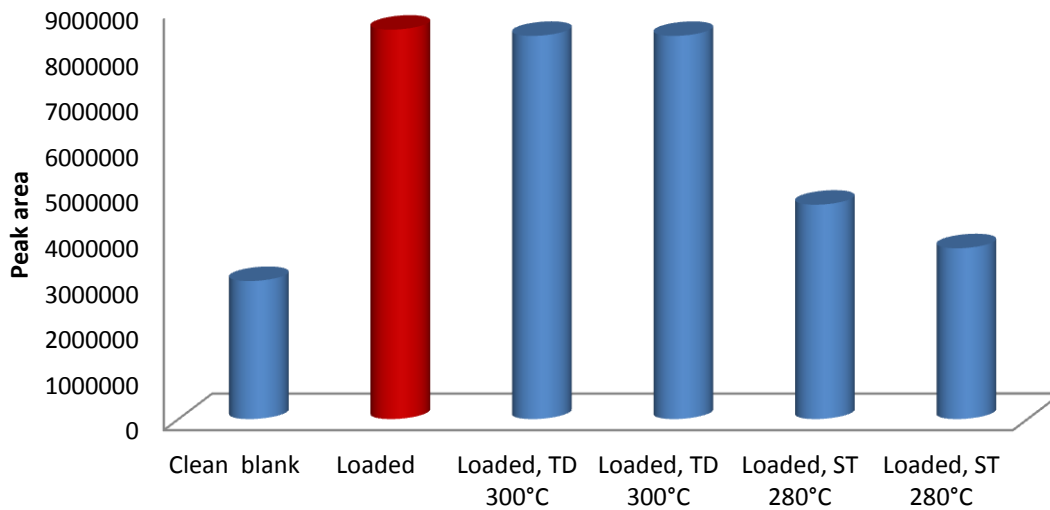


Figure 3-15 Absolute peak area of D-pyrene from spiked filters including: clean blank filter, loaded filter (analysed by method described in Section 3.2.3), loaded filter that was thermally desorbed (TD) at 300 °C (ST at 200 °C) as well a loaded filter that was analysed with a source temperature (ST) of 280°C (TD at 300 °C) (n=2).

### 3.6.4 Desorption efficiency

Desorption efficiency was investigated by analysing a loaded trap sample which was taken from the workshop at Plat mine B for a period of 10 minutes. The conditions listed in Table 3-4 were used to analyse the same trap sample twice to compare PAH ion extracted chromatograms as seen in Fig. 3-16 below.

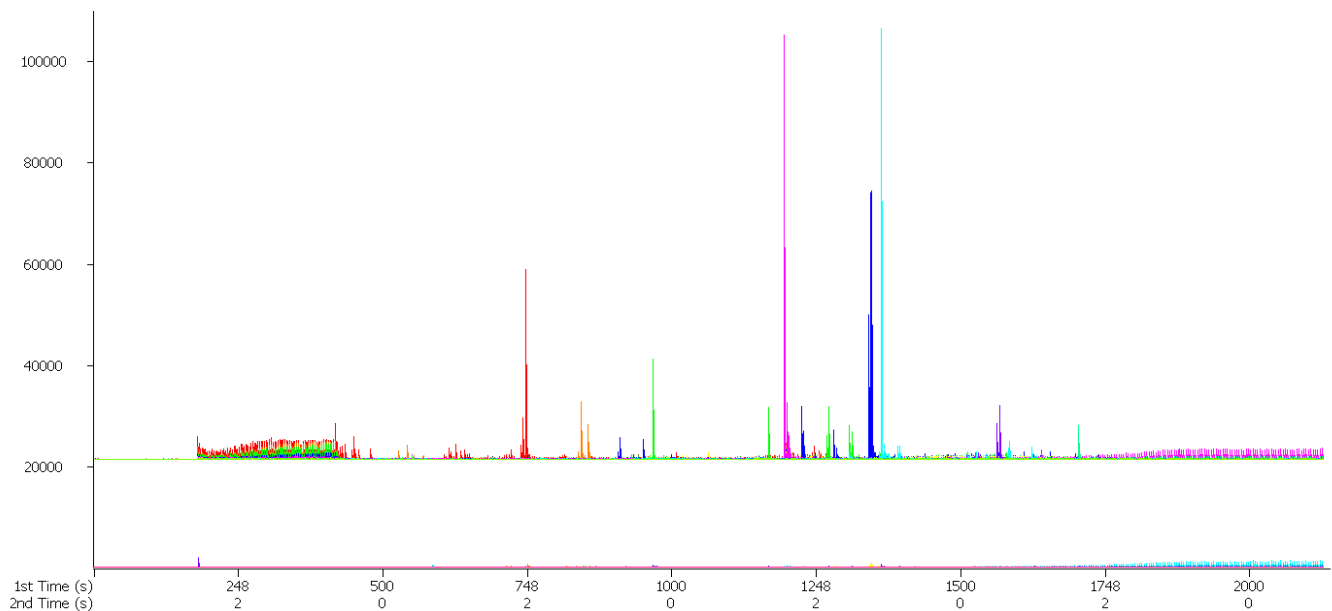


Figure 3-16 PAH ion extracted chromatograms of a loaded trap sample (taken from the workshop at Plat mine B) after first (top chromatogram) and second (bottom chromatogram) desorption of the same trap.

Fig. 3-16 showed the first (top chromatogram) and second (bottom chromatogram) desorption of the same loaded trap. The chromatograms were ion selected for the PAH masses and it was visibly clear that after the first desorption there were no PAH analytes that were detected on the trap, which was also confirmed by the peak table that showed that there were no detected PAHs on the trap after it had already been thermally desorbed once. This gives confidence to the efficiency of the desorption method with respect to contamination and carry over. Fig. 3-16 also implies that traps could potentially be reused.

### 3.6.5 Future validation

- Desorption efficiency of the filters should be further investigated.
- Method validation should be performed on the same trap for each replicate.
- The NIST DPM standard should to be analysed repeatedly (approximately 5 times), preferably on the same day where the instrument conditions are unchanged, to show repeatability. The instrument need not be baked out in between runs but rather an empty trap should be analysed to assess the carry-over although in the past only naphthalene and sometimes phenanthrene were carried over, due to the high concentrations of these analytes.
- A deuterated benzo(k)fluoranthene standard should be used to investigate parameters as per Section 3.6.4.

### 3.6.6 Calibration and linearity study

Linearity of an analysis shows the correlation between the instrument response and the amount of the analyte. The analysis should give as good linearity ( $R^2$  as close to 1 as possible) to ensure quality of results. The linearity of the GC response was tested by analyzing a range of known concentrations of analytes (in toluene) spiked onto traps and filters under the same analysis conditions and the linearity of each of these analytes was shown by a calibration curve and statistically by the coefficient of determination ( $R^2$ ) (Dasgupta 2010).

Linear regression analysis was performed using the Data Analysis Tool Kit in Excel. The standard error (–) as well as the coefficients of the slope (b) and intercept (a) were obtained from the analysis and were used to set up regression equations in order to quantify the results.

The limit of detection (LOD) and limit of quantification (LOQ) are used in analytical chemistry to define the limitations of a method and evaluate the method suitability. The LOD is defined as the lowest

concentration of an analyte in a sample that can be detected (under the method conditions) whereas the LOQ is defined as the lowest concentration of an analyte in a sample that can be quantified with acceptable accuracy and precision (de Vos *et al.* 2011). Only results that exceeded the corresponding LOQ were reported in Chapter 4.

The signal-to-noise (S/N) method was used to determine the LOD and LOQ values whereby peak noise around the analyte peak was used to estimate the concentration of the analyte that would yield a signal equal to certain value of S/N ratio at the defined retention times, in this case, the LOD was estimated as three times the noise value (Dasgupta 2010, de Vos 2011) and LOQ was estimated as ten times noise value as shown in Table 3-13 & 3-14. The S/N ratio was obtained from the auto-integrator results and the peaks were inspected manually to ensure they were correctly integrated. This method is widely used for different instrumental methods such as gas chromatography, as it is easy to implement.

The instrumental limit of detection was 1 pg therefore it was used as the cut off point for all results. The LOD and LOQ values that are reported in Table 3-13 and 3-14 were calculated using a sampling volume of 5 L which was the volume for most of the samples and it was the desired sample volume. A few of the samples had volumes that were higher than 5 L which resulted in even better (lower) LOD and LOQ values and were therefore not tabulated. However the quantification concentrations in Chapter 4 were compared to the LOD and LOQ corrected for each sample volume collected.

#### 3.6.6.1 Calibration of traps

The calibration of the traps was done by analysing 0.1, 1, 5 and 10 ng standards that were spiked onto empty traps (clean and conditioned). As expected the lighter PAHs, up to pyrene, generated calibration curves with good linearity ( $R^2 > 0.98$ ) as they readily desorbed from the traps and were not lost in the system. The heavier PAHs showed less linearity than the lighter PAHs and at best only three points could be plotted therefore the calibration curves were not included. This was not a concern as these heavier PAHs were not detected in any of the trap samples in this study. All of the other calibration curves showed excellent linearity with coefficients of determination ranging from 0.9817-1.000.

The limits of detection of PAHs on PDMS traps range from 0.2-4.07 ng.m<sup>-3</sup> as seen in Table 3-13. The lighter PAHs were all less than 1.0 ng.m<sup>-3</sup>. Fig. 3-17 represents examples of calibration curves obtained from a PDMS trap for naphthalene and pyrene. It should be noted that each standard was spiked on a separate trap which is not ideal. In future, the same trap should be used throughout; starting with the smallest concentration standard to the highest concentration. From the trap repeatability study the



inter-trap variation was evident therefore using the same trap will ensure that the effect of the trap matrix will be the same in every sample and the linearity should be even better.

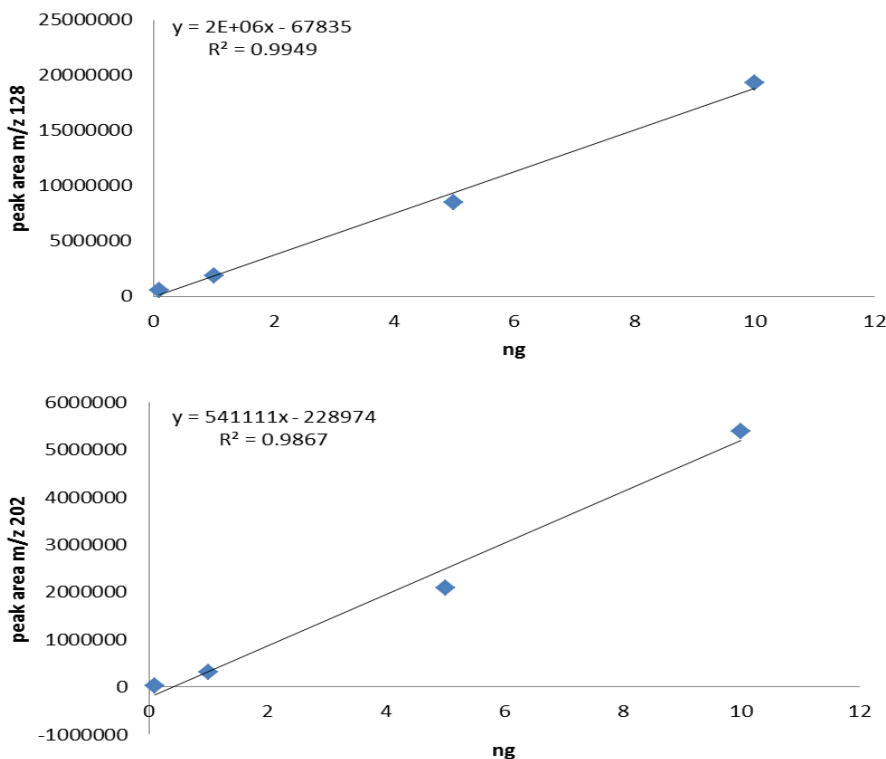
**Table 3-13 Coefficients of determination and limits of detection and quantification of PAHs on traps.**

PAH	m/z	R <sup>2</sup>	Equation	<sup>b</sup> LOD (pg)	<sup>c</sup> LOQ (pg)	<sup>b</sup> LOD (ng.m <sup>-3</sup> )	<sup>c</sup> LOQ (ng.m <sup>-3</sup> )
Naphthalene	128	0.9949	Y= 1893241x -67835	1.0	3.3	0.20	0.67
Naphthalene, 2-methyl-	142	0.9953	Y= 948218x -185685	1.0	3.3	0.20	0.67
Naphthalene, 1-methyl-	142	0.9899	Y= 1079149x -338232	1.0	3.3	0.20	0.67
Acenaphthylene	152	0.9975	Y= 613792x -127873	1.0	3.3	0.20	0.67
Acenaphthene	154	1.0000	Y= 754548x -17815	1.0	3.3	0.20	0.67
Fluorene	166	0.9863	Y= 698537x -192547	1.0	3.3	0.20	0.67
Phenanthrene	178	0.9849	Y= 1260468x -646079	1.0	3.3	0.20	0.67
Fluoranthene	202	0.9888	Y= 475468x -175354	1.0	3.3	0.20	0.67
Pyrene	202	0.9867	Y= 541111x -228974	1.4	4.6	0.27	0.92
Chrysene+benz(a)anthracene	228	0.9817	Y= 717408x -403439	1.4	4.8	0.29	0.95
<sup>a</sup> Benzo(k)fluoranthene	252	0.9837	Y= 636974x -357267	2.2	7.3	0.44	1.46
<sup>a</sup> Benzo(a)pyrene	252	0.9794	Y= 284850x -176737	5.7	19	1.15	3.83
<sup>a</sup> Indeno(1,2,3-cd)pyrene	276	0.9671	Y= 233022x -179840	20	68	4.07	13.58
<sup>a</sup> Benzo(ghi)perylene	276	0.9739	Y= 229394x -159078	9.5	32	1.90	6.32
<sup>a</sup> Dibenz(a,h)anthracene	278	0.9789	Y= 181928x -259908	4.1	14	0.82	2.73

<sup>a</sup> Calibration curves not included

<sup>b</sup> Limit of detection (LOD) calculated as the concentration that gives a signal-to-noise ratio of 3

<sup>c</sup> Limit of quantification (LOQ) calculated as the concentration that gives a signal-to-noise ratio of 10



**Figure 3-17 Calibration curves for naphthalene (top) and pyrene (bottom) from the PDMS traps across the range 0.1-10 ng.m<sup>-3</sup>**

### 3.6.6.2 Calibration of filters

Calibration of the filters was performed by analysing 0.001, 0.01, 0.1, 0.5 and 1.0 ng standards that were spiked onto a specific loaded filter (obtained from the CSIR). The lower standard concentration range was selected after consulting the peak areas that were obtained from the actual samples. It should be noted that the lower concentrations will have an impact on the results. Dibenz(a,h)anthracene had only two data points which was insufficient for a calibration curve, therefore the regression results were not included in Table 3-14. Coefficient of determination ranges were from  $R^2 = 0.9746-0.9999$  for the more volatile PAHs and  $R^2 = 0.9679-0.9990$  for the heavier PAHs. Fig. 3-18 represents examples of calibration curves obtained from a spiked filter for heavier PAHs: benzo(k)fluoranthene and benzo(a)pyrene.

The limits of detection for PAHs on filters were all less than  $1.1 \text{ ng.m}^{-3}$  for each PAH. It can be seen that the LOD of the heavier PAHs are lower on the filter samples than on the trap samples, which can be due to the DPM matrix that serves as a coating on the filter and therefore deactivates the silica from the filter making the analytes more recoverable as compared to the traps. From the filter repeatability study the variation within the same filter is evident and this may affect the calibration to some extent.

**Table 3-14 Coefficients of determination and limits of detection and quantification of PAHs on filters.**

PAH	m/z	$R^2$	Equation	<sup>b</sup> LOD (pg)	<sup>c</sup> LOQ (pg)	<sup>b</sup> LOD (ng.m <sup>-3</sup> )	<sup>c</sup> LOQ (ng.m <sup>-3</sup> )
Naphthalene	128	0.9746	Y= 3768115x -93846	1.0	3.3	0.20	0.67
Naphthalene, 2-methyl-	142	0.9766	Y= 1904134 -46190	1.0	3.3	0.20	0.67
Naphthalene, 1-methyl-	142	0.9910	Y= 1934552x -44162	1.0	3.3	0.20	0.67
Acenaphthylene	152	0.9906	Y= 2601402x -47923	1.0	3.3	0.20	0.67
Acenaphthene	154	0.9919	Y= 1566621x -27420	1.0	3.3	0.20	0.67
Fluorene	166	0.9881	Y= 1714950x -19273	1.0	3.3	0.20	0.67
Phenanthrene	178	0.9986	Y= 1932614 +45473	1.0	3.3	0.20	0.67
Anthracene	178	1.0000	Y= 1613439x +6634	1.0	3.3	0.20	0.67
Fluoranthene	202	0.9969	Y= 1117440x +14451	1.0	3.3	0.20	0.67
Pyrene	202	0.9877	Y= 1082375x +33809	1.0	3.3	0.20	0.67
Chrysene+benz(a)anthracene	228	0.9990	Y= 920095x +19139	1.0	3.3	0.20	0.67
Benzo(k)fluoranthene	252	0.9980	Y= 748045x +12601	1.0	3.3	0.20	0.67
Benzo(a)pyrene	252	0.9997	Y= 326680x +2249	1.1	3.5	0.21	0.70
Indeno(1,2,3-cd)pyrene	276	0.9679	Y= 163260x -8579	5.2	17	1.00	3.5
Benzo(ghi)perylene	276	0.9871	Y= 207298x -5647	2.3	7.7	0.46	1.5
<sup>a</sup> Dibenz(a,h)anthracene	278					1.10	3.7

<sup>a</sup> Calibration curves not included

<sup>b</sup> Limit of detection (LOD) calculated as the concentration that gives a signal-to-noise ratio of 3

<sup>c</sup> Limit of quantification (LOQ) calculated as the concentration that gives a signal-to-noise ratio of 10

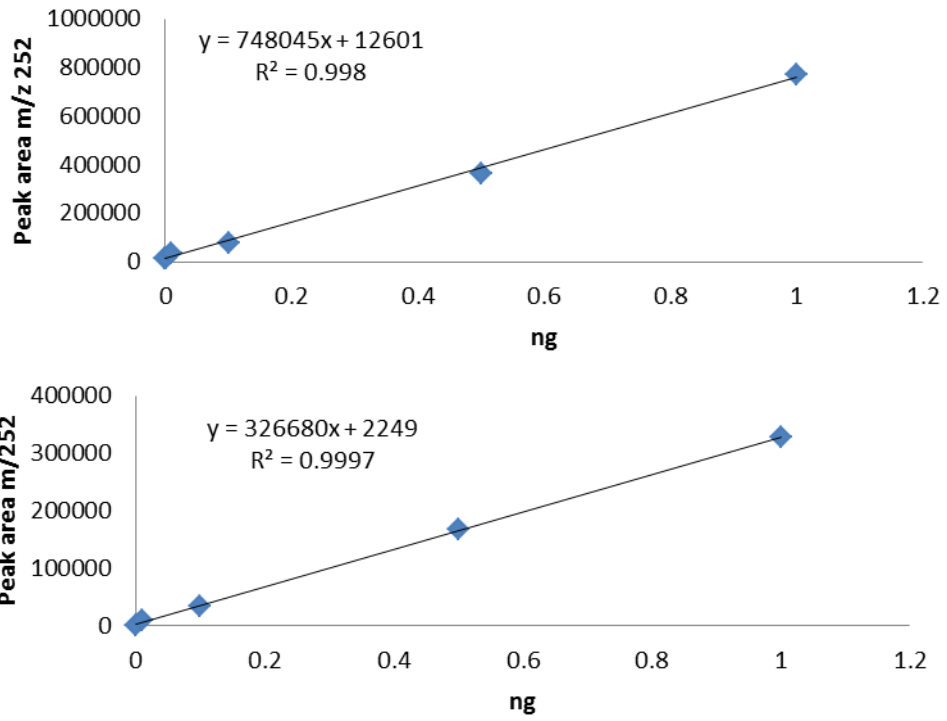


Figure 3-18 Calibration curves for benzo(k)fluoranthene (top) and benzo(a)pyrene (bottom) from filters across the range 0.001-1.0 ng.m<sup>-3</sup>

### 3.7 References

- Dasgupta, S., Banerjee, K., Patil, S.H., Ghaste, M., Dhumal, K.N. & Adsule, P.G. 2010, "Optimization of two-dimensional gas chromatography time-of-flight mass spectrometry for separation and estimation of the residues of 160 pesticides and 25 persistent organic pollutants in grape and wine", *Journal of Chromatography A*, vol. 1217, no. 24, pp. 3881-3889.
- Ellison, S.T.R., Barwick, V.J. & Duguid Farrant, T.J. 2009, *Practical Statistics for the Analytical Chemist*, 2<sup>nd</sup> edn. RSC Publishing, Cambridge, pp. 49-51.
- de Vos, J., Gorst-Allman, P. & Rohwer, E. 2011, "Establishing an alternative method for the quantitative analysis of polychlorinated dibenzo-p-dioxins and polychlorinated dibenzofurans by comprehensive two dimensional gas chromatography–time-of-flight mass spectrometry for developing countries", *Journal of Chromatography A*, vol. 1218, no. 21, pp. 3282-3290.
- Forbes, P.B.C. & Rohwer, E.R. 2009, "Investigations into a novel method for atmospheric polycyclic aromatic hydrocarbon monitoring", *Environmental Pollution*, vol. 157, no. 8-9, pp. 2529-2535.
- Forbes, P.B.C., Karg, E.W., Zimmermann, R. & Rohwer, E.R. 2012a, "The use of multi-channel silicone rubber traps as denuders for polycyclic aromatic hydrocarbons", *Analytica Chimica Acta*, vol. 730, pp. 71-79.
- Forbes, P.B.C. 2012b, "Particle emissions from household fires in South Africa", Air Pollution Conference, 16-18 May 2012, La Coruna, Spain. Published in *Air Pollution XX, WIT Transactions on Ecology and the Environment*, vol. 157, pp. 445-456, ISSN 1743-3541.
- May, A.A., Presto, A.A., Hennigan, C.J., Nguyen, N.T., Gordon, T.D. & Robinson, A.L. 2013, "Gas-particle partitioning of primary organic aerosol emissions: (1) gasoline vehicle exhaust", *Atmospheric Environment*, ISSN 1352-2310.
- NIST. 2009, Certificate of Analysis of Standard Reference Material 2975, National Institute of Standards and Technology, Certificate issue date: 19 March 2009, pp. 1-10.
- Particulate sampling, n.d. image, viewed 10 June 2013, <<http://www.skcgulfcoast.com/products/filters.asp>>
- Schnelle-Kreis, J., Orasche, J., Abbaszade, G., Schäfer, K., Harlos, D.P., Hansen, A.D.A. & Zimmermann, R. 2011, "Application of direct thermal desorption gas chromatography time-of-flight mass spectrometry for determination of nonpolar organics in low-volume samples from ambient particulate matter and personal samplers", *Analytical and Bioanalytical Chemistry*, vol. 401, no. 10, pp. 3083-3094.
- Wold, S., Esbensen, K. & Geladi, P. 1987, "Principal Component Analysis", *Chemometrics and Intelligent Laboratory Systems*, vol. 2, pp. 37-52.

## 4 Results and Discussion of Platinum Mine Study

### 4.1 Introduction

Thousands of peaks were found in the two-dimensional chromatograms of the mine samples when the automated peak identification routine, based on deconvolution methods, was used. Single ion masses of PAHs were extracted and classified and the NIST library was consulted to compare the similarities of spectra, where only library matches of greater than 80 % were used for tentative identification purposes (refer to Appendix A for sample chromatograms).

Peak areas were an indication of the concentration of a given substance. In order to do inter-mine or inter-sample comparisons the remaining peak areas were used simply as the sum of the normalised peak areas (i.e. peak area per litre sampled) for a specific compound class (such as hydrocarbons and PAHs) or a specific PAH.

Relative % peak areas were calculated using the peak area of a given compound divided by the total peak area (sum of every peak in sample) which was then multiplied by 100, this was useful to see the apportionment patterns or profiles of a sample using relative amounts of the compounds.

Section 4.2 that follows will show both relative % peak area illustrations and direct peak area illustrations that give an indication of the concentrations of a substance.

Principle component analysis (PCA) was performed using JMP 10 software and was based on covariance. Score plots, loading plots and eigenvalue bar graphs were generated. These terms are defined and discussed in Section 4.12.

Diagnostic ratios are tools that can be used to identify and assess emission sources of PAHs, however they should be used with caution as the ratios may change due to the different environmental fates of PAHs (Tobiszewski 2012). It is for this reason that degradation and transport correction factors should be applied to the PAHs which is not always a simple task. Additionally, supporting information such as molecular markers should be used in conjunction with diagnostic ratios for confirmation. Table 4-1 shows diagnostic ratios that apply to diesel emissions

Table 4-1 Diagnostic ratios of PAHs

PAH ratio	Value		
FL/(FL+PYR)	>0.5	Diesel emissions	Ravindra <i>et al.</i> 2008b
BaA/(BaA+CHR)	>0.35	Combustion	Yunker <i>et al.</i> 2002
FLA/(FLA + PYR)	0.4-0.5	Fossil fuel combustion	De La Torre-Roche <i>et al.</i> 2009
$\Sigma$ LMW/ $\Sigma$ HMW	<1	pyrogenic	Zhang <i>et al.</i> 2008
$\Sigma$ COMB/ $\Sigma$ PAHs	~1	Combustion	Ravindra <i>et al.</i> 2008a
FL	-fluorene		
FLA	-fluoranthene		
PYR	-pyrene		
BaA	-benzo(a)anthracene		
$\Sigma$ LMW	-sum of the low molecular weight PAHs (2-3 rings)		
$\Sigma$ HMW	-sum of the higher molecular weight PAHs (4-5 rings)		
$\Sigma$ COMB	-FLA, PYR, BaA, CHR, BkF, BbF, BaP, IcdP and BghiP		
$\Sigma$ PAHs	-sum of the non-alkylated PAHs		

The diagnostic ratio concept has also included signatures of profiles where relative amounts of multiple species are studied using multivariate methods and a review by Galarneau *et al.* examined two of the assumptions necessary for profile or ratio based source apportionment methods for PAHs. They presented a set of conditions under which conventional source apportionment may be valid as these limitations were not yet accounted for in literature (Galarneau *et al.* 2008). It should also be noted that available literature investigates ambient air environments, however underground mine environments are completely different with a new set of limitations requiring further research.

In a study by Borrás *et al.* a total of 16 PAHs were identified in the diesel emission sample namely: naphthalene, acenaphthylene, fluorene, acenaphthene, phenanthrene, anthracene, fluoranthene, pyrene, benzo(a)anthracene, chrysene, benzo(k)fluoranthene, benzo(b)fluoranthene, benzo(a)pyrene, indeno(1,2,3-cd)pyrene, benzo(ghi)perylene and dibenz(a,h)anthracene. The PAHs found in the diesel emissions were extracted ultrasonically from microfiber filters with two cycles of 15 mL of dichloromethane (CH<sub>2</sub>Cl<sub>2</sub>) for 15 minutes and then concentrated, fractionated, dissolved and finally analysed by GC-MS (Borrás *et al.* 2009).

In 2010 the identification of 13 PAHs in diesel exhaust was performed by Yadav *et al.* where the particulate phase was collected on Whatman filter paper. After Soxhlet extraction, PAHs were identified by reverse phase high performance liquid chromatography using a C18 column and UV detection (Yadav *et al.* 2010). PAHs that were identified were: naphthalene, acenaphthylene, fluorene, acenaphthene,

phenanthrene, anthracene, fluoranthene, pyrene, benzo(a)anthracene, chrysene, benzo(k)fluoranthene, benzo(a)pyrene and dibenz(a,h)anthracene

PAH exposure can be assessed by the use of biomarkers such as pyrene which is a frequently used biomarker of internal dose for carcinogenic PAHs (Yadav *et al.* 2010). Benzo(a)pyrene is considered as one of the most carcinogenic PAHs hence its use as an environmental PAH exposure indicator and is often correlated to PAH-metabolite or DNA adduct biomarkers (Ono-Ogasawara & Smith 2004).

#### 4.1.1 Sample Identification

Throughout this study the sample names will be abbreviated and will have corresponding numbers that will appear on the y-axis of the bubble plots. The samples and their abbreviations together with the corresponding numbers are given in Table 4-2. It should also be noted that each mine is consistently represented by a colour.

Table 4-2. Sample name abbreviations and corresponding numbers

Sample Description	Abbreviation	Number	Colour
30 minute ambient sample from Plat mine A	30MIN A	1	BLUE
30 minute ambient sample from Plat mine B	30MIN B	2	RED
30 minute ambient sample from Plat mine C	30MIN C	3	GREEN
Workshop sample from Plat mine A	WS A	4	
Workshop sample from Plat mine B	WS B	5	
Workshop sample from Plat mine C	WS C	6	
LHD sample from Plat mine A	LHD A	7	
LHD sample from Plat mine B	LHD B	8	
LHD sample from Plat mine C	LHD C	9	
10 minute ambient sample from Plat mine A	10MIN A	10	
10 minute ambient sample from Plat mine B	10MIN B	11 <sup>#</sup>	
10 minute ambient sample from Plat mine C	10MIN C	12	
Non-diesel sample from Plat mine A	ND A	13	
Non-diesel sample from Plat mine B	ND B	14	

<sup>#</sup> Not sampled due to sampling equipment constraints

Table 4-3 Temperature, humidity, air velocity and sampled volume of each sample

Sample no:	Temperature (°C)	Humidity (%)	Ambient air velocity (m/s)	Volume sampled (L)	Sampling flow rate (L/min <sup>-1</sup> )
1	31.4	63.0	0.4	14.5	0.483
2	23.2	55.0	0.8	33.4	1.115
3	25.2	70.0	0.7	30.0	1.000
4	27.3	36.0	0.0	5.0	0.503
5	20.4	49.8	-	4.9	1.115
6	22.8	47.2	0.0	7.0	1.000
7	27.3	36.0	0.0	5.0	0.503
8	23.2	55.0	0.8	11.1	1.115
9	20.7	76.0	-	5.0	1.000
10	31.4	63.0	0.4	5.0	0.503
11	-	-	-	-	-
12	22.3	81.6	0.9	10.0	1.000
13	30.9	48.3	0.5	5.0	0.503
14	23.2	62.4	8.45	22.3	1.115

#### 4.1.2 Factors influencing analytical results

Ideally the sample volumes should be the same for comparison but due to pump limitations it could not practically be done therefore all results are normalized to peak area per litre of air sampled. The silicone of the trap acts as a solvent to the non-polar PAH molecules and therefore “traps” the analytes. The filter, post primary trap, will collect PAHs that occurred in the particulate phase, and this can be visually seen after sampling. The secondary trap will collect any gas phase PAHs that had not been successfully trapped by the primary trap or had blown off from the filter. It was expected for the secondary trap to have much lower concentrations than the primary trap unless breakthrough had occurred or the concentration of gas phase analytes changed during sampling. According to Forbes *et al.*, the breakthrough volume of 10 % breakthrough of naphthalene was experimentally determined to be 5 L therefore breakthrough of PAHs was not expected to occur in this study (Forbes & Rohwer 2009). If any heavier PAHs were seen on the secondary trap it was likely due to blow off from the filter as it is much less likely that breakthrough conditions have occurred for the less volatile PAHs. Due to these effects, samples could show unpredictable results but anomalies can be accounted for if results are properly interpreted taking all limitations into consideration.

The analytical method employed a thermal desorption temperature of 280 °C which was high enough to desorb the smaller, lighter PAHs but was less favourable for the desorption of the heavy PAHs. This instrumental limitation could result in incomplete desorption of heavy PAHs (such as coronene) in some of the samples. Previous PAH monitoring had been carried out successfully at 270 °C (hold time of 2 min)



by Forbes *et al.* in which multi-channel polydimethylsiloxane traps were used for sampling (Forbes & Rohwer 2009). Other studies employed a desorption temperature of 300 °C for PAH analysis where samples were collected on quartz fibre filters (Pietrogrande *et al.* 2011, Orasche *et al.* 2011). It was decided that 280 °C would be sufficient in this study and this temperature was used when developing the method which resulted in good desorption. A NIST 2975 DPM standard was desorbed with the method employed for this study and it showed that PAHs up to benzo(ghi)perylene and dibenz(a,h)anthracene were detected which gave confidence in the developed method for desorption. The desorption temperature was increased to 300 °C in order to investigate the effect of the higher temperature but no significant increase in peak intensity was found.

It should also be noted that the samples that were taken were grab samples, insinuating that they were “snapshots” representing the instantaneous environment and did not represent the section or shaft as a whole. For this same reason the samples may not represent average PAH levels and may have omitted short, time based peaks in PAH concentration in the “snapshot”. It was also noted that there were a limited number of samples that were taken due to cost and time considerations.

The GilAir portable personal sampling pumps that were used to take the mine samples switched off on a regular basis during sampling and had to be switched back on to complete the required sampling time. It was for this reason that the pump flow rates and sampling times were not consistent. The low flow rates that were required ( $\sim 0.5 \text{ L}\cdot\text{min}^{-1}$ ) for PAH sampling and the back pressures from the denuders were possible factors influencing the pump instability. New pumps with lower flow rate and higher back pressure capabilities should be considered for future research. The inconsistent sampling conditions can be seen in Table 4-3. The peak areas that were detected were normalized so that all results were expressed as peak area per litre of air sampled. The normalisation of the results was necessary when comparisons were to be made.

#### 4.1.3 Observations made during the sampling campaign

Trackless diesel machinery (TM3) that was used for platinum mining included: load haul dump vehicles (LHDs), utility vehicles (UVs), dump trucks and drill rigs. Equipment, material and personnel are transported by UVs and the drill rigs are used to drill holes into the rock face for the explosives to be inserted. Diesel powered LHDs (see Fig. 4-1) are then used to load, haul and dump blasted ore and ore

residue onto underground conveyor belts or onto dump trucks which then transport the ore into designated areas.

Whilst sampling at the different mines the ambient conditions were all different in terms of the number of diesel vehicles being used whilst the sampling period elapsed, the type of vehicles being used, the condition of the used vehicles and the location of the diesel bays for re-fueling. The workshops were also all different with respect to number and condition of vehicles being housed as well as the amount of oil spills on the ground. All of these variables were taken into account when interpreting results.



Figure 4-1 LHD vehicle used underground showing the size of the diesel powered engine next to a mine worker  
(Photographed by G. Geldenhuys)

## 4.2 Semi-volatile organic compound profiles expressed in relative % peak areas

The relative % peak area of each compound class was expressed in the form of bubble plot illustrations with the size of the bubble being proportional to the relative amount of each compound class. The relative % peak area was defined as the absolute peak area (of a compound class) divided by the total peak area which was then multiplied by 100 to obtain a percentage. The absolute peak area per litre of air sampled is presented in Section 4.5. The plot of each sample was combined and the total emission profile could be seen as a whole. The dominating compound classes could be identified however they did not provide quantitative concentration data. Relative % peak areas were illustrated with 3 separate figures for the primary trap, filter and secondary trap samples respectively, where the compound classes were displayed on the x-axis and the sample numbers on the y-axis.

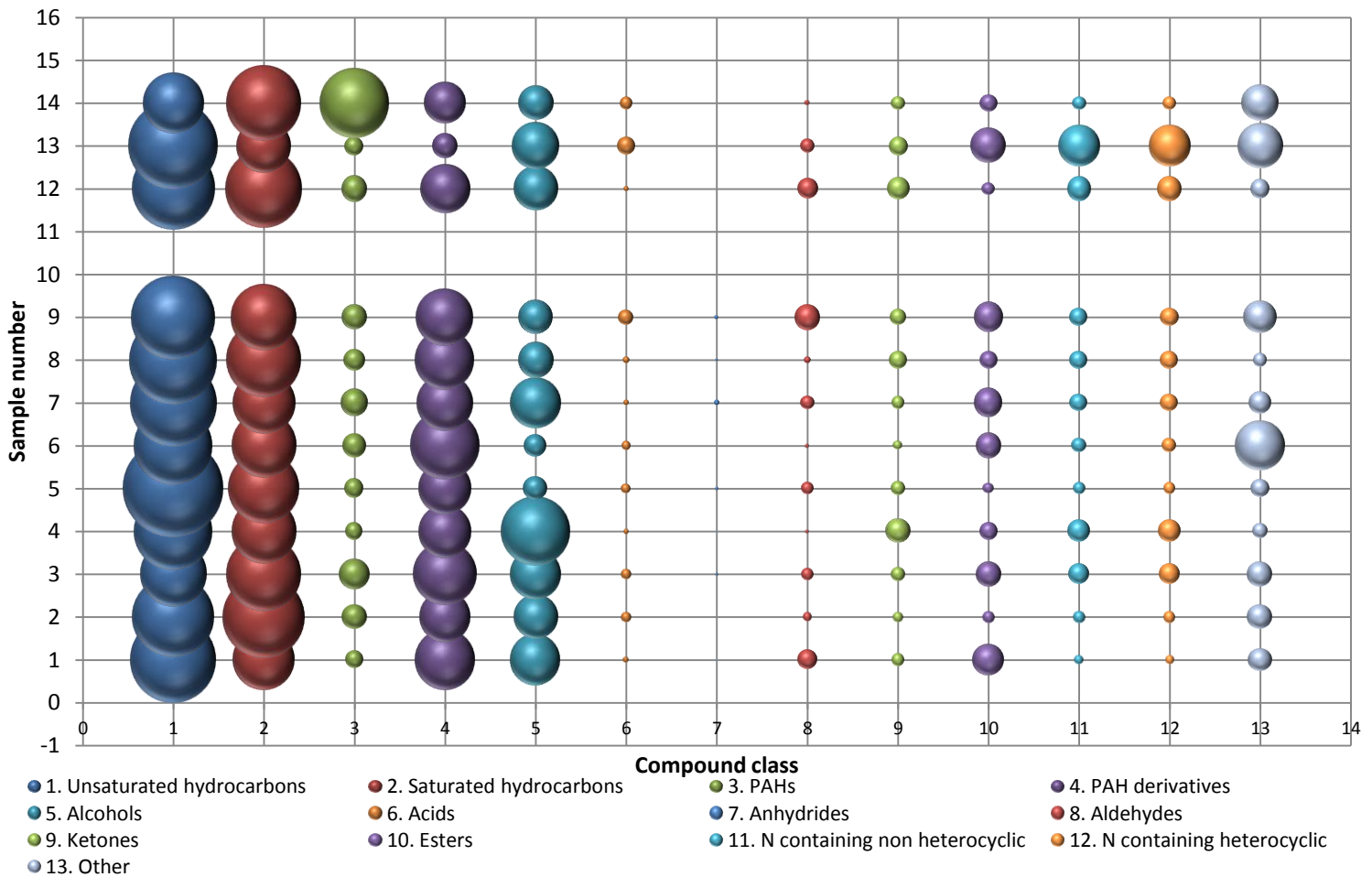


Figure 4-2 Relative % peak areas of SVOC classes found in primary trap samples

Fig. 4-2 represented the relative % peak area of each compound class as found on the primary trap samples. Sample number 10 was not featured in this figure due to analytical complications and due to sampling complications, sample 11 was not included. The figure showed that the relative composition pattern of the air samples from the diesel shafts remained relatively consistent throughout the samples with few discrepancies. The non-diesel shaft samples showed less consistency.

The unsaturated and saturated hydrocarbons presented the highest contributions which were likely due to incomplete combustion of diesel fuel. Alcohols also presented high contributions whereas the acid and acid anhydrides had low contributions due to their reactivity (hence instability). The oxidized species such as: aldehydes, ketones and esters had significant contributions arising from oxidative reactions with the organic emissions. There was a trend between the nitrogen containing non-heterocyclic and the heterocyclic groups in that they were very similar to one another in every sample.

When looking at the separate mines, it was seen that Plat mine A generally showed higher alcohol contributions than the other mines. Plat mine C showed higher contributions of aldehydes than the other mines whereas Plat mine B showed the lowest ester contributions in some of the samples. Plat mine C also showed higher relative % peak areas for the unclassified compounds specifically for samples 6 & 9 which were the workshop and LHD samples respectively. The compound class labeled “other” included compounds that could not be characterized into the other classes such as dibenzofuran, dibenzothiophene and other thiols.

PAHs were consistently found in every primary trap sample with similar relative % peak areas and PAH derivatives were generally found more abundantly than the parent PAH compounds. The PAH derivatives showed the highest relative % peak areas in the diesel shaft samples apart from the hydrocarbons.

There were PAH and PAH derivative contributions found in the non-diesel shaft samples, the composition of which will be discussed in more detail in the sections to follow.

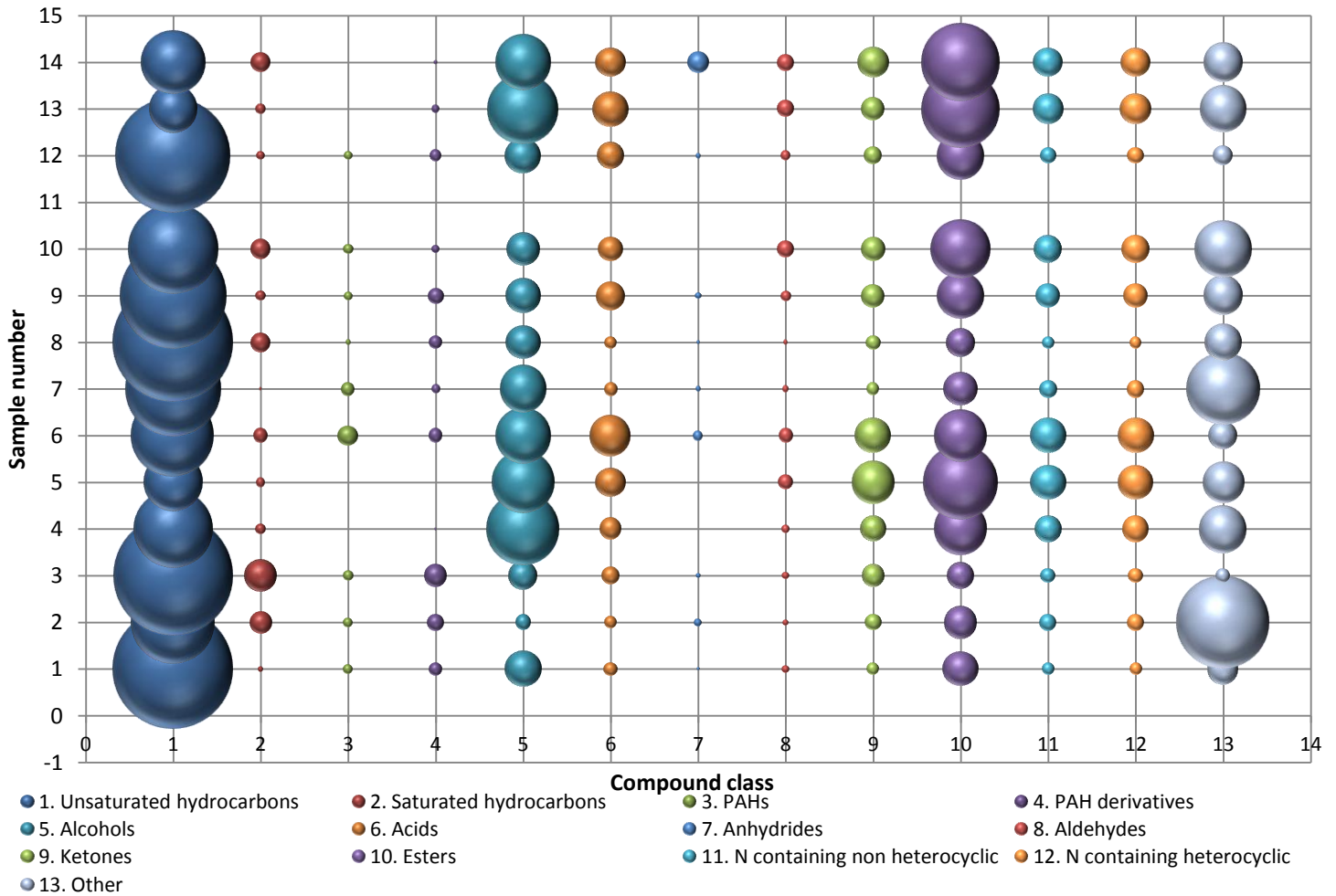


Figure 4-3 Relative % peak areas of SVOC classes found in filter samples

Fig. 4-3 represented the relative % peak area of each compound class as found on the filter. It showed that the composition of the diesel and non-diesel shaft samples were less consistent than the composition reflected from the primary trap samples, with bubble sizes showing a lot more variation. Samples showed more discrepancies particularly in the group named “other”. The results were however more consistent within sample types (e.g. between workshop samples) for the filter samples when compared to the primary traps.

It was evident from Fig. 4-3 that the unsaturated hydrocarbons had the highest contributions in every sample and was the most dominant compound class but the saturated hydrocarbon contribution was significantly lower than in the primary traps. Alcohol and ester contributions were also dominant in Fig. 4-3. The trend between the nitrogen containing groups was once again evident. The relative concentration of acids found on the filter was generally higher than that of the primary trap, particularly in the workshop samples but the acid anhydrides still had very small relative contributions. The oxidized species particularly esters had significantly higher relative contributions on the filter samples than for the primary traps.

From Fig. 4-3 it was also evident that PAHs were not consistently found in every sample and the relative % peak areas varied much more than the primary trap samples. The relative % peak areas of the PAH derivatives also varied and were in some cases less than the parent PAH relative % peak areas, which was not the case in the primary trap samples where the derivatives were always more abundant than the parent PAHs. Overall the relative % peak areas were lower for PAH and PAH derivatives in the filter samples as compared to the primary trap samples which indicated higher gas phase loading. This implied that sampling of only particle associated PAHs in this environment would lead to an under estimation of potential human health effects due to exposure.

Very similar relative % peak areas were found for all three mines' ambient samples (30 minute & 10 minute) for all the compound classes especially the PAHs and PAH derivatives.

Regarding the workshop samples, the sample profiles had lower contributions from PAH and PAH derivatives, but more oxidized products compared to that of the ambient samples. This was most likely due to the difference in localized environments at these sampling points (such as light and ventilation).

The non-diesel profile was similar to that of the workshop (#4) samples. No PAHs were detected in the non-diesel samples, but PAH derivatives were detected which will be discussed in more detail in the next sections. The source of these should be determined in a future study.

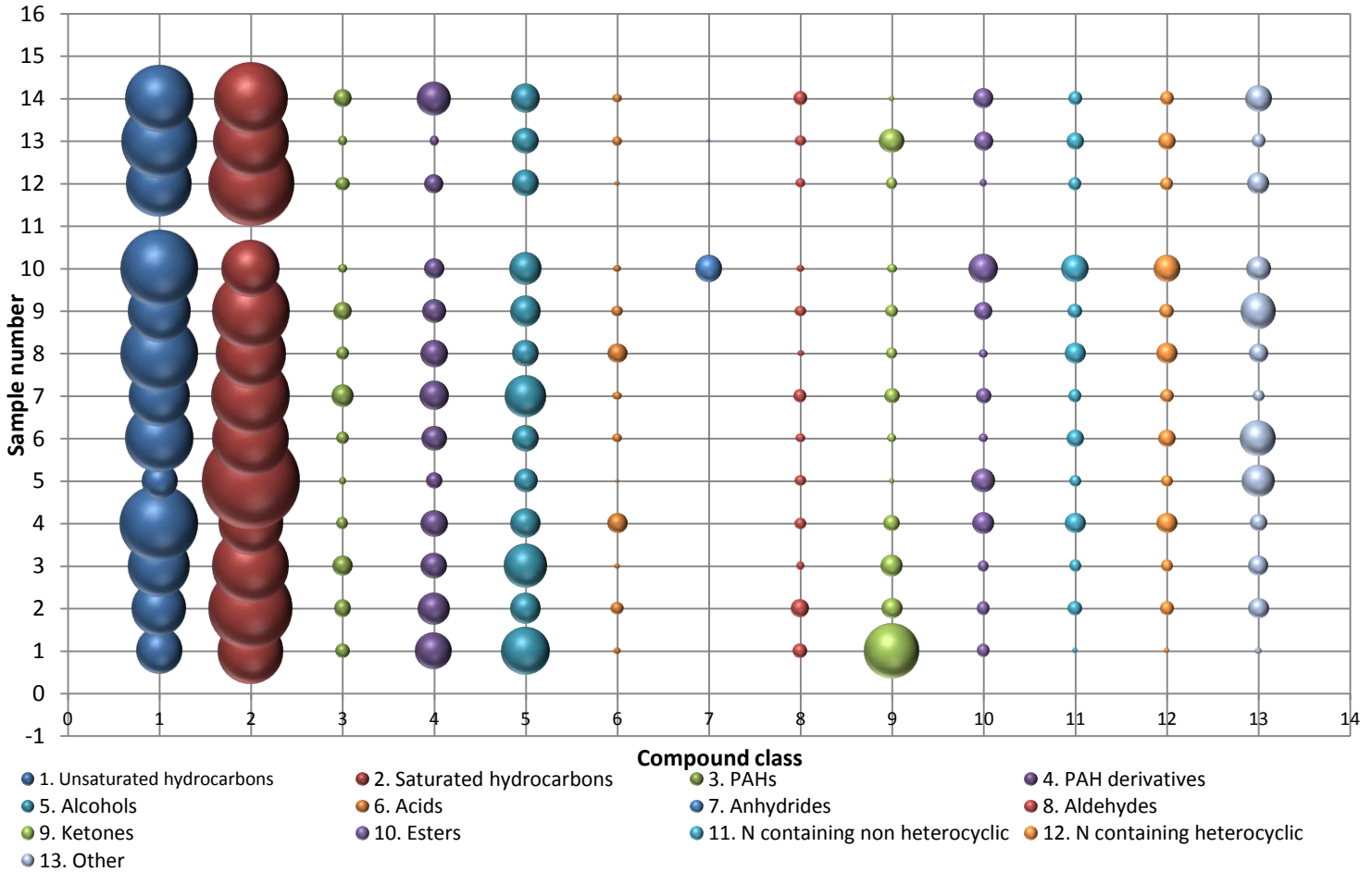


Figure 4-4 Relative % peak areas of SVOC classes found in secondary trap samples

Fig. 4-4 represented the relative % peak area of each compound class as found on the secondary traps. It showed that the compositions of each sample (from each shaft) revealed similar trends to that of the primary trap samples in Fig. 4-2 but there were a few differences. The key difference between the primary and secondary traps was that the secondary traps were dominated by the hydrocarbons and the relative contributions from the PAHs and their derivatives were significantly smaller. This was to be expected as the majority of the gas phase PAHs would be trapped on the primary trap with only small amount of PAHs that experienced blowoff or breakthrough being trapped on the secondary trap. The hydrocarbons were generally more volatile than the PAHs and would therefore have lower breakthrough volumes and would thus breakthrough before the PAHs and oxidized species.

From Fig. 4-4 it was also evident that PAHs were consistently found in every sample with similar relative % peak areas and PAH derivatives were also found more abundantly than the parent PAH compounds (as in the primary traps) however, the relative % peak areas were significantly lower. This showed the

importance of employing a secondary trap to ensure that all PAHs were effectively trapped. From the relative % peak area analysis of the diesel and non-diesel shaft samples it could be clearly seen that the PAHs and PAH derivatives were predominantly found in the gas phase. The source of PAHs in the non-diesel samples needs to be investigated.

### 4.3 Compound class profiles per sample expressed in total normalised peak areas.

This section provides radar plots of each sample that represented the total normalized peak areas for each compound class. This was illustrated so that inter-mine and inter-sample comparisons could be made with respect to relative concentrations. Although some detail is hidden in these radar plots due to dominance of some samples, they are useful in presenting the dominant compound class and sample information in a visual manner which can be easily compared. The primary trap, filter and secondary trap samples for each sampling site were compared.

#### 4.3.1.1 30 minute ambient samples

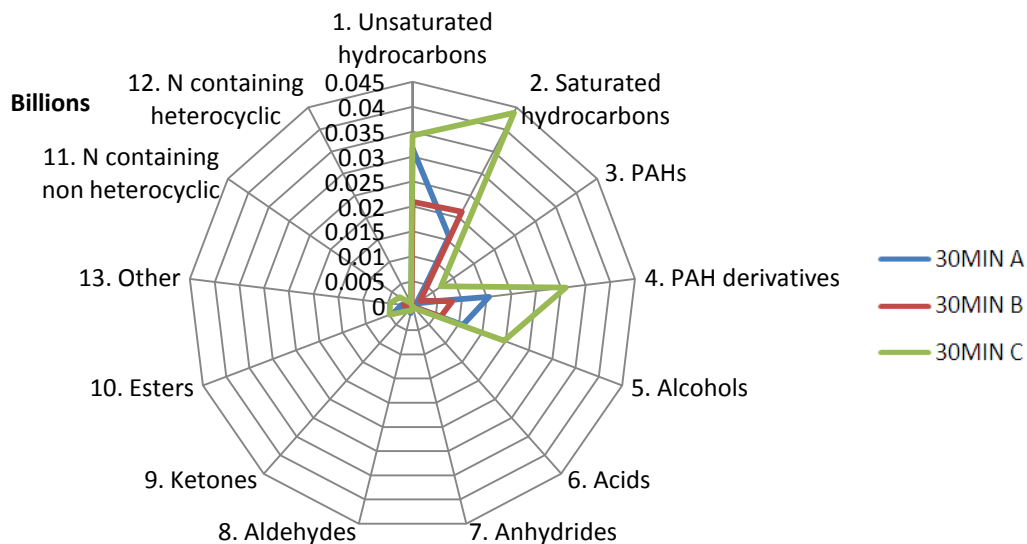


Figure 4-5 Composition of SVOCs from primary traps for 30 minute ambient diesel shaft samples



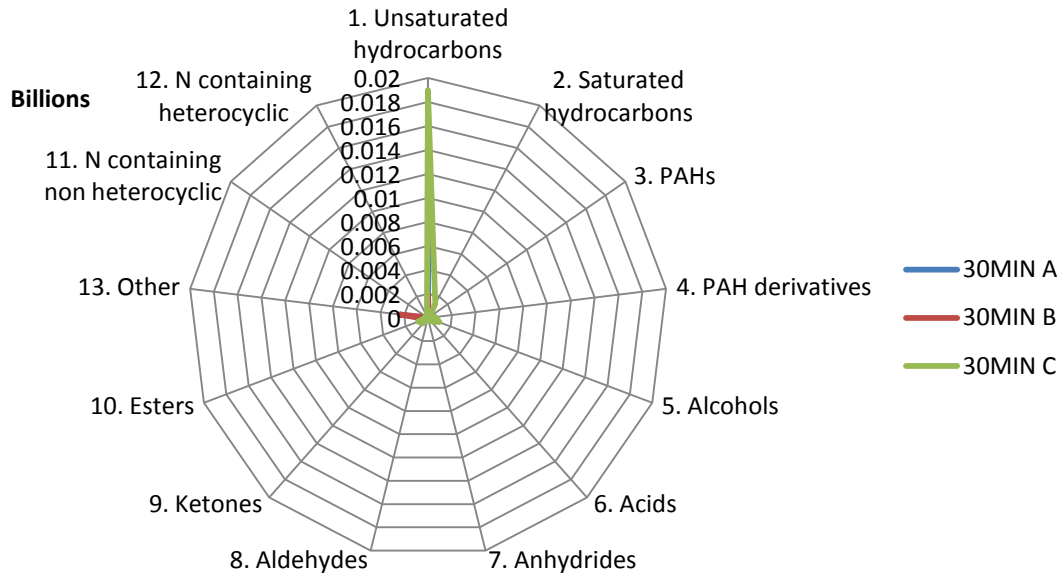


Figure 4-6 Composition of SVOCs from filters for 30 minute ambient diesel shaft samples

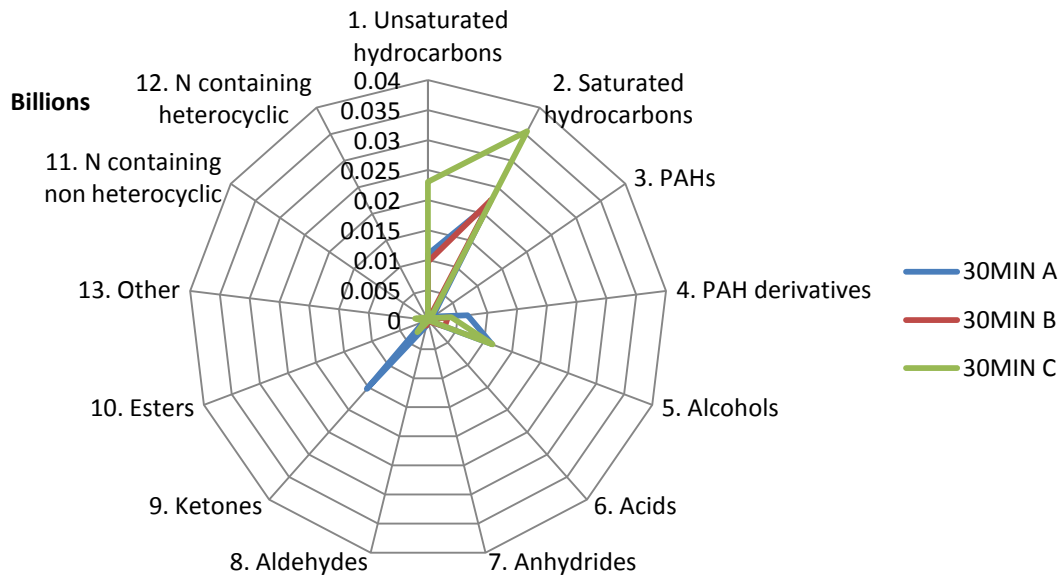


Figure 4-7 Composition of SVOCs from secondary traps for 30 minute ambient diesel shaft samples

Figures 4-5 to 4-7 represented the composition of the SVOC profiles of the samples that were taken over a 30 minute period in diesel shafts underground for the primary trap, filter and secondary trap respectively. It should be noted that the environments where samples were taken were reasonably different (see Section 4.1.3). Whilst sampling at Plat mine A, the sampling area was busy with LHD vehicles ( $\pm 30$  vehicles) passing by at short intervals whereas at Plat mine B: a LHD would pass by every 8 minutes or so without stopping or idling.

The radar graphs represented the actual peak area (normalized) obtained from each class and therefore showed comparisons between Plat mine A, B and C.

From Fig. 4-5 it could be clearly seen that the saturated and unsaturated hydrocarbons revealed the highest areas with the PAH derivatives and alcohols also having significant contributions. These results were consistent with Fig. 4-2 that showed the relative % peak areas from the primary traps. The radar graph clearly showed that the Plat mine C sample had the highest quantities of each compound class and Plat mine A sample had the least. Samples were analysed from low to high concentrations, the instrument was baked out in between runs and blanks were analysed to ensure that there was no carry over.

Fig. 4-6 showed the abundance of unsaturated hydrocarbons with the Plat mine C sample showing the largest contributions (this was also consistent with the relative % peak area from filters as seen in Fig. 4-3).

Fig. 4-7 showed the compound class composition obtained from the secondary traps. This revealed a similar pattern to that of the primary traps in Fig. 4-5 in that the hydrocarbons were dominant with significant amounts of alcohols being present. The Plat mine A sample showed a high peak area for ketones. The Plat mine C sample had the highest peak areas for a number of compound classes. The amount of PAH derivatives was much less than in the primary traps.

For future reference the samples should be spiked with an internal standard before TD to demonstrate that the variation in peak areas is due to a difference in samples and not due to possible run-to-run variation over time.

4.3.1.2 LHD exhaust samples

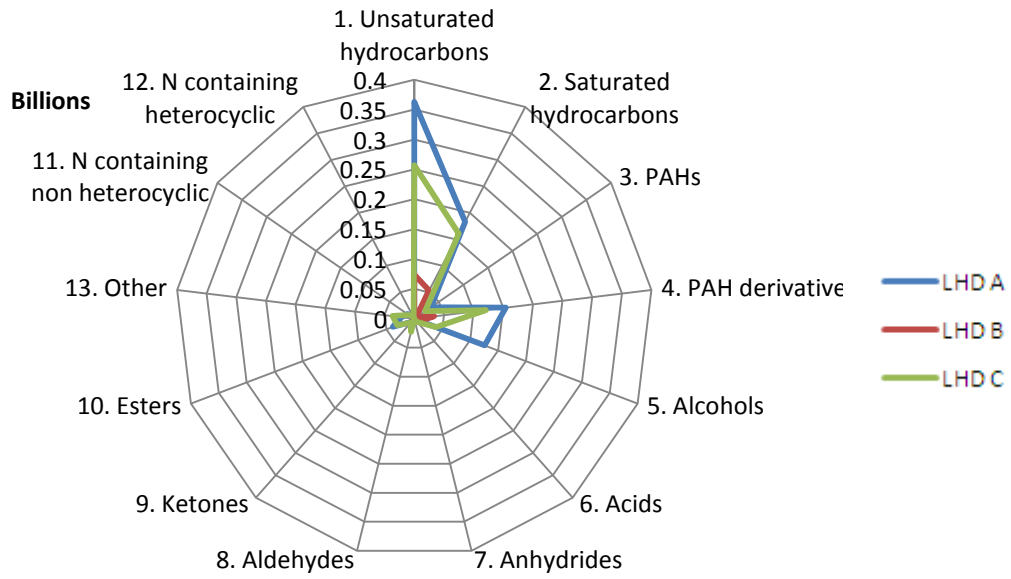


Figure 4-8 Composition of SVOCs from primary traps for LHD diesel shaft samples

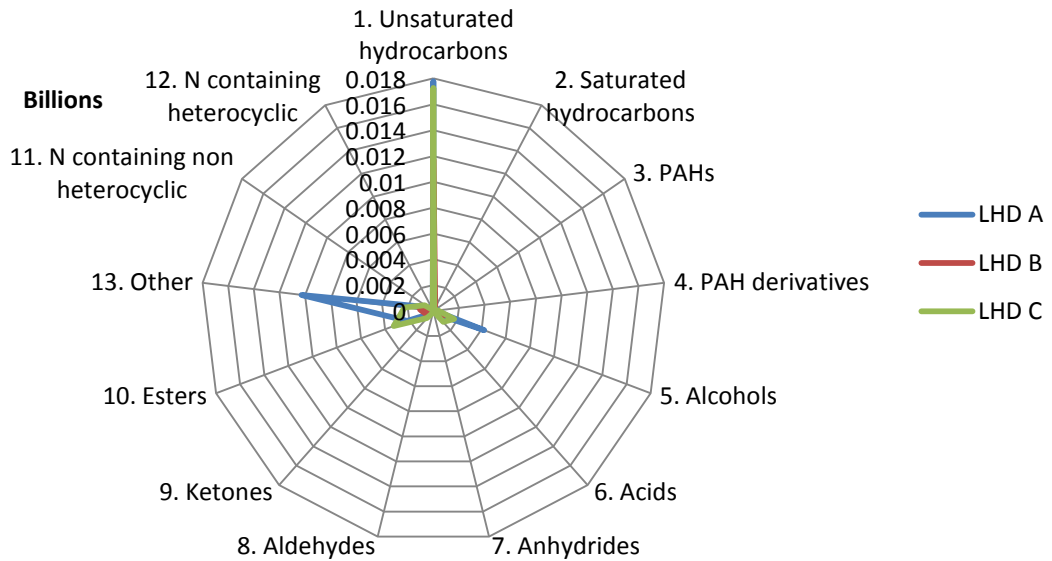


Figure 4-9 Composition of SVOCs from filters for LHD diesel shaft samples

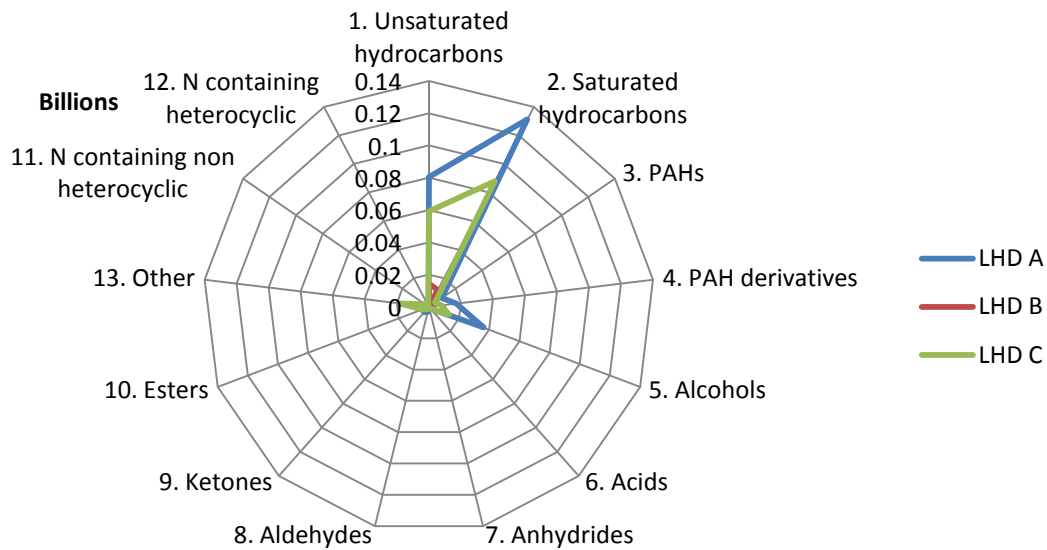


Figure 4-10 Composition of SVOCs from secondary traps for LHD diesel shaft samples

Figures 4-8 to 4-10 represented the composition of SVOC profiles of the samples that were taken over a 10 minute period at the LHD exhaust in shafts utilising diesel powered machinery of the primary trap, filter and secondary trap respectively. It should be noted that the LHD condition, age and level of maintenance will all contribute to the variation in the results and variation between the three mines.

From Fig. 4-8 it could be clearly seen that the saturated and unsaturated hydrocarbons had the highest peak areas with the PAH derivatives also having significant contributions. The radar graph clearly showed that the Plat mine A sample had the highest amounts of each compound class in the primary trap samples and the Plat mine B sample had the least.

Fig. 4-9 showed the abundance of unsaturated hydrocarbons in the Plat mine A and C samples which revealed the largest peak areas. The Plat mine A sample revealed a significant peak for the compound class "other" and a small peak for "alcohols".

In Fig. 4-10 the compound classes obtained from the secondary traps showed a similar pattern to that of the primary traps in Fig. 4-8 in that the hydrocarbons were dominant but the areas were much smaller as expected from the secondary trap as it was post primary trap. There were more saturated

hydrocarbons than unsaturated hydrocarbons on the secondary traps which was the opposite of what the primary trap revealed, this suggested that the saturated hydrocarbons may be more volatile in nature and thus broke through the primary trap. There was a significant amount of alcohols present in the secondary trap samples. The Plat mine A sample had the largest peak areas for each compound class whereas the Plat mine B sample the smallest.

Therefore the Plat mine A LHD exhaust contained the largest proportion of gas phase SVOCs, whilst the Plat mine C LHD filter sample showed higher particle loading. This was relevant in terms of potential human health effects, as the fate of the two phases in the human respiratory system would be different. It should be noted that the ambient temperature at this sampling point was highest for Plat mine A, which would enhance gas phase partitioning of the PAHs.

The higher particle SVOC loading of the LHD samples compared to the other 10 minute sample types was evident upon comparison of the graphical scales of the filter samples in each case (e.g. Fig. 4-9 compared to Fig. 4-12). The gas phase content was higher in the primary traps and secondary traps of the LHD samples when compared to all the other sample types.

#### 4.3.1.3 Workshop samples

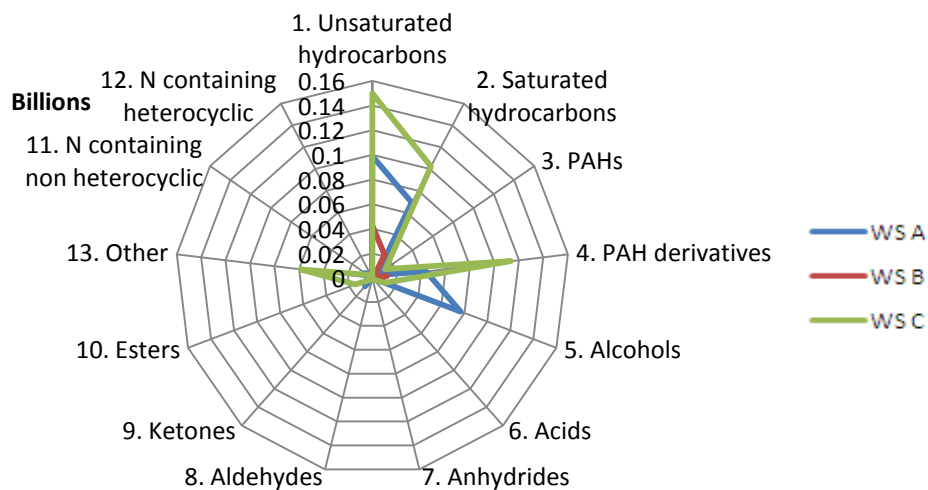


Figure 4-11 Composition of SVOCs from primary traps for workshop diesel shaft samples

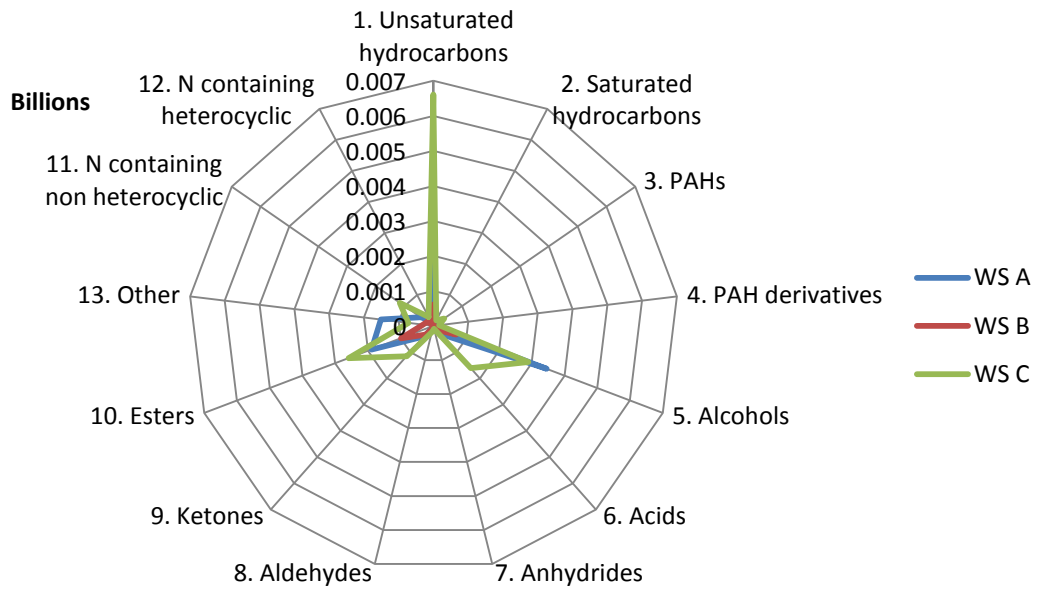


Figure 4-12 Composition of SVOCs from filters for workshop diesel shaft samples

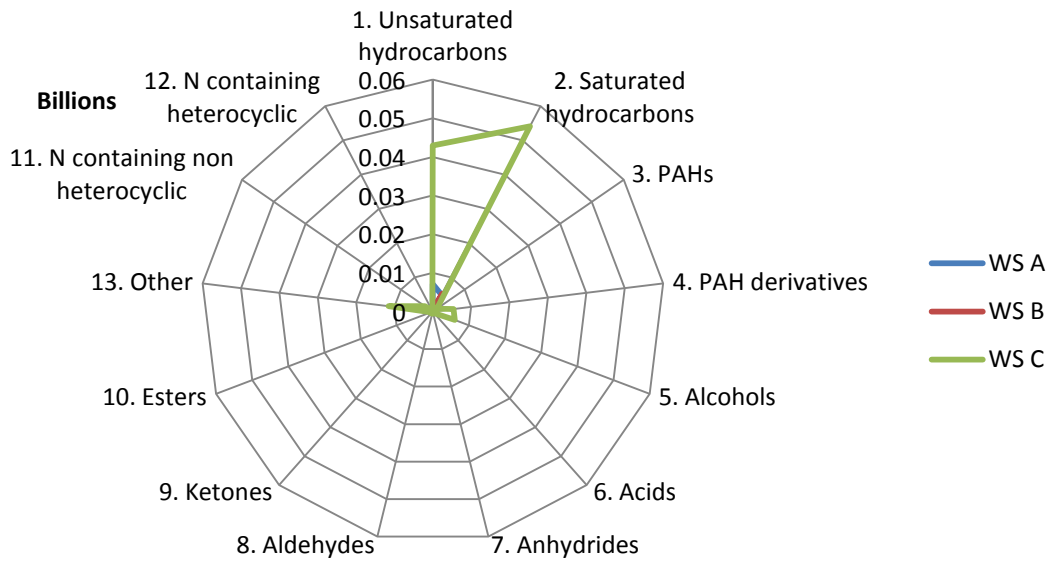


Figure 4-13 Composition of SVOCs from secondary traps for workshop diesel shaft samples

Figures 4-11 to 4-13 represented the composition of SVOC profiles of the samples that were taken from within the workshops underground in diesel shafts where the sampling period was approximately 10 minutes for the primary trap, filter and secondary trap respectively. The workshop at every mine differed in size, number of stored vehicles, number of vehicles in need of maintenance, the area relative to the mining area and ventilation, therefore if all these factors are considered results were expected to vary.

From Fig. 4-11 it could be clearly seen that saturated and unsaturated hydrocarbons had the highest peak areas in the primary traps from each mine with the Plat mine C sample having the largest peak areas. PAH derivatives were significant in the Plat mine C sample. The peak areas obtained from the Plat mine B sample were overshadowed by the other two mines which was to be expected as Plat mine B had the smallest workshop of the three and whilst sampling the workshop was empty and relatively clean. Plat mine A on the other hand had a busy workshop with many vehicles coming and going.

Fig. 4-12 showed the abundance of particle associated unsaturated hydrocarbons. The Plat mine C sample also contained a relatively significant amount of acids, ketones and esters. The Plat mine A sample showed the highest peak area for alcohols.

Particle loading of SVOCs was very low compared to the other sample types (possibly due to lower particle concentration), as seen from the scale of Fig. 4-12.

Fig. 4-13 revealed that the Plat mine C sample had the highest amount of hydrocarbons on the secondary traps, and had more hydrocarbon breakthrough than in the 30 minute and non-diesel samples (refer to the scale of Fig. 4-16).

4.3.1.4 Non-Diesel samples

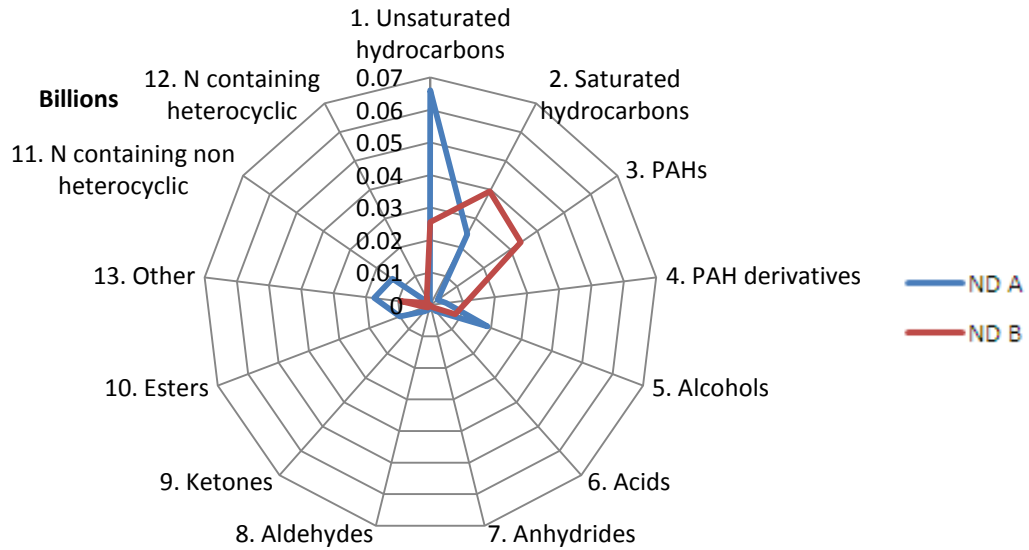


Figure 4-14 Composition of SVOCs from primary traps for ambient 10 minute non-diesel shaft samples

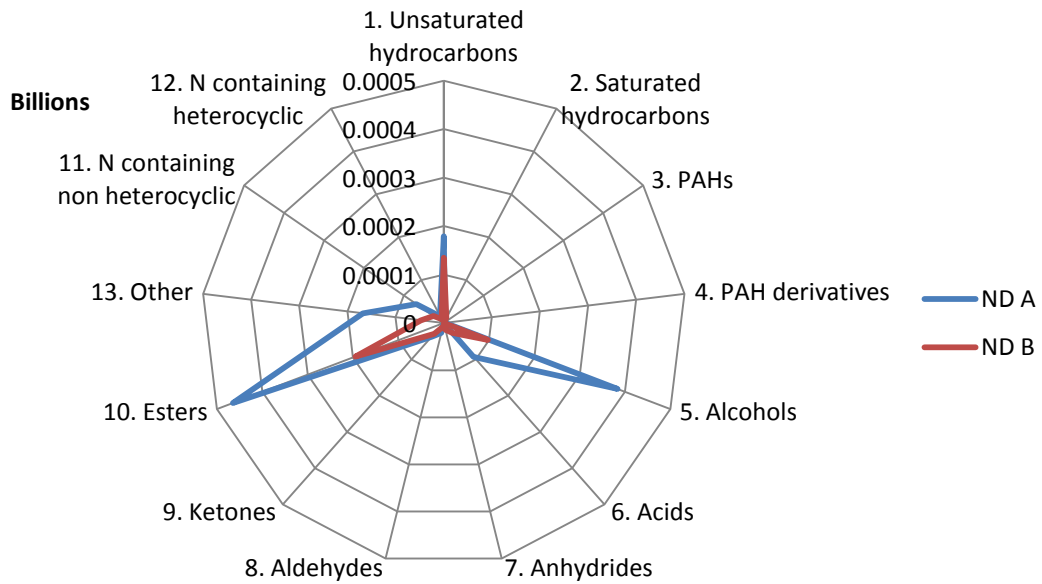


Figure 4-15 Composition of SVOCs from filters for ambient 10 minute non-diesel shaft samples



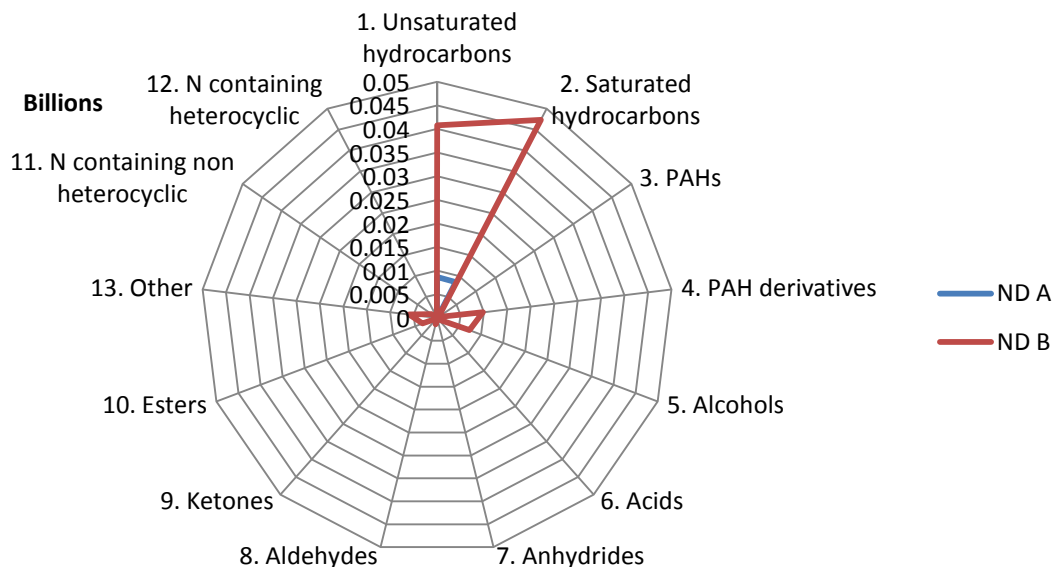


Figure 4-16 Composition of SVOCs from secondary traps for ambient 10 minute non-diesel shaft samples

Figures 4-14 to 4-16 represented the composition of SVOC profiles of the samples that were taken in non-diesel shafts, where the samples were taken for an approximately 10 minute period for primary trap, filter and secondary trap respectively. No sampling could take place at Plat mine C due to industrial unrest at the time.

Fig. 4-14 and 4-16 showed the peak areas of each compound class found on the primary and secondary traps respectively at the shafts where no diesel vehicles were used. The primary trap of the Plat mine B sample showed larger peak areas for saturated hydrocarbons and PAHs. The Plat mine A sample showed larger peak areas than that of the Plat mine B sample for unsaturated hydrocarbons and alcohols in the primary trap (Fig. 4-14). The Plat mine B secondary trap sample showed larger peak areas than the Plat mine A sample, specifically with regards to unsaturated and saturated hydrocarbons, PAH derivatives and alcohols. The source(s) of the PAHs and PAH derivatives seen in the primary and secondary trap, particularly for the Plat mine B sample, should be investigated.

Fig. 4-15 revealed that the Plat mine A and B filter samples had relatively large peak areas for unsaturated hydrocarbons, alcohols and esters. The peak areas of the esters were substantially larger (relative to the area of the unsaturated hydrocarbons) than in other samples, which could be due to

conventional mining practices in the non-diesel shaft. The scale of Fig. 4-15 indicated that there was a very low particle loading of SVOCs probably due to low particle levels.

From the radar graphs it could be generally concluded that the hydrocarbons were always detected and possessed the highest peak areas. Pentatriacontane ( $C_{35}H_{72}$ ), eicosane ( $C_{20}H_{42}$ ) and octasane ( $C_{28}H_{58}$ ) were amongst some of the longer chain unsaturated hydrocarbons that were detected. Nonane ( $C_9H_{20}$ ), decane ( $C_{10}H_{22}$ ), cyclotetradecane ( $C_{14}H_{28}$ ), indene ( $C_9H_8$ ) and docosene ( $C_{22}H_{44}$ ) were amongst other hydrocarbons that were found with high peak areas. Primary traps contained the highest peak areas followed by the secondary traps. The importance of gas phase SVOC sampling was again evident.

No particle phase PAHs were detected in the non-diesel shafts.

#### 4.4 PAH profiles expressed as relative % peak areas

The relative % peak areas (individual PAH peak area relative to total peak area of all compounds in sample) of the PAHs found in the primary traps, filters and secondary traps respectively were represented in bubble plot figures in this section which gave a clear PAH profile for each sample medium and it showed the clustering patterns of the PAHs.

Plots of the absolute peak area of PAHs, per litre of air sampled, are presented in Section 4.5 to 4.7 for the primary trap, filter and secondary trap respectively.

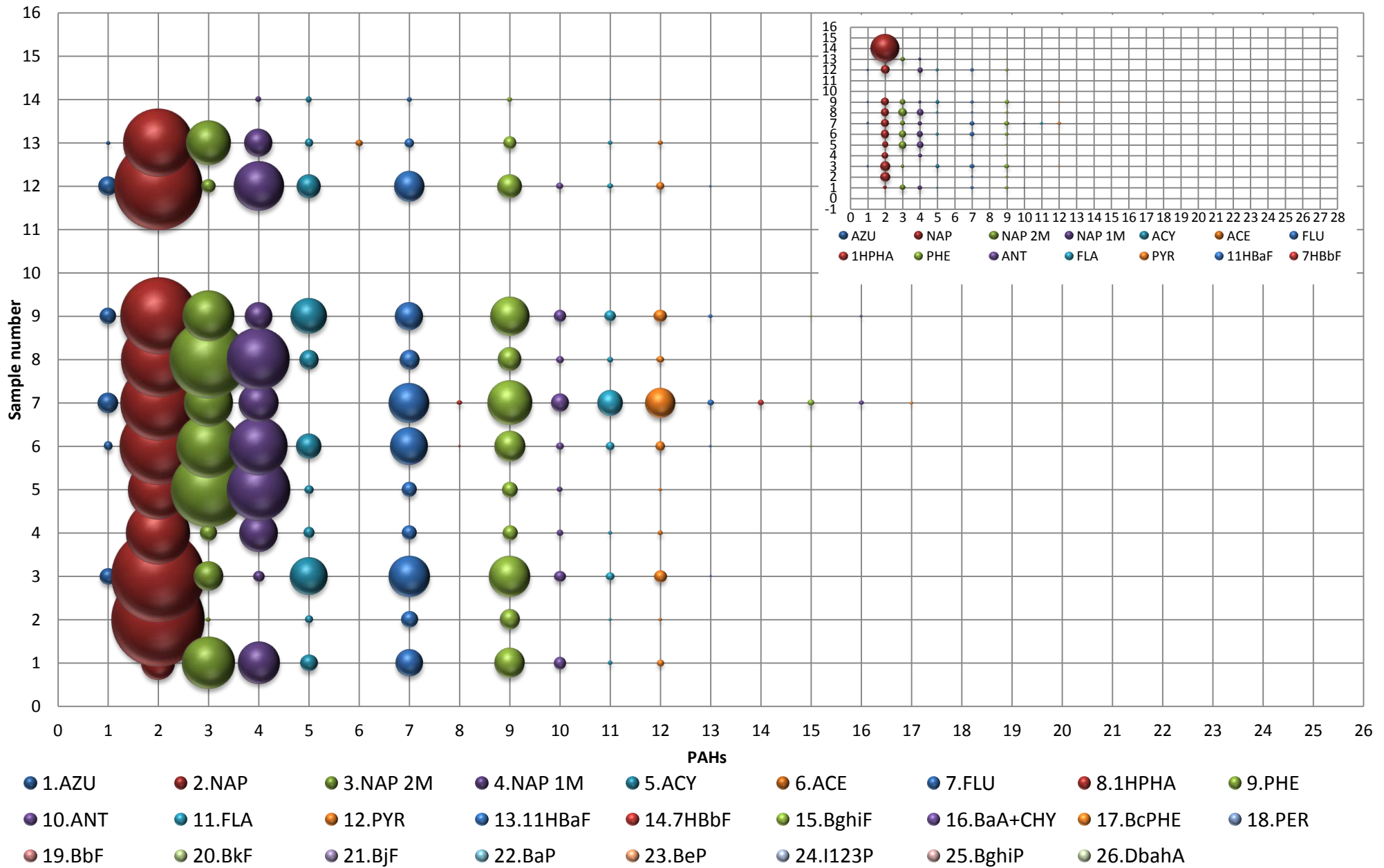


Figure 4-17 A: Relative % peak areas of PAHs from the primary trap samples excluding sample # 14. Figure 4-7 B: (insert) Relative % peak areas of PAHs from the primary trap samples including sample # 14

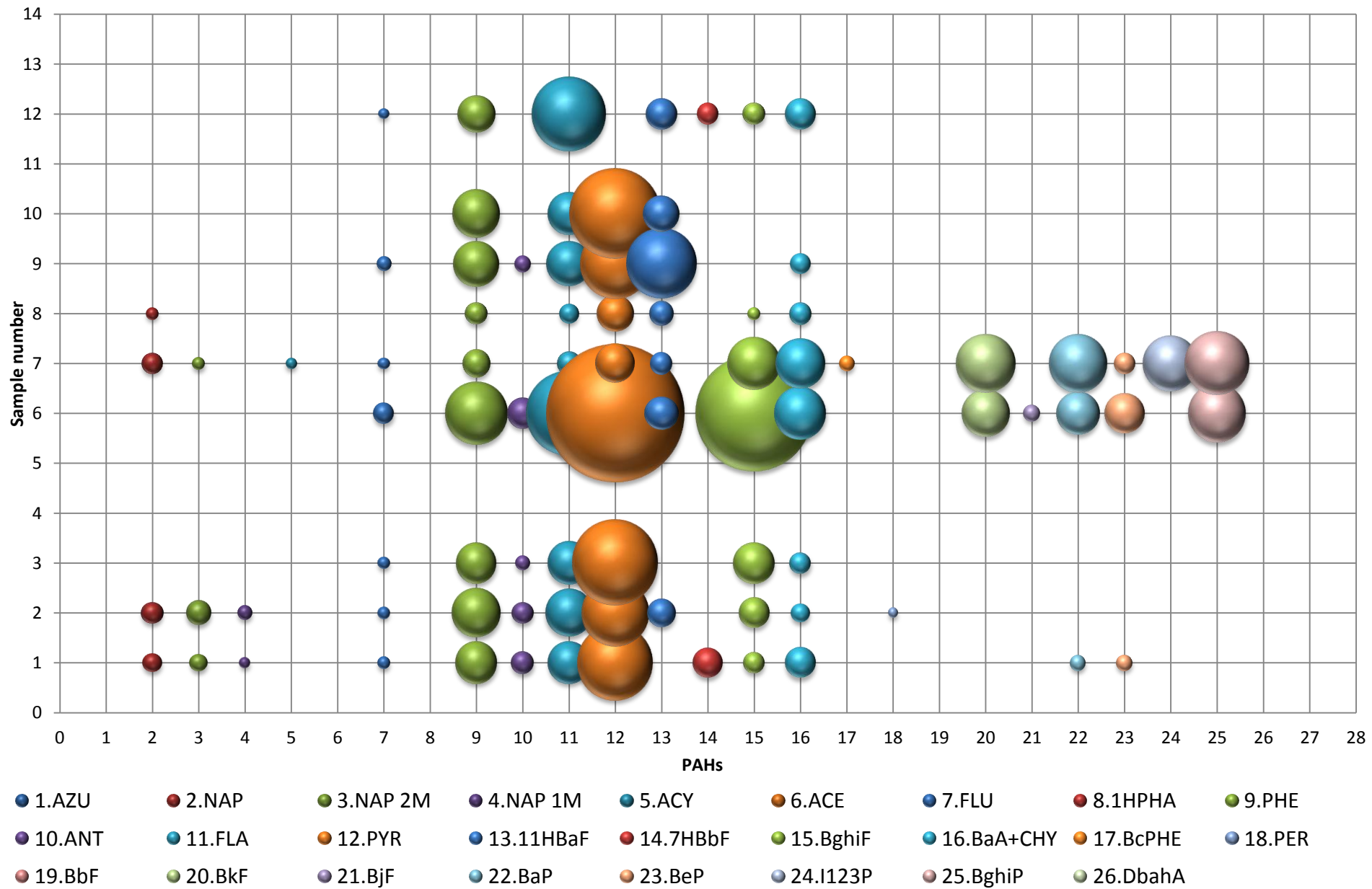


Figure 4-18 Relative % peak areas of PAHs from the filter samples

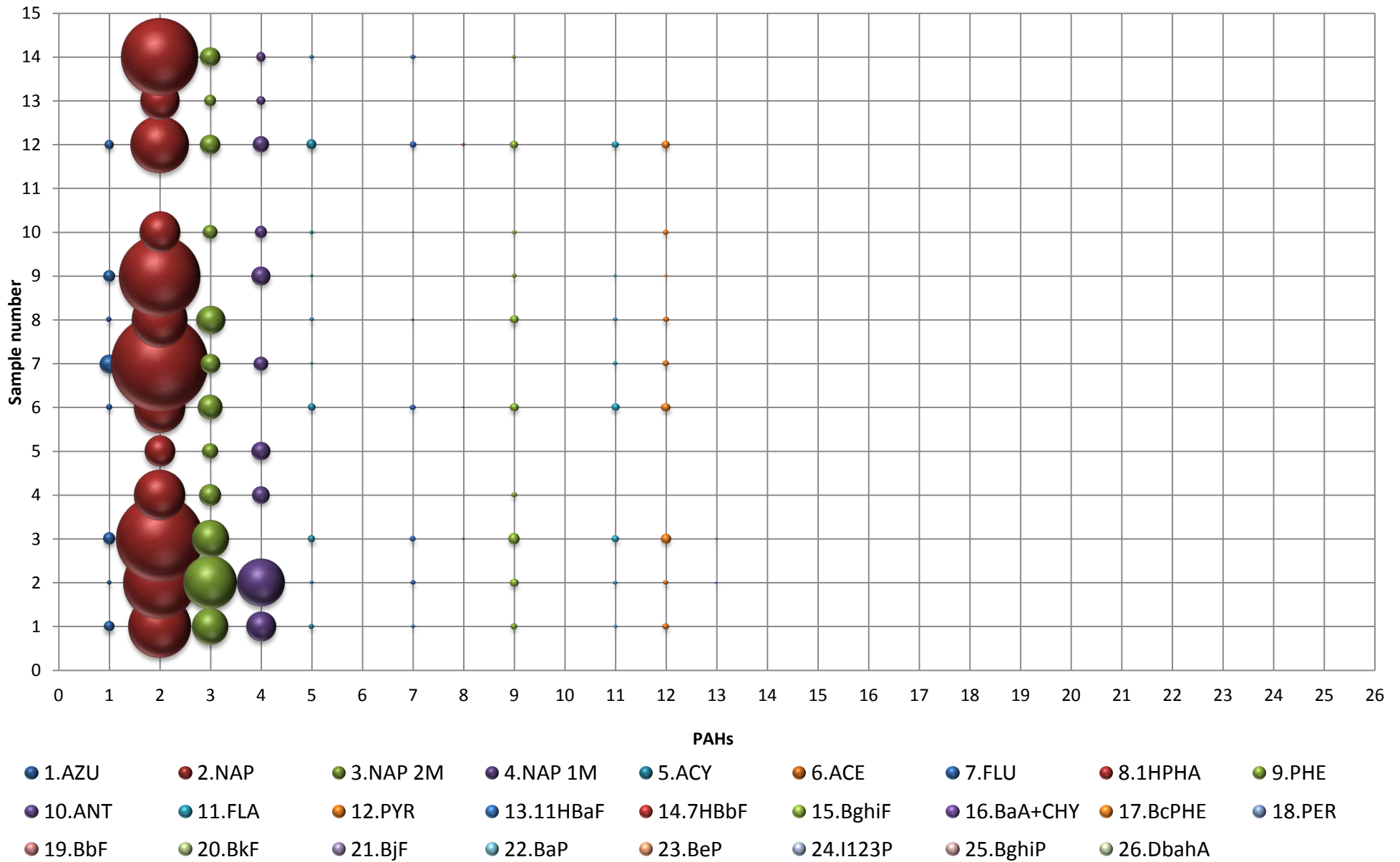


Figure 4-19 Relative % peak areas of PAHs from the secondary trap samples

Figures 4-17 to 4-19 represented the relative % peak area of PAHs obtained from the primary trap, filter and secondary trap samples respectively. The theory of the denuder sampling devices (Fig. 3-2) is that the primary trap will collect gaseous PAHs which are generally the lower molecular weight PAHs. PAHs with molecular weights up to  $202 \text{ g.mol}^{-1}$ , such as pyrene, are considered more volatile and are found mostly in the gaseous phase (Forbes *et al.* 2012). The silicone acts as a solvent to the non-polar molecules and therefore “traps” the analytes. The filter, post primary trap, will collect PAHs that occur in the particulate phase or PAHs that were adsorbed onto filter fibres whereas the secondary trap will collect any PAHs that have blown off from the filter. It could happen that analytes may have broken through the primary trap, however the small sampling volumes would prevent breakthrough as it was previously found that the breakthrough volume ( $V_B$ ) of the more volatile naphthalene was 5 L (Forbes & Rohwer 2009). It was expected that the secondary trap have much lower concentrations than the primary trap unless significant breakthrough had occurred or if analyte concentrations varied over the sampling interval. It should be noted that desorption efficiencies from PDMS traps may differ from that of a loaded filter.

Fig. 4-17A showed that smaller PAHs (2-4 rings) were trapped on the primary trap as expected. PAHs up to pyrene were seen in the majority of the samples. Naphthalene and the mono substituted naphthalene derivatives were the most abundant of the PAHs found on the primary traps. Acenaphthylene and fluorene also had significant relative % peak areas. A more detailed inter sample comparison is presented in the following sections. The Plat mine B non-diesel sample (number 14) revealed a very high relative % peak area for naphthalene which could be seen in Fig. 4-17B however the sample was omitted in Fig. 4-17A to allow for the other samples to be visible. The large bubble representing the relative % peak area for naphthalene corresponded to a peak that was 24 % of the total peak area whereas PAH relative % areas generally did not exceed 2.4 %.

Fig. 4-18 showed the relative % peak areas of PAHs on the filter samples i.e. particulate associated PAHs, and it was evident that the heavier PAHs were trapped on the filters. When comparing Fig.4-17 & 4-18, the shift from the smaller, lower weight PAHs found on the trap to the larger, heavier, PAHs found on the filters was undoubtedly seen. Pyrene and fluoranthene had the highest relative % peak areas in most of the filter samples. A similar profile was evident for the three 30 minute ambient samples. Overall it could be concluded that the majority of the PAHs trapped on the filters were from phenanthrene ( $178 \text{ g.mol}^{-1}$ ) to benzo(ghi)fluoranthene ( $216 \text{ g.mol}^{-1}$ ). Heavy PAHs, such as benzo(k)fluoranthene, benzo(a)pyrene and benzo(ghi)perylene were seen in a few of the samples which

were identified in the following sections. These PAHs were consistent with the PAHs recorded in the literature for diesel sources (Section 4.1). However, the instrumental limitations (Section 4.1.2), with respect to the TD temperature, were considered when interpreting the filter sample results presented here.

Fig. 4-19 showed that smaller PAHs (2-4 rings) were trapped on the secondary trap. Naphthalene and the mono substituted naphthalene derivatives were the most abundant of the PAHs found on the secondary traps which is expected as they have higher ambient gas phase concentrations and they are the more volatile species. Should the smaller, more volatile PAHs be adsorbed onto filter particles they may be readily blown off and are thus trapped by the secondary trap. Significantly lower amounts of PAHs (up to pyrene) could be seen on the secondary traps.

The relative % peak area figures (Fig. 4-17 to 4.19) gave a good indication of profiles of the PAHs found on the traps and filter samples. To gain more quantitative insight, bar graphs of actual peak areas (normalised) will be shown in the following section where the total peak areas of PAHs in each sample can be compared.

#### 4.5 PAH profiles expressed as total normalized peak areas

This section provides bar graphs of the normalized peak areas (with respect to sample volumes) for each PAH obtained for each sample. This was done to get a general overview as to which PAHs (or clusters of PAHs) were most commonly detected and which were most abundant. It also allowed for inter-mine comparison with respect to the PAH profiles. It should be noted that the sample names were not labeled in these graphs as the PAH profiles for each sample will be discussed in Section 4.6.

Figures 4-20 to 4-22 showed normalised peak areas (with respect to sample volumes) obtained from the primary traps, filters and secondary traps respectively. Plat mine A was always represented by blue, Plat mine B by red and Plat mine C by green. Ideally, for comparative purposes the PAH peak areas should be relative to an internal standard that would account for possible run-to-run variation, this should be considered in a future study.

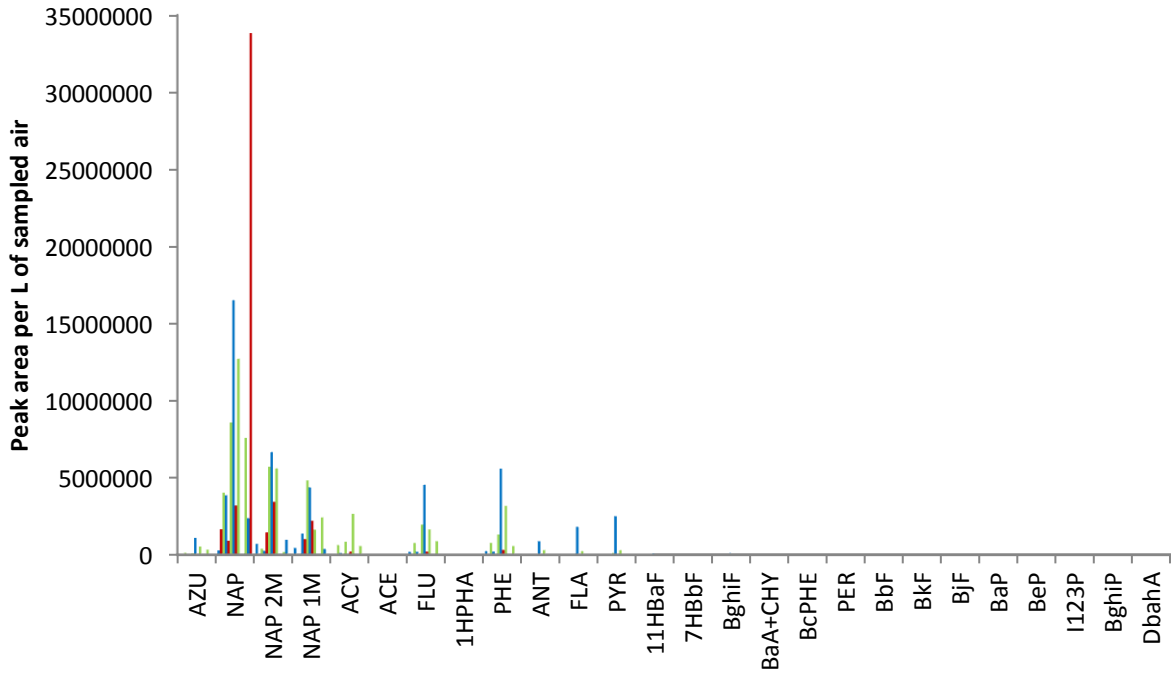


Figure 4-20 Total peak areas of PAHs from the primary trap samples

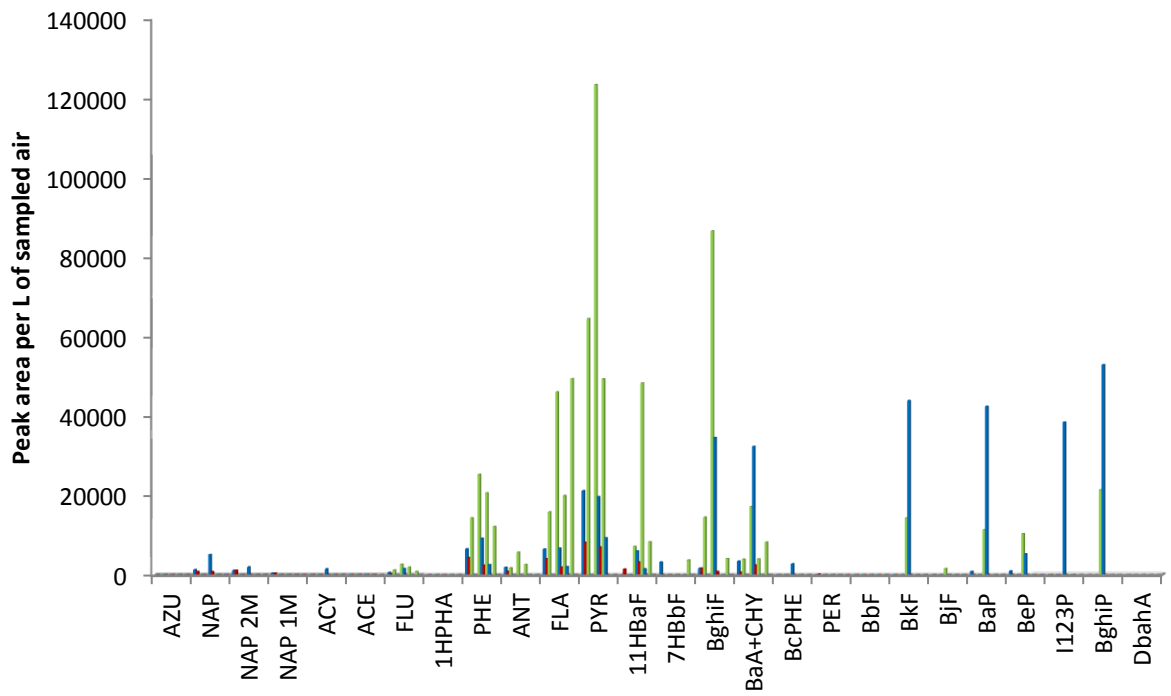


Figure 4-21 Total peak areas of PAHs from the filter samples



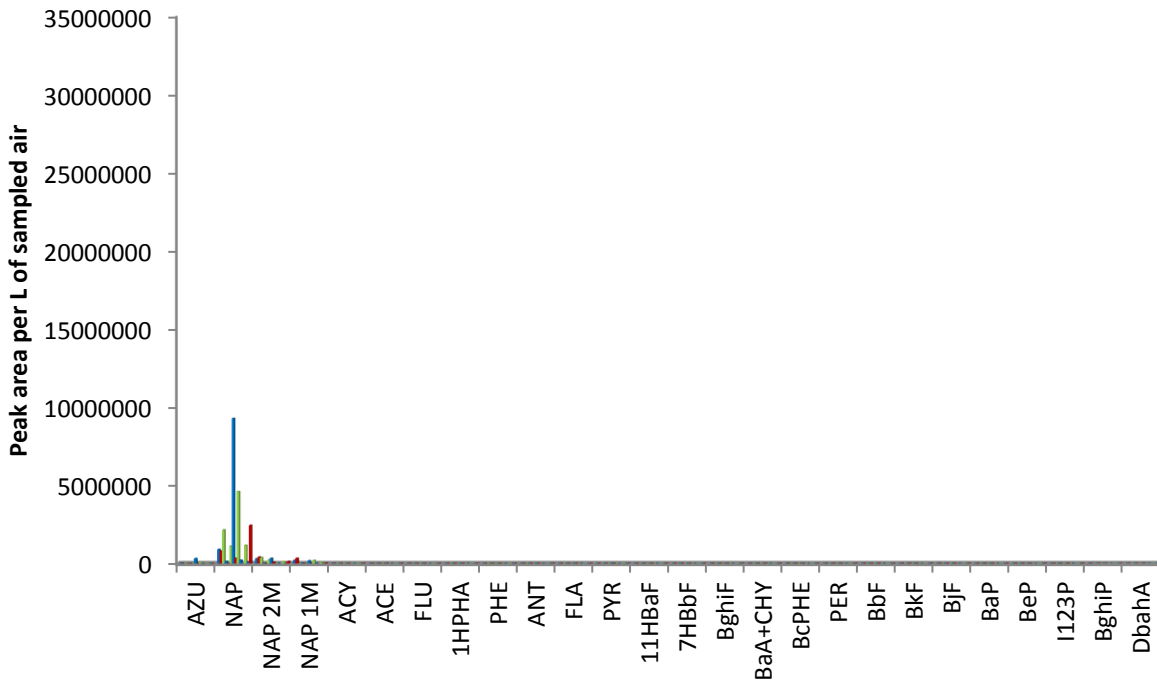


Figure 4-22 Total peak areas of PAHs from the secondary trap samples (y axis was kept the same as in Figure 4-20 for comparative purposes).

Fig. 4-20 showed that smaller PAHs (2-4 rings) were trapped on the primary trap and PAHs up to pyrene were seen in the majority of the samples. Naphthalene and the mono substituted naphthalene derivatives were the most abundant of the PAHs found on the primary traps as seen in Fig. 4-20. The peak area of 1-methyl naphthalene was the highest in a Plat mine C sample whereas 2-methyl naphthalene was found at the highest levels in Plat mine A samples. Plat mine B showed one very high peak area for naphthalene (corresponds to the non-diesel sample described in the previous section and Fig. 4-17B) but for every other PAH, this mine had the lowest levels. The Plat mine C samples showed the highest peak area for acenaphthylene with the Plat mine A samples revealing the highest peak areas for that of pyrene, fluoranthene, anthracene and phenanthrene. The primary traps contained the highest concentrations of PAHs as seen from the scale of the x-axis.

Fig. 4-21 showed the peak areas of PAHs found on the filter samples and it was evident that the heavier PAHs were trapped on the filters as seen in Fig. 4-18. The Plat mine C samples generally showed high concentrations of PAHs in the particulate phase with a significantly large area for pyrene, fluoranthene, anthracene and phenanthrene when compared to the other mines. The red bars representing the Plat mine B samples showed very little particulate loading compared to the other two mines. The Plat mine A and C samples showed traces of heavy PAHs. The Plat mine A filter samples contained the highest

amount of the heavier PAHs namely: benzo(a)pyrene, benzo(ghi)perylene and indeno(1,2,3-cd)pyrene. Heavier PAHs were not detected on the Plat mine B filter samples. The PAH profiles of Plat mine B and C were similar with higher peak areas for the 4 ring PAHs whereas the Plat mine A profiles showed a dominance of the 5 and 6 ring PAHs.

Fig. 4-22 showed that smaller PAHs (2-3 rings) were trapped on the secondary trap consistent with Fig. 4-19. The highest peak areas for naphthalene were found in a Plat mine A sample whereas the Plat mine B samples showed the highest peak areas for the mono-substituted naphthalene. The finding that Plat mine A and B had relatively high peak areas in the secondary trap may be due to blow off from the filter or due to a variation in PAH concentration over the sampling period. This was confirmed with the observation made during the sampling where LHD vehicles would pass by which caused a spike in the PAH concentration. At Plat mine B, the LHDs would pass by at approximately 8 min intervals whereas the LHDs passed by more frequently in the other mines during the sampling, all of which would result in a changing ambient concentration.

By looking at the results from all three mines, it was evident that similar PAH clusters were seen in all the mines on the primary trap and secondary trap. The primary trap revealed that naphthalene, 1 & 2-methyl naphthalene, acenaphthylene, fluorene and phenanthrene were present in every mine sample, however the amounts were fairly different. The secondary trap showed clustering of the more volatile naphthalenes from all mines. The profiles for the filter samples differ particularly due to the presence of the heavier PAHs in the Plat mine A samples, although the mines seemed to have similar clustering of PAHs around pyrene which was the most intense peak. From the scales of the graphs, the PAHs existed dominantly in the gaseous phase with peak areas of the filter samples being 20 times less than that of the primary trap samples, when the Plat mine B non-diesel primary trap sample was excluded.

The peak areas of PAHs (Fig. 4-20 to 4-22) gave a good comparison between mines with respect to the amount of PAHs found in all of the samples but in order to understand the individual contributions of each sample type, a more in-depth study was conducted. Bar graphs of peak areas of each PAH will be shown in the following section, where the total peak areas of each PAH from each sample type from each mine were compared.

## 4.6 Sample PAH fingerprints expressed as total normalised peak area for inter-mine comparison

This section shows bar graphs of normalised peak areas for each PAH in the individual samples. These graphs revealed how much (peak area is related to concentration) of a certain PAH there was at a specific sampling site at the three different mines, allowing for inter-mine comparisons. Comparing the different bar graphs to each other also allowed for inter-sample comparisons. All the primary traps were compared to each other and they were discussed first, followed by the filters then the secondary traps.

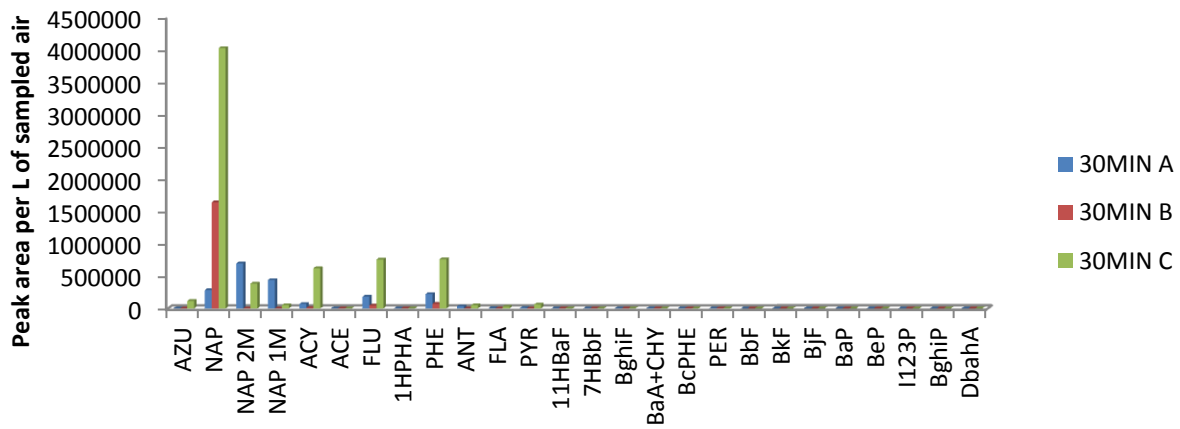


Figure 4-23 Peak areas of PAHs detected in 30 minute ambient samples from primary traps.

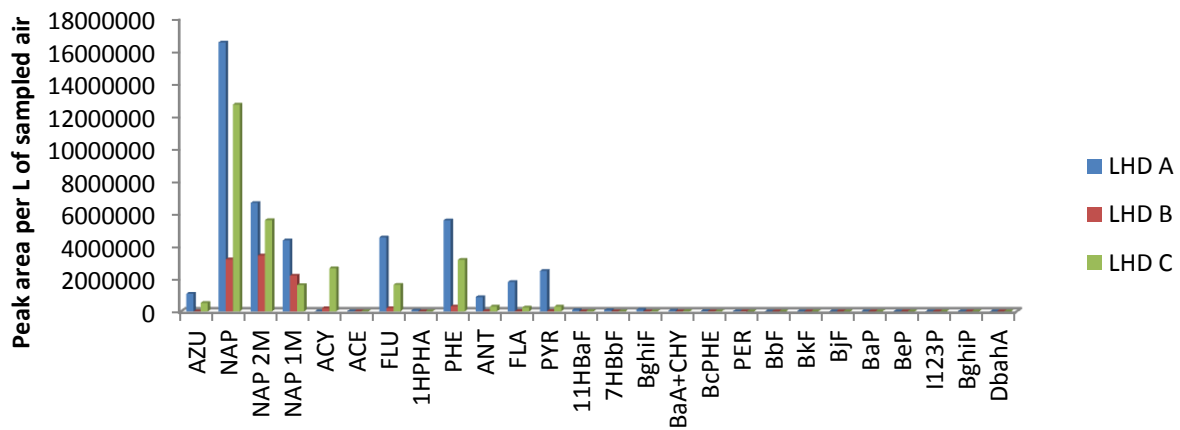


Figure 4-24 Peak areas of PAHs detected in LHD exhaust samples from primary traps.

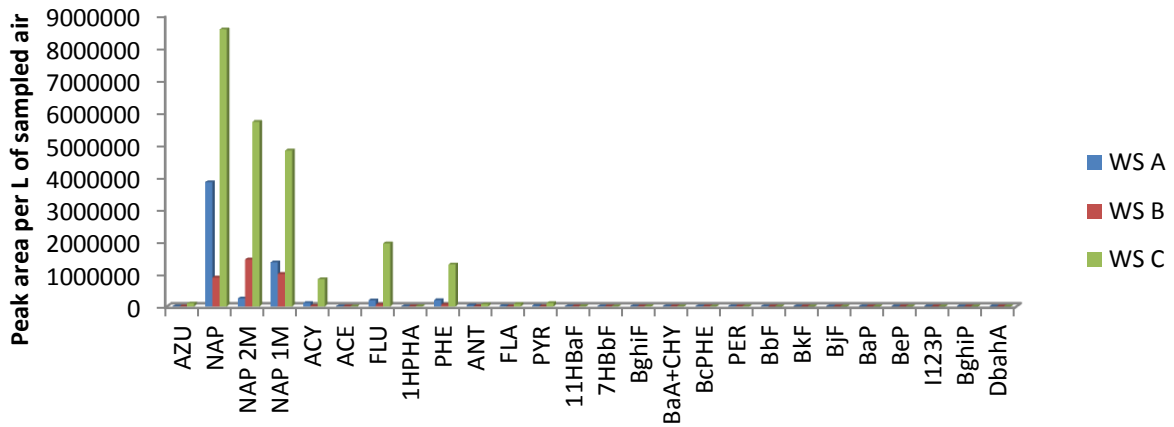


Figure 4-25 Peak area of PAHs detected in workshop samples from primary traps.

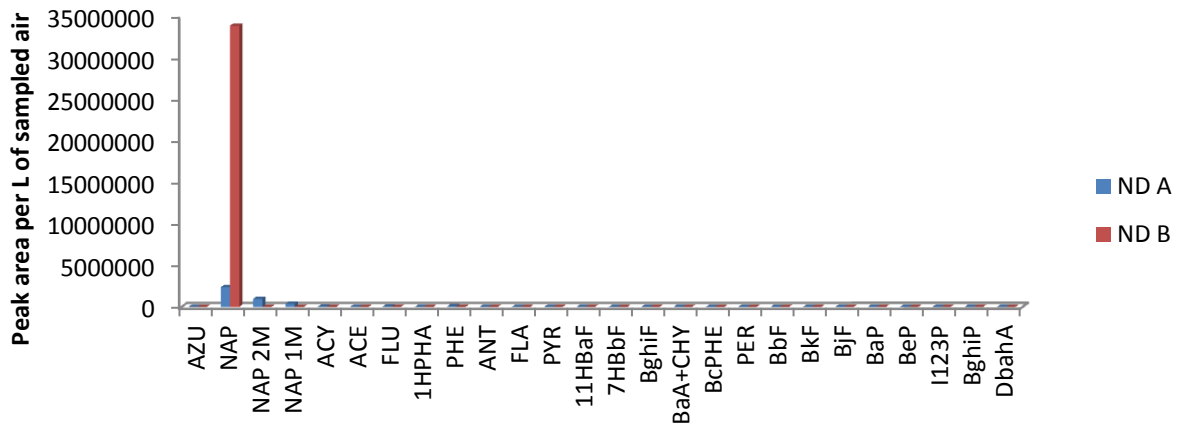


Figure 4-26 Peak area of PAHs detected in non-diesel samples from primary traps.

Figures 4-23 to 4-26 represented the PAHs detected from the primary traps from a range of sampling locations. The graphs showed the common detection of the lighter, more volatile PAHs (typically up to pyrene) as previously shown in other sections. There was no 10 minute Plat mine B sample and the 10 minute Plat mine A sample was not included in the sample set, due to analytical complications, therefore no 10 minute bar graph was provided for the primary traps.

High peak areas were expected for the 30 minute samples (Fig. 4-23) due to the larger sampling volume, but the maximum areas were less than that found in the LHD samples. This was attributed to the fact that the LHD samples were taken at the exhaust (the source of emission in a LHD usage area) whereas the 30 minute samples were taken at ambient conditions. For the 30 minute samples, the Plat mine C sample showed the highest peak areas for naphthalene, acenaphthylene, fluorene and phenanthrene

with the naphthalene peak being twice as high as any other peak. Plat mine A sample showed the highest peak areas for 2-methyl naphthalene and 1-methyl naphthalene. The highest peak found in the 30 minute ambient sample at Plat mine B was naphthalene, however the peak area for every other PAH was much less than at the other mines.

The LHD (Fig. 4-24) samples had the highest amount of PAHs than in any other type of sample (higher peak areas than in any other sample type as seen from the graphical scale), with the exception of the high naphthalene level found in the non-diesel Plat mine B sample, and there was more consistency between sample profiles. The Plat mine B sample showed the lowest peak area for every PAH from the LHD exhaust samples, except for 1-methyl naphthalene where the peak area was slightly higher than that of the Plat mine C sample.

The workshop samples in Fig. 4-25 revealed that the Plat mine C sample contained the most PAHs with dominating peak areas almost double those of the other mines. The maximum peak area as seen in Fig. 4-25 was approximately 9 000 000 which was in the same range as most of the peaks found in the LHD samples (Fig. 4-24), which suggested that the workshop at Plat mine C was either polluted with diesel fumes due to a high amount of vehicles or the ventilation might not have been adequate during sampling. Alternatively, the position of the workshop could be in very close proximity to mining operations.

The non-diesel samples revealed that the Plat mine A sample contained naphthalene, 2-methyl naphthalene and 1-methyl naphthalene. The Plat mine B sample showed only naphthalene with a peak area higher than in any other sample.

The next few pages provide the results obtained from the filters followed by the results obtained for the secondary traps.

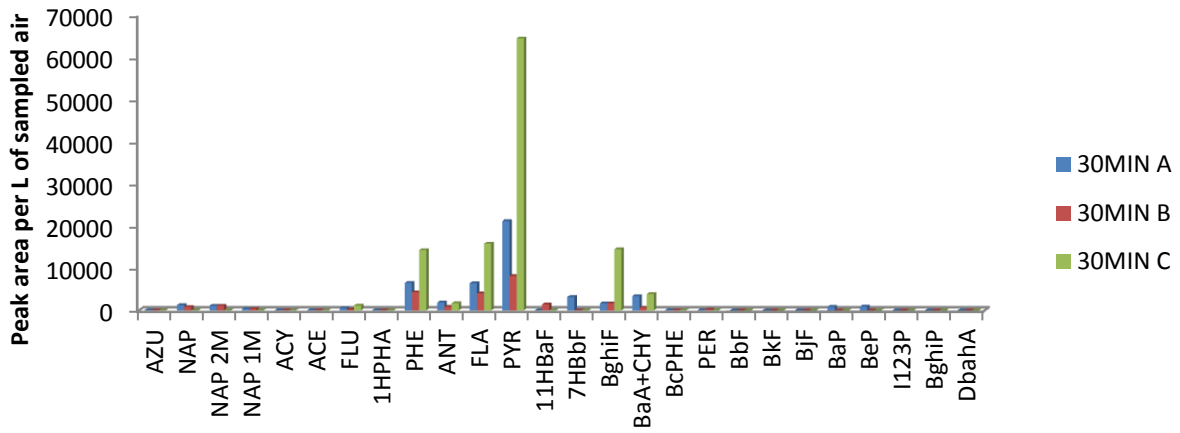


Figure 4-27 Peak areas of PAHs detected in 30 minute ambient samples from filters.

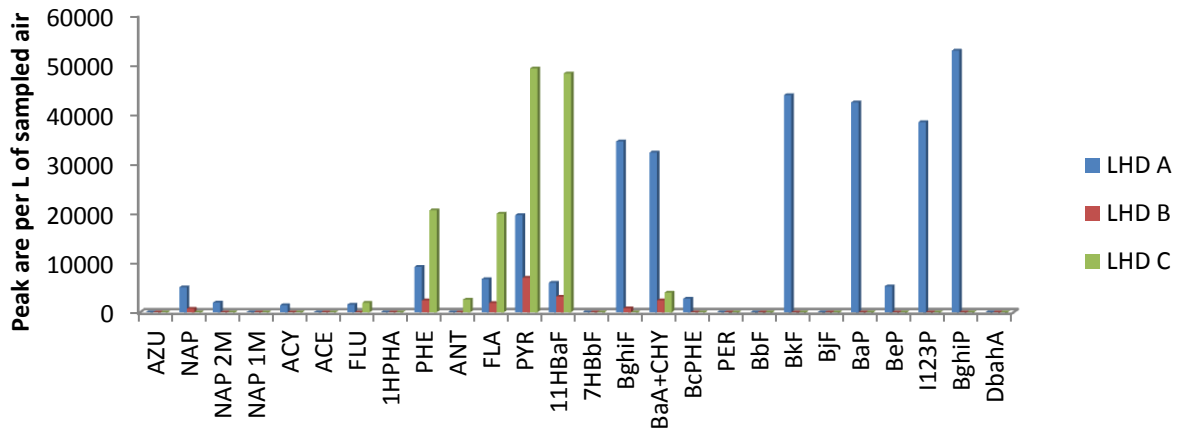


Figure 4-28 Peak areas of PAHs detected in LHD exhaust samples from filters.

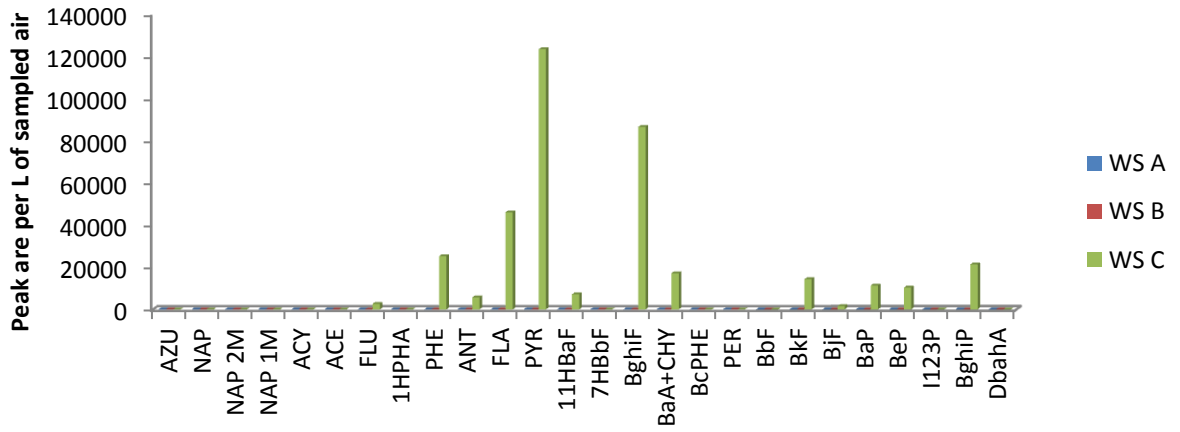


Figure 4-29 Peak areas of PAHs detected in workshop samples from filters.

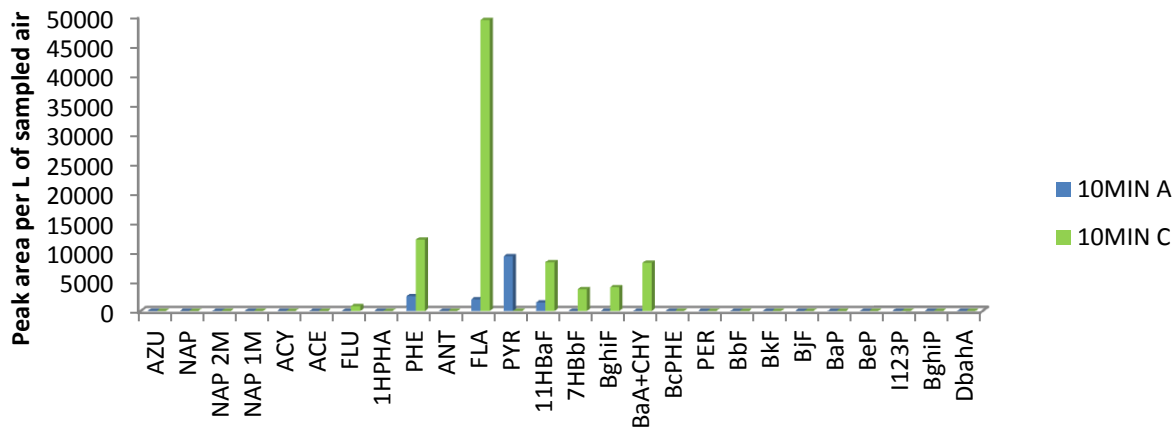


Figure 4-30 Peak areas of PAHs detected in 10 minute ambient samples from filters.

Figures 4-27 to 4-30 represented the PAHs detected from the filters. The general overview showed consistency with what had previously been discussed with respect to the occurrence of the heavier PAHs and less of the lighter PAHs.

The 30 minute samples showed high particle loading (peak area scale was in the same range as the LHD filter samples) which could be explained by the increased activity of diesel vehicles that was observed during sampling. Pyrene was the most dominant PAH for all mines, and the Plat mine C sample had the highest peak areas for each PAH. The Plat mine B sample had the lowest particle loading of PAHs which was in order as during the sampling period there was not as much activity (scooping, loading and idling) of the diesel machinery as there was at Plat mine A or C.

The LHD samples in Fig. 4-28 showed that the Plat mine C sample had the highest peak areas for phenanthrene, anthracene, fluoranthene and pyrene, whilst the Plat mine A sample profile was dominated by heavier PAHs which could be linked to the cold start conditions of the LHD that was selected for the Plat mine A sample. Benzo(ghi)perylene had the highest peak area of all of the LHD filter samples. Vehicle age, maintenance and operating condition impacted on profiles that were obtained. The LHD profiles were different to the 30 minute and 10 minute ambient sample profiles, in that the heavier PAHs were not present in the ambient profiles. This indicated that the particles with which the heavier PAHs were associated deposited rapidly after emission by dry deposition and were thus not present in the ambient air.

The workshop samples revealed that only the Plat mine C filter sample contained particulate PAHs. Once again it should be noted that the workshop at each mine was different and the number of factors influencing the results were numerous.

The 10 minute samples (Fig. 4-30) showed similar trends to the 30 minute ambient samples which was expected as they were taken in the same environments. Lower peak areas for the 10 minute samples were likely the result of a decreased probability of diesel vehicle activity in the area over a shorter time interval.

There were no PAHs detected in the filter samples from the non-diesel shafts thus the graphs were not included. The fact that no PAHs were detected on the filter implied that either PAHs were solely found in the gas phase or the volatile PAHs that were particle loaded had blown off from the filter and were therefore not detected.

From the filter graphs it was concluded that pyrene was found in the particulate phase in every type of filter sample from diesel shafts therefore this compound may serve as a useful indicator of PAHs in mining environments in the future.

The results obtained from the secondary traps are presented in Fig. 4-31 to 4-35.

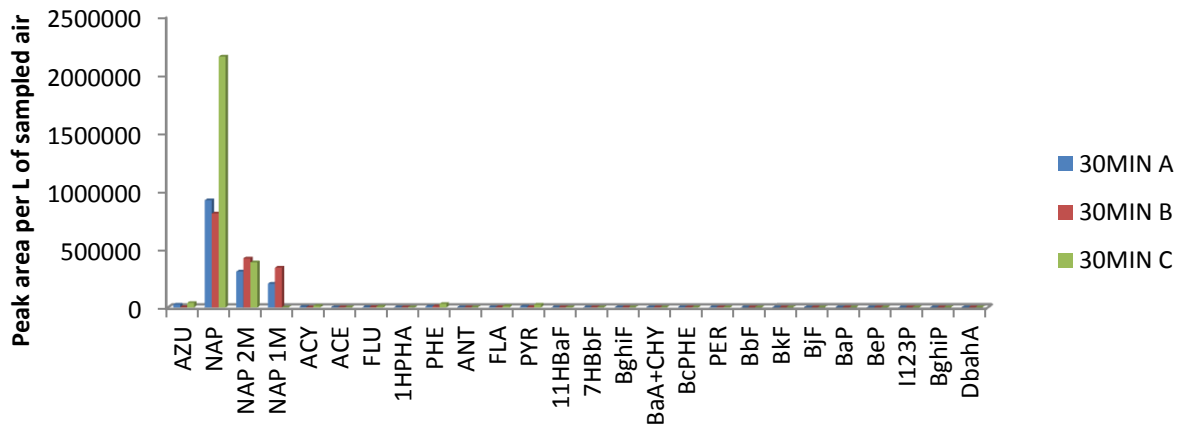


Figure 4-31 Peak areas of PAHs detected in 30 minute ambient samples from secondary traps.



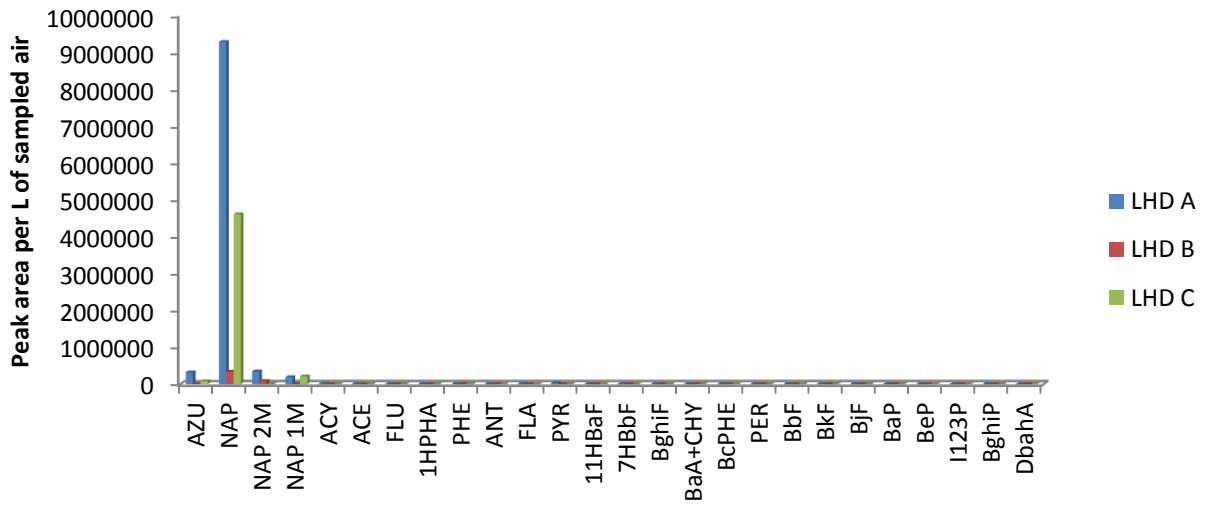


Figure 4-32 Peak areas of PAHs detected in LHD exhaust samples from secondary traps.

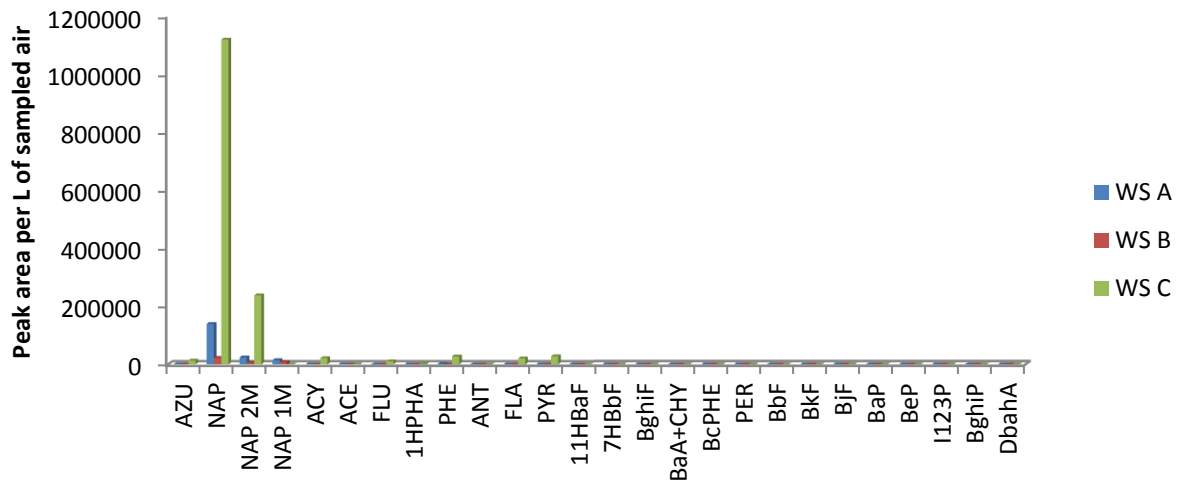


Figure 4-33 Peak areas of PAHs detected in workshop samples from secondary traps.

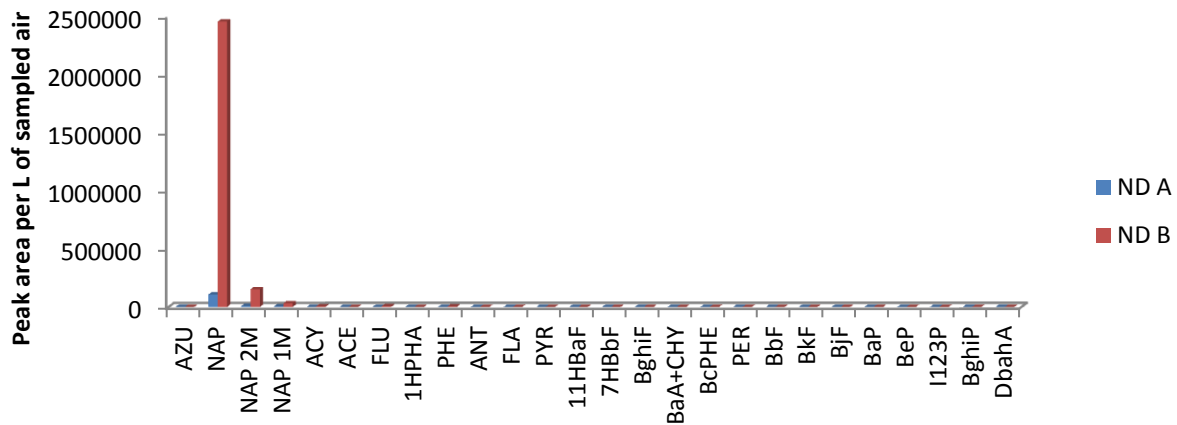


Figure 4-34 Peak areas of PAHs detected in non-diesel samples from secondary traps.

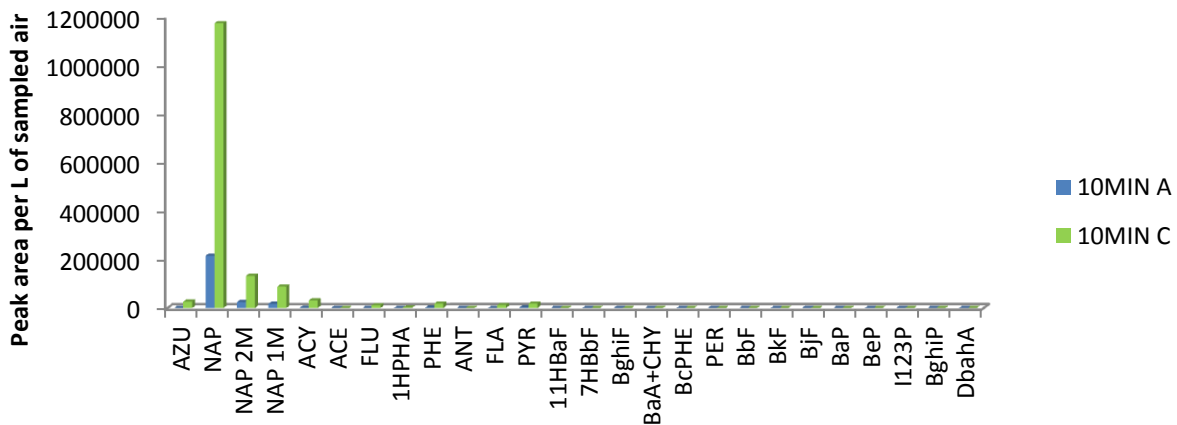


Figure 4-35 Peak areas of PAHs detected in 10 minute ambient samples from secondary traps.

The detection of PAHs on the secondary traps (Fig. 4.31 to 4.35) could be due to blow off from the filter or as a result of a change in analyte concentrations whilst sampling. The activity of the mining operations (i.e. change in source emissions) during sampling and the changing of the instantaneous environment (such as variation in ventilation rates) resulted in change in concentrations of analyte species and this could be the reason for analytes that were detected on the secondary traps.

Overall it was evident that the smaller 2 ring PAHs dominated the secondary trap PAH profiles and there was no evidence of heavier PAHs as expected. It was clearly seen that the 30 minute sample and the LHD samples revealed the highest peak areas of PAHs with naphthalene and its derivatives being the most abundant. High naphthalene levels were also found in the non-diesel sample from Plat mine B. The longer sampling time (i.e. larger sample volume) of the 30 minute ambient samples may have resulted in

breakthrough of the more volatile species from the primary trap. Regarding the LHD samples, high concentrations of PAHs were available to be adsorbed onto particles and the consequent blow off resulted in PAHs on the secondary trap.

Some of the analytes on the secondary trap may be as a result of breakthrough from the primary trap, for sample volumes > 5 L, as the breakthrough volume is 5 L for naphthalene (Forbes & Rohwer 2009).

#### 4.7 Inter-sample comparisons

In this section the normalised peak areas of two different sample types are plotted on one graph in order to compare the PAH fingerprints between the different sampling environments.

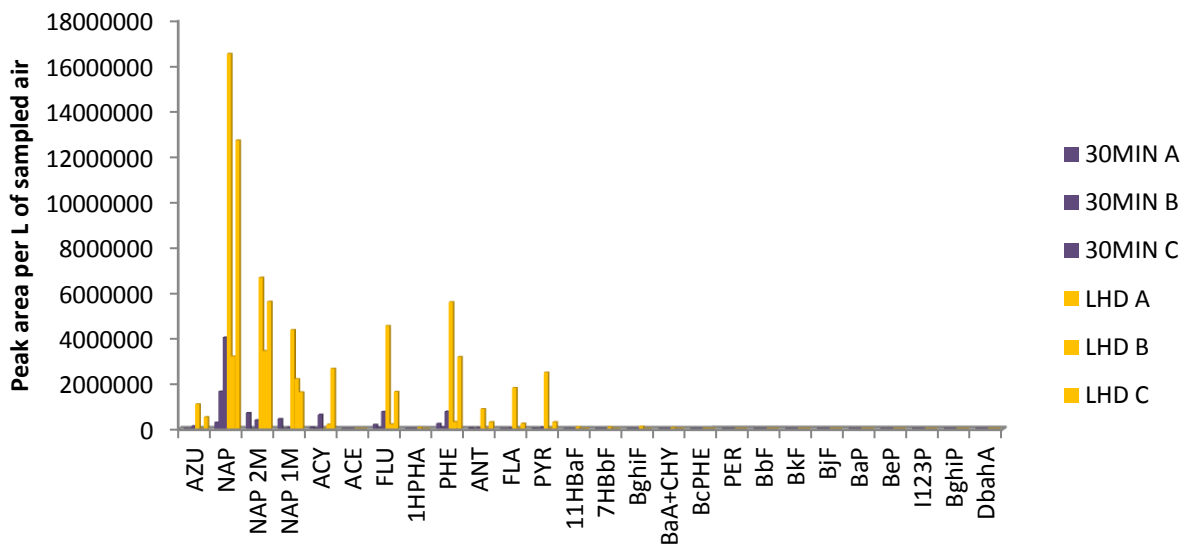


Figure 4-36 Comparison of LHD and 30 minute ambient primary trap samples

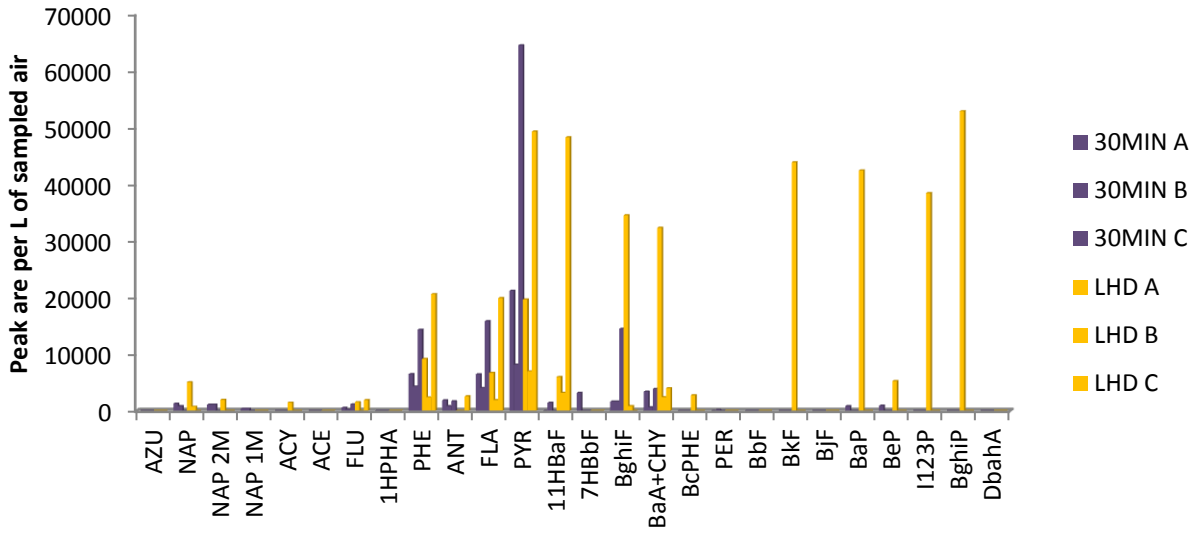


Figure 4-37 Comparison of LHD and 30 minute ambient filter samples

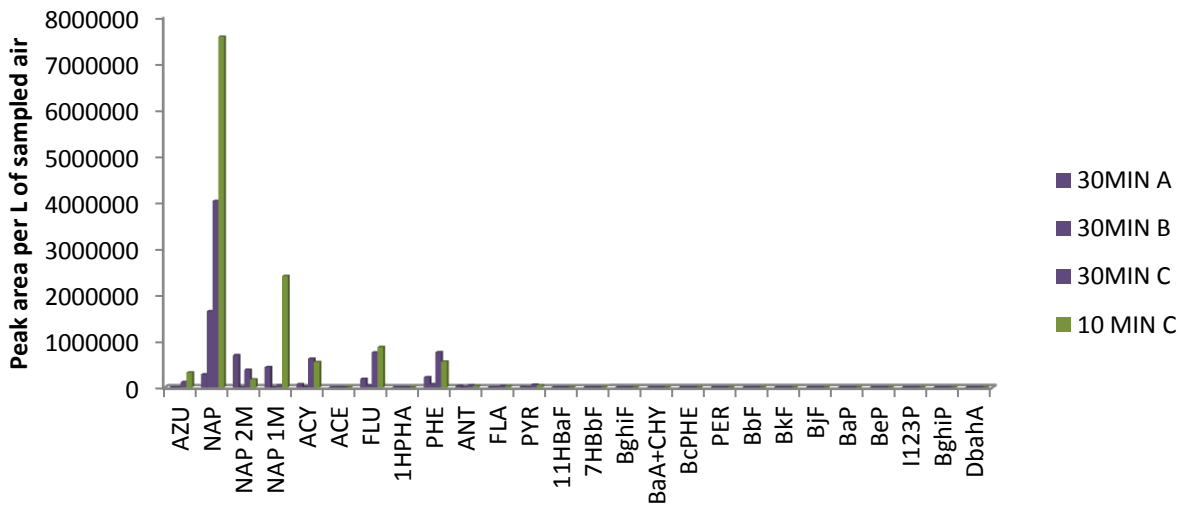


Figure 4-38 Comparison of the 10 minute and 30 minute ambient primary trap samples

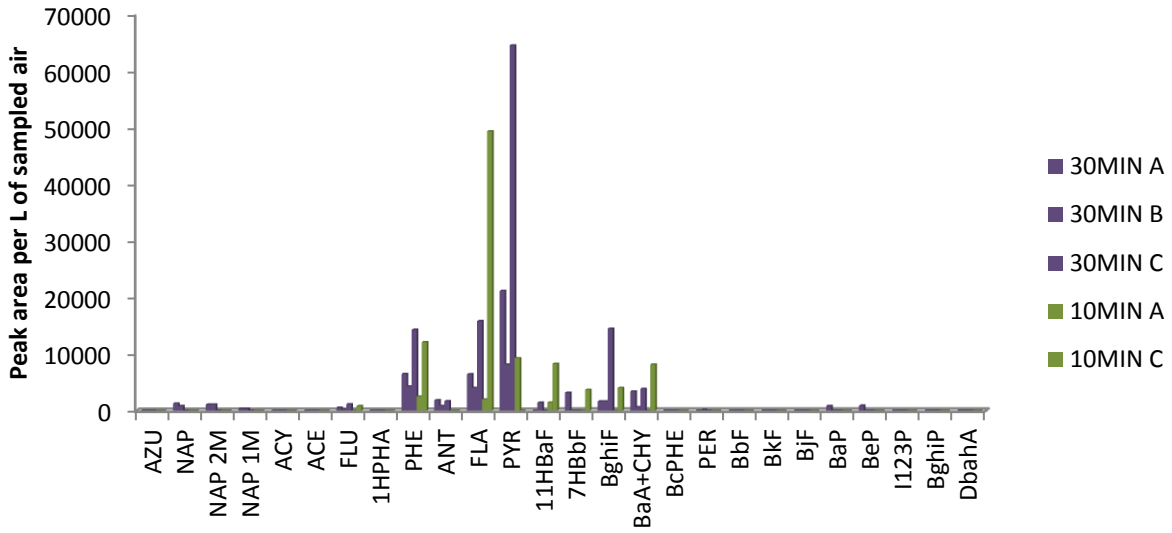


Figure 4-39 Comparison of the 10 minute and 30 minute ambient filter samples

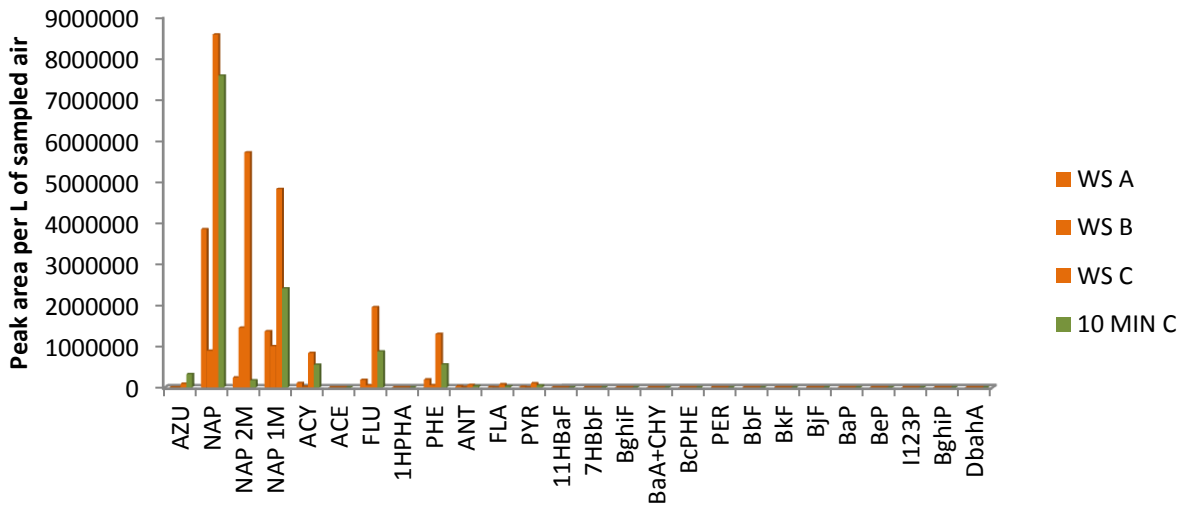


Figure 4-40 Comparison of the workshop and 10 minute ambient primary trap samples

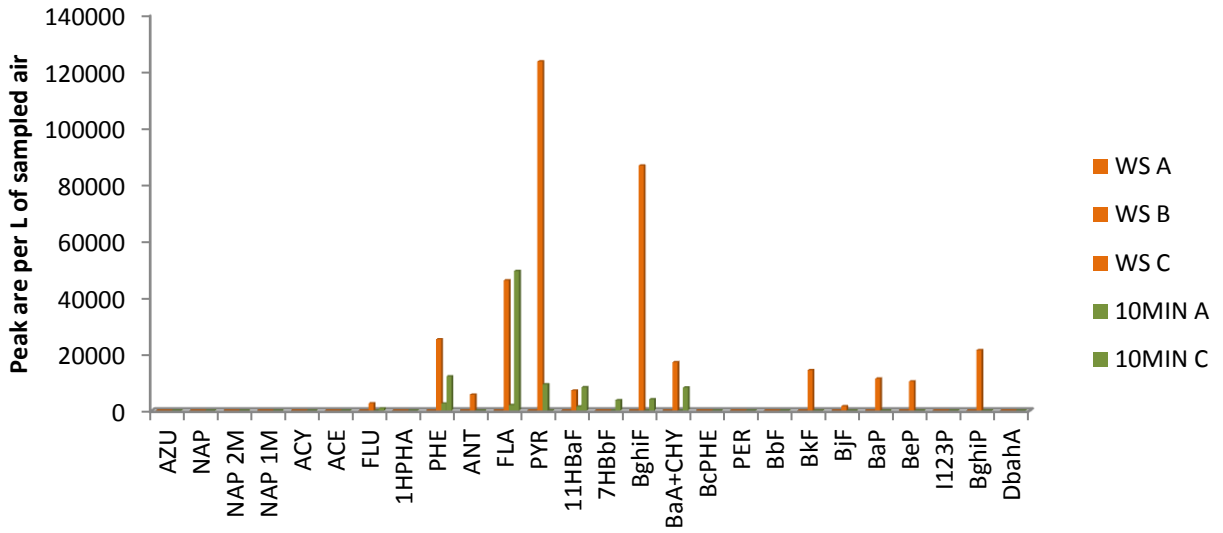


Figure 4-41 Comparison of the workshop and 10 minute ambient filter samples

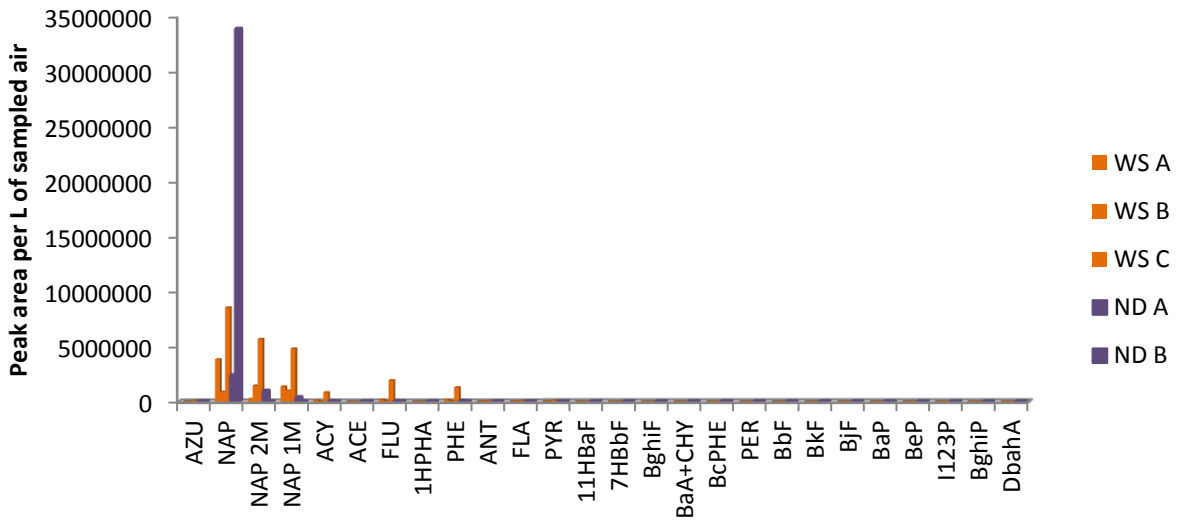


Figure 4-42 Comparison of the workshop and non-diesel ambient primary trap samples

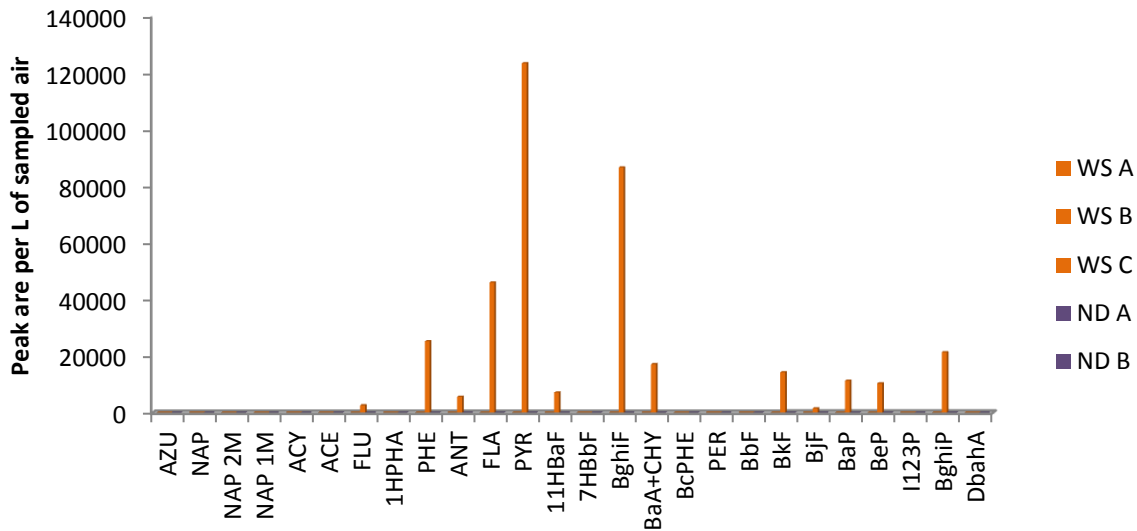


Figure 4-43 Comparison of the workshop and non-diesel ambient filter samples

Figures 4-36 and 4-37 showed the dominance of the LHD samples with respect to the PAH emissions, whilst dilution effects contributed to the decreased levels of PAHs in the ambient 30 min samples. The significant presence of the heavier PAHs in the particulate phase from the LHD samples were expected to correlate to the heavier PAHs in the ambient samples, as these vehicles were operated in the area where the ambient samples were taken. However this was not the case, as the PAH profiles for the particulate samples were very different for the two types of samples. Heavier PAHs seen in the LHD particulate phase samples were not detected in the 30 minute ambient samples. This could have been due to the fact that the sampled LHD was not in the same working condition as the other LHDs in operation in that area and therefore had different emissions. Alternatively, the heavier PAHs from the exhaust may have been associated with heavier particles which settled rapidly and were therefore not present in the ambient atmosphere.

The comparison of the ambient 10 minute and 30 minute samples (Fig. 4-38 and 4-39) showed very similar PAH emission profiles, as expected, as they were taken in the same environment.

The workshop samples showed higher PAH peak areas than the ambient 10 minute samples for both gas and particulate phases (Fig. 4-40 and 4-41). The emission profiles showed similar patterns which link the types of environments of each sample type regarding emissions from various types of diesel vehicles. The workshop filter sample (specifically that of Plat mine C) showed the presence of heavier PAHs that were not found in the ambient samples but were found to exist in the exhaust samples, which indicated that the workshop was polluted with diesel exhaust fumes (LHD fumes) at the time of sampling.

Fig. 4-43 revealed that the workshop filter samples showed the presence of PAHs that were not detected at the non-diesel shafts which implied that the presence of these PAHs was due to the presence of diesel engines. The workshop primary trap samples (Fig. 4-42) showed higher peak areas of the 2 ringed PAHs than in the non-diesel shaft's samples, except for the high amount of naphthalene that was detected at Plat mine B. The number of detected PAHs was the lowest in the samples from the shafts where diesel vehicles were not used.

#### 4.8 Other source indicators

There were many classes of molecular markers that could be used as tracers for the particulate matter emitted by sources such as n-alkanes, polycyclic aromatic hydrocarbons (PAHs), oxidized PAHs as well as more polar compounds such as cholesterol or levoglucosan. Composition profiles of diesel and gasoline powered vehicles as sources have been widely studied and the markers that were included in this section have been selected after considering previous publications (Kotianová *et al.* 2008, Schnelle-Kreis *et al.* 2005).

Vehicle emissions are dominated by n-alkanes ( $C_{19}$  to  $C_{32}$ ) with a maximum at  $C_{20}$  for HDV (Pietrogrande *et al.* 2011). Alkanes with chain length  $>C_{26}$  mainly derive from vehicle emissions and heavier n-alkanes ( $>C_{27}$ ) are indicators of products of incomplete combustion, such as octacosane and heptacosane which were detected in the mine samples (Pietrogrande *et al.* 2011). All of the samples that were analysed showed higher alkanes with  $>C_{27}$  indicating vehicular emissions and incomplete combustion as sources of pollution.

Eicosane ( $C_{20}$ ) and nonadecane ( $C_{19}$ ) were found in all of the diesel samples from the primary traps which indicated vehicle emissions from heavy duty engines. Eicosane was also detected in all the diesel filter samples except the ambient sample from Plat mine A (10 minute) and Plat mine C (30 minute). Nonadecane was detected in all of the filter samples from the diesel shafts except for the workshop filter samples from Plat mine A and B. The Plat mine C workshop filter sample however contained both  $C_{19}$  and  $C_{20}$  compounds. The secondary traps revealed eicosane detection in all of the LHD samples. This indicates that heavy duty diesel vehicles were a main source in these samples.

There was no eicosane detected in the Plat mine A non-diesel primary trap sample and no nonadecane in the Plat mine B primary trap non-diesel sample. The filter non-diesel samples also revealed that there



was no eicosane or nonadecane detected which confirmed that diesel vehicular emissions were not a source of the particulate matter found in the non-diesel shafts.

Target PAHs (that were detected) could also be used as relevant anthropogenic source tracers as they are all constituents of emissions from combustion (of fuel, coal, gas and oil) and traffic. These PAHs include: the smaller, 4 ringed PAHs such as pyrene, fluoranthene, benz(a)anthracene and chrysene as well as the larger, 5-6 ringed PAHs which include the benzofluoranthenes, benzopyrenes, benzo(ghi)perylene and indeno(1,2,3-cd)pyrene (Ravindra *et al.* 2008a).

Cyclopenta(def)phenanthrenone, benzo(a)fluorene-11-one were amongst the very few oxygenated PAHs that were detected in the diesel filter samples. There was no detection of levoglucosan in any of the mine samples.

#### 4.9 Effectiveness of the denuder sampling device

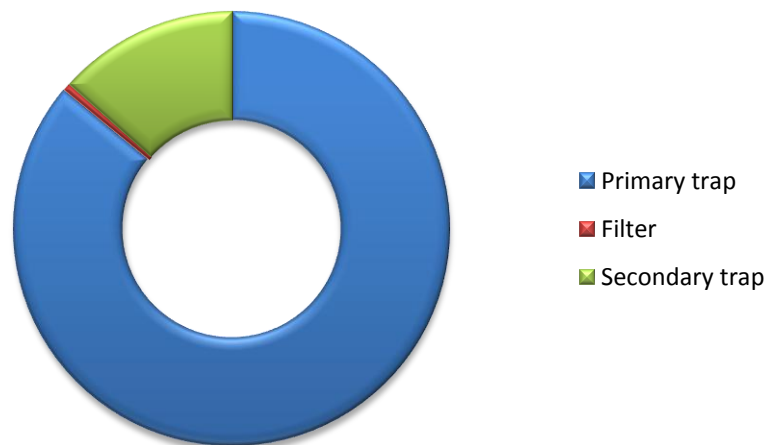


Figure 4-44 Total PAH peak area detected from each denuder component

Fig. 4-44 showed that the denuder as a sampling device functioned as theoretically expected. The primary trap was responsible for the majority of the PAH trapping, with the secondary trap only trapping a small amount of analytes that were not trapped by the primary trap. As previously discussed, this could be due to a change in analyte concentration during sampling (which was likely) or alternatively as a result of analytes that were blown off from the filter. Breakthrough was not likely when the sampling volumes did not exceed the breakthrough volume of 5 L of the most volatile PAH (naphthalene) as experimentally determined in another study (Forbes & Rohwer 2009). The filter trapped PAHs in the particulate phase which were typically PAHs that were heavier than pyrene.

Fig. 4-45 showed that all of the samples for which the sampling period was 10 minutes had the highest amounts of PAHs detected from the primary trap, which was expected based on denuder theory. For the 30 min Plat mine B sample, the secondary trap accounted for more PAHs than the primary trap, as here the breakthrough volume of the more volatile species was exceeded and analyte concentration variations may also have contributed to this effect.

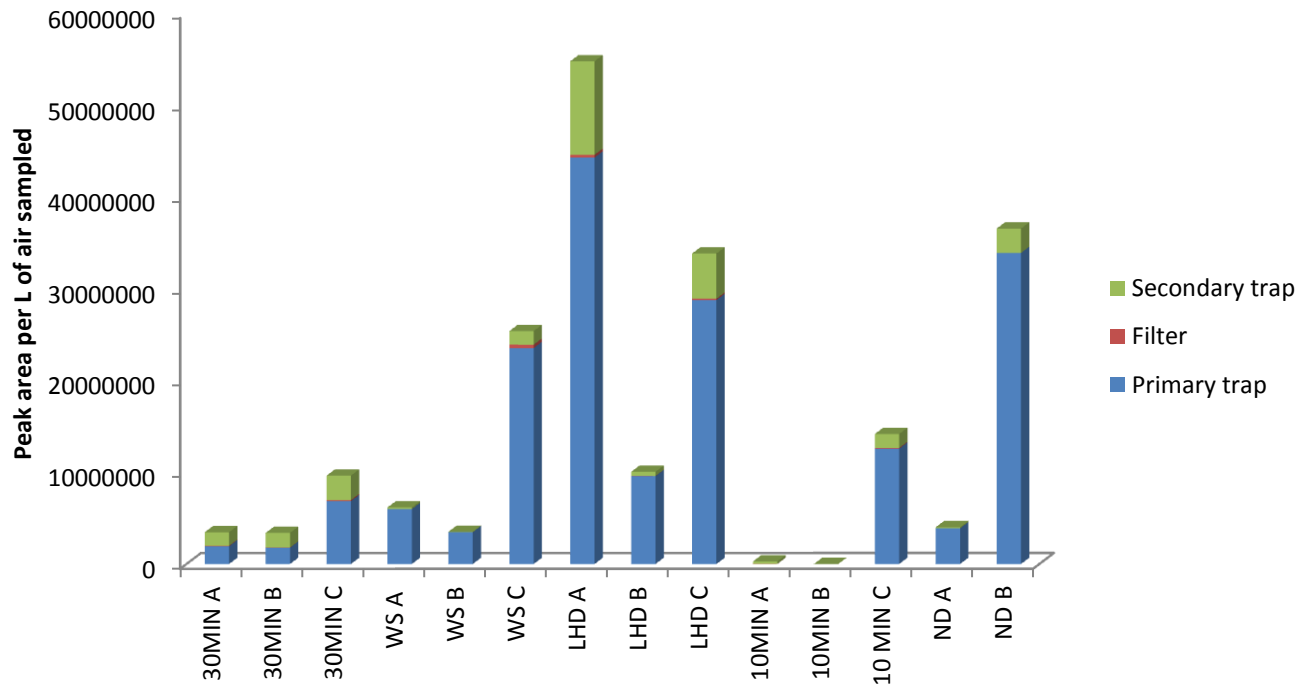


Figure 4-45 PAH peak areas for different sample types from the different sampling media

#### 4.10 Effect of ambient temperature and humidity

Humidity was a factor that may have affected both the trap samples as well as the filter samples. Moisture can deactivate any active sites on the surfaces of the silica of the filter and PDMS of the trap (especially the primary trap), which may result in analytes passing through the primary trap and getting trapped on the secondary trap. Figures 4-46 & 4-47 show the ambient temperature readings at different sampling sites with the corresponding PAH peak areas in gas and particulate phase.

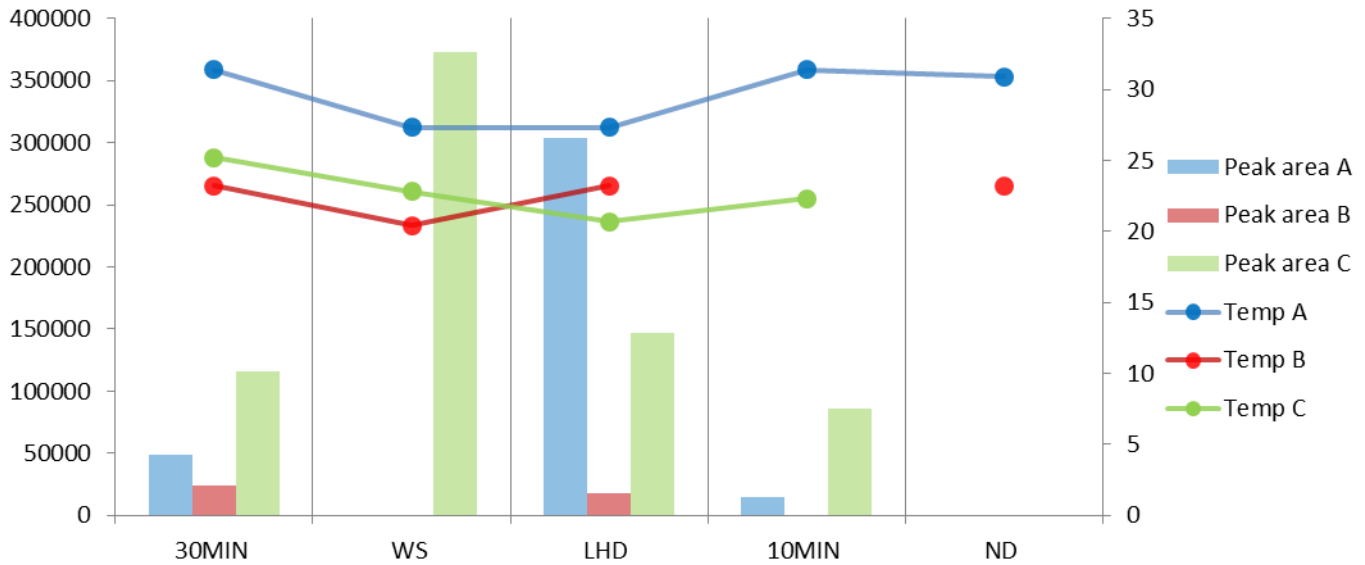


Figure 4-46 Total particulate phase PAH peak areas per litre of air sampled with corresponding ambient temperature readings at each sampling site (filter samples)

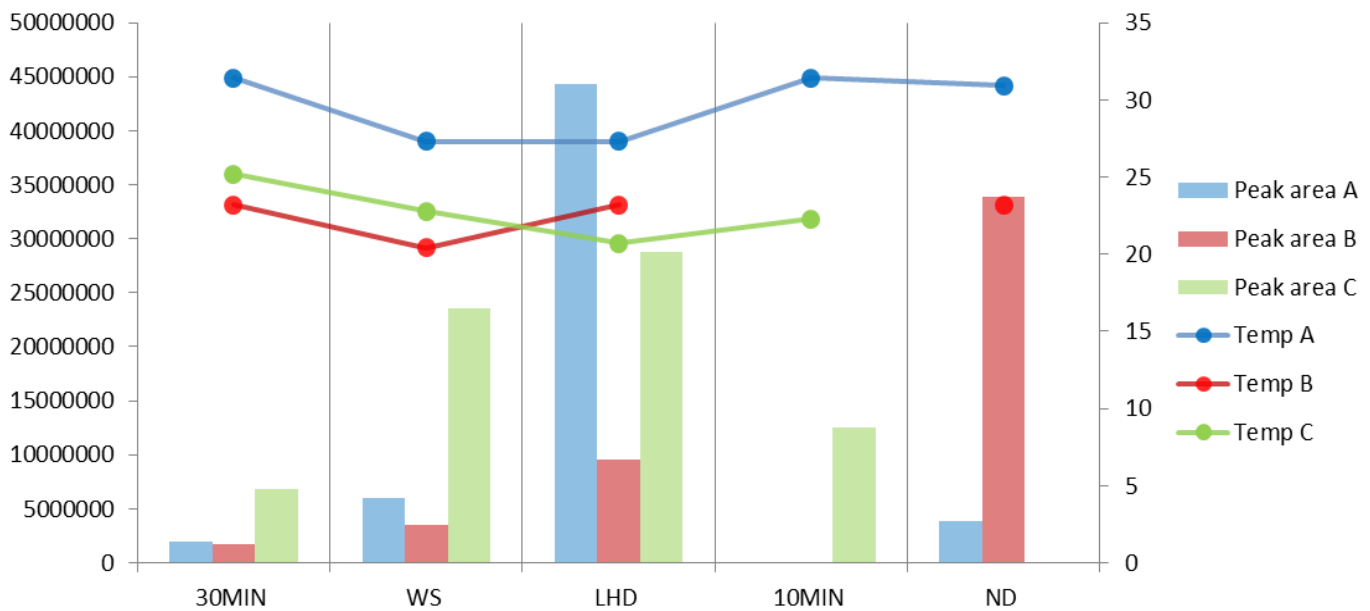


Figure 4-47 Total gas phase PAH peak areas per litre of air sampled with corresponding ambient temperature readings at each sampling site (primary trap samples)

Overall the ambient temperature underground was high (refer to Fig. 4-46 and 4-47) as it is a confined environment, with no natural air flow, where the vehicles generate heat when operated and the fact that the temperature increases as you move towards the core of the earth. Plat mine A had the highest ambient temperatures at every sampling site but this did not result in the highest gas phase PAH peak areas for every sample type. It can therefore be said that although the higher ambient temperatures result in the favourable partitioning of PAHs into the gas phase it has no influence on the amount of gas phase PAHs, which is ultimately determined by the number, type and operating condition of the sources.

#### 4.11 Quantification

This study was undertaken to provide qualitative SVOC (primarily PAHs) chemical profiles for the mines concerned. Later, quantification was performed and the following results were found.

Table 4-4 PAHs ( $\mu\text{g}\cdot\text{m}^{-3}$ ) detected in the primary trap samples

PAH	30MIN A	30MIN B	30MIN C	WS A	WS B	WS C	LHD A	LHD B	LHD C	10MIN C	ND A	ND B
NAP	0.15	0.87	2.13	2.04	0.48	4.53	8.73	1.69	6.72	4.00	1.26	17.88
NAP 2M	0.75	0.01	0.41	0.29	1.57	6.04	7.06	3.63	5.95	0.20	1.05	-
NAP 1M	0.43	-	0.06	1.32	0.99	4.51	4.10	2.06	1.56	2.26	0.41	0.02
ACY	0.13	0.02	1.02	0.22	0.07	1.39	-	0.34	4.36	0.92	0.09	0.03
ACE	-	-	-	-	-	-	-	-	-	-	0.03	-
FLU	0.28	0.07	1.09	0.32	0.13	2.83	6.55	0.31	2.40	1.28	0.11	0.02
PHE	0.21	0.07	0.62	0.26	0.15	1.10	4.53	0.29	2.61	0.49	0.16	0.03
ANT	-	-	-	-	-	-	-	-	-	-	-	-
FLA	0.03	0.01	0.07	0.09	-	0.21	3.86	0.06	0.57	0.09	0.09	0.02
PYR	0.05	0.02	0.13	0.11	0.09	0.25	4.67	0.08	0.63	0.13	0.10	0.02
BaA+CHY	-	-	-	-	-	-	0.18	-	0.13	-	-	-
BbF	-	-	-	-	-	-	-	-	-	-	-	-
BkF	-	-	-	-	-	-	0.12	-	-	-	-	-
BjF	-	-	-	-	-	-	-	-	-	-	-	-
BaP	-	-	-	-	-	-	0.14	-	-	-	-	-
BeP	-	-	-	-	-	-	-	-	-	-	-	-
I123P	-	-	-	-	-	-	-	-	-	-	-	-
BghiP	-	-	-	-	-	-	-	-	-	-	-	-

The absolute peak areas that were obtained from analysis were used to calculate the concentrations by using linear regression equations. These concentrations were then compared to the LOD and LOQ values and were all found to be higher than the LOQ (refer to Section 3.6.6). The concentrations were then

corrected for the various sampling volumes and all of the results are tabulated as  $\mu\text{g.m}^{-3}$  (trap samples) or  $\text{ng.m}^{-3}$  (filter samples), as shown in Tables 4-4 to 4-6.

Table 4-4 showed that PAHs up to pyrene on the primary trap were quantified and the concentrations were higher than the LOD and LOQ values. Naphthalene showed the highest concentrations which confirmed what was found based on peak areas. PAHs from acenaphthylene to pyrene generally had concentrations less than  $1.00 \mu\text{g.m}^{-3}$  except for the LHD samples, where higher values were detected. The Plat mine B non-diesel sample showed the highest concentration of  $17.88 \mu\text{g.m}^{-3}$  for naphthalene.

The LHD samples generally showed the highest concentration for all PAHs. The Plat mine A LHD samples ranged from  $3.86\text{--}8.73 \mu\text{g.m}^{-3}$  for the lighter PAHs and  $0.12 \mu\text{g.m}^{-3}$  was the minimum concentration for the few heavier PAHs that were detected.

**Table 4-5 PAHs ( $\text{ng.m}^{-3}$ ) detected in the filter samples**

PAH	30MIN A	30MIN B	30MIN C	WS C	LHD A	LHD B	LHD C	10 MIN C
NAP	2.05	0.96	-	-	6.32	2.44	-	-
NAP 2M	2.24	1.30	-	-	5.88	-	-	-
NAP 1M	1.76	-	-	-	-	-	-	-
ACY	-	-	-	-	-	-	-	-
ACE	-	-	-	-	-	-	-	-
FLU	1.09	0.47	1.05	3.12	3.14	-	3.36	1.61
PHE	1.74	1.52	6.62	9.70	3.17	0.82	5.96	3.92
ANT	-	-	-	-	-	-	-	-
FLA	4.88	3.23	13.74	39.35	3.40	0.52	15.23	42.88
PYR	17.41	6.59	58.56	109.60	11.90	3.63	39.29	-
BaA+CHY	2.26	0.05	3.50	15.64	30.94	0.75	0.17	6.80
BbF	-	-	-	-	-	-	-	-
BkF	-	-	-	16.73	55.29	-	-	-
BjF	-	-	-	-	-	-	-	-
BaP	2.07	-	-	33.66	128.46	-	-	-
BeP	-	-	-	-	-	-	-	-
I123P	-	-	-	7.51	245.94	-	-	-
BghiP	-	-	-	106.98	260.59	-	-	-

Table 4-5 revealed that the concentration of analytes that were found on the filter samples were orders of magnitude smaller than the concentrations found on the trap samples. The filter samples had analyte concentrations in the  $\text{ng.m}^{-3}$  range. This confirmed the importance of sampling both gas and particle phases when determining human exposure levels to PAHs.

Fluorene and phenanthrene were found to range from 0.47-9.70 ng.m<sup>-3</sup> whereas fluoranthene and pyrene were found to have higher concentrations of 0.52-109.60 ng.m<sup>-3</sup>. These four PAHs were commonly seen in the filter samples with pyrene having highest concentrations in most samples. The Plat mine C workshop sample showed the highest concentration for pyrene of 109.60 ng.m<sup>-3</sup>. Relatively high concentrations were also seen for the heavier PAHs in this workshop sample which resembled the LHD sample. As previously mentioned, this could be due to a high number of diesel vehicles being present in the workshop whilst sampling.

The highest concentrations that were found were in fact for the heavier PAHs: benzo(a)pyrene, indeno(1,2,3-cd)perylene and benzo(ghi)perylene in the Plat mine A LHD filter sample. This sample also contained the largest range of PAHs with a concentration range of 3.14-260.59 ng.m<sup>-3</sup>. In contrast, the Plat mine B LHD filter sample showed very few PAHs at low concentrations with a maximum of 3.63 ng.m<sup>-3</sup> for pyrene.

**Table 4-6 PAHs (µg.m<sup>-3</sup>) detected in the secondary trap samples**

	30MIN A	30MIN B	30MIN C	WS A	WS B	WS C	LHD A	LHD B	LHD C	10MIN A	10MIN C	ND A	ND B
NAP	0.49	0.43	1.14	0.08	0.02	0.60	4.91	0.18	2.44	0.12	0.62	0.06	1.30
NAP 2M	0.34	0.45	0.41	0.06	0.05	0.28	0.41	0.11	-	0.07	0.16	0.05	0.17
NAP 1M	0.21	0.33	-	0.08	0.07	-	0.24	-	0.26	0.08	0.11	0.07	0.04
ACY	0.02	0.01	0.03	-	-	0.06	0.05	0.02	0.05	0.04	0.07	0.04	0.02
ACE	-	-	-	-	-	-	-	-	-	-	-	-	-
FLU	0.02	0.01	0.02	-	-	0.05	0.05	0.03	0.05	0.06	0.04	-	0.02
PHE	0.04	0.02	0.04	0.10	-	0.09	0.10	0.05	0.11	0.10	0.07	-	0.03
ANT	-	-	-	-	-	-	-	-	-	-	-	-	-
FLA	0.03	0.01	0.03	-	-	0.10	0.09	0.04	0.08	-	0.06	-	-
PYR	0.04	0.02	0.06	-	-	0.11	0.13	0.04	0.09	0.09	0.08	-	0.02

Table 4-6 showed concentrations with lower values than what was detected on the primary traps. Naphthalene shows the highest concentrations for most samples with a maximum value of 4.91 µg.m<sup>-3</sup> in the Plat mine A LHD sample. The concentration of every other analyte is less than 1 µg.m<sup>-3</sup> and only the lighter PAHs (up to pyrene) were detected. Overall the concentrations found on the secondary trap were much lower than the concentrations found on the primary trap.

The concentrations that were found in this study show benzo(a)pyrene had a maximum concentration of  $0.26 \mu\text{g.m}^{-3}$  from the LHD sample from Plat mine A. According to existing limits (refer to Table 1-4 in Chapter 1) the concentrations in Tables 4-4 to 4-6 were less than the limits of the regulated anthracene, chrysene and benzo(a)pyrene, which had limits ranging from  $0.1\text{-}0.2 \text{ mg.m}^{-3}$ .

The PAH profiles in this study and the partitioning between the gas and particulate PAHs compared well with what was found in other ambient and tunnel studies i.e. PAHs up to PYR were found in gas phase samples and filter samples showed PAHs heavier than, and including PYR (Refer to Table 2-1 in Chapter 2). The mine filter samples revealed similar PAH profiling patterns and concentrations to that of the filter samples reported in the literature, that were taken in different urban and tunnel environments. PYR had relatively high concentrations ranging from  $3.63\text{-}109.6 \text{ ng.m}^{-3}$  in mine samples reported here, compared to  $0.38\text{-}173 \text{ ng.m}^{-3}$  in urban and tunnel environments, reported in the literature. The Plat Mine A LHD and Plat Mine C WS samples also revealed relatively high concentrations of the heavier PAHs namely: BaP, I123P and BghiP that ranged from  $7.51\text{-}260.59 \text{ ng m}^{-3}$  which was less than, but comparable, to the range of  $31.25\text{-}494.52 \text{ ng.m}^{-3}$  that was recorded in Dehli, India which has a heavy traffic density (Sharma *et al.* 2008).

The gas phase PAHs were in the range of  $\mu\text{g.m}^{-3}$  in the mine samples, which was an order of magnitude greater than the  $\text{ng.m}^{-3}$  range of the urban and tunnel environments as mentioned before in the literature. NAP ranged from  $0.15\text{-}8.73 \mu\text{g.m}^{-3}$  in the mine samples with the LHD samples possessing the highest concentrations whereas the maximum NAP concentration of  $0.5 \mu\text{g.m}^{-3}$  was reported in the Gothenburg tunnel in Sweden. Although the concentrations of gas phase PAHs in underground mine environments are significantly higher than urban and tunnel environments, the PAH profiles are very similar.

## 4.12 Scanning electron microscopy

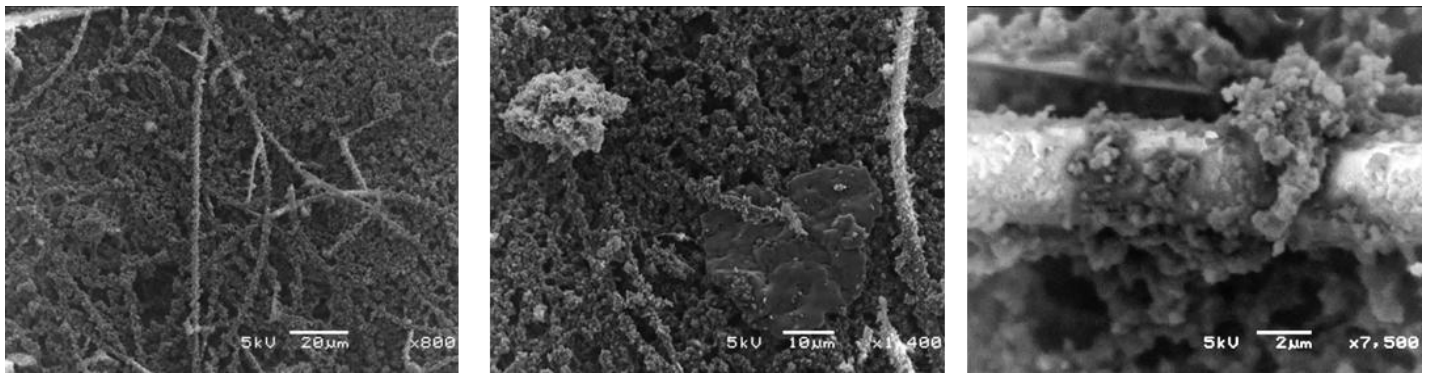


Figure 4-48 Plat mine A filter sample from a LHD operator at 800, 1400 & 7500 magnifications.

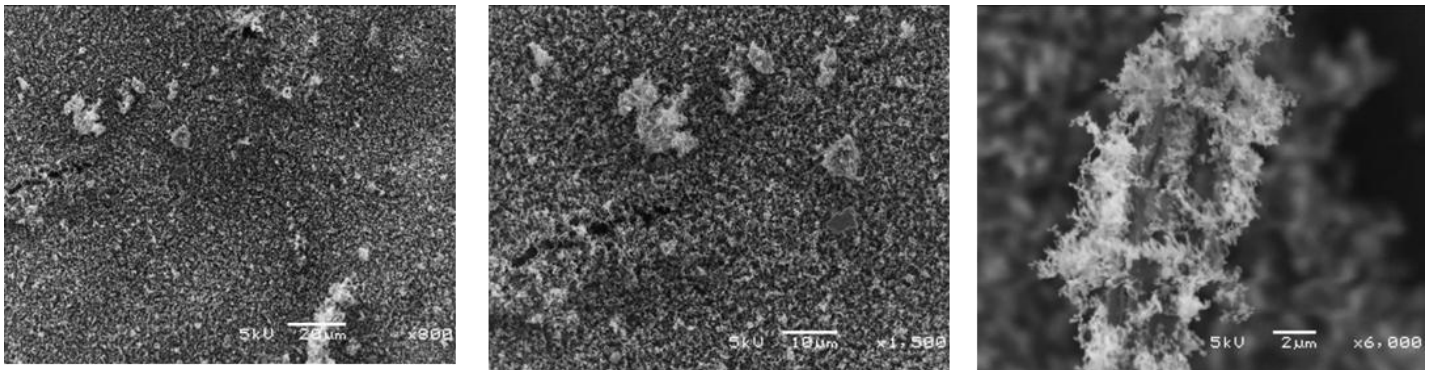


Figure 4-49 Plat mine B filter sample from a LHD operator at 800, 1500 & 6000 magnifications.

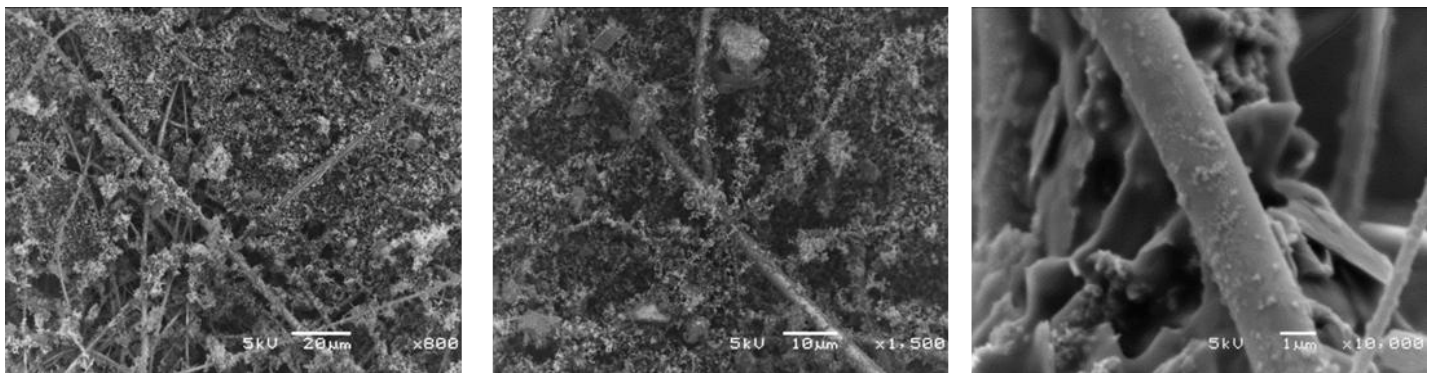


Figure 4-50 Plat mine C filter sample from a LHD operator at 800, 1500 & 10 000 magnifications.



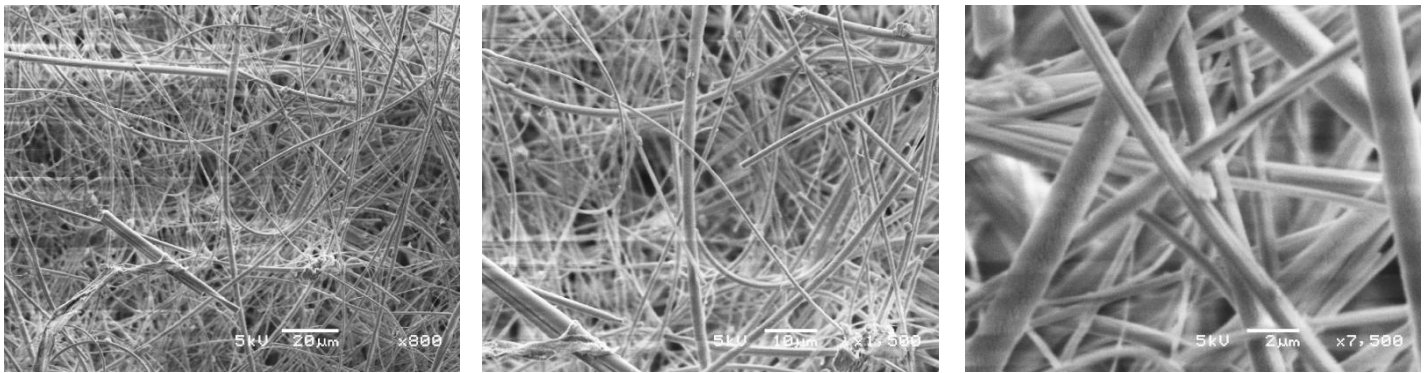


Figure 4-51 102(Plat mine C) filter sample from a winch operator at 800, 1500 & 7500 magnifications.

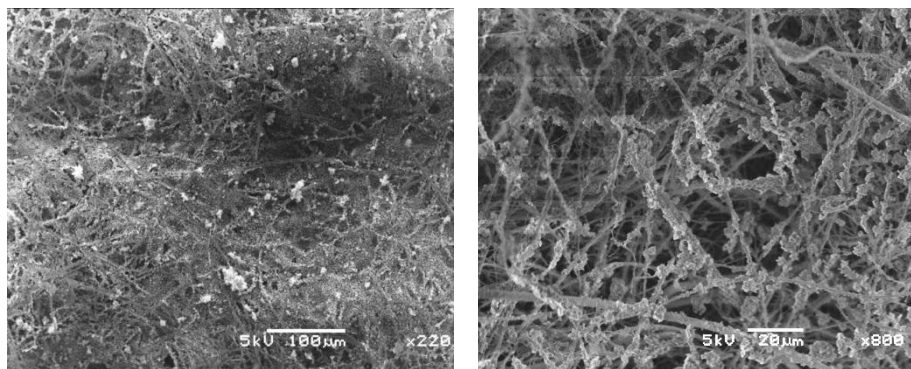


Figure 4-52 105 (Plat mine B) filter sample from a winch operator at 220 & 800 magnifications.

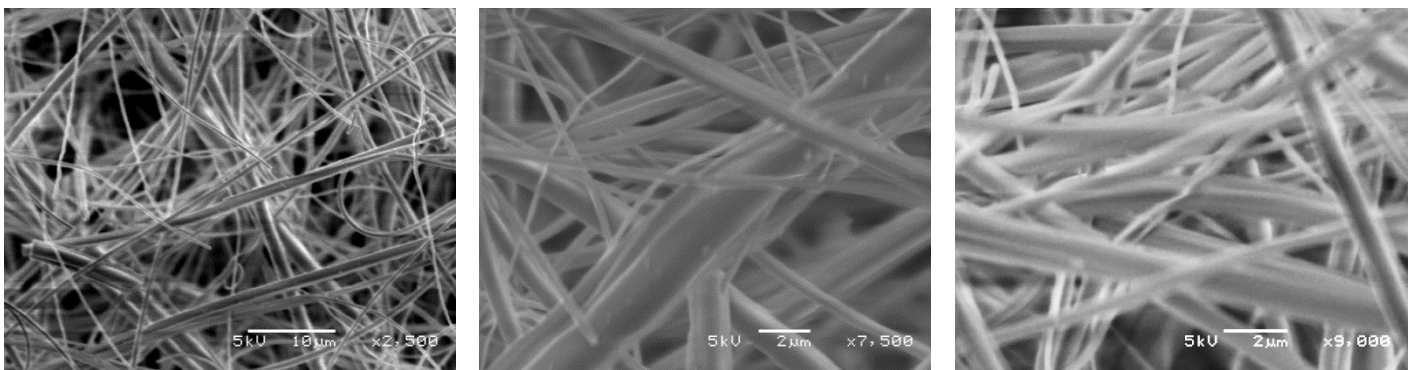


Figure 4-53 Blank filter samples at 2500, 7500 & 9000 magnifications.

The images from the LHD operator's personal filters (Fig. 4-48 to 4-50) were clearly more heavily loaded than the winch operator's personal filters (Fig. 4-51 to 4-52). The LHDs use diesel engines whereas the winches are electrical (non-diesel) so the images gave a comparison between diesel versus non-diesel environments underground. The different magnifications show a range of particulate matter (PM) from  $\text{PM}_{10}$  to  $\text{PM}_{2.5}$ . There was also evidence of ultrafine PM from the LHD images which could be seen on the individual filter fibres with a light, fluffy appearance which are typical for DPM (Ancelet *et al.* 2011).

The smaller DPM is easier to inhale and it can penetrate the deepest part of the lung, where oxygen enters the blood stream, thus having adverse health implications (DEEP 2001).

The DPM could be identified and was consistent with literature findings (Ancelet *et al.* 2011). It was also confirmed to be DPM by performing spot energy dispersive spectrometry (EDS) analyses on the particles with the results showing that the highest mass % of the particle consisted of carbon as expected.

There were also particles found on the filters that contained metals and were more mineral than carbonaceous in nature. These mineral particles are expected to be denser than the DPM and therefore gravitationally settle to the ground more rapidly than the DPM which may remain airborne. This may be of concern in a confined environment, such as a mine, as DPM will consequently be present in ambient air and will only be removed by the ventilation.

When comparing the LHD filters from the three different mines, it appeared that Plat mine B (Fig. 4-49) had the most loaded filter where the filter fibres were not even visible in the images at 800 x magnification. The other two mines clearly showed visible filter fibres at the same magnification indicating that they were not as heavily loaded. Plat mine B and C showed particles with similar fluffy appearances at a high magnification whereas Plat mine A showed slightly different particles with a more dense appearance. As mentioned previously, the operating patterns can influence the type and amount of emissions so it was expected that the mines differ with respect to the amount of DPM on the filters, which provided mere snapshots of exposure in an individual area over a particular time period. Comparisons between mines should be made with great caution, as the filters that were analysed were chosen randomly from a sample set.

The winch operator samples showed that there were particles on the filter fibres; but they had a very different morphology to those collected for the LHD operators. The images revealed that the 105 winch sample was much more loaded than the 102 winch sample. This could be due to the working conditions during the sampling period or the nature of the operations in close proximity to the sampling area where the particular winch was being operated.

From the SEM images it could be concluded that diesel versus non-diesel samples appeared to show very different filter loadings with respect to the amount and nature of particles found on the filters.

### 4.13 Principal component analysis

Principal component analysis (PCA) is a mathematical method that converts potentially correlated variables of a large data set into a set of values of linearly uncorrelated variables (called principal components (PCs)) using orthogonal transformation (Wold *et al.* 1987). PCs allow for multivariate data to be simplified in such a way that it can be interpreted graphically. The first PC is the linear combination of the standardised original variables that account for the maximum variability in a data set with each succeeding PC having the highest variance possible under the restriction that it be orthogonal to the former PC (Wold *et al.* 1987).

For this study the PCA was based on covariance which gave the variance and covariance of the variables (relative % peak areas were used for analysis). Score plots were generated which involved the projection of the data onto the PCs in two dimensions and it was used to interpret relationships between observations. Loading plots revealed the relationships between variables in the space of the first two components. The PCA results also gave the eigenvalues and a bar chart that represents the % of variation accounted for by each PC. A scree plot was also a useful visual aid for determining the appropriate number of principal components needed.

Even though PCA reduces the dimensionality of multivariate data, it did have limitations with respect to the data that was presented in this study. For instance, the samples were taken with denuder sampling devices which introduced a great amount of variance with respect to the different sample medium (primary trap, filter or secondary trap). The differences introduced from the sample medium were in addition to the differences that were introduced as a result of sampling at different mines, on different days for different durations and at different sampling sites. The number of variables that came into play was already enormous and it must also be noted that the samples were analysed on different days which may also introduce instrumental variation.

PCA was thus performed on 10 minute ambient versus 30 minute ambient samples (sampling site in common) as well as 10 minute ambient versus LHD samples (sampling time in common).

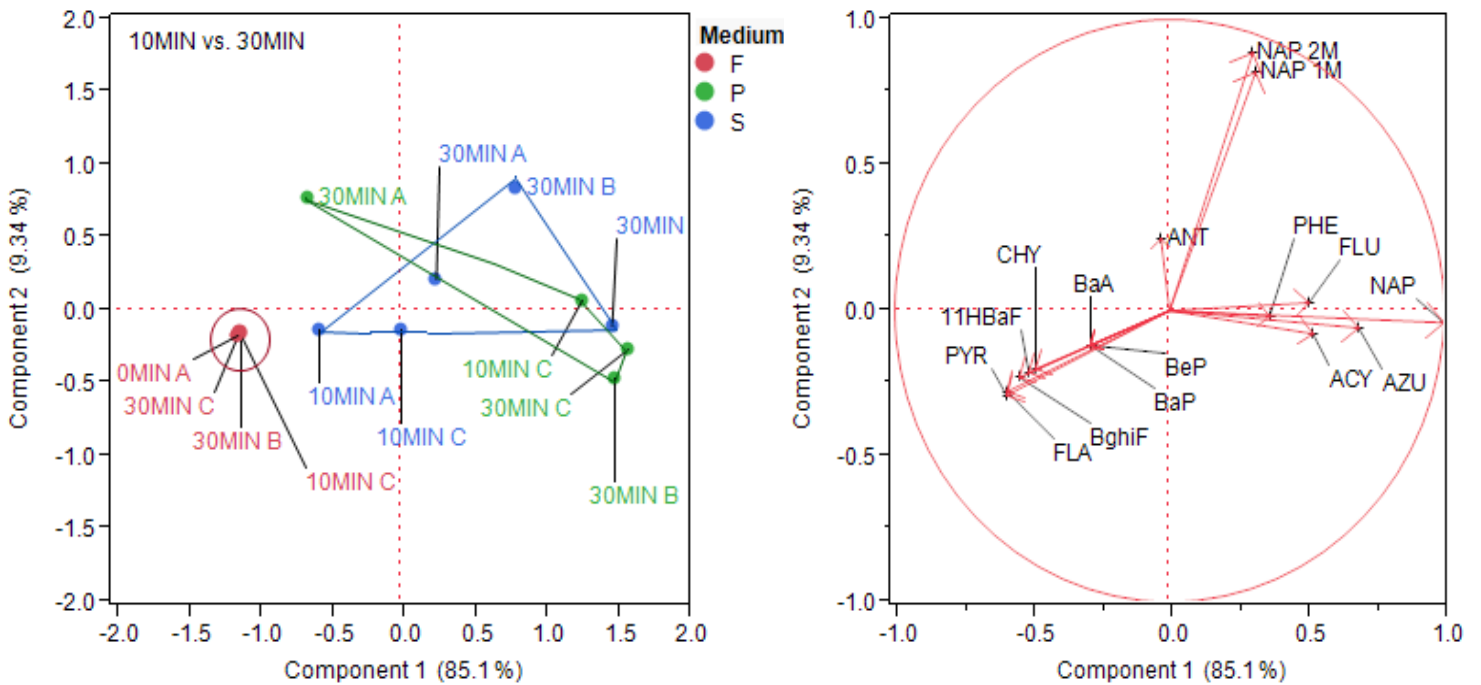


Figure 4-54 Score plot (left) and loading plot (right) resulting from PCA on samples with different sampling times: 10 minute and 30 minute ambient samples (with F; P; S denoting filter, primary trap and secondary trap respectively)

Fig. 4-54 showed that the first principal component accounted for 85.1 % of the explained variance and the principal components were illustrated according to covariance. The relative % peak areas of PAHs (relative to the total peak area of sample) were used to generate these plots. The eigenvalues indicated that at least 4 PCs were needed to account for at least 80 % of the variance if principal components were based on correlation. The scores plot showed that all the filter samples were grouped together and were separated from the trap samples in the first principal component. The primary and secondary traps were distinguishable from the filters but were not as clearly distinguishable from each other as there was overlap of the groups. This was expected as they were both gas phase samples and the 30 minute samples would include breakthrough from the primary trap, causing the primary and secondary trap results to be similar. The samples could therefore be grouped according to the sample medium (trap or filter represented by colours), however they could not be effectively grouped according to the sample type (10 min or 30 min labelled for each marker).

Fluoranthene, naphthalene, 2-methyl naphthalene, 1-methyl naphthalene and pyrene showed similar heavy loading in either PC1 or PC2.

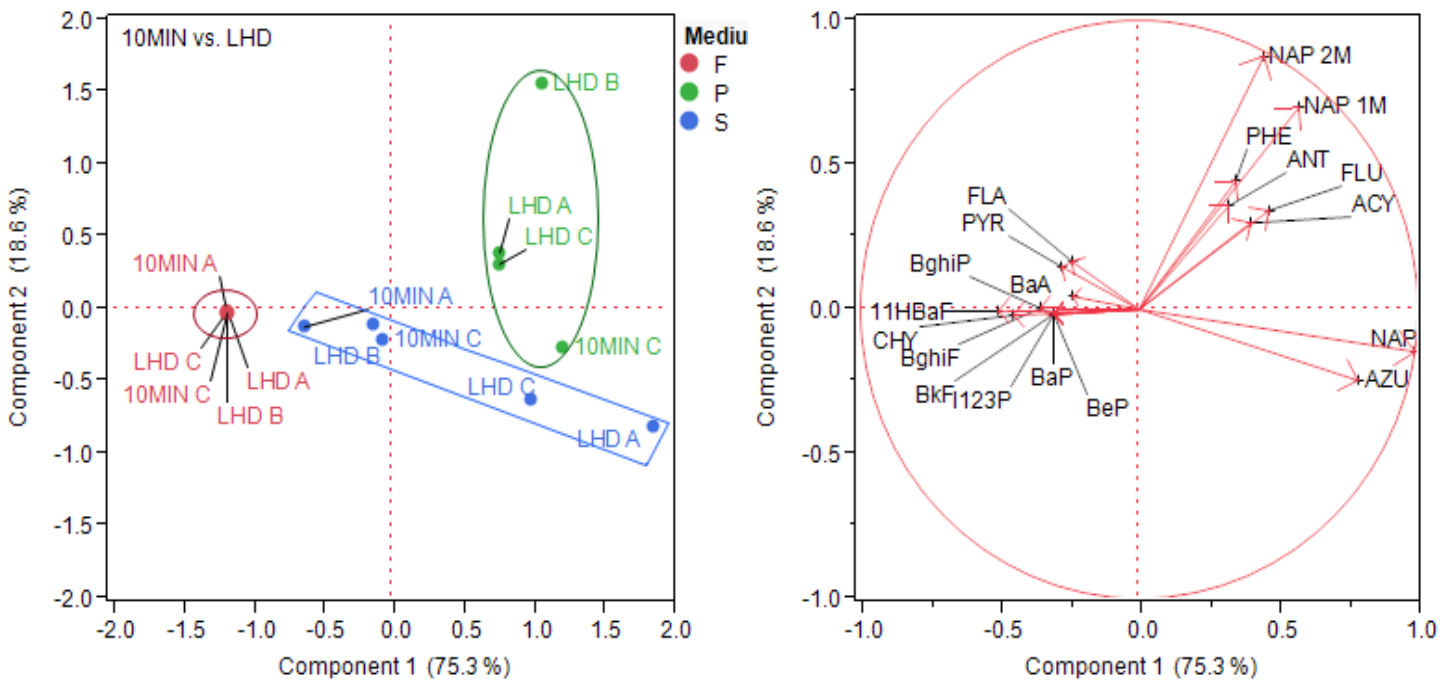


Figure 4-55 Score plot (left) and loading plot (right) resulting from PCA on samples with different sampling sites: 10 minute ambient and LHD samples (with F; P; S denoting filter, primary trap and secondary trap respectively)

Fig. 4-55 showed that the first principal component accounted for 75.3 % of the explained variance between ambient and LHD samples. The eigenvalues indicated that at least 2 PCs were needed to account for at least 80 % of the variance. The scores plot showed that there was very good grouping of samples with respect to the different sample medium (primary trap, filter and secondary trap represented by the colours). The sample type did not show grouping patterns as they were sporadically distributed within the groups of the different colours. Therefore it can be concluded that samples could be grouped according to the sample medium (primary trap, secondary trap or filter represented by colours) however they could not be grouped effectively according to the sample type (10 min ambient or LHD labelled for each marker).

The loading plot showed that primary traps' variance was largely due to the methylated naphthalenes as naphthalene was the main contributor to variance in the secondary traps. It should also be noted that inter-mine results were inconclusive, in that the plots were random with no apparent grouping patterns.

#### 4.14 Diagnostic ratios

Diagnostic ratios were employed in this section in order to identify different emission sources of PAHs in underground platinum mine environments. Source identification was improved by using more than one ratio and all the ratios were calculated for total PAHs (primary trap samples+filter samples+secondary trap samples) which accounted for the gas and particulate phases.

Table 4-7 Diagnostic ratios of PAHs in the different sample types of the mine samples.

	FL/(FL+PYR) <sup>1</sup>	FLA/(FLA+PYR) <sup>2</sup>	ANT/(ANT+PHE) <sup>3</sup>	ΣLMW/ΣHMW <sup>4</sup>	FLA/PYR <sup>5</sup>
30MIN A	>0.5	<0.4	>0.1	>1	0.3
30MIN B	<0.5	<0.4	~0.1	>1	0.5
30MIN C	>0.5	<0.4	~0.1	>1	0.3
WS A	>0.5	<0.4	>0.1	>>1	0.5
WS B	>0.5	<0.4	>0.1	>>1	0.0
WS C	<0.5	<0.4	~0.1	>1	0.4
LHD A	>0.5	<0.4	>0.1	>1	0.7
LHD B	>0.5	<0.4	~0.1	>1	0.4
LHD C	>0.5	<0.4	>0.1	>1	0.5
10MIN C	>0.5	>0.5	<0.1	>1	6.8
ND A	>0.5	~0.5	<0.1	>>1	0.8
ND B	>0.5	>0.5	<0.1	>>1	1.0
Sources	Diesel emissions (>0.5) Petrol emissions (<0.5)	Fossil fuel combustion (0.4-0.5) Coal and wood combustion (>0.5) Petrogenic (<0.4)	Pyrogenic (>0.1) Petrogenic (<0.1)	Petrogenic (>1) Pyrogenic (<1)	Vehicles (~0.6)

ANT -anthracene

FLA -fluoranthene

FL -fluorene

PHE -phenanthrene

PYR -pyrene

ΣLMW -sum of the low molecular weight PAHs (2-3 rings)

ΣHMW -sum of the higher molecular weight PAHs (4-5 rings)

<sup>1</sup> Ravindra *et al.* 2008b

<sup>2</sup> De La Torre-Roche *et al.* 2009

<sup>3</sup> Pies *et al.* 2008

<sup>4</sup> Zhang *et al.* 2008

<sup>5</sup> Ravindra *et al.* 2008a

The diagnostic ratio of FL/(FL+PYR) confirmed the presence of diesel emissions in all sampling locations except for the Plat mine C workshop and 30 minute ambient Plat mine B samples where ratios were more representative of petrol emissions (Ravindra *et al.* 2008a). The FLA/PYR ratio of approximately 0.6 confirmed vehicular emissions as a source and when used in conjunction with the FL/(FL+PYR) ratio gave confidence to conclude that diesel vehicular emissions were a dominant source of PAH emissions underground. The ANT/(ANT+PHE) ratio, however indicated pyrogenic sources for all of the samples, except for the Plat mine C 10 minute ambient and non-diesel samples, which indicated petrogenic sources. The FLA/(FLA+PYR) ratios showed petrogenic sources for all of the samples, except for the 10 minute Plat mine C sample and the non-diesel samples, which indicated the presence of coal and wood

combustion sources. The FLA/PYR ratio for the Plat mine C 10 minute sample was significantly different when compared to other diesel shaft samples, possibly due to high humidity of 81 % for this sample (refer to Table 4.3).

As previously mentioned, the diagnostic ratios should be used with caution as the difference in physiochemical properties such as volatility, solubility and reactivity of each PAH may introduce a bias. This can be minimized by using ratios of PAHs with similar properties and using more than one ratio to draw conclusions (Ravindra *et al.* 2008a, 2008b).

## 4.15 Conclusion

PAHs coexist in vapour and particle phase, each of which has different human health impacts in terms of the fate of the PAHs in the human body. It was for this reason that it was vital to sample the PAHs in both phases which was made possible by the denuder sampling devices. The denuders were easily prepared in the laboratory, with little cost, and were convenient to use and transport as they are small, lightweight and mobile. The PDMS multi-channel traps act as a non-polar solvent for the SVOCs (including PAHs) therefore sample recovery is higher due to absorption taking place rather than adsorption. The effective trapping of the PAHs in both vapour and particulate phases was made evident in this study and the results were consistent with denuder theory.

From the relative % peak area analysis of the diesel and non-diesel shaft samples, it was clearly seen that the PAHs and PAH derivatives were predominantly found in the gas phase. Overall the relative % peak areas were lower for PAHs and PAH derivatives in the filter samples as compared to the primary trap samples, which indicated higher gas phase loading. This implied that sampling of only particulate PAHs in this environment would lead to an underestimation of potential human health effects due to exposure. No PAHs or PAH derivatives were detected in the non-diesel filter samples, but PAHs were detected in the gas phase. The source of these PAHs should be determined in a future study.

From the radar graphs it was generally concluded that the hydrocarbons were always detected and possessed high peak areas in comparison to the other SVOC compound classes. Pentatriacontane ( $C_{35}H_{72}$ ), eicosane ( $C_{20}H_{42}$ ) and octasane ( $C_{28}H_{58}$ ) were some of the longer chain unsaturated hydrocarbons that were detected. The radar plots of SVOC peak areas revealed that the Plat mine A LHD exhaust contained a larger proportion of gas phase SVOCs, whilst the Plat mine C sample contained primarily particle phase SVOCs, which can be explained by the higher ambient temperature at the Plat mine A sample site. This was relevant in terms of potential human health effects, as the fate of the two phases in the human respiratory system would be different.

The high amount of hydrocarbons in the diesel emission profiles illustrated by the radar plots indicated that combustion was incomplete, suggesting that the diesel engines were not operating optimally. This in turn affected all other emissions including PAH emissions. Underground mines are a confined environment thus it was assumed that diesel emissions were the primary source of PAHs but it was not the sole source (as evident from the presence of smaller PAHs in the non-diesel trap samples). Source apportionment methods currently have many limitations and were derived for ambient environments,



therefore more research should be done for underground environments which are unique and will present new limitations. Suggested future research in this regard as proposed by Galarneau *et al.* includes: firstly, the creation of an emission factor database that accounts for a variety of sources so as to evaluate the individuality of relative PAH species emissions among various sources, and secondly, the determination of reactivities of measured PAHs under realistic conditions (Galarneau *et al.* 2008).

The relative % peak area PAH graphs showed that the primary trap consisted mainly of lighter PAHs with naphthalene and its derivatives having the highest relative % peak areas and other PAHs up to pyrene were all detected with significant relative % peak areas. The filter samples contained heavier PAHs that are commonly found in the particulate phase. The secondary traps showed lower concentrations of only lower volatility PAHs that could be due to blow off of these abundant PAHs that were adsorbed to particles on the filter or possibly due to the change of the analyte concentration whilst sampling, due to the dynamic nature of the mining activities. Breakthrough would have occurred for sampling volumes > 5 L. These results were consistent with the theory of the denuder. All the PAHs that were detected were consistent with previous findings in the literature regarding diesel emissions.

All three mines showed similarity when comparing the overall PAH profiles on the primary trap, secondary trap and filter sample in that they revealed similar clustering of certain PAHs. The profiles were dissimilar in that the amounts and ratios of PAHs were all very different.

The dissimilarity was clearly seen when the individual sample type PAH profiles were considered. The LHD samples showed the highest PAH peak areas for the primary trap (excluding the Plat mine B non-diesel sample), secondary trap and filter at the diesel shafts which was expected as the LHD sample was taken from the exhaust where the concentration of pollutants was the highest.

The Plat mine C samples showed very high PAHs in the workshop compared to the other two mines which can be due to numerous reasons regarding the sampling or the workshop environment. The LHD Plat mine A filter sample showed heavy PAHs which were not present in the other mines samples. It was mentioned that the driving patterns influenced the emissions and the Plat mine A LHD sample was taken when the vehicle was experiencing cold start and idling conditions, which are associated with heavy PAH emissions. The 10 minute ambient samples generally showed fewer PAHs and smaller peak areas than that of the 30 minute ambient samples for the filter and secondary trap samples, as expected. The non-diesel samples showed significantly fewer PAH compounds than that of the diesel samples, indicating that the primary source of PAHs was diesel emissions. The source of the high naphthalene levels in the

Plat mine B non-diesel sample requires further investigation. From the filter results it can be concluded that pyrene was found in the particulate phase in every type of filter sample therefore this compound may serve as a useful indicator of PAH exposure in mining environments.

All of the samples that were analysed showed higher alkanes with  $>C_{27}$  which indicated that vehicular emissions and incomplete combustion were sources of pollution. The  $C_{19}$  and  $C_{20}$  compounds were indicators of heavy duty diesel vehicles as sources. LHD samples showed the detection of both eicosane and nonadecane which confirmed that the alkane tracers reflected the diesel vehicle source. The  $C_{19}$  and  $C_{20}$  compounds were seen in all the diesel shaft samples, therefore diesel vehicles were the primary source of pollution in these shafts. The non-diesel filter samples revealed that there was no trace of eicosane or nonadecane which indicated that diesel vehicular emissions were not a source of the particulate matter found in the non-diesel shafts which was to be expected.

The PAHs that were detected were also used as relevant source tracers as they are constituents of traffic and combustion emissions (Ravindra *et al.* 2008a, 2008b). There was no trace of levoglucosan or any other polar compound markers in the samples. The source indicators are valuable tools to distinguish between the different sources of pollution but in order to get an understanding as to the relative contributions made by each source it is vital to perform full quantitation of all of the organic compounds in the samples.

From the SEM images it can be concluded that diesel samples (LHD) versus non-diesel samples (winch) showed very different filter loadings with respect to the amount and nature of particles found on filters.

PCA proved to be valuable. Even though the variables were kept at a minimum, there were no evident grouping patterns according to sample type but very good grouping according to sample medium. The PCA analysis was yet another confirmation of the denuder theory as the different sampling media were clearly grouped and separated in the scores plots.

For future research it is recommended that a larger sample set should be taken for a more accurate understanding and comparison as well as for statistical purposes. The consistency of the sampling should be improved in terms of the sampling times and volumes. The inconsistency in this case related to the problem that was encountered with the portable pumps that could not meet the low flow rate requirements due to the relatively high back pressures of the denuders. Pump technology has since improved and the encountered problem can easily be overcome. The thermal desorption method did have limitations and incomplete desorption of the heavier PAHs was a possibility so further optimization should be performed for future research.

## 4.16 References

- Ancelet, T., Davy, P.K., Trompetter, W.J., Markwitz, A. & Weatherburn, D.C. 2011, "Carbonaceous aerosols in an urban tunnel", *Atmospheric Environment*, vol. 45, no. 26, pp. 4463-4469.
- Borrás, E., Tortajada-Genaro, L.A., Vázquez, M. & Zielinska, B. 2009, "Polycyclic aromatic hydrocarbon exhaust emissions from different reformulated diesel fuels and engine operating conditions", *Atmospheric Environment*, vol. 43, no. 37, pp. 5944-5952.
- DEEP (Diesel emissions evaluation programme). 2001, "Sampling for diesel particulate matter in mines", *CANMET: Mining and Mineral Science Laboratories*, report (MMSL) 01-052.
- De La Torre-Roche, R.J., Lee, W. & Campos-Díaz, S.I. 2009, "Soil-borne polycyclic aromatic hydrocarbons in El Paso, Texas: Analysis of a potential problem in the United States/Mexico border region", *Journal of Hazardous Materials*, vol. 163, no. 2-3, pp. 946-958.
- Forbes, P.B.C. & Rohwer, E.R. 2009, "Investigations into a novel method for atmospheric polycyclic aromatic hydrocarbon monitoring", *Environmental Pollution*, vol. 157, no. 8-9, pp. 2529-2535.
- Forbes, P.B.C., Karg, E.W., Zimmermann, R. & Rohwer, E.R. 2012, "The use of multi-channel silicone rubber traps as denuders for polycyclic aromatic hydrocarbons", *Analytica Chimica Acta*, vol. 730, pp. 71-79.
- Galarneau, E. 2008, "Source specificity and atmospheric processing of airborne PAHs: Implications for source apportionment", *Atmospheric Environment*, vol. 42, no. 35, pp. 8139-8149.
- Kotianová, P., Puxbaum, H., Bauer, H., Caseiro, A., Marr, I.L. & Cík, G. 2008, "Temporal patterns of n-alkanes at traffic exposed and suburban sites in Vienna", *Atmospheric Environment*, vol. 42, no. 13, pp. 2993-3005.
- Ono-Ogasawara, M. & Smith, T.J. 2004, "Diesel exhaust particles in the work environment and their analysis", *Industrial Health*, vol. 42, no. 4, pp. 389-399.
- Orasche, J., Schnelle-Kreis, J., Abbaszade, G. & Zimmermann, R. 2011, "Technical Note: In-situ derivatization thermal desorption GC-TOFMS for direct analysis of particle-bound non-polar and polar organic species", *Atmospheric Chemistry and Physics*, vol. 11, no. 17, pp. 8977-8993.
- Pies, C., Hoffmann, B., Petrowsky, J., Yang, Y., Ternes, T.A. & Hofmann, T. 2008, "Characterization and source identification of polycyclic aromatic hydrocarbons (PAHs) in river bank soils", *Chemosphere*, vol. 72, no. 10, pp. 1594-1601.
- Pietrogrande, M.C., Abbaszade, G., Schnelle-Kreis, J., Bacco, D., Mercuriali, M. & Zimmermann, R. 2011, "Seasonal variation and source estimation of organic compounds in urban aerosol of Augsburg, Germany", *Environmental Pollution*, vol. 159, no. 7, pp. 1861-1868.

- Ravindra, K., Sokhi, R. & Van Grieken, R. 2008a, "Atmospheric polycyclic aromatic hydrocarbons: Source attribution, emission factors and regulation", *Atmospheric Environment*, vol. 42, no. 13, pp. 2895-2921.
- Ravindra, K., Wauters, E. & Van Grieken, R. 2008b, "Variation in particulate PAHs levels and their relation with the transboundary movement of the air masses", *Science of the Total Environment*, vol. 396, no. 2-3, pp. 100-110.
- Schnelle-Kreis, J., Sklorz, M., Peters, A., Cyrys, J. & Zimmermann, R. 2005, "Analysis of particle-associated semi-volatile aromatic and aliphatic hydrocarbons in urban particulate matter on a daily basis", *Atmospheric Environment*, vol. 39, no. 40, pp. 7702-7714.
- Sharma, H., Jain, V.K. & Khan, Z.H. 2008, "Atmospheric polycyclic aromatic hydrocarbons (PAHs) in the urban air of Delhi during 2003", *Environmental Monitoring and Assessment*, vol. 147, no. 1-3, pp. 43-55.
- Tobiszewski, M. & Namieśnik, J. 2012, "PAH diagnostic ratios for the identification of pollution emission sources", *Environmental Pollution*, vol. 162, pp. 110-119.
- Wold, S., Esbensen, K. & Geladi, P. 1987, "Principal Component Analysis", *Chemometrics and Intelligent Laboratory Systems*, vol. 2, pp. 37-52.
- Yadav, V.K., Prasad, S., Patel, D.K., Khan, A.H., Tripathi, M. & Shukla, Y. 2010, "Identification of polycyclic aromatic hydrocarbons in unleaded petrol and diesel exhaust emission", *Environmental Monitoring and Assessment*, vol. 168, no. 1-4, pp. 173-178.
- Yunker, M.B., Macdonald, R.W., Vingarzan, R., Mitchell, R.H., Goyette, D. & Sylvestre, S. 2002, "PAHs in the Fraser River basin: A critical appraisal of PAH ratios as indicators of PAH source and composition", *Organic Geochemistry*, vol. 33, no. 4, pp. 489-515.
- Zhang, W., Zhang, S., Wan, C., Yue, D., Ye, Y. & Wang, X. 2008, "Source diagnostics of polycyclic aromatic hydrocarbons in urban road runoff, dust, rain and canopy throughfall", *Environmental Pollution*, vol. 153, no. 3, pp. 594-601.

## 5 Results and Discussion of the study involving other environments where diesel engines are used

### 5.1 Introduction

Diesel emissions are characterized by accompanying range of pollutants of which DPM and PAHs are of particular interest for the purpose of this study due to their carcinogenic properties (El-Fadel & Hashisho 2001, IARC 2012). Exposure time in a tunnel is typically short but due to the confined environment, pollutant concentrations may be elevated to levels of potential health and safety risks. Safety becomes an issue as the presence of suspended particulate matter can decrease the visibility inside the tunnel and potentially cause car accidents (El-Fadel & Hashisho 2001 and HEI 2010). DPM emissions may not only affect vehicle passengers/drivers and pedestrians but also potentially affect people and neighbourhoods in the near vicinity of the ventilation buildings where the discharged plume is dispersed. Occupational exposure is generally limited to workers responsible for the maintenance of the tunnel, however numerous pedestrians, cyclists and motorists pass through the tunnel regularly, as discussed in Section 1.5.2. This chapter compares other environments where diesel engines are used to those of the mine environment as presented in Chapter 4.

### 5.2 Sample identification

The samples that were taken from the Daspoort Tunnel are represented by sample numbers which are tabulated in Table 5-1 and 5-2 and these numbers correspond to the y-axis of the bubble charts.

**Table 5-1 Sample details for the gas phase sampling of PAHs in the Daspoort Tunnel using PDMS multi-channel (MC22) traps.**

Sample no:	Sample name	Sample type	Traffic time	Sample height (m)	Tunnel position
1	936	single trap	off peak	1.0	entrance
2	934	single trap	peak	1.0	entrance
3	928	single trap	off peak	1.5	inside
4	927	single trap	off peak	1.0	inside
5	926	single trap	peak	1.5	inside
6	929	single trap	peak	1.0	inside
7	550	denuder primary trap*	off peak	1.0	entrance
8	324	denuder secondary trap#	peak	1.0	inside
9	334	denuder primary trap#	peak	1.0	inside

\*Indicating a component of denuder set 1

# indicating a component of denuder set 2

Table 5-2 Sample details for the particulate sampling of PAHs in the Daspoort Tunnel using quartz fibre filters.

Sample no:	Sample name	Sample type	Traffic time	Sample height (m)	Tunnel position
10	DTSF08	denuder filter*	off peak	1.0	entrance
11	DTSF09	denuder filter#	peak	1.0	inside
12	TS01	swab sample	-	from railing	¼ way inside
13	TS02	swab sample	-	from railing	middle
14	TS04	swab sample	-	from railing	entrance
15	WEEK 1	weekly filter	continous	2.5	inside
16	WEEK 2	weekly filter	continous	2.5	inside
17	WEEK 3	weekly filter	continous	2.5	inside
18	WEEK 4	weekly filter	continous	2.5	inside
19	WEEK 6	weekly filter	continous	2.5	inside

\*Indicating a component of denuder set 1

# indicating a component of denuder set 2

A traffic count was also conducted, in collaboration with students from St Mary’s DSG High School in Pretoria, to gain better understanding as to the number and types of vehicles passing through the tunnel during peak (07:00 a.m- 08:00 a.m) and off-peak (08:00 a.m- 10:00 a.m) hours of the mornings (Forbes *et al.* 2011). It can clearly be seen from Fig. 5-1 that cars (light duty vehicles) contributed the most to the traffic count and no real peak and off-peak periods were evident.

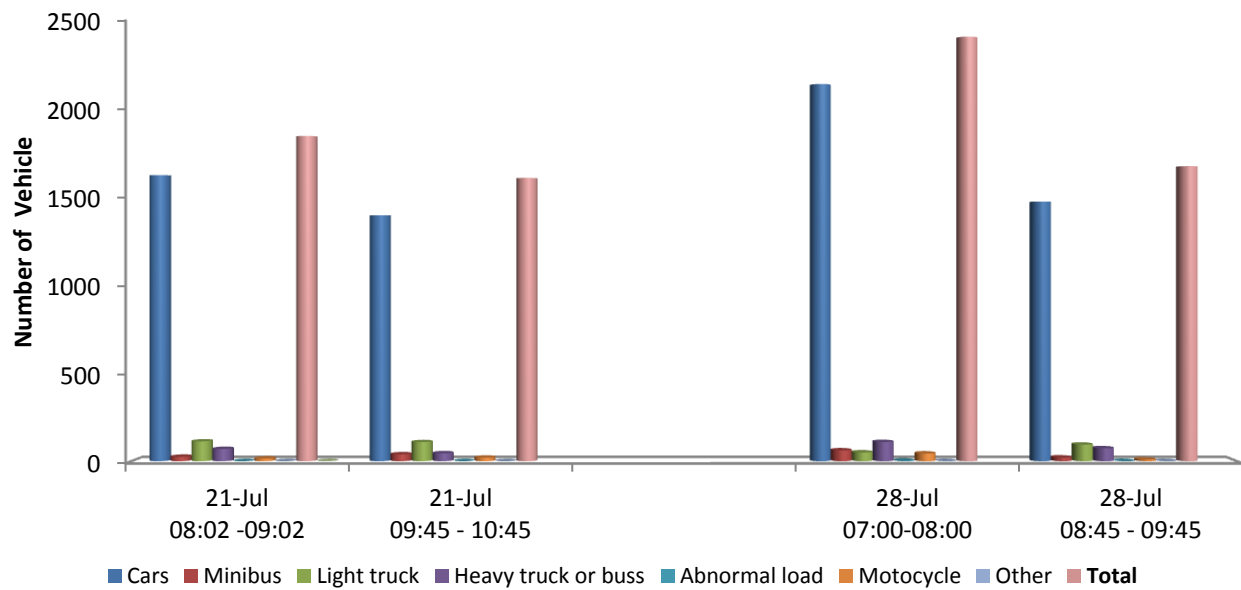


Figure 5-1 Vehicle count in the Daspoort Tunnel (Forbes *et al.* 2011)

### 5.3 Semi-volatile organic compound profiles for Daspoort Tunnel samples expressed as relative % peak areas

The relative % peak area of each compound class was given in the form of bubble plot illustrations with the size of the bubble being proportional to the relative % peak area. The plot of each sample was combined and the total SVOC profile can be seen as a whole. The dominating compound classes were identified, however they did not provide concentration data. The bubble plot was illustrated with 2 separate figures for the gaseous trap samples and for the particulate phase filter samples respectively, where the compound classes were displayed on the x-axis and the sample numbers are on the y-axis.

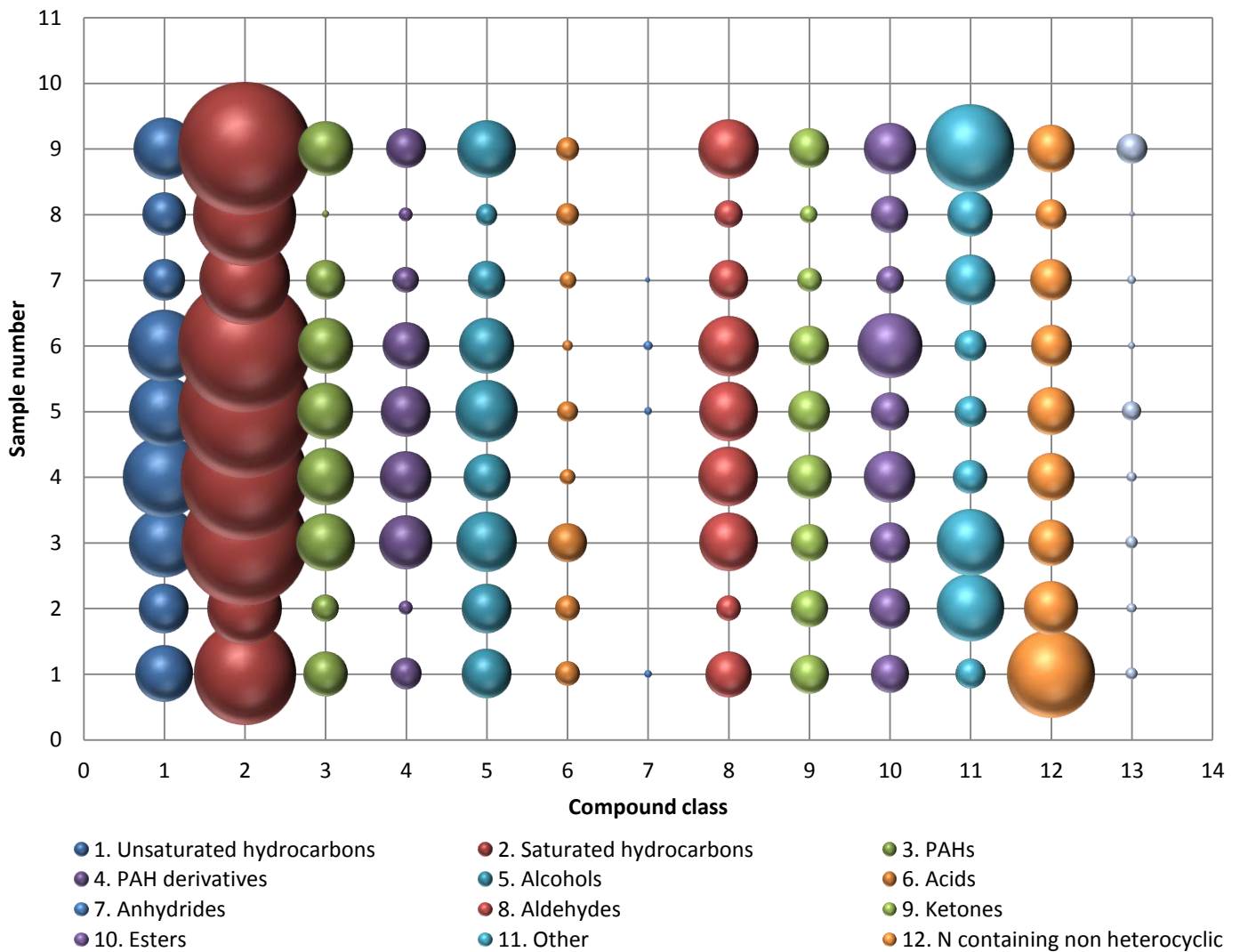


Figure 5-2 Relative % peak area SVOC profile of trap samples (gas phase) from the Daspoort Tunnel



Fig. 5-2 represented the relative % peak area of each compound class as found on the trap samples. The figure showed that the relative composition pattern remained relatively consistent for all the samples with few discrepancies.

The unsaturated and saturated hydrocarbons presented the highest contributions (similar to the mine trap samples) with the saturated hydrocarbons being dominant whereas the mine samples revealed a dominance of unsaturated hydrocarbons.

Aldehyde, ketone and ester contributions were higher and more consistent in the tunnel samples than in the mine samples most likely due to the larger, more constant amount of oxidising species within the tunnel.

Acid and acid anhydrides had low contributions as in the mine samples due to their reactivity (hence instability). There were very small contributions from the “other” group.

PAHs were consistently found in every primary trap sample with similar relative % peak areas and parent PAHs were found more abundantly than the PAH derivatives. There were expectedly less PAH and PAH derivative contributions found in sample 8, which corresponded to the secondary trap denuder sample. PAH contributions were relatively higher in the tunnel samples than in the mine samples, however the mine samples revealed much larger PAH derivative contributions and smaller PAH contributions.

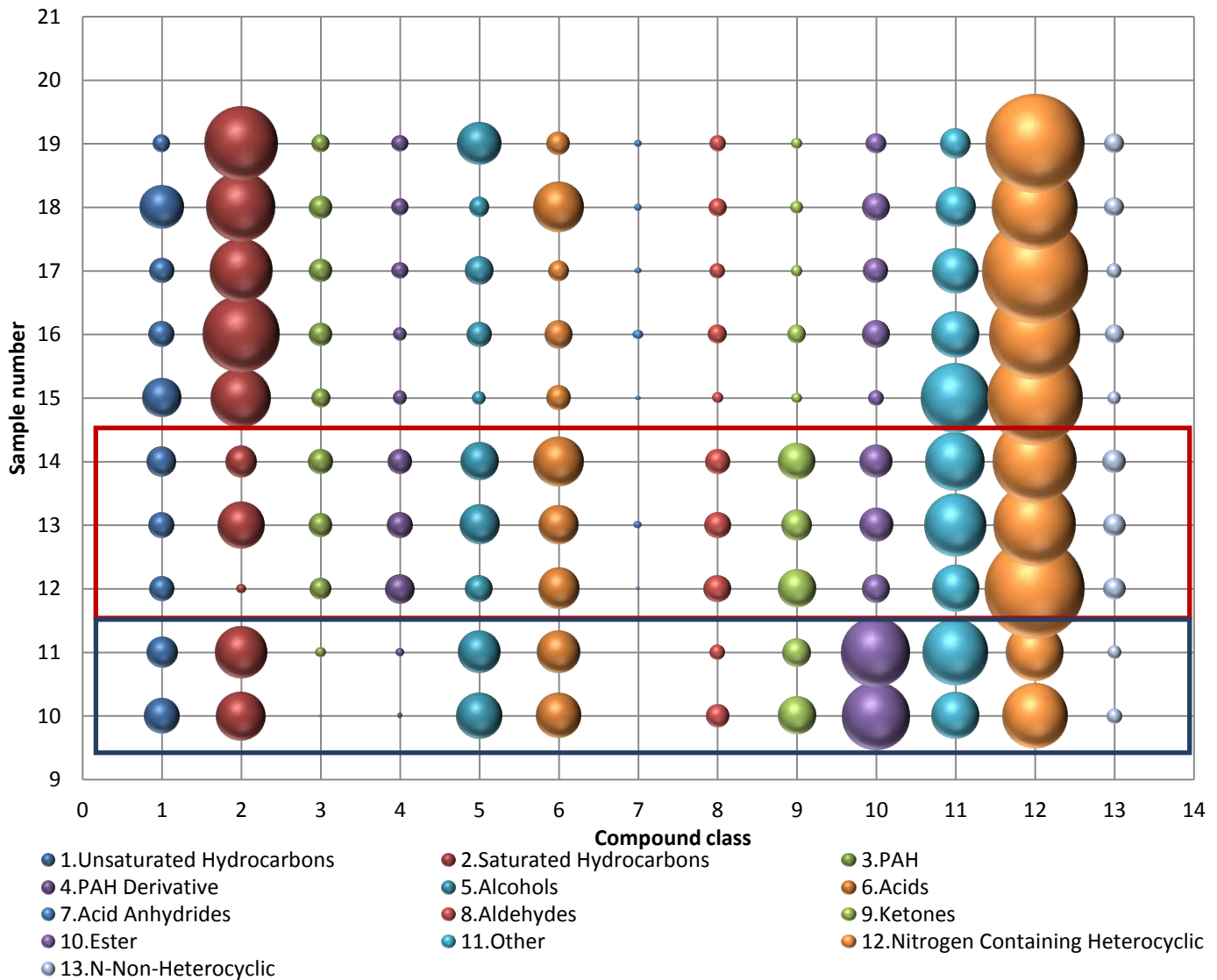


Figure 5-3 Relative % peak area SVOC profile of filter samples from the Daspoort Tunnel where the blue box groups the denuder filters and the red box groups the swab samples.

Fig. 5-3 represented the relative % peak area of each compound class as found on the filter samples; the blue box grouped the denuder filter samples together and the red box grouped the three swab samples together and good consistency was seen within these different types of samples. Fig. 5-3 also showed that the composition of the SVOCs was less consistent over all samples as a whole when compared to the overall composition reflected from the primary traps which was also the case for the mine samples. The results showed good consistency within sample types. The inconsistency for the filter profiles could be due to the different methods of sampling that was used (swab & trap).

It was evident from Fig. 5-3 that the saturated hydrocarbons consistently had the highest contributions in the weekly filter samples as well as in the denuder filter samples whereas unsaturated hydrocarbons (straight chain or cyclic) were dominant in the underground mine filter samples.

Fig. 5-3 showed very good consistency of the denuder filter samples which showed high relative % peak areas for esters when compared to the other filter sample types which was also the case for the underground denuder filter samples. The relative % peak areas for nitrogen containing compounds found on the filter were generally higher than that found on the primary trap in every sample. The oxidized species, particularly esters, had significantly higher relative contributions on the filter samples than for the primary traps in both the mine and tunnel denuder samples. Both the nitrogen-containing and oxidised species were primarily secondary pollutants.

Overall the relative % peak areas were lower for PAH and PAH derivatives in the filter samples as compared to the primary trap samples which indicated higher gas phase loading which corresponded to the mine samples. This implied that sampling of only particle associated PAHs in both the mine and tunnel environment would lead to an under estimation of potential human health effects due to exposure. The relative % peak areas for PAHs and PAH derivatives were substantially higher in the tunnel samples than in the mine filter samples. This could be due to increased emissions in the tunnel or possibly more stagnant air in the tunnel. There appeared to be an increased number of atmospheric reactions (to form derivatives) in the tunnel environment.

There were good correlations between the PAHs and PAH derivatives for each sample type with the swab samples having the highest contributions of both. The mine filter samples revealed higher contributions of PAH derivatives than PAHs whereas as the tunnel filter samples revealed very similar contributions of PAHs and their derivatives with some cases having higher contributions of the parent PAHs as in the weekly filter samples.

The swab samples had higher contributions of oxidized products compared to that of the other samples; this was most likely due to the accumulation of aged and fresh compounds on the railings. The tunnel samples in general had larger contributions from acids, alcohols and oxidised species (aldehydes and ketones). This was expected due the tunnel having more oxidant species available for reaction.

## 5.4 PAH profiles for Daspoort Tunnel samples expressed in relative % peak areas

The relative % peak areas (relative to total area of all compounds in sample) of the PAHs found in the traps and filters respectively were represented in bubble plot figures in this section, which gave a clear PAH profile for each sample medium and it showed the clustering patterns of the PAHs.

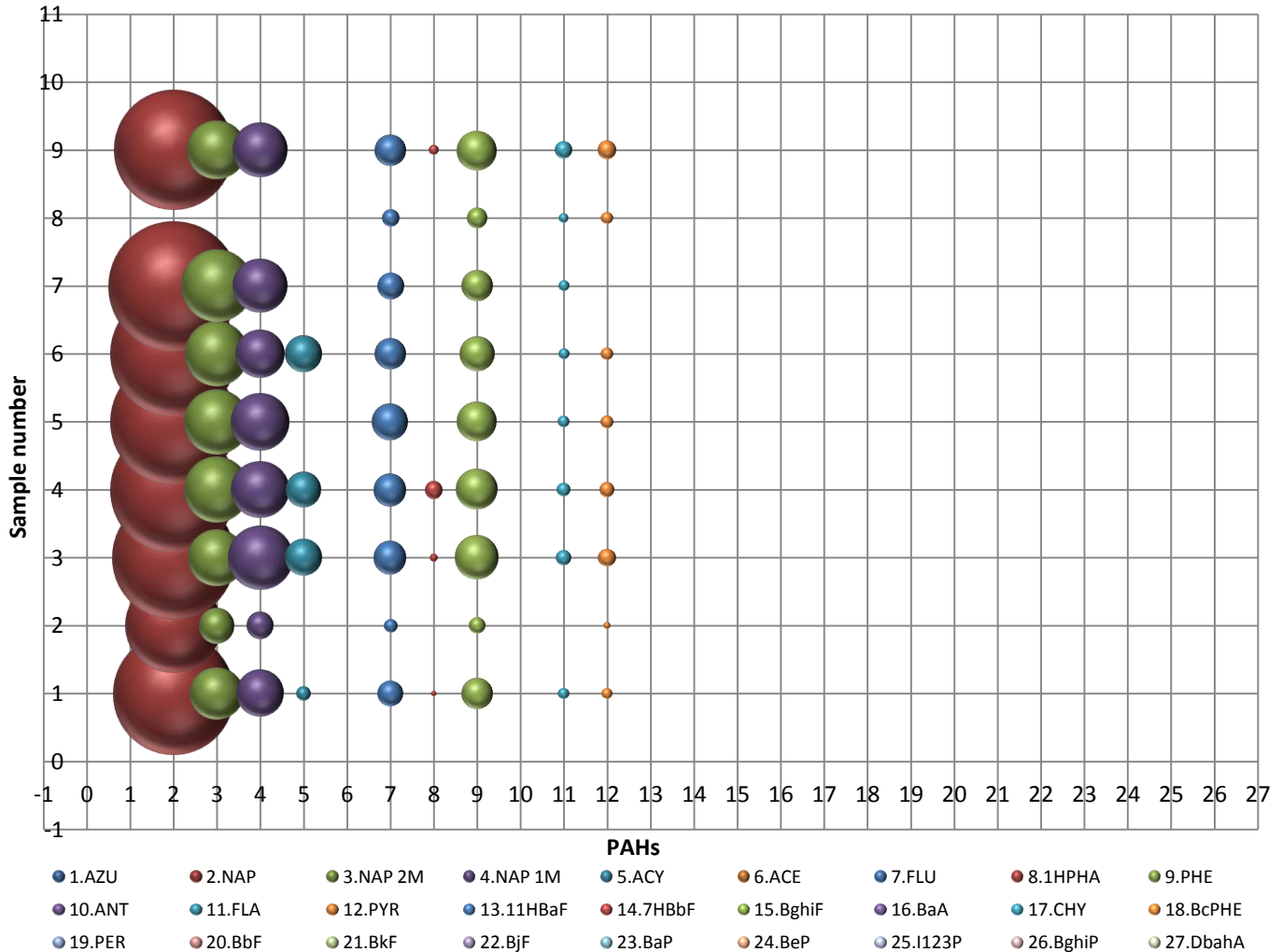


Figure 5-4 Relative % peak area PAH profile for trap samples (gas phase) from the Daspoort Tunnel

Fig. 5-4 and 5-5 represented the relative % peak area of PAHs obtained from the trap samples and filter samples respectively. The traps collected gaseous PAHs which were generally the lower molecular weight PAHs (up to  $202 \text{ g.mol}^{-1}$ ), such as pyrene, which was expected as they are considered more volatile and are found mostly in the gaseous phase (Phuleria 2006, Wingfors 2001). The filters collected PAHs that occur in the particulate phase and are generally the less volatile PAHs.

Fig. 5-4 showed that smaller PAHs (2-4 rings) were trapped on the primary trap as expected. The PAH profile was consistent in all the samples, except sample 8 which corresponds to the secondary trap. PAHs up to pyrene were seen in the majority of the samples. Naphthalene was the most abundant of the PAHs found on the traps with its derivatives also showing significant contributions. Fluorene and phenanthrene also had significant relative % peak areas.

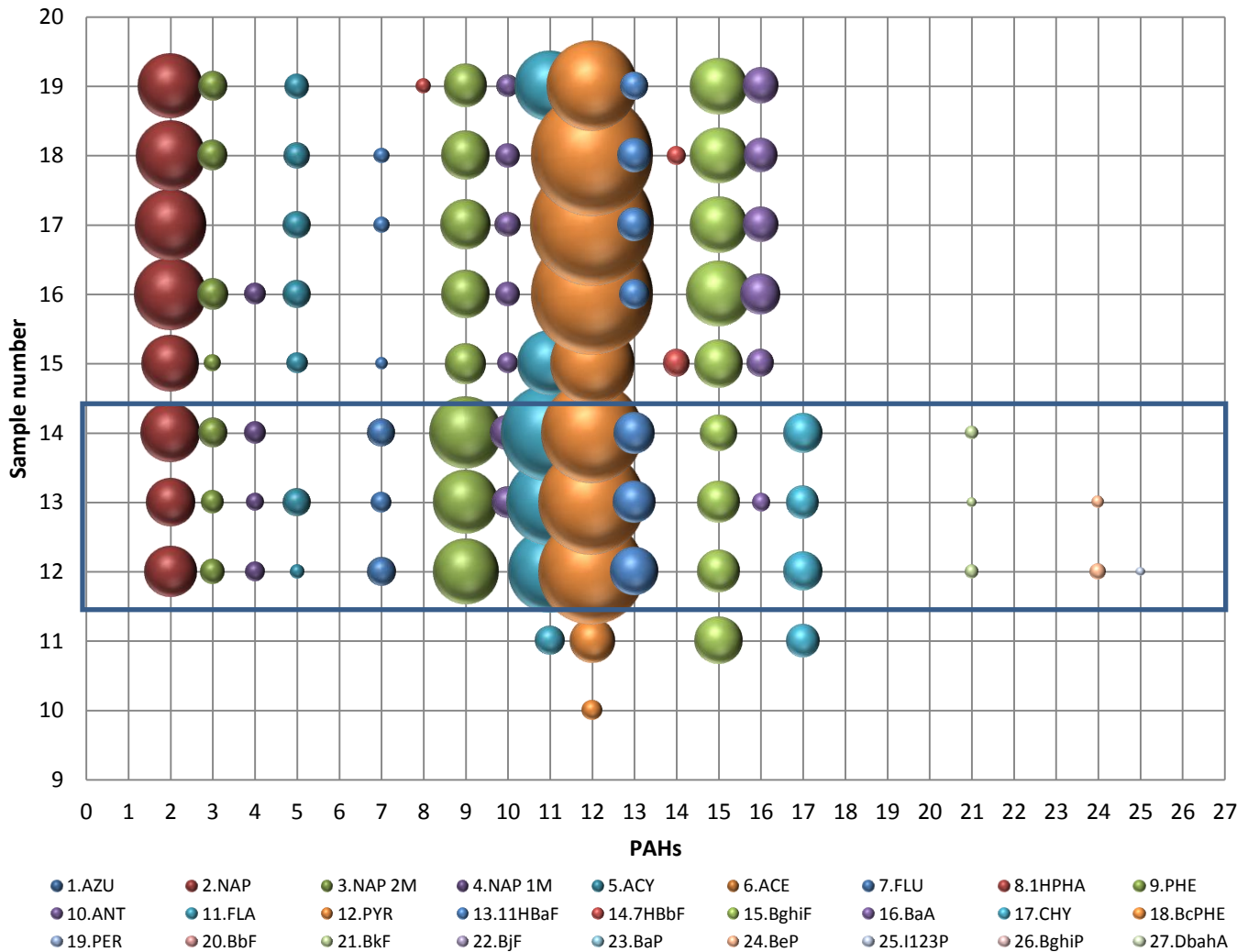


Figure 5-5 Relative % peak area PAH profile for filter samples (particulate phase) from the Daspoort Tunnel where the blue box groups the swab samples.

Fig. 5-5 showed the relative % peak areas of PAHs on the filter samples i.e. particulate associated PAHs, and it was evident that the heavier PAHs were trapped on the filters. Pyrene was found in every sample and was consistently the largest contributor to the relative % peak area. The denuder filter samples

showed the smallest contributions of PAHs whereas the swab samples showed the largest. Heavy PAHs, such as benzo(k)fluoranthene, benzo(e)pyrene and indeno(1,2, a-cd)pyrene were seen in the swab samples (enclosed in blue box) and not in any other filter sample, they were also seen in the underground LHD samples.

The swab sample taken at the tunnel entrance (as opposed to inside the tunnel) revealed less of the heavier PAHs. These PAHs were consistent with the PAHs found in the literature (Section 5.1). The instrumental limitations that were identified in Section 4.1.2 with respect to the TD temperature were considered when interpreting the filter sample results.

When the mine results were compared with the tunnel results it was evident that the PAH profiles from the tunnel samples showed much more consistency (with respect to the presence of certain PAHs and their corresponding bubble sizes) than the mine profiles. This was expected due to the consistent sampling at the Daspoort Tunnel. The underground samples were taken at different areas, for different periods of time, with different local environments.

The trap samples for both the mine samples and the tunnel samples were similar in that generally the same PAHs were detected with naphthalene and its mono methylated derivatives having dominant contributions. The mine samples revealed the presence of slightly heavier PAHs such as benzo(a)anthracene that were also found in the gas phase whereas the tunnel samples showed pyrene as the heaviest PAH detected in the gas phase.

The filter samples of the tunnel and the mine samples showed pyrene as the most dominant PAH with clustering of other PAHs around pyrene. The tunnel samples showed particulate loading of the more volatile PAHs such as naphthalene and 2-methyl naphthalene with significant relative % peak area contributions whereas the mine sample showed little to none of these 2 ring PAHs.

## 5.5 PAH profiles for Daspoort Tunnel samples expressed in total peak areas

### 5.5.1 Gas phase samples

The sum of all peak areas of each detected PAH was graphically represented in this following section in order compare the gas phase tunnel samples.

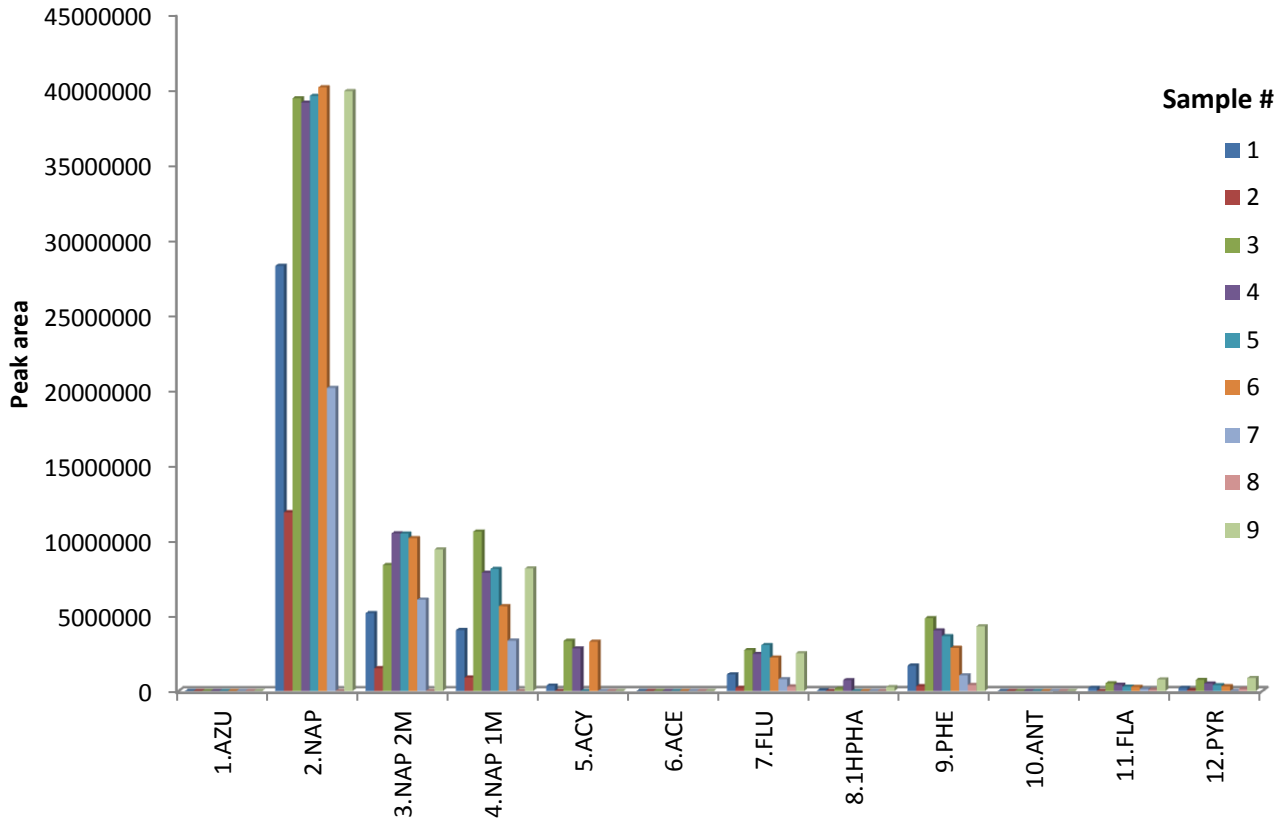


Figure 5-6 Sum of all PAH peak areas detected in the Daspoort Tunnel trap samples

It was seen from Fig. 5-6 that the PAH peak area profiles were generally very consistent between all of the gas phase samples, with naphthalene being the most abundant PAH. The mono-methylated naphthalene derivatives, acenaphthylene, fluorene and phenanthrene were the commonly detected PAHs in the gas phase which corresponded to the literature (Ho, 2009, Wingfors 2001) with smaller peak areas for fluoranthene and pyrene.

### 5.5.2 Particulate phase samples

The sum of all peak areas of each detected PAH was graphically represented in this following section in order compare the particulate phase tunnel samples.

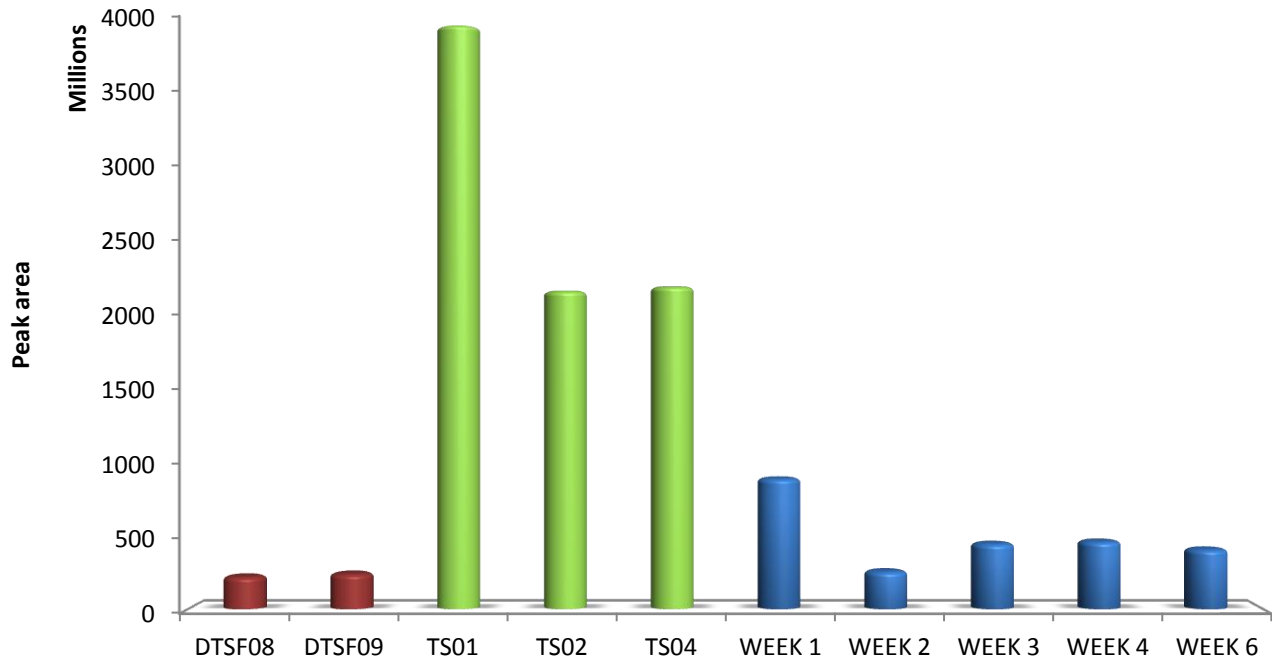


Figure 5-7 Sum of all PAH peak areas detected in the Daspoort Tunnel for all particulate samples

Fig. 5-7 showed the total PAH peak areas for each type of filter sample. The PAH peak areas showed good consistency within each sample type but showed a large variation between the sample types. It was noted that the volumes sampled and manner of sampling was different for each sample type. Consequently the swab samples showed the highest total peak areas for PAHs as they were the largest samples. The weekly samples were sampled for a 7 day period but still showed significantly lower PAHs than the swab samples collected. This was due to the accumulation of particulate matter on the railings in the tunnel, which was also physically seen in Fig. 3-3 where the filter was blackened with the railing soot. TS01 showed the highest amount of PAHs and it was taken  $\frac{1}{4}$  of the way inside the tunnel. The other swabs show lower PAH peak areas as the one was taken at the entrance, where dilution with fresh air took place, and the other was taken from the middle of the tunnel underneath the extraction duct which would extract some of the emissions.

This is of concern as pedestrians may use the railing for support when walking through the tunnel. If this was the case for the railings in the tunnel, the same may apply to underground environments where



DPM will be deposited and accumulated on the vehicles, barricades and supports and even on the rock faces. The tunnel railings (and thus also the tunnel walls) can be manually cleaned with little effort and a cleaning strategy should be implemented but it is more of a challenge in underground environments where the DPM is also deposited on the rock.

The next section gives a better description of the PAH apportionment in each sample type.

### 5.5.2.1 PAH apportionment for denuder filters, swabs and weekly filters.

The following section provides the absolute peak areas of each PAH from the different filter samples, whereby the overall PAH apportionment for each sample type can be seen. The samples were plotted with a separate graph for each sample type for simplicity. The fact that the sampling was significantly different for each sample type (with respect to volume sampled or the manner of sampling) prevented the direct comparison of tunnel samples, as was done for the mine samples.

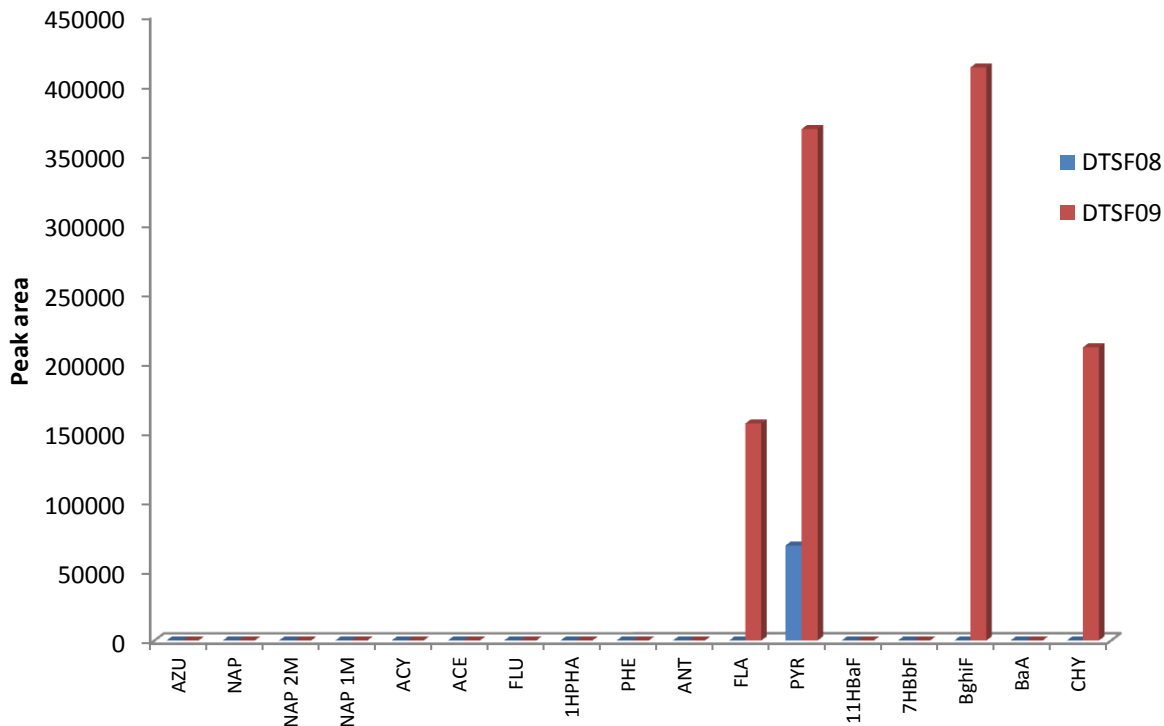


Figure 5-8 PAH peak areas detected in the denuder filter samples

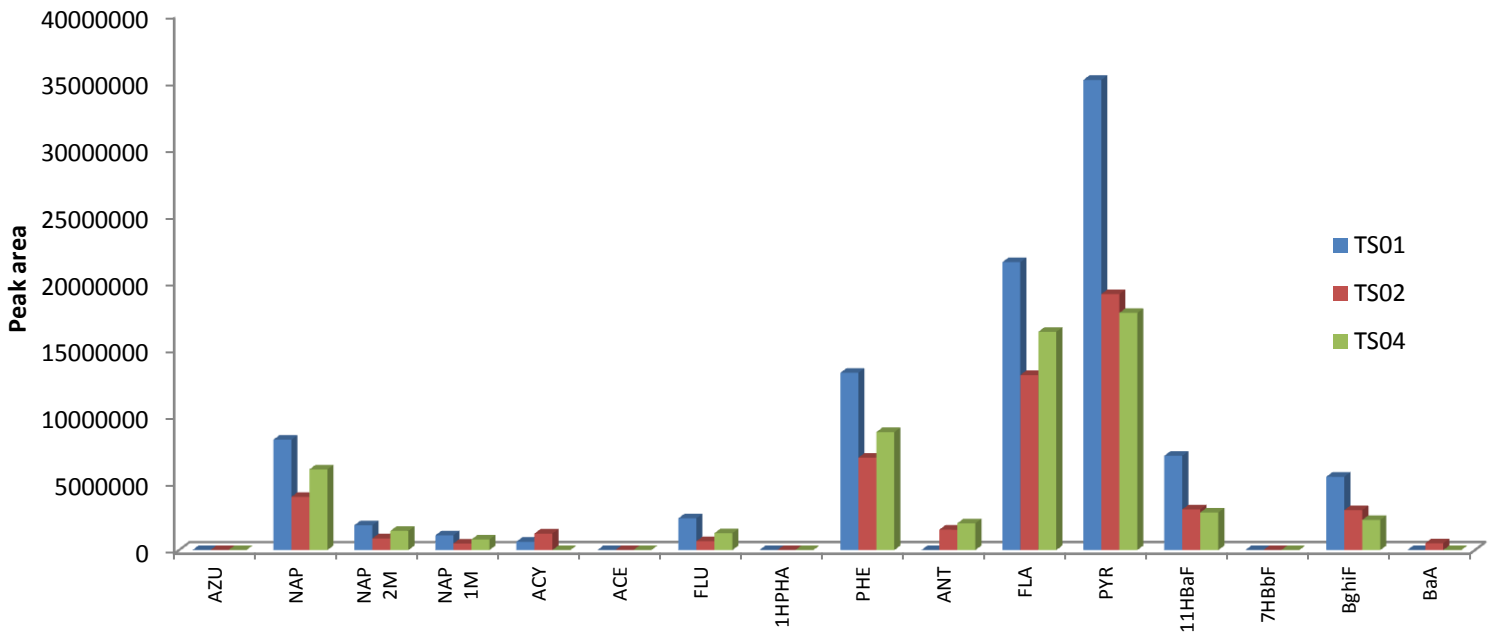


Figure 5-9 Sum of all PAH peak areas detected in the swab filter samples

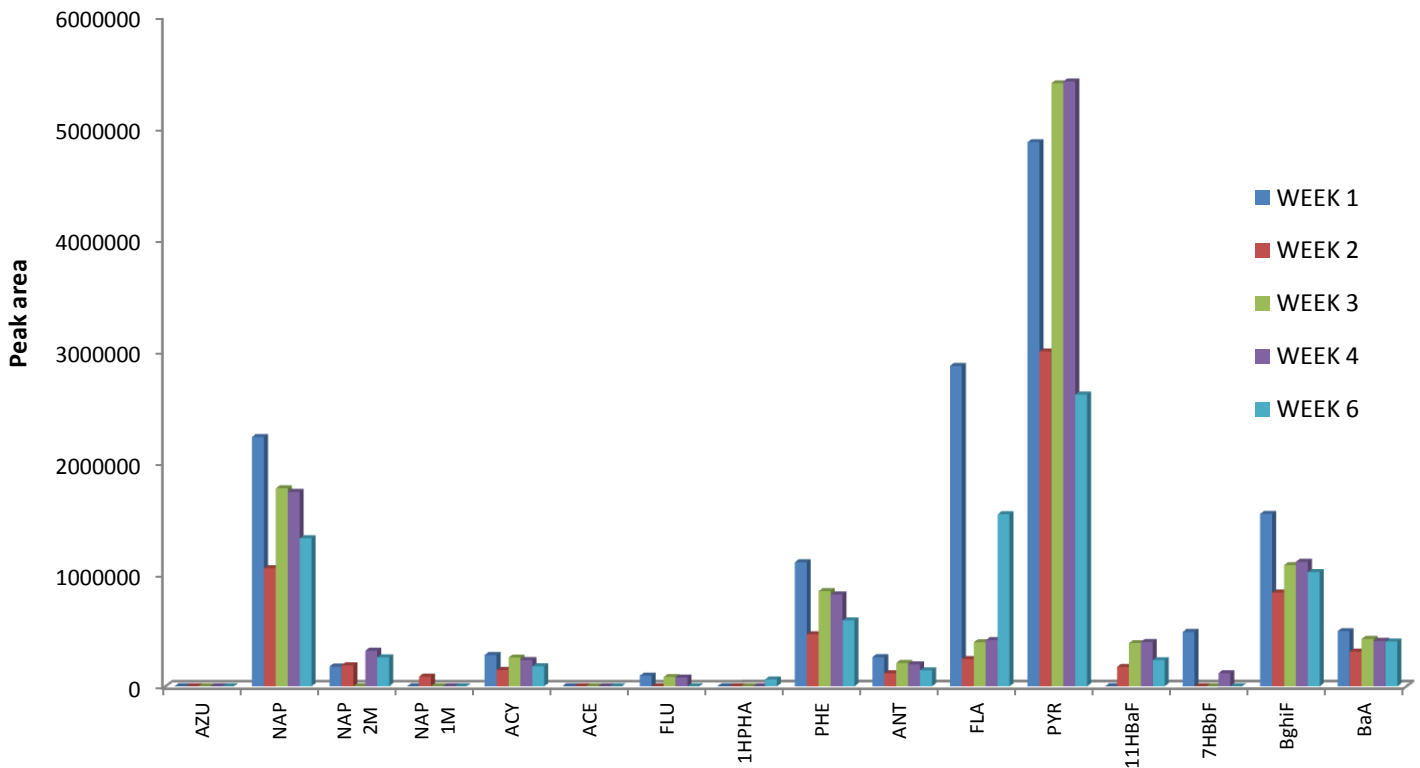


Figure 5-10 Sum of all PAH peak areas detected in the weekly filter samples

Fig. 5-8 showed that the denuder filters contained only a few PAHs with DTSF08 containing only pyrene. The DTSF08 sample was taken at the tunnel entrance, where dilution occurred, and it was taken during off peak traffic times where emissions were less. It was therefore expected to have less PAH loading than DTSF09 which was taken from inside the tunnel during peak traffic times. DTSF09 showed fluoranthene, pyrene and chrysene, which are 4 ringed PAHs that are typically found in the particle phase and are associated with diesel emissions. Fluoranthene and pyrene are used as diesel markers (Ho 2009).

Fig. 5-9 revealed similar PAH loading profiles for all the swab samples. The TS01 sample that was taken from  $\frac{1}{4}$  of the way inside the tunnel showed the highest peak areas as previously discussed. Pyrene was the most dominant PAH.

Fig. 5-10 showed the particle PAH loading on the weekly filter samples. The profiles generally had the same pattern with pyrene being the most abundant PAH. There was a significant presence of naphthalene in the weekly samples. Acenaphthylene, fluorene, phenanthrene, anthracene, fluoranthene and benzo(a)pyrene were amongst other PAHs detected in the weekly samples.

## 5.6 HICE 2012 Campaign: Emissions from ship's engine using light fuel oil

In this brief section, the PAH peak areas were divided by the total peak area (sum of all peak areas) and then multiplied by 100 to give relative % peak areas. Relative % peak areas did not provide actual concentration data in this section, but they gave clear PAH profiles for each engine load and showed clustering patterns of these PAHs.

From Fig. 5-11 it was seen that PAHs that were detected ranged from very volatile two ringed naphthalene to the less volatile benzo(k)fluoranthene. The PAH profile was consistent for all of the loads but at 75 % load there were intensified relative % peak areas for a few of the PAHs. The 50 % load showed higher relative % peak areas than for the 75 % load for benzo(k)fluoranthene, chrysene and fluoranthene.

Pyrene and fluoranthene were the dominant PAHs that were detected for every engine load which was consistent with literature findings for filter samples of diesel exhaust emissions (Ho 2009). Fluoranthene had the highest relative % peak area at 100 % engine load, as did pyrene which is also the most abundant PAH for all of the other engine loads.

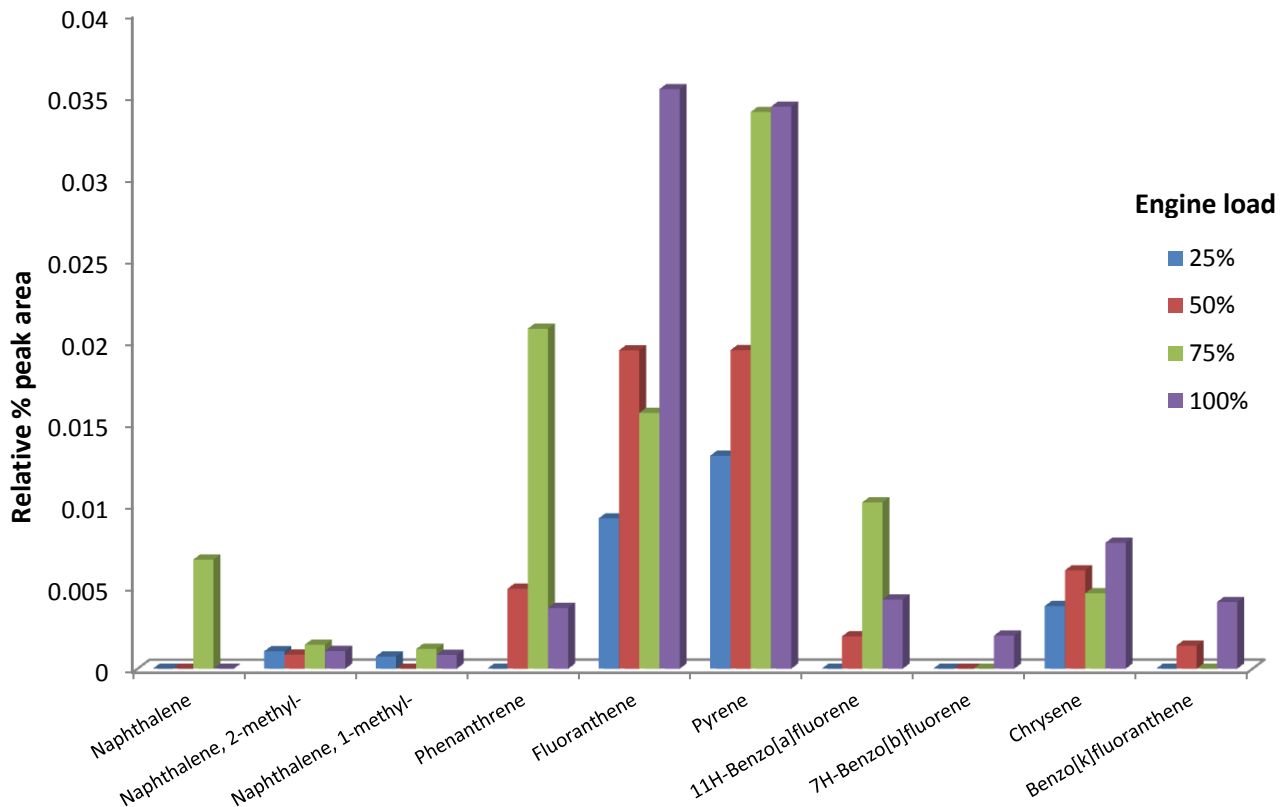


Figure 5-11 Relative % peak area of PAHs from a ship engine exhaust at different operating loads with LFO.

At 25 % engine load, there were less PAHs detected than at the higher operating loads and the relative % peak areas were generally lower. The 75 % engine load revealed the highest relative % peak areas for most of the more volatile PAHs and showed significantly higher naphthalene, phenanthrene and benzo(a)fluorene contributions than the other loads. The heavier PAHs such as chrysene and benzo(k)fluoranthene had higher relative % peak areas for 100 % engine load.

The number of detected PAHs increased linearly with increasing the engine load but the total relative % peak area of these PAHs did not follow the same trend which can be seen in Fig. 5-12.

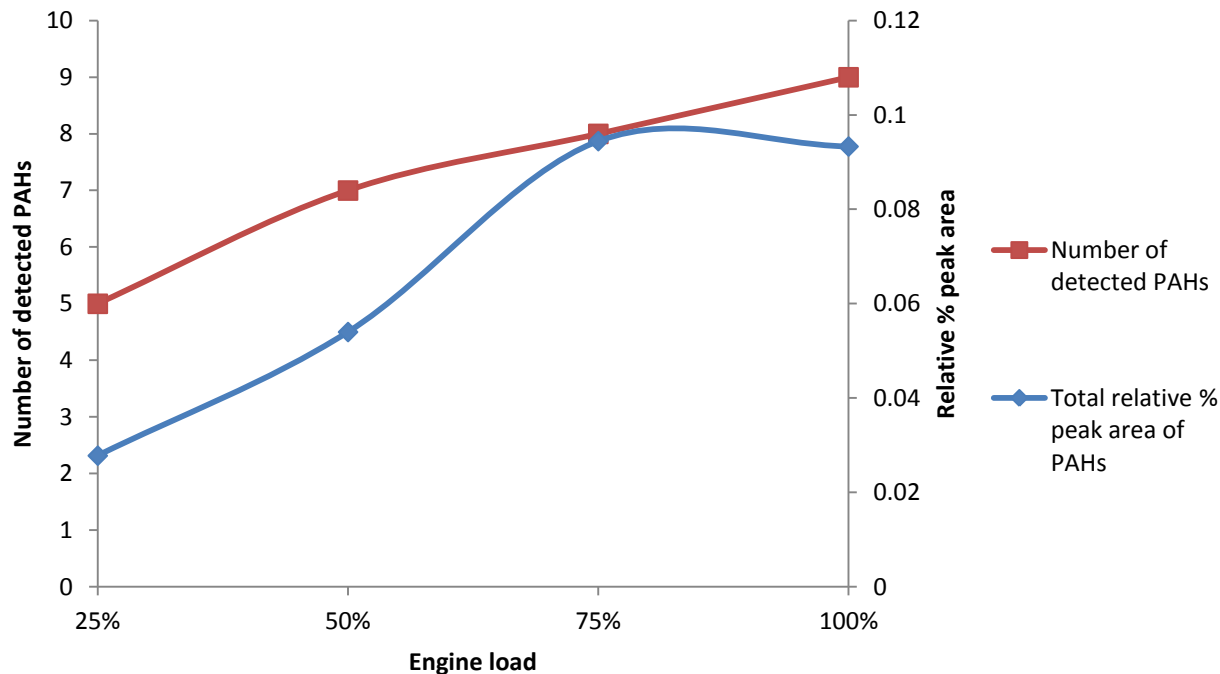


Figure 5-12 Number and relative % peak areas of detected PAHs from a ship engine exhaust emissions at different operating loads

## 5.7 Conclusion

The SVOC relative % peak area profiles from the tunnel were compared to underground mine profiles. In the tunnel profiles, the unsaturated and saturated hydrocarbons presented the highest contributions (corresponding to the mine trap samples) with the saturated hydrocarbons being dominant whereas the mine samples revealed a dominance of unsaturated hydrocarbons. Aldehyde, ketone and ester contributions were higher and more consistent in the tunnel samples, than in the mine samples, likely due to the larger, more constant amount of oxidising species in the tunnel.

The relative % peak areas were lower for PAH and PAH derivatives in the tunnel filter samples as compared to the tunnel gas phase trap samples indicating higher gas phase loading which corresponds to the mine samples. Sampling of only particle associated PAHs in both the mine and tunnel environment would lead to an under estimation of potential human health effects due to exposure.

The PAH relative % peak area profiles were very consistent between all of the tunnel gas phase samples with naphthalene being the most abundant PAH. The mono methylated naphthalene derivatives, acenaphthylene, fluorene and phenanthrene were the commonly detected PAHs in the gas phase.

Particulate tunnel filter samples from the Daspoort Tunnel revealed the dominance of pyrene, which corresponded to the samples taken from underground platinum mines and the literature with respect to diesel emissions. The tunnel sample PAH profiles were more consistent when compared to the mine samples due to the fact that the tunnel environment and sampling regime was more consistent and constant than underground, where different local environments were sampled.

Tunnel swab samples showed high peak areas for the PAHs that were associated with the larger, denser particles which deposited out and settled onto the tunnel railings, which is a cause for concern as pedestrians use the railing for support when walking through the tunnel. The same scenario applies to underground environments where DPM may be deposited and accumulated on the vehicles, barricades and supports and even on the rock faces.

## 5.8 References

- El-Fadel, M. & Hashisho, Z. 2001, "Vehicular emissions in roadway tunnels: A critical review", *Critical Reviews in Environmental Science and Technology*, vol. 31, no. 2, pp. 125-174.
- Forbes, P.B.C., Garland, R.M., Wright, C.Y., Louw, W., L. Phiri, L., Gawler, N., Mabe, M., Molisiwa, J. and Brown, J. 2011, "Air quality measurements in the Daspoort Tunnel, Pretoria", *National Air Quality Officers News*, July-September, pp. 11-13.
- HEI Panel on the Health Effects of Traffic-Related Air Pollution. 2010, "*Traffic-Related Air Pollution: A Critical Review of the Literature on Emissions*", Exposure, and Health Effects. HEI Special Report 17. Health Effects Institute, Boston, MA, viewed 10 June 2013, <<http://www.healtheffects.org/getfile.php?u=553>>.
- Ho, K.F., Ho, S.S.H., Lee, S.C., Cheng, Y., Chow, J.C., Watson, J.G., Louie, P.K.K. & Tian, L. 2009, "Emissions of gas- and particle-phase polycyclic aromatic hydrocarbons (PAHs) in the Shing Mun Tunnel, Hong Kong", *Atmospheric Environment*, vol. 43, no. 40, pp. 6343-6351.
- IARC. 2012, Diesel engine exhaust carcinogenic 2012, Press Release no. 213.
- Phuleria, H.C., Geller, M.D., Fine, P.M. & Sioutas, C. 2006, "Size-resolved emissions of organic tracers from light- and heavy-duty vehicles measured in a California roadway tunnel", *Environmental Science and Technology*, vol. 40, no. 13, pp. 4109-4118.
- Wingfors, H., Sjödin, A., Haglund, P. & Brorström-Lundén, E. 2001, "Characterisation and determination of profiles of polycyclic aromatic hydrocarbons in a traffic tunnel in Gothenburg, Sweden", *Atmospheric Environment*, vol. 35, no. 36, pp. 6361-6369.

## 6 Conclusion

South Africa is a developing country in which the mining sector contributes immensely to the country's revenue as it is the world's frontrunner in platinum production and one of the top producers of diamonds, gold, coal and base metals. The mining process involves the use of diesel engines for a number of underground operations and combustion emissions contribute to ambient particulate and gaseous air pollutant levels, including those of semi-volatile organic compounds and PAHs. The mining sector provides hundreds of thousands of jobs of which most are for underground miners which is why occupational exposure to diesel engine exhaust is a great concern. The DEE particles contain concentrations of toxic components which can be very high at times, especially in confined work environments with inadequate ventilation such as underground mines. Since recently being confirmed as carcinogenic (IARC 2012), DEE are a global hot topic from environmental as well as human health perspectives and occupational limits are soon to be adopted in South Africa.

The aim of the research presented was to test the application of a novel denuder sampling device for underground environments, and use these findings to conduct a preliminary survey to evaluate SVOCs in South African platinum mines, with emphasis on PAHs. PAHs coexist in both the vapour and particle phase and each of these has different environmental impacts as well as human health impacts, in terms of the fate of the PAHs in the human body. It was for this reason that it was vital to sample the PAHs in both gas and particulate phases.

The setup of a conventional partitioning sampling device consists of a high volume sampler that draws large volumes of air through a GFF prior to an adsorbent such as PUF. This sampling methodology would not be suitable for underground monitoring as the set-up is heavy, bulky and expensive. Standard partitioning measurements also possess other limitations, including adsorption and blow off effects whilst sampling, which would result in an under or over estimation of human exposure to PAHs.

Contrary to the conventional partitioning sampling devices; the denuders were cost effectively prepared in the laboratory and were very easy to use and transport underground as they are small, lightweight and portable. The blow off and adsorption effects that are typically experienced with the conventional setup were overcome with the denuder as they were fitted with an additional PDMS trap post filter. In addition, low sampling volumes were employed and the system has a relatively low back pressure.



The effective trapping of the PAHs in both vapour and particulate phases was demonstrated in this study and the results were consistent with denuder theory. The denuder devices proved to be very effective for this investigative preliminary study and could potentially be used for future routine monitoring of SVOCs in underground environments. The PDMS multi-channel traps of the denuder served as a solvent for the SVOCs (including PAHs) therefore analyte recovery was expected to be higher due to absorption of SVOCs rather than adsorption. The sorbent was well suited to the type of analytes to be sampled as well as the TD-GC<sub>x</sub>GC-ToFMS analysis, as the PDMS had high enough thermal stability for thermal desorption. The use of thermal desorption eliminated the use of toxic organic solvents and time consuming extraction techniques which was beneficial from human health, environmental and cost perspectives. TD also allows for total transfer of the sample analytes onto the GC column which enhances sensitivity when compared to solvent extraction based methods and thereby facilitates shorter sampling times and smaller sampling volumes.

The method that was developed for characterisation of DPM in underground platinum mines with emphasis on PAHs was proven to be successful. The sampling was rapid and effective and low limits of detection for PAHs were found for the experimental method (0.2-3.7 ng.m<sup>-3</sup> for filters and 0.2-13.6 ng.m<sup>-3</sup> for PDMS traps). The method calibration showed good correlation coefficients ranging from 0.9746-0.9999.

Three participating underground platinum mines were involved in this study. Samples were taken from each mine, at different mining environments, in shafts that use trackless mining methods (use of diesel vehicles) as well as shafts that use conventional track mining methods (no diesel vehicles). When comparing the three mines; varying amounts of emissions were detected which can be attributed to the fact that the instantaneous environments whilst sampling were different at each mine, with respect to the number and type of possible emission sources that were observed. This was the main difficulty with comparative monitoring in this environment.

The PAH emissions from different areas were compared as were the PAH fingerprints in both gaseous and particulate phases. PAHs that were detected underground ranged from 2- ringed gas phase PAHs, that were found on the trap samples, to 5-6 ringed PAHs that were detected on the filter samples. PAHs were predominantly found to exist in the gas phase with naphthalene and its mono-methylated derivatives being the most abundant (0.15-8.73 µg.m<sup>-3</sup>). This finding emphasised the need for gas phase sampling as sampling of only the particle phase would lead to an underestimation of potential human

exposure. Pyrene was the most abundant PAH that was found in the particulate phase and it was present in every filter sample from the diesel shafts, therefore this compound may serve as a useful indicator of PAH exposure in mining environments. The particle bound PAHs were found in the highest concentrations at the LHD exhaust, with dominance of fluoranthene and pyrene at concentrations that ranged from 0.52-109.60 ng.m<sup>-3</sup>. The LHD exhaust samples included heavier PAHs such as benzo(e)pyrene, benzo(a)pyrene, and indeno(1,2,3-cd)pyrene.

The FLA/PYR diagnostic ratio of approximately 0.6 confirms vehicular emissions as a source. When this ratio is used in conjunction with the FL/(FL+PYR) ratio, this gives confidence to conclude that diesel vehicular emissions were a dominant source of PAH emissions underground. Diagnostic ratios from literature were used as source indicators to verify the results. All of the mine samples that were analysed showed higher alkanes, with >C<sub>27</sub>, indicating that vehicular emissions and incomplete combustion were sources of pollution. The non-diesel filter samples revealed no traces of eicosane or nonadecane, indicating that diesel vehicular emissions were not a source of the particulate matter found in the non-diesel shafts, which was to be expected. There was no trace of levoglucosan or any other polar compound markers in the samples analysed.

The PAH fingerprints from the underground mine samples compared well with the Daspoort Tunnel samples, in that naphthalene was the most dominant gas phase PAH that was detected and pyrene was the most abundant particulate phase PAH. This also concurred with literature studies regarding diesel exhaust emissions. The filter samples that were taken from a diesel ship's engine exhaust also correlated well with the mine and tunnel filter samples showing pyrene and fluoranthene as the most abundant particulate PAHs.

This study focused on the chemical characterisation of PM from DEE at a time when engine technology, diesel fuel quality and emission regulations are undergoing major changes, as are the analysis techniques for particle characterisation. Human health and climate change are global topics which is why there is an enormous interest in the composition of particles. New developments in engine technology and after-treatments have made it possible to significantly reduce PM emissions although it does not apply to South African mines, at this time, as the age and condition of the vehicle fleet in South African mines limits the use of much of the new technology.

The new proposed DPM limits that are to be adopted by South Africa call for a decrease in the emissions of DPM, and correspondingly less PAH emissions. In order to achieve this, there are a number of factors

that need to be considered which will require an integrated strategy that incorporates efforts from all departments of a mine including: maintenance, ventilation, Safety, Health, Environmental and Quality (SHEQ) and all levels of management.

The quality of the fuel and lubrication oil affects the concentration of emissions as well as the type of emissions. Low sulphur fuel should be used as sulphur inhibits the implementation of new technology and effective after-treatments. The sulphur content also increases the maintenance cost of engines due to corrosion resulting from the formation of sulphuric acid. In addition to lowering the sulphur content, the aromatic content in fuels and oils should also be lowered to decrease the resulting PAH emissions.

Diesel particulate filter (DPF), disposable filter element (DFE), partial flow filter (PFF), diesel oxidation catalysts (DOC), or hybrids of these, are possible engine after-treatments that can be used to drastically reduce emissions. These after-treatments are dependent on the engine type, engine loading and fuel quality. Therefore older engine technologies, which are currently in use in South Africa, may not be compatible with these options and if they are, the costs of incorporating them may exceed the cost of the engine.

From the emission profiles discussed in Chapter 4, it was noted that there was a high degree of incomplete combustion, as was evident from the high amounts of hydrocarbons, indicating that the engines were not operating optimally. Maintenance of the diesel engines is vital to ensure that optimum combustion is achieved and that the engines are operated optimally. There should not only be a maintenance plan for the vehicles but also for the roads/pathways of these vehicles and the driving conditions of each vehicle should be managed. Speed limits and one way travel routes could be introduced to prevent traffic congestion as well as the restriction of unnecessary idling or lugging of vehicles. When there are large rocks on the path, the vehicle has to be laboured excessively to move beyond the obstacle therefore roads should be cleared prior to the start of the shift.

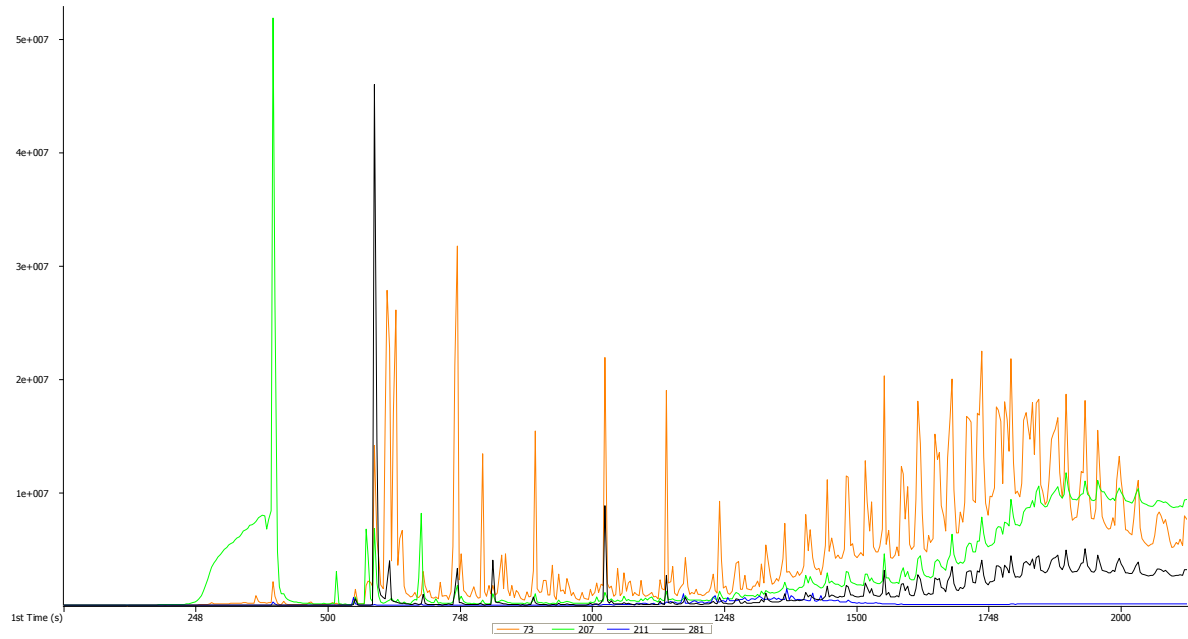
A high cost but effective option would be to replace the old diesel engines that are unrated or Tier 0 and opt for Tier 2 technology, which has been proven to decrease DPM emissions by over 50 %. The older engines generate more emissions and are limited regarding the after-treatments that can be fitted.

Ventilation should be working as effectively as possible and should be checked before commencement of the shift. The exhaust emission levels in working environments and worker exposure to these emissions should be continuously assessed to ensure that the emissions are decreasing and to ensure compliance to the OELs.

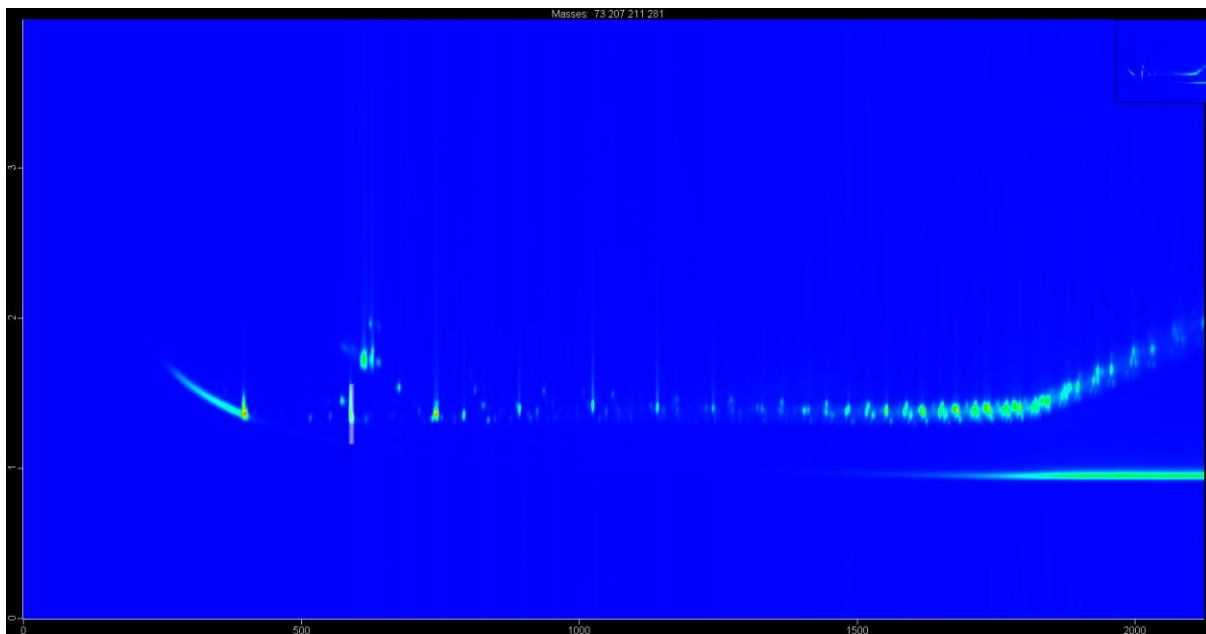
## 6.1. Recommendations

- For future research it is recommended that a larger sample set with replicates should be taken for a more accurate understanding and comparison and for statistical purposes.
- The thermal desorption method did have limitations and incomplete desorption of the heavier PAHs is a possibility, therefore further optimization should be performed for future research.
- The source indicators are valuable tools to distinguish between the different sources of pollution, but in order to get an understanding as to the relative contributions made by each source it is vital to perform full quantitation of all of the organic compounds in the samples.
- NIST 2975 DPM standard should be used to fully validate the method for PAH analysis underground.
- The question of breakthrough needs to be addressed. Although the majority of sampling was done under theoretically non-breakthrough conditions, the secondary traps contained more volatile analytes. It was not clear as to whether these analytes in fact broke through from the primary trap or if they were adsorbed onto particles that were caught on the filter and were then blown off. In order to test this: two PDMS traps should be connected in series without a filter (trap-trap). This sampler should be used in parallel with the conventional denuder (trap-filter-trap). When analysing the trap-trap denuder, it will be possible to determine what was in fact breakthrough by what appears on the secondary trap. The analytes (specifically PAHs) that appear on the secondary trap of the conventional denuder that do not appear on the secondary trap of the trap-trap denuder can therefore be confirmed as blow off of particle adsorbed PAHs. In order to reduce breakthrough, lower flow rates and smaller total sampling volumes should be tested however, it should be noted that this may have an impact on the detection limits.
- In future the mass of particles collected should be recorded in order to calculate partitioning ratios.

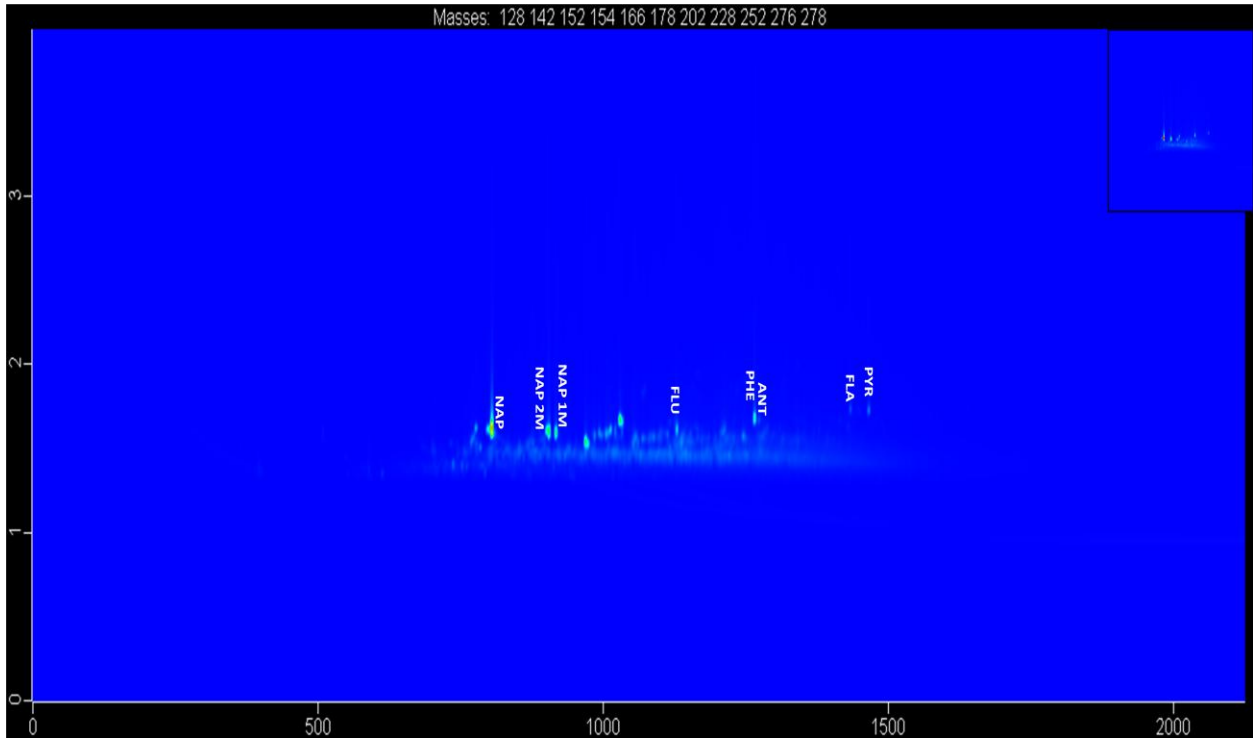
## 7 Appendix A: Sample chromatograms



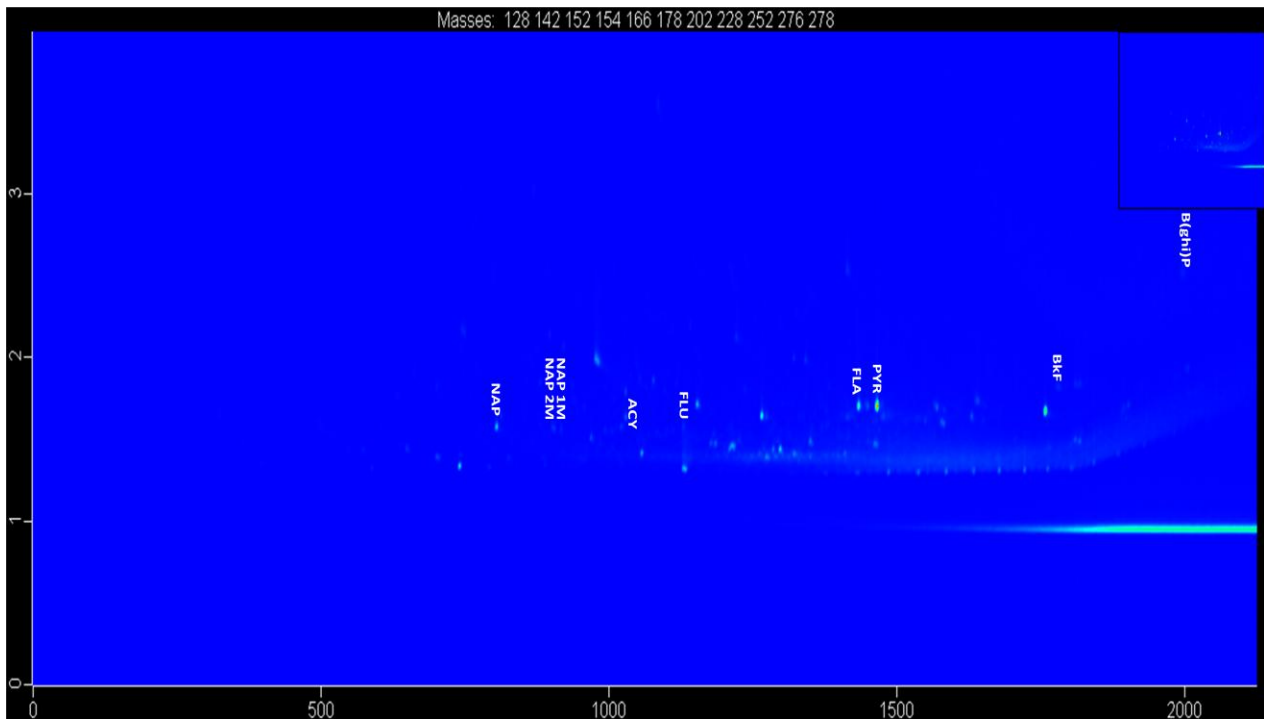
7-1 Reconstructed 1st dimension extracted ion chromatograms for typical PDMS degradation product ions (73, 207, 211 and 281 Da) for a LHD exhaust sample



7-2 Contour plot of a reconstructed ion chromatogram for typical PDMS degradation product ions (73, 207, 211 and 281 Da) for a LHD exhaust sample



7-3 Contour plot of a reconstructed ion chromatogram (128, 142, 152, 154, 166, 178, 202, 228, 252, 276, and 278 Da) of a thermally desorbed PDMS primary trap sample (gas phase) taken at a Load Haul Dump (LHD) vehicle exhaust



7-4 Contour plot of a reconstructed ion chromatogram (128, 142, 152, 154, 166, 178, 202, 228, 252, 276, and 278 Da) of a thermally desorbed quartz fibre filter sample (particle phase) taken in an underground workshop

## Appendix B: Project outputs

### 7.1 Publications

Forbes P.B.C., Karg, E.W., **Geldenhuis G.**, Nsibande S.A., Zimmermann, R. and Rohwer, E.R., Characterisation of atmospheric semi-volatile organic compounds, *The Clean Air Journal*, 2013, 23 (1), 3-6, ISSN 1017-1703.

### 7.2 Conference proceedings

Forbes P.B.C., **Geldenhuis G** and Rohwer E.R., "Characterisation of atmospheric polycyclic aromatic hydrocarbons in South African platinum mines", 11th GCxGC Symposium and 38th International Symposium on Capillary Chromatography, 18-24 May 2014, Riva del Garda, Italy.

**Geldenhuis G.**, Rohwer E.R. and Forbes P.B.C., "Chromatographic analysis of diesel particulate matter in South African Platinum Mines with emphasis on polycyclic aromatic hydrocarbons", IUAPPA/National Association of Clean Air (NACA) 2013 Conference, 29 September - 4 October 2013, Cape Town.

**Geldenhuis G.**, Rohwer E. and Forbes P., "Atmospheric polycyclic aromatic hydrocarbon fingerprinting in South African platinum mines", 12th International Chemistry Conference Africa 2013, 7-12 July 2013, Pretoria.

**Geldenhuis G.**, Rohwer E.R. and Forbes P.B.C., "Analysis of diesel particulate matter and polycyclic aromatic hydrocarbons in confined environments", National Association of Clean Air (NACA) 2012 Conference, 1-2 November 2012, Rustenburg.

\* awarded the Best Student Poster award for presentation.

Nsibande S., **Geldenhuis G.** and Forbes P.B.C., "Characterisation of particulate matter in the Daspoort Tunnel, Pretoria", National Association of Clean Air (NACA) 2012 Conference, 1-2 November 2012, Rustenburg. Annual Conference Proceedings ISBN 978-0-620-53886-2, Electronic Proceedings ISBN 978-0-620-53885-5.

**Geldenhuis G.**, Rohwer E.R. and Forbes P.B.C., "Analysis of diesel particulate matter and polycyclic aromatic hydrocarbons in confined environments", ChromSAAMS 2012 Conference, 7-10 October 2012, Dikhololo.

P.B.C. Forbes and **G. Geldenhuis**, "Careers in Science: Chemistry", A Day of Discovery, St Mary's Diocesan School for Girls, 7 June 2012, Pretoria.

7.2.1 Poster presentation

# Analysis of diesel particulate matter and polycyclic aromatic hydrocarbons in confined environments

Geldenhuis G<sup>1,2</sup>, Rohwer ER<sup>1</sup> and Forbes PBC<sup>1</sup>

<sup>1</sup> Department of Chemistry, Faculty of Natural and Agricultural Sciences, University of Pretoria, Lynnwood Road, 0002

<sup>2</sup> Mineral Processing Laboratory, Impala Platinum Limited, 123 Bethlehem Drive, Rustenburg, 0299

## INTRODUCTION

The International Agency for Research on Cancer, which is part of the World Health Organization (WHO), recently classified diesel engine exhaust as **carcinogenic to humans - Group 1** (IARC, 2012). Evidence reveals that exposure is associated with an increased risk for lung cancer. In addition to lung cancer, cancers of the bladder and lymphatic tissue are the other most common cancers associated with exposures to diesel exhaust emissions (Lewtas, 2007).

Polycyclic aromatic hydrocarbons (PAHs) adsorb onto diesel particulate matter (DPM) and are common by-products of incomplete diesel combustion. PAHs are toxic to humans and animals (Lewtas, 2007).

The wide use of trackless diesel vehicles underground poses a risk towards the health and safety of employees due to exposure to diesel exhaust emissions. Sampling was performed at 3 different Platinum mines in South Africa. Not only is DPM exposure an occupational threat for mine workers but is potentially a risk for everyday road users which is why samples were also taken in the Daspoort tunnel in Pretoria.

The particulate matter was characterised by means of scanning electron microscopy (SEM) and comprehensive two dimensional gas chromatography with mass spectrometric detection (GCxGC-MS).



Fig. 1 Sources of DPM: (A) Load haul dump (LHD) vehicle and (B) diesel powered vehicle.

## EXPERIMENTAL

### SAMPLING

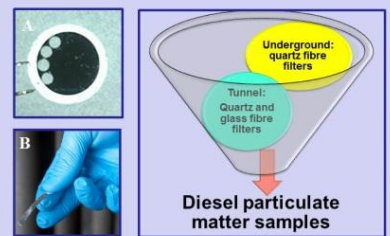


Fig. 2 (A) Heavily loaded DPM filter and (B) tunnel swab.

### Tunnel samples

Tunnel weekly samples: A Thermo Scientific Area Dust Monitor, Model ADR-1500, sampled at 1.19 l.min<sup>-1</sup> onto a Whatman 934-AH 37 mm glass filter paper.

Tunnel swab samples: Whatman quartz fibre filter strips were used to take swab samples from a hand rail in the tunnel to determine aged soot composition.

### Underground samples

Sampled onto quartz fibre filters according to NIOSH 5040 method. Heavy, medium & lightly loaded filters from each Platinum mine were selected for analysis.

### TD-GCxC-TOFMS

5mm diameter punches from the filters were used for analysis. Comprehensive two dimensional gas chromatography with time of flight mass spectrometric detection (GCxGC-TOFMS, LECO Pegasus 4D) was employed in the analysis of thermally desorbed (Gerstel) filters (particle associated organic emissions). Helium was used at a desorption flow rate of 100 ml.min<sup>-1</sup> and analytes were cryogenically focussed at -50 °C. The primary column was a 30 m RTX 55iIMS (250 µm id; 0.25 µm film thickness) and the secondary column was a 1.79 m RTX 200 (150 µm id; 0.15 µm film thickness). The modulation period was 4 s.

### SCANNING ELECTRON MICROSCOPE

A 5mm punch from quartz and glass fibre filters were sputter coated with gold prior to analysis by SEM (JSM 5800LV).

## RESULTS

Fig. 3 DPM composition in tunnel and underground samples based on the peak areas of filter punches by TD-GCxC-MS.

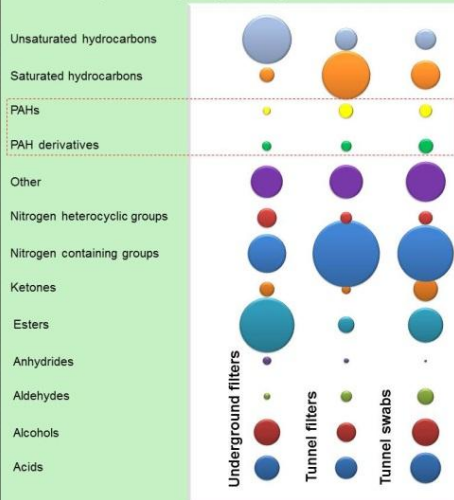


Fig. 4 Ratio % Area of PAHs and PAH derivatives for (A) underground filters, (B) tunnel filters and (C) tunnel swabs.

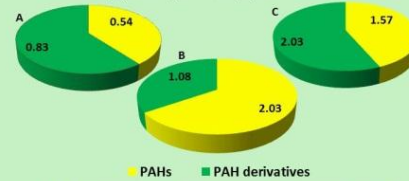


Fig. 5 PAH composition in tunnel and underground samples.

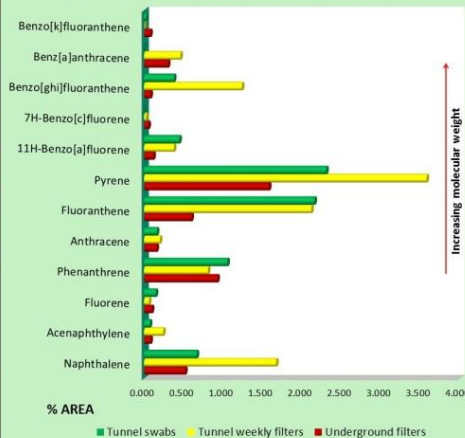
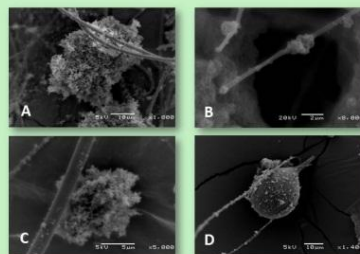


Fig. 6 SEM images of underground (A, B) and tunnel samples (C, D).



## DISCUSSION & CONCLUSIONS

From the bubble plot in Fig. 3 it can be seen that the general composition of DPM is consistent throughout the samples. The high level of unsaturated hydrocarbons indicate inefficient fuel combustion. The highest percentage of unsaturated hydrocarbons is clearly seen in the underground samples, which may be attributed to the generally more aged and worn vehicles underground that do not operate optimally. Esters and nitrogen containing compounds were also found abundantly in the samples.

The fresh, weekly tunnel samples reflect more PAHs than PAH derivatives however the opposite is seen for the underground and tunnel swab samples (Fig. 4). Derivatives are formed due to the transformations and atmospheric reactions that PAHs undergo such as the reactions with: ozone (O<sub>3</sub>), as well as hydroxyl (•OH) and nitrate (•NO<sub>3</sub>) radicals to form a wide range of derivatives.

Pyrene is by far the most abundant PAH found in both underground and tunnel samples. Fluoranthene, phenanthrene and naphthalene were seen in all samples in relatively high amounts.

The heavier PAHs such as benzo(e)pyrene, benzo(k)fluoranthene and indeno (1, 2, 3-cd) pyrene were found in the underground filters and not in the tunnel filters. Benzo(a)pyrene is considered as one of the most carcinogenic PAHs hence its use as an environmental PAH exposure indicator (Ono-Ogasawara & Smith, 2004).

The SEM images in Fig. 6A & C reveal similar carbonaceous DPM agglomerates in both tunnel and underground samples. The findings were consistent with the literature (Ancelet *et al.*, 2011). Particulate matter smaller than 2.5 µm in diameter can be inhaled by humans and penetrate into the lungs resulting in cardiopulmonary health effects (Yu *et al.*, 2011). Fig. 6B shows the fine particles present in the DPM samples. These small particles contain adsorbed PAHs as seen in Fig. 7 below.



Fig. 7 The physico-chemical composition and structure of DPM (adapted by Maricq, 2007). Green portion represents adsorbed hydrocarbons on the soot.

Future work: this study focused on particulate matter only however, PAHs coexist in particulate and gaseous phase. It is recommended to use denuder sampling devices to trap PAHs in gas and particulate form after which characterisation and quantification should be performed to indicate potential human health and environmental risks corresponding to each phase.

## REFERENCES

- Ancelet, T., Davy, P.K., Trompeter, W.J., Markwitz, A., & Weatherburn D.C. 2011, *Atmospheric Environment*, 45: 4463-4469.
- IARC. 2012, IARC (International Agency for Research on Cancer), World Health Organisation, 2012, 'Diesel engine exhaust carcinogenic', Press Release no. 213, 12 June 2012.
- Lewtas, J. 2007, *Mutation Research - Reviews in Mutation Research*, 636: 95-133.
- Maricq, M. 2007, *Journal of Aerosol Science*, 38: 1079-1118.
- Ono-Ogasawara, M. & Smith, T.J. 2004, *Industrial Health*, 42: 389-399.
- Yu, C., Fan, Z., McCandlish, E., Stern, A.H. & Lioy, P.J. 2011, *Journal of Air and Waste Management*, 61: 1015-1025.

## ACKNOWLEDGEMENTS

- Department of Chemistry, University of Pretoria, South Africa, with special thanks to Yvette Naudé for all your technical assistance.
- LECD Africa, specifically Peter Gorst-Aliman for use of the LECD instrument.
- CSIR, Centre for Mining Innovation, particularly Cecilia Pretorius.
- CSIR, Natural Resources & the Environment.
- Ero Technologies for use of the Area Dust Monitor as well as assistance with the tunnel sampling.
- University of Pretoria Microscopy Unit
- Platinum Mines
- ChromSA for generous funding to attend ChromSAAMS 2012
- Impala Platinum for the opportunity to do my MSc as well as the sponsorship they provided.



## 7.2.2 Paper presentation

### Chromatographic analysis of diesel particulate matter in South African platinum mines with emphasis on polycyclic aromatic hydrocarbons

Genna-Leigh Geldenhuys G<sup>\*1,2</sup>, Egmont R. Rohwer<sup>1</sup> and Patricia B.C. Forbes<sup>1</sup>

<sup>1</sup>Laboratory for Separation Science, Department of Chemistry, Faculty of Natural and Agricultural Sciences, University of Pretoria, Lynnwood Road, Pretoria, 0002, South Africa, patricia.forbes@up.ac.za

<sup>2</sup>Impala Platinum Limited, Mineral Processing Laboratory, 123 Bethlehem Drive, Rustenburg, 0299, South Africa, Genna-Leigh.Geldenhuys@implats.co.za

Diesel engines are used widely throughout the mining industry; however they emit a mixture of gaseous and particulate pollutants. Multi-channel silicone rubber traps were used in a denuder configuration with quartz fibre filters to trap polycyclic aromatic hydrocarbons (PAHs) in gas and particulate phases. Samples were analysed directly using thermal desorption-GCxGC-ToFMS. Higher concentrations of PAHs were found in the gas phase than in the particulate phase with a prevalence of naphthalene and its methylated derivatives. The samples taken directly at the vehicle exhaust corresponded to the highest concentration of PAHs and also contained some of the heavier PAHs. This work highlights the need to establish South African occupational exposure limits for diesel particulate matter (DPM) and PAHs.

*Keywords:* polycyclic aromatic hydrocarbons, diesel particulate matter, gas chromatography, diesel exhaust emissions.

## 1. Introduction

Diesel engines are widely used for transportation, mining, construction and in many other industries due to their high power output. Diesel exhaust emissions (DEE) are a mixture of gaseous and particulate substances originating from unburned fuel, lubricant oil and combustion products (Ono-Ogasawara, 2004). Main constituents of DPM are elemental carbon (EC) and organic carbon (OC). The OC fraction contains trace concentrations of polycyclic aromatic hydrocarbons (PAHs) and their methylated, nitrated and oxygenated derivatives (Ono-Ogasawara 2004). Diesel engine PAH particulate emissions originate from high temperature combustion of fossil fuels (pyrosynthesis of aromatic compounds), unburned fuel and lubricating oil (Borrás 2009).

Exposure to DEE has been linked to an array of respiratory and allergic diseases (Laumbach 2012) and has recently been confirmed as carcinogenic (IARC 2012). Concentrations of DPM and PAHs in platinum mine environments are likely to be higher than in ambient air. The high numbers of heavy duty diesel powered vehicles that are used underground serve as sources of PAHs. The aim of the research presented was to test the application of a novel denuder sampling device for underground environments and use the results to conduct a preliminary survey to evaluate exhaust emissions from different areas (from different

mines) in shafts where diesel engines are used (diesel shafts) and those where diesel engines are not used (non-diesel) for comparison. The PAH emissions from different areas were compared as was the PAH fingerprints in both gaseous and particulate phases.

## 2. Method

### 2.1 Sampling setup

The mine samples were collected with Gilair personal sampling pumps that were attached to denuder sampling devices via rubber tubing. The denuders consisted of two multi-channel silicone rubber traps (MC22) separated by a 6 mm diameter quartz fibre filter, held in position by a Teflon connector, this configuration allowed for both gas and particulate phase sampling (Forbes 2012). The gas phase semi volatile organic compounds (including PAHs) were trapped by the first (primary) trap as the polydimethylsiloxane serves as a solvent for these compounds and the particles were trapped downstream on the quartz fiber filter. The post filter trap (secondary trap) served to sample any remaining gas phase SVOCs including PAHs that had blown off from particles or had broken through from the primary trap. A low flow rate of approximately 500 ml.min<sup>-1</sup> and a sampling time of 10 min was used to prevent breakthrough of volatile compounds.

## 2.2 Sampling sites

Samples were taken from diesel shafts as well as non-diesel shafts from three underground platinum mines (Plat mine A, B & C) in the North West province of South Africa (see Figure 1). The samples from the diesel shafts included: ambient samples from a general mining area (10 minute and 30 minute sampling periods), ambient samples from within a workshop (10 minutes) and exhaust samples (10 minutes). The non-diesel shaft sample consisted of a 10 minute ambient sample taken from a general working area.



Figure 1 Provincial map of South Africa (*Map of South Africa, n.d.*)

## 2.3 Instrumental analysis

The TD-GCxGC-ToFMS that was employed was a Pegasus 4D system (Leco, St. Joseph, MI, USA), equipped with an Agilent Technologies 6890 GC (Palo Alto, CA, USA). Data acquisition and processing was carried out using ChromaTOF software version 4.0 (LECO Corp., St. Joseph, MI). The GC column set consisted of a Rxi-5Sil, 5%-phenyl-95%-methylsiloxane (30 m, 0.25 mm i.d., 0.25  $\mu\text{m}$  df) as the first dimension (1D) and a Rxi-200 (Restek), 50%-phenyl-50%-methylsiloxane (1.5 m, 0.1 mm i.d., 0.1  $\mu\text{m}$  df) as the second dimension (2D). All columns were obtained from Restek (Bellefonte, PA, USA). Thermal desorption was carried out at 280  $^{\circ}\text{C}$  for 5 minutes after which the desorbed semi-volatiles were cryogenically focused via a cooled injection system (CIS) at -50  $^{\circ}\text{C}$  using liquid nitrogen. The temperature was rapidly ramped to 280  $^{\circ}\text{C}$  in order to introduce the analytes onto the GC. The primary oven was ramped at 10  $^{\circ}\text{C min}^{-1}$  from 40  $^{\circ}\text{C}$  to 315  $^{\circ}\text{C}$  which was held for 5 min and the secondary oven was

ramped at 10  $^{\circ}\text{C min}^{-1}$  from 45  $^{\circ}\text{C}$  to 320  $^{\circ}\text{C}$  which was also held for 5 min. The MS transfer line temperature was set to 280  $^{\circ}\text{C}$  with a modulator temperature offset of 30  $^{\circ}\text{C}$ . The modulation period was 4 s with a hot pulse time of 1.0 s. The electron energy was 70 eV.

Thousands of peaks were found in the two-dimensional chromatograms when the automated peak identification routine methods were used, based on deconvolution. Single ion masses of PAHs were extracted and classified and the NIST library was consulted to compare the similarities of spectra, where only library matches of greater than 80% were used for tentative identification purposes. Individual peak areas were automatically acquired, and compound identification was performed by comparison with pure and mixed PAH standards (Supelco, Bellefonte, USA), where the exact retention times and elution orders were obtained.

## 3. Results and discussion

The PAHs that were detected in the gas phase samples were the more volatile PAHs such as naphthalene and its mono methylated derivatives. The PAH composition can be seen in Figure 2 which gives an indication of which PAHs were prominently detected in each phase and it was expressed as total PAH peak area (normalised per litre of air sampled) for all of the samples.

The PAHs that were detected in the particulate phase were the heavier, less volatile PAHs with pyrene being the most dominant PAH. The difference in the PAH fingerprint in each phase confirms the theory behind the denuder sampling device. Benzo(a)pyrene, benzo(e)pyrene, indeno(1,2,3-cd)pyrene and benzo(ghi)perylene were amongst the heavier PAHs that were detected underground and were mainly seen in the samples that were taken at the diesel engine exhaust. The heavier PAHs are associated with cold start conditions of diesel vehicles and it should be noted that the nature of the emissions are affected by the way the vehicle was operated and maintained. Figure 3 shows the total detected PAHs at each sampling location and it differentiates between the three different mines. Gas phase and particle phase are represented by the 1st trap and filter samples respectively as we were working under breakthrough conditions and thus the 2nd trap content is inconsistent with blow off only. From the scales of the two graphs it can be seen that PAHs were predominantly found in the gas phase which emphasises the need for gas phase sampling as sampling of only one phase would lead to an underestimation of potential human exposure.

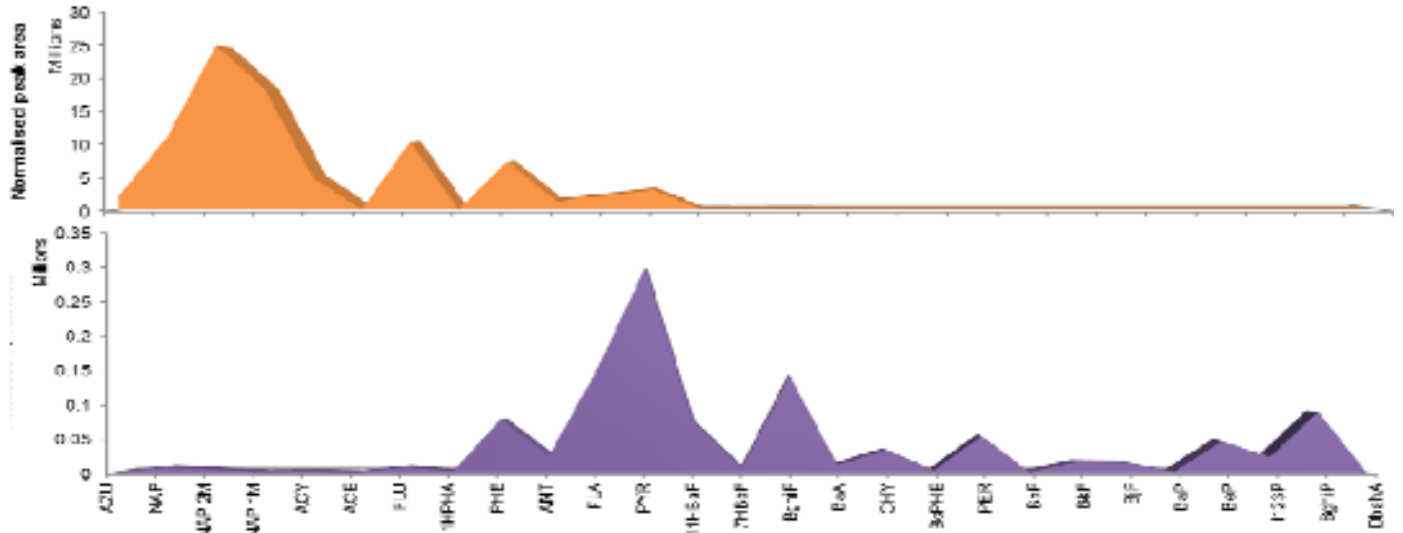


Figure 2 Total PAH peak areas (combination of all of the samples) that were detected in gaseous phase (top) and particulate phase (bottom). See Appendix A for an abbreviation list.

The samples that were taken at the vehicle exhausts had the highest peak areas for PAHs in both phases which was expected as the samples were taken directly at the source of the emissions. Plat mine A showed the highest PAH peak areas in the exhaust samples which can be attributed to the specific vehicle that was sampled with respect to age and maintenance of the vehicle as well as the

cold start conditions during the sampling period. Plat mine C showed the highest PAH peak areas for all of the ambient samples with significantly high peak areas found in the workshop sample. The workshops are used to store and service all of the vehicles and can have a high volume of vehicles at a given time which will influence the concentration of diesel exhaust emissions and thus PAHs. It

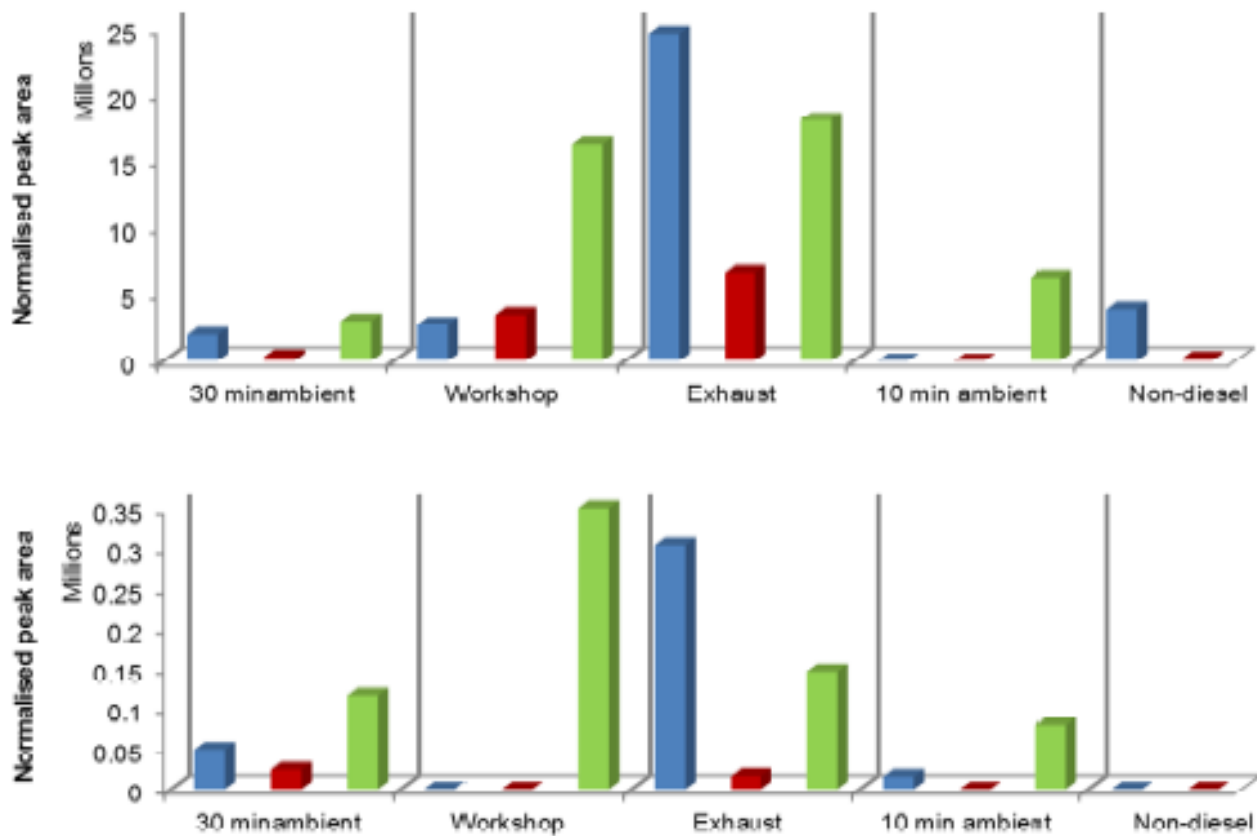


Figure 3 Total PAH peak areas that were detected in gas phase (top graph) and particle phase (bottom graph) from each mine at different sample locations. Plat mines A, B & C are represented by blue, red & green bars respectively.

should be noted that the samples that were taken are grab samples therefore they do not represent an area, shaft or mine as a whole but merely give a snapshot look at the instantaneous environmental conditions. Plat mine B showed generally the lowest amounts of PAHs for every sample type. There was no 10 min ambient samples from Plat mine B therefore they are not included in this discussion. The non-diesel shafts showed less PAH particle loading than the diesel shafts and low levels of gas phase PAHs which indicates that diesel exhaust emissions are the main source of PAHs in underground environments.

#### 4. Conclusion

PAHs that were detected underground range from 2 ringed gas phase PAHs that were found on the trap samples to benzo(ghi)perylene which was detected on the filter samples. PAHs were predominantly found to exist in the gas phase with naphthalene and its mono methylated derivatives being the most abundant. Pyrene was the most abundant particulate phase PAH that was detected. The use of this small, portable denuder proved to be a very effective device for this investigative preliminary study. Samples taken at the exhaust were found to have the highest amounts of PAHs in both phases. The three investigated mines showed varying amounts of PAHs which can be attributed to the fact that the instantaneous environments whilst sampling were different at each mine with respect to the number and type of possible emission sources that were observed.

#### 5. Acknowledgments

Resources provided by Leco Africa are gratefully acknowledged. Thanks to the CSIR, Centre for Mining Innovation particularly Cecilia Pretorius. Thank you to the NRF and SASOL for the finance that was generously provided. Impala Platinum is acknowledged for granting Genna-Leigh Goldenhuys study leave and funding in order for her to complete her MSc. The Plat Mines are gratefully acknowledged for funding and guided underground sampling visits. Yvette Naudé is thanked for technical assistance.

#### 6. References

Borrás E., Tortajada-Genaro L.A., Vázquez M. & Zielinska B. 2009, 'Polycyclic aromatic hydrocarbon exhaust emissions from different reformulated diesel fuels and engine operating conditions', *Atmospheric Environment* **43**:5944-5952.  
 Forbes P.B.C., Karg E.W., Zimmermann R. & Rohwer E.R. 2012, 'The use of multi-channel silicone rubber traps as denuders for polycyclic

aromatic hydrocarbons', *Analytica Chimica Acta* **730**:71-79.

IARC (International Agency for Research on Cancer) 2012, 'Diesel engine exhaust carcinogenic'. Press Release no. 213.

Laumbach R.J. and Kipen H.M. 2012, 'Respiratory health effects of air pollution: Update on biomass smoke and traffic pollution', *Journal of Allergy and Clinical Immunology* **129**:3-11.

Ono-Ogasawara M. and Smith T.J. 2004, 'Diesel exhaust particles in the work environment and their analysis', *Industrial Health*. **42**:389-399.

*Provincial map of South Africa*, n.d. image, viewed 19 June 2013, <<http://www.agsa.co.za/AboutUs/Ourregionaloffices.aspx>>

#### Appendix A

List of PAHs and their corresponding abbreviations.

Name of PAH	Abbreviaton
Azulene	AZU
Naphthalene	NAP
Naphthalene, 2-methyl-	NAP 2M
Naphthalene, 1-methyl-	NAP 1M
Acenaphthylene	ACY
Acenaphthene	ACE
Fluorene	FLU
1H-Phenalene	1HPHA
Phenanthrene	PHE
Anthracene	ANT
Fluoranthene	FLA
Pyrene	PYR
11H-Benzo[a]fluorene	11HBaF
7H-Benzo[b]fluorene	7HBbF
Benzo[ghi]fluoranthene	BghiF
Benz[a]anthracene	BaA
Chrysene	CHY
Benzo[c]phenanthrene	BcPHE
Perylene	PER
Benzo[b]fluoranthene	BbF
Benzo[k]fluoranthene	BkF
Benzo[j]fluoranthene	BjF
Benzo[a]pyrene	BaP
Benzo[e]pyrene	BeP
Indeno[1,2,3-cd]pyrene	I123P
Benzo[ghi]perylene	BghiP
Dibenz[a,h]anthracene	DbahA

## 7.2.3 Journal publication

### Characterisation of atmospheric semi-volatile organic compounds

Patricia B.C. Forbes<sup>1\*</sup>, Erwin W. Karg<sup>2</sup>, Genna-Leigh Geldenhuys<sup>1,3</sup>, Sifiso A. Nsibande<sup>1</sup>, Ralf Zimmermann<sup>2,4</sup> and Egmont R. Rohwer<sup>1</sup>

<sup>1</sup> Laboratory for Separation Science, Department of Chemistry, University of Pretoria, Lynnwood Road, Pretoria, 0002, South Africa, patricia.forbes@up.ac.za

<sup>2</sup> Cooperation Group "Analysis of Complex Molecular Systems", Joint Mass Spectrometry Centre, Helmholtz Zentrum München, D-85758 Neuherberg, Germany

<sup>3</sup> Mineral Processing Laboratory, Impala Platinum Limited, 123 Bethlehem Drive, Rustenberg, 0299

<sup>4</sup> University of Rostock, Division of Analytical and Technical Chemistry, D-18059 Rostock, Germany

Atmospheric semi-volatile organic compounds (SVOCs), including polycyclic aromatic hydrocarbons (PAHs), are ubiquitous environmental pollutants, which may be present in the gaseous phase and adsorbed onto the surface of aerosol particles. A novel portable miniature denuder consisting of two multi-channel silicone rubber traps separated by a quartz fibre filter has been developed for such applications. It allows for the concentration of SVOCs in each phase to be determined, which is important for human health risk assessments. The overall particle transmission efficiency through the denuder was found to be  $92 \pm 4\%$  for particles between 16 and 320 nm. SVOCs in the traps (gas phase) or on the filter (particle phase) are analysed by GC-MS, or by GCxGC-MS for enhanced separation capability. This enhances detection limits and allows for lower sampling flow rates and shorter sampling times. These denuders have been applied in studies involving the monitoring of emissions from domestic fires, vehicles and underground mine diesel engines.

**Keywords:** denuder; particulate matter; aerosol; semi-volatile organic compounds; polycyclic aromatic hydrocarbons; silicone; GCxGC-MS; air quality; human health.

## 1. Introduction

Atmospheric semi-volatile organic compounds (SVOCs), including polycyclic aromatic hydrocarbons (PAHs), are emitted from widespread anthropogenic sources such as domestic fires and internal combustion engines. This is of concern due to the potential human health effects of a number of these compounds, especially in light of the recent declaration of diesel exhaust emissions as a human carcinogen (IARC, 2012).

In the atmosphere, SVOCs partition between the vapour phase and particulate phase, where they are adsorbed onto the surface of aerosols. This partitioning depends on the vapour pressure of the particular SVOC as well as the total suspended particulate loading and may be described in terms of a partition coefficient,  $K_{p,g}$  (Krieger and Hites, 1994).

It is important to be able to quantify the relative contributions of each of these phases of the analyte, as they may have different environmental impacts. Deposition and uptake of inhaled toxic species in the human respiratory system depends on phase distribution (Temime-Roussel, 2004a). Environmental cycling, such as atmospheric transport and transformations, are also phase dependent (Bidleman, 1988).

Sampling of each of these phases is complex, as it must be ensured that blowoff of particle adsorbed analyte does not occur (which would underestimate the particle phase concentration and overestimate the gas phase). Similarly, adsorption of gas phase

analyte onto the particles collected during sampling must be prevented (this would underestimate gas phase concentrations and overestimate particle phase loading).

This paper describes a novel, miniature and portable denuder device which has been shown to be effective in sampling and pre-concentrating atmospheric SVOCs in both the gas and particle phases.

## 2. Methodology

### 2.1 The denuder device

The denuder consists of two multi-channel silicone rubber traps in series, which are separated by a 6 mm diameter quartz fibre filter held in place by a Teflon connector. Each trap contains 22 parallel polydimethylsiloxane (PDMS) tubes (55 mm long, 0.3 mm i.d. and 0.64 mm o.d.) which are housed in a 178 mm long glass tube (Fig. 1).

The gas phase SVOCs are sorbed into the PDMS in the first (primary) trap (Ortner, 1996), whilst particle phase analytes pass through the trap and are collected on the downstream filter. The transmission efficiency was evaluated theoretically and was found to be promising, therefore particle transmission tests were performed to confirm these results, as discussed in Section 2.2. Blowoff of SVOCs from the filter should be minimal due to the low pressure drop across the sampling system, the short sampling time (10 min) and the constant ambient sampling temperature. However, any gas phase analytes

which breakthrough the primary trap are collected on the downstream secondary PDMS trap.

## 2.2 Laboratory particle transmission tests

A multi-channel silicone rubber trap and a bypass line were connected in parallel by means of electrically conducting tubing with valve connections to allow for switching of aerosol flow between them (Forbes, 2012). The flow rate in each line was maintained at  $500 \text{ mL}\cdot\text{min}^{-1}$ , which is the same flow rate as used in

the denuder field applications.

Ammonium sulphate aerosol particles were generated by a jet nebulizer (Trijet, Model 3460, TSI, USA). The particle size distribution had a modal diameter of  $\sim 50 \text{ nm}$  and there were  $>10^5 \text{ particles}\cdot\text{cm}^{-3}$ . Particle size analysis was performed by a scanning mobility particle sizer (SMPS, Model 3081, TSI, USA) and a condensation particle counter (CPC, Model 3775, TSI, USA) was used to determine particle number concentrations (Fig. 2).

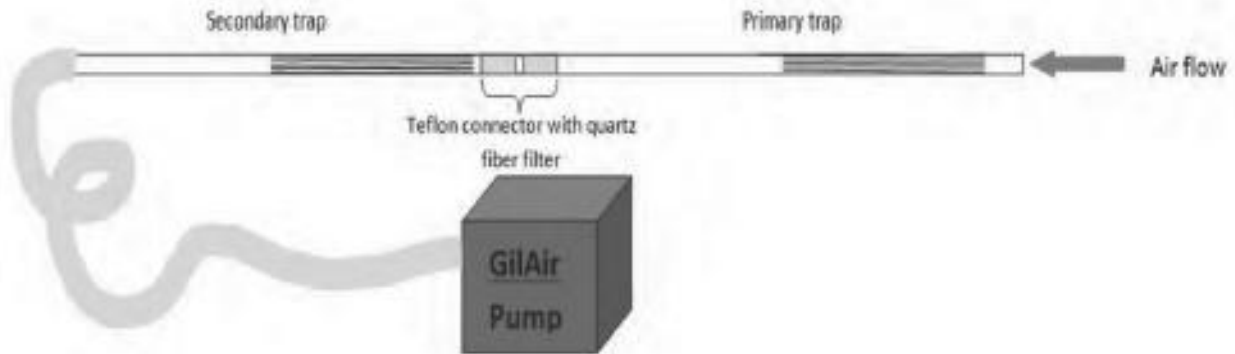


Figure 1 Multi-channel silicone rubber trap based denuder device.

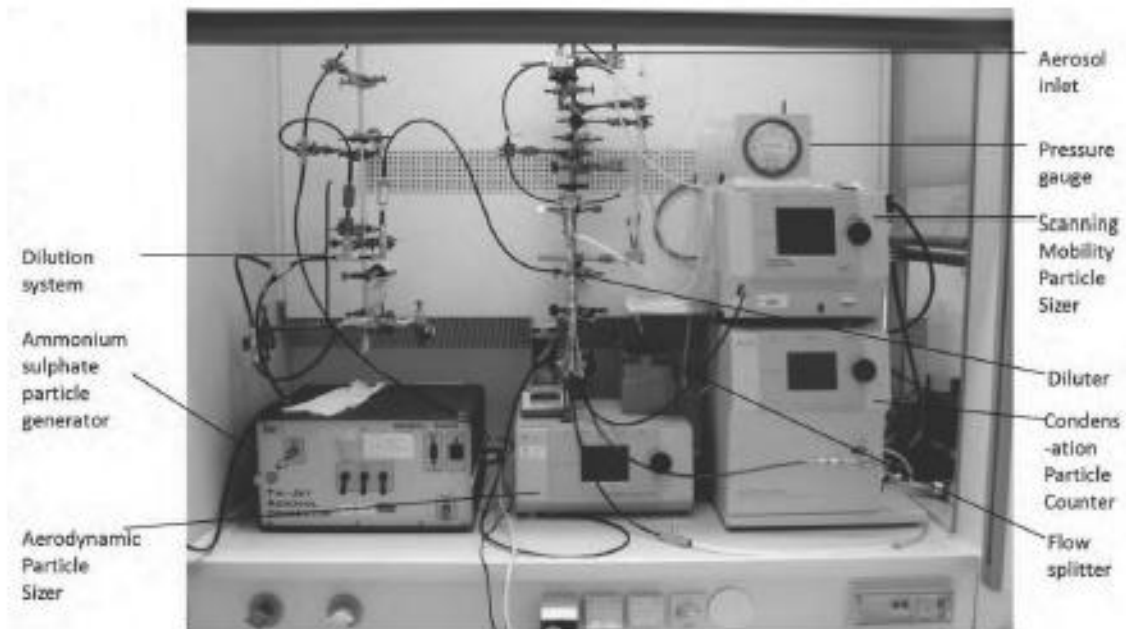


Figure 2 Experimental setup used for the determination of the denuder particle transmission efficiency.

## 2.3 Field applications

Domestic fires (wood and charcoal fuel mix) were lit in traditional braziers using either the traditional or the basa njengo Magogo (upside down) methods of lighting a fire. Air samples were taken at the fire using our denuder device coupled to a portable Gilair sampling pump operating at  $500 \text{ mL}\cdot\text{min}^{-1}$  for 10 min. The traditional fire was sampled 40 min after ignition, whilst the basa njengo Magogo fire was sampled directly after ignition.

Similarly, air samples were taken at the exhaust of an idling diesel passenger vehicle under cold start conditions. Here 2 traps in series as well as an empty glass tube followed by a filter and a secondary PDMS trap were used to sample both in parallel to a full denuder setup.

In a third study, air samples were taken onto denuders in underground platinum mines.

## 2.4 Analytical methodology

Comprehensive two-dimensional gas chromatography with time of flight mass spectrometric detection (GCxGC-TOFMS, LECO Pegasus 4D) was employed in the analysis of thermally desorbed (TD) (Gerstel TDS 3) filter samples (particle associated SVOC emissions) and silicone rubber traps (gas phase SVOC emissions). Helium was used at a desorption flow rate of  $50 \text{ mL}\cdot\text{min}^{-1}$  and analytes were cryogenically focussed at  $-40 \text{ }^\circ\text{C}$ . The primary column was a 30 m RTx 5SiMS ( $250 \mu\text{m}$  id;  $0.25 \mu\text{m}$  film thickness) and the secondary column was a 0.790 m RTx 200 ( $180 \mu\text{m}$  id;  $0.2 \mu\text{m}$  film thickness). The modulation period was 4 s.

## 3. Results and discussion

The particle transmission efficiency was determined from the ratio of the denuder and bypass particle concentrations, and was found to be  $92 \pm 4\%$  and the particles ranged from 16 to 320 nm. The transmission efficiency was found to be constant during the sampling period. The median diameter of the particles transmitted by the denuder was 64 nm and 59 nm for the bypass.

The particle size distributions of transmitted particles was very similar for the denuder and bypass line for particle sizes  $>100 \text{ nm}$ . However, the transmission efficiency of the denuder decreased for particles  $<80 \text{ nm}$ , with transmission efficiencies of  $<60\%$  for particles  $<20 \text{ nm}$ . It is likely that electrostatic and diffusional effects contributed to loss of these very small particles inside the denuder.

TD-GCxGC-MS analysis of the gas phase domestic fire samples yielded chemical fingerprints of the semi-volatile organic compounds present based on relative peak areas and MS library matching (Fig. 3). Differences between the two compound classification profiles are evident, and the traditional fire appeared to have poorer combustion conditions (higher unsaturated hydrocarbon levels) even 40 min after ignition, by which time combustion conditions should have been favourable. Higher levels of PAHs and PAH derivatives were found in the case of the traditional fire.

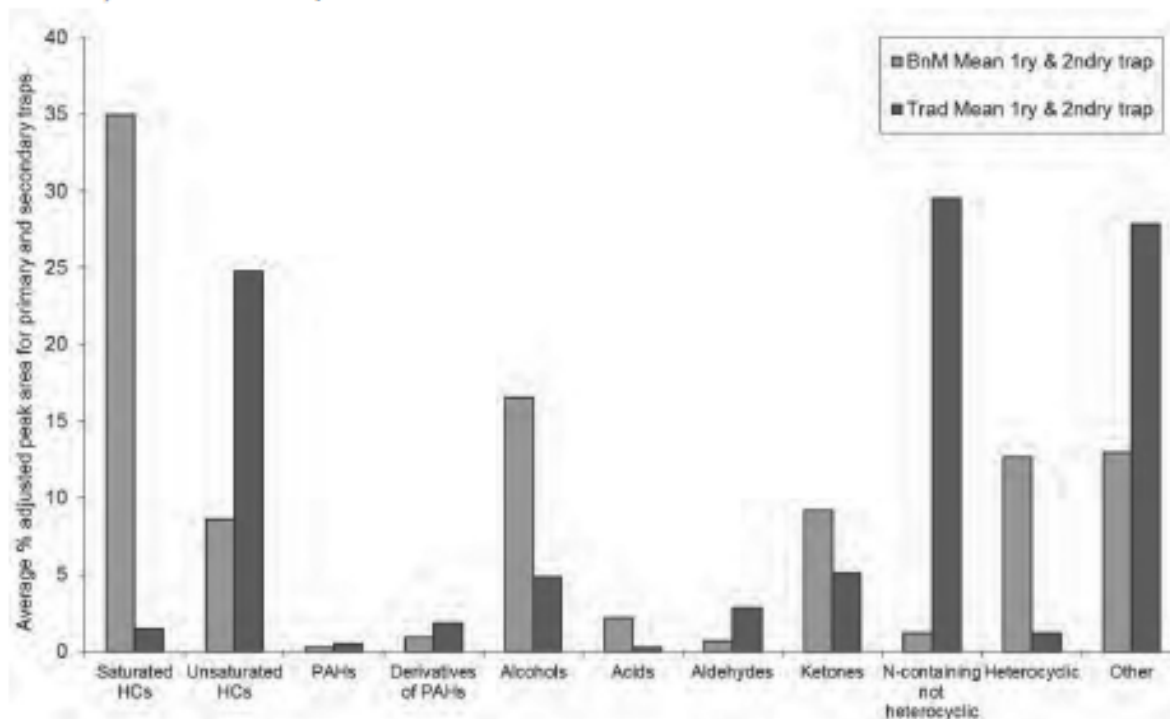


Figure 3 Gas phase semi-volatile organic compound profiles (primary and secondary trap) found for the traditional and the Basa njengo Magogo domestic fire lighting methods.

Analysis of the naphthalene content of the vehicle exhaust samples revealed that no gas phase naphthalene was adsorbing onto the filter or sampled particulate matter, as the same amount of this PAH was found in the primary trap of the trap-trap and in the trap of the tube-filter-trap configurations (Forbes, 2012). Moreover, no breakthrough of naphthalene was evident, in that this compound was not detected in the secondary trap of the denuder sample (the sampling volume was 5 L).

The underground mining samples contained a range of SVOCs, including PAHs, with one of the main sources of these compounds being diesel engine exhaust emissions. The denuder samples were taken in a range of underground environments, and allowed for the chemical fingerprinting of compounds present in both gas and particle phases. The results (which are provided in more detail in a separate paper to this conference) revealed the importance of sampling both phases in order to prevent the underestimation of concentrations and therefore exposures.

There was also a clear difference in SVOC and specifically PAH profiles between the gas and particle phase samples. Heavier PAHs were found associated with the particles, whilst the lighter PAHs, including naphthalene and methylated naphthalene derivatives, dominated the gas phase profiles. In addition, principal component analyses (PCA) confirmed that the denuder was operating effectively, as the gas (trap) and particle (filter) phase samples were clearly separated.

#### 4. Conclusion

From a theoretical perspective, this novel denuder met the requirements to effectively sample gas and particle phase SVOCs concurrently. Particle transmission experiments confirmed that  $92 \pm 4\%$  of particles ranging from 16 to 320 nm were transmitted by the multi-channel silicone rubber trap. Transmission efficiency through the trap was  $\sim 100\%$  for particles  $>50$  nm at a flow rate of  $500 \text{ mL}\cdot\text{min}^{-1}$ . It has been reported that  $>95\%$  of particle bound PAHs are associated with particles in the size range between 0.1 and 8  $\mu\text{m}$  (Temime-Roussel, 2004b), and the denuder transmits particles very efficiently in this size range.

TD-GC $\times$ GC-MS analysis allowed for the identification of SVOCs, including PAHs, present in the gas and particle phases, as each component of the denuder (PDMS traps and the filter) is analysed separately.

The denuder has been shown to operate effectively in a range of applications, including domestic fuel combustion and in monitoring emissions from diesel engines, both from passenger vehicles and in underground mines.

The denuder is small and is highly portable, and only requires the use of a small, portable battery operated sampling pump.

The German-South African Year of Science Programme is acknowledged for funding. LECO South Africa, SASOL and the NRF are thanked for resources provided. The CSIR and Plat Mines are acknowledged for funding and assistance with the mining samples.

#### 6. References

Bidleman T.F., 1988, 'Atmospheric processes', *Environmental Science and Technology*, **22**:361-367.

Forbes P.B.C., Karg E.W., Zimmernann R. & Rohwer E.R. 2012, 'The use of multi-channel silicone rubber traps as denuders for polycyclic aromatic hydrocarbons', *Analytica Chimica Acta*, **730**:71-79.

IARC (International Agency for Research on Cancer), World Health Organisation, 2012, 'Diesel engine exhaust carcinogenic', Press Release no. 213, 12 June 2012.

Krieger M.S., Hites, R.A., 1994, 'Measurement of Polychlorinated Biphenyls and Polycyclic Aromatic Hydrocarbons in Air with a Diffusion Denuder', *Environmental Science and Technology*, **28** (6):1129-1133.

Ortner E.K. & Rohwer E.R., 1996, 'Trace analysis of semi-volatile organic air pollutants using thick film silicone rubber traps with capillary gas chromatography', *Journal of High Resolution Chromatography*, **19**:339-344.

Temime-Roussel B., Monod A., Massiani C. & Wortham H., 2004a 'Evaluation of an annular denuder tubes for atmospheric PAH partitioning studies—1: evaluation of the trapping efficiency of gaseous PAHS', *Atmospheric Environment*, **38**:1913-1924.

Temime-Roussel B., Monod A., Massiani C. & Wortham H., 2004b 'Evaluation of an annular denuder for atmospheric PAH partitioning studies—2: evaluation of mass and number particle losses', *Atmospheric Environment*, **38**:1925-1932.